The Molecular Basis and Pathology of Phenotypic Variability in Urea Cycle Disorders

---

Dissertation

zur

Erlangung der naturwissenschaftlichen Doktorwürde
(Dr. sc. nat.)

vorgelegt der
Mathematisch-naturwissenschaftlichen Fakultät

der

Universität Zürich
von

Liyan HU

aus

Taizhou, Zhejiang der V.R. China

Promotionskomitee

Prof. Dr. sc. nat. Beat W. Schäfer (Vorsitz)

Prof. Dr. med. Johannes Häberle (Leitung der Dissertation)

Prof. Dr. sc. nat. Thierry Hennet

PD Dr. med. Jean-Marc Nuoffer

Zürich, March 2014

The present study was performed from October 2010 till March 2014 in the metabolic laboratory at the Division of Metabolism, University Children's Hospital Zürich under the supervision of Prof. Dr. med. Johannes Häberle.

Publications represented in this study:

1. **Understanding the Role of Argininosuccinate Lyase Transcript Variants in the Clinical and Biochemical Variability of the Urea Cycle Disorder Argininosuccinic Aciduria**
   Liyan Hu, Amit V. Pandey, Sandra Eggimann, Véronique Rüfenacht, Dorothea Möslinger, Jean-Marc Nuoffer, Johannes Häberle (2013) *The Journal of biological chemistry* 288(48), 34599-34611

2. **Variant forms of the urea cycle disorder argininosuccinic aciduria are caused by folding defects of argininosuccinate lyase**
   Liyan Hu, Amit V. Pandey, Cécile Balmer, Sandra Eggimann, Véronique Rüfenacht, Jean-Marc Nuoffer, and Johannes Häberle
   Manuscript submitted to *Human Molecular Genetics*, 2014

3. **Molecular characterization of the only recurrent mutation in carbamoyl phosphate synthetase 1 (CPS1) deficiency**
   Liyan Hu, Carmen Diez-Fernandez, Véronique Rüfenacht, Erdogan Soyucen, Mahmut Çoker, Bilge Tanyeri, Jordi Pérez Tur,Vicente Rubio, Johannes Häberle
   Manuscript in preparation, 2014

Contributions to other studies:

4. **Phytohemagglutinin stimulation of lymphocytes improves mutation analysis of carbamoylphosphate synthetase 1**
   Kretz R, **Hu L**, Wettstein V, Leiteritz D, Häberle J (2012). *Mol Genet Metab*. 106(3): p. 375-8

5. **Understanding carbamoyl phosphate synthetase (CPS1) deficiency by using the recombinantly purified human enzyme: effects of clinical CPS1 mutations that concentrate in a central domain of unkown function**
   Carmen Diez-Fernandez, **Liyan Hu**, Javier Cervera, Johannes Häberle, and Vicente Rubio
   Manuscript submitted to *Mol Genet Metab.* 2014 (currently minor revisions)

Personal contributions to the above related projects

1. Design and planning the studies, performing DNA and RNA studies, cloning of the vectors, sequencing, cultivation and transfection of mammalian cells, establishment of expression system, expression of recombinant ASL transcript variants constructs in 293T cells, protein extraction and immunoblotting, enzymatic activity assays, analysis of the data and statistics, drafting and editing the manuscript
2. Design and planning the studies, cultivation and transfection of 293T cells, expression of recombinant ASL constructs in 293T cells, protein extraction and immunoblotting, enzymatic activity, kinetics and thermostability assays, analysis of the data and statistics, drafting and editing the manuscript
3. Design and planning the studies, site-directed mutagenesis and cloning, cultivation of insect Sf9 cells, expression of recombinant CPS1 constructs in Sf9 cells using baculovirus, protein extraction and purification, immunoblotting, enzymatic activity assays, thermostability assay using differential scanning fluorimetry, analysis of the data and statistics, drafting and editing the manuscript
4. Protein extractions from different cell lines, western blot analysis for lymphocytes with or without PHA-M stimulation
5. Assistance to establish the baculovirus/insect expression system in our lab and to perform the experiments

Abbreviations

aCGH	array comparative genomic hybridization
ADC	arginine decarboxylase
AGAT	arginine:glycine amidinotransferase
ARG1	arginase1
ARG1D	arginase1 deficiency
ASA	argininosuccinic aciduria
ASD	allosteric doman
ASL	argininosuccinate lyase
ASLD	argininosuccinate lyase deficiency
ASS	argininosuccinate synthetase
ASS1D	argininosuccinate synthetase1 deficiency
AVV	adeno-associated virus
bp	base pair
BPSD	bicarbonate phosphorylation domain
CNS	central nervous system
CP	carbamoyl phosphate
CPS1	carbamoyl phosphate synthetase1
CPS1D	carbamoyl phosphate synthetase1 deficiency
CPSD	carbamate phosphorylation domain
DSF	differential scanning fluorimetry
DTT	dithiothreitol
EC	enzyme commission
ex2del	exon 2-deleted
ex7del	exon 7-deleted
EV	empty vector pcDNA3
GAMT	guanidinoacetate methyltransferase
GAPDH	glyceraldehyde-3-phosphate dehydrogenase
GSD	glutaminase domain
GS	glutamine synthetase
H	hour
HEK	human embryonic kidney
HHH syndrome	hyperornithinemia-hyperammonemia-homocitrullinuria syndrome

HPLC	high performance liquid chromatography
HRP	horseradish peroxidase
IEMs	inborn errors of metabolism
Indels	insertions/deletions
ISD	intersubunit interaction domain
kb	kilo bases
kDa	kilo daltons
Mb	million bases
MD	molecular dynamics
min	minute
NAG	N-acetylglutamate
NAGS	N-acetylglutamate synthase
NAGSD	N-acetylglutamate synthase deficiency
NBS	Newborn screening
NCG	N-carbamyl-L-glutamate
NO	nitric oxide
NOS	nitric oxide synthase
NT	non-transfected 293T cells
OAT	ornithine aminotransferase
ODC	ornithine decarboxylase
OMIM	Online Mendelian Inheritance in Man
OTC	ornithine transcarbamoylase
OTCD	ornithine transcarbamoylase deficiency
PAGE	polyacrylamide gel electrophoresis
P-D31N	pcDNA3-ASL-Asp31Asn
P-E189G	pcDNA3-ASL-Glu189Gly
P-ex2del	pcDNA3-ASL-ex2del
P-ex7del	pcDNA3-ASL-ex7del
P-I100T	pcDNA3-ASL-Ile100Thr
P-Q286R	pcDNA3-ASL-Gln286Arg
P-R12Q	pcDNA3-ASL-Arg12Gln
P-R95C	pcDNA3-ASL-Arg95Cys
P-R193W	pcDNA3-ASL-Arg193Trp
P-R379C	pcDNA3-ASL-Arg379Cys

P-R385C	pcDNA3-ASL-Arg385Cys
P-R385L	pcDNA3-ASL-Arg385Leu
P-R445P	pcDNA3-ASL-Arg445Pro
P-V178M	pcDNA3-ASL-Val178Met
P-V335L	pcDNA3-ASL-Val335Leu
P-wt	pcDNA3-ASL-wt
PCR	polymerase chain reaction
PDB	protein data bank
PKU	phenylketonuria
S.D.	standard deviation
SDM	site directed mutator
SDS	sodiumdodecyl sulphate
shRNA	short hairpin RNA
TMS	tandem mass spectrometry
UCDs	urea cycle disorders
UFSD	unknown function domain
UMP	uridine monophosphate
V1013del	pFastBac carrying deletion of valine1013 CPS1
wt/WT	wild type

Table of Contents

1 Summary

1.1 Summary

The urea cycle comprises a series of biochemical reactions and converts the waste nitrogen into urea. This cycle is located exclusively in the liver. A genetic defect in any of the enzymes and transporters involved in this pathway can cause a urea cycle disorder (UCD) resulting in hyperammonemia with a high mortality and morbidity. The affected UCD patients can manifest at any age with a broad phenotypic variability of which the molecular basis and pathology is not yet fully understood. The present work focuses on two UCDs, caused by mutations in the *argininosuccinate lyase (ASL)* or *carbamoyl phosphate synthetase 1 (CPS1)* genes leading to deficiency in ASL or CPS1, respectively.

ASL, a cytosolic homotetrameric urea cycle enzyme, catalyzes the cleavage of argininosuccinate into arginine and fumarate. Argininosuccinic aciduria (ASA, OMIM #207900), caused by ASL deficiency (ASLD), is a rare autosomal-recessive UCD with a wide clinical spectrum ranging from asymptomatic to severe neonatal-onset life-threatening forms. We investigated the role of naturally occurring *ASL* transcript variants and of the residual activities of mutant ASL to understand better the clinical and biochemical variability of ASA. We found that exon 2 and 7-deleted (ex2del and ex7del) ASL are the most common transcript variants expressed in different tissues at low levels compared to wild type (WT). The transcript variant ASL-ex2del forms a stable truncated protein with no relevant activity but a dose-dependent dominant negative effect on the enzymatic activity after co-expression with WT or mutant ASL p.E189G, whereas the variant ASL-ex7del is unstable but, nevertheless, appears to have a dominant negative effect on mutant ASL. The predominant occurrence of ASL-ex7del transcript found in two ASA patients in combination with the heterozygous mutant p.E189G suggested the pathophysiological relevance of this transcript variant. Further, we found residual activities > 3% of ASL WT in nine of all known (n=11) variant ASL mutants identified in patients associated with late-onset and/or mild clinical and biochemical courses. Surprisingly, six variant ASL mutants (p.R95C, p.I100T, p.V178M, p.E189G, p.V335L and p.R379C) with high residual activities (≥18% of ASL WT) showed no or only slightly increased (<2 folds of WT) K_m values, but nevertheless displayed thermal instability. These findings were supported by structural modelling predictions for ASL heterotetramer/homotetramer formation.

Taken together, our results suggest that the investigated ASL transcript variants, if expressed at high levels, as well as relevant levels of ASL residual activities of mutant proteins mainly caused by a folding defect can contribute to the phenotypic variability in ASA patients. Especially, in a stable mutant such as the ex2del ASL variant, the effect is even more striking leading to marked impairment of ASL activity.

CPS1, the first rate-limiting mitochondrial urea cycle enzyme, catalyzes carbamoyl phosphate (CP) formation from ammonia, bicarbonate and two ATPs, and requires the essential allosteric activator N-acetyl-L-glutamate (NAG) in a global reaction with three steps: phosphorylation of bicarbonate, formation of carbamate and phosphorylation of carbamate. Most clinical mutations found in CPS1 deficiency (CPS1D, OMIM #237300) are “private”, i.e. only found in single families with no or little recurrence. Here, we investigated the molecular characteristics of the only known frequently recurrent *CPS1* mutation, p.Val1013del, found in nine unrelated patients of Turkish descent using recombinant CPS1s (WT or V1013del) expressed in baculovirus/insect cells. We found that CPS1 WT and V1013del mutant were expressed at comparable levels and could be purified to homogeneity. The mutant exhibited no significant residual activities in the assays for the CP synthesis reaction and neither for the partial reactions. In the CPS1 structural model, the location of valine 1013 is close to the predicted carbamate tunnel that links both phosphorylation sites. The deletion of this residue, by shortening the β-strand of the A subdomain of the carbamate phosphorylation domain (an ATP grasp domain), could distort this carbamate tunnel and possibly hamper the connection between both phosphorylation steps. Our findings indicate that the mutation p.Val1013del inactivates the enzyme but does not render the enzyme grossly unstable or insoluble.

With these investigations, we contribute to the understanding of non-classical UCDs, namely the variant ASA forms and a recurrent CPS1 mutant on the molecular basis. At the same time, the results obtained open the way towards novel therapeutic targets. Specifically, further studies should determine the stabilising potential of pharmacological chaperons on instable mutant ASL.

1.2 Zusammenfassung

Der Harnstoffzyklus ist der Hauptweg zur Entgiftung von neurotoxischem Ammoniak und besteht aus einer Serie biochemischer Reaktionen, an deren Ende Harnstoff entsteht. Der Zyklus ist ausschliesslich in der Leber lokalisiert. Ein genetischer Defekt eines der am Harnstoffzyklus beteiligten Enzyme oder Transporter kann eine entsprechende Harnstoffzyklusstörung auslösen, die zu Hyperammonämie mit einer hohen Mortalität und Morbidität führen kann. Die betroffenen Patienten können in jedem Alter erstmals erkranken und eine breite phänotypische Variabilität zeigen, wobei die molekularen Mechanismen und deren Pathologie noch nicht völlig verstanden sind. Die vorliegende Arbeit ist auf zwei Harnstoffzyklusstörungen fokussiert, den Defekt der Argininosukzinat Lyase (ASL) und der Carbamoylphosphat Synthetase 1 (CPS1), welche zu ASL oder CPS1 Mangel führen.

ASL ist ein zytosolisches homotetrameres Harnstoffzyklusenzym, das die Reaktion von Argininosukzinat zu Arginin und Fumarat katalysiert. Die Argininbernsteinsäurekrankheit (ASA, OMIM #207900), die durch einen ASL-Mangel verursacht wird, ist eine seltene autosomal-rezessiv vererbte Harnstoffzyklusstörung mit breitem klinischem Spektrum, das von asymptomatischen bis hin zu lebensgefährlichen Verlaufsformen reicht. Um die klinische und biochemische Variabilität der ASA besser zu verstehen, haben wir untersucht, welche Rolle natürlich vorkommende ASL Transkript-Varianten und die Restaktivitäten der ASL Mutanten spielen. Wir konnten zeigen, daß exon 2- und 7-Deletionen (ex2del und ex7del) von ASL die am meisten vorkommenden Transkript-Varianten sind und in unterschiedlichen Geweben auf niedrigem Level im Vergleich zum Wildtyp (WT) exprimiert werden. Die Transkript-Variante ASL-ex2del bildet ein stabiles, verkürztes Protein ohne relevante Enzymaktivität. Hingegen hat das mutierte Protein einen dosierungsabhängigen dominant-negativen Effekt auf die Enzymaktivität, wenn es mit WT oder der Mutante p.E189G ko-exprimiert wird. Die Variante ASL-ex7del ist dagegen instabil, weist aber dennoch einen dominant-negativen Effekt auf das mutierte ASL Protein p.E189G auf. Das überwiegende Auftreten der ASL-ex7del Transkript-Varianten, das in zwei ASA Patienten in Kombination mit einer heterozygoten Mutation p.E189G gefunden wurde, deutet auf die pathophysiologische Relevanz dieser Transkript-Variante hin.

Ausserdem haben wir eine Restaktivität >3% von ASL WT) bei 9 der 11 bekannten varianten ASL Mutanten detektiert, welche in Patienten mit spät

einsetzendem und/oder mildem klinischen und biochemischen Verlauf identifiziert wurden. Erstaunlicherweise zeigten die sechs varianten ASL Mutanten (p.R95C, p.I100T, p.V178M, p.E189G, p.V335L und p.R379C) mit hoher enzymatischer Restaktivität (≥18% von ASL WT) keine oder nur leicht gesteigerte (< 2-fach von WT) K_m Werte, aber dennoch thermische Instabilität. Diese Untersuchungsergebnisse wurden von Strukturmodellen, welche die ASL Heterotetramer/Homotetramer-Bildung darstellen, unterstützt. Insgesamt deuten unsere Ergebnisse drauf hin, dass sowohl die untersuchten ASL Transkript-Varianten, die stark exprimiert sind, als auch die relevanten ASL Restaktivitäten der mutierten Proteine, welche hauptsälich von einem Faltungsdefekt verursacht sind, zur phänotypischen Variabilität von ASA Patienten beitragen. Besonders auffallend ist der Effekt in einer stabilen Mutante wie der ASL-ex2del Variante, die eine ausgeprägte Beeinträchtigung der ASL Aktivität zur Folge hat.

CPS1 ist das erste und geschwindigkeitsbestimmende mitochondriale Harnstoffzyklusenzym, das die Synthese von Carbamoylphosphat (CP) aus Ammoniak, Bikarbonat und zwei ATP-Molekülen katalysiert. Die globale Reaktion erfordert obligat den allosterischen Aktivator N-Acetyl-L-Glutamat (NAG) und erfolgt in drei Teilschritten: Phosphorylierung von Bikarbonat, Entstehung von Carbamat durch die Anlagerung von Ammoniak unter Abspaltung des Phosphatrestes sowie Phosphorylierung von Carbamat. Die meisten klinischen Mutationen bei einem CPS1 Mangel (CPS1D, OMIM #237300) sind „privat“, d.h. sie treten fast nur in einzelnen Familien auf.

In der vorliegender Arbeit haben wir die molekularen Eigenschaften der einzigen bekannten häufig auftretenden Mutation, p.Val1013del, die in neun nicht verwandten Patienten türkischer Abstammung identifiziert wurde, mittels in Bakulovirus/Insektenzellen exprimierter rekombinanter CPS1 Proteine (WT oder V1013del) untersucht. CPS1 WT und V1013del Mutante wurden auf vergleichbarem Niveau exprimiert und zur Homogenität gereinigt. Die Mutante zeigte keine signifikanten Restaktivitäten in den Assays für die Reaktion der CP Synthese und auch nicht für die beiden Teilreaktionen. In dem CPS1 Strukturmodell liegt der Valinrest V1013 nah beim prognostizierten Carbamat Tunnel, der beide Phosphorylierungsstellen verknüpft. Die Entfernung des Valinrestes im β-Strang der A Subdomäne der Carbamat Phosphorylierungsdomäne (eine ATP Zugriffsdomäne) könnte den Carbamat Tunnel deformieren und damit das Zusammenspiel der beiden

Phosphorylierungsschritte verhindern. Unsere Ergebnisse deuten darauf hin, dass die Mutation p.V1013del das Enzym inaktiviert, jedoch nicht zu Instabilität oder Unlöslichkeit des Enzyms führt.

Mit diesen Untersuchungen können wir zum besseren Verständnis der nicht-klassischen Harnstoffzyklusstörungen, insbesondere der varianten ASA Formen und einer relativ häufig auftretenden CPS1 Mutante auf molekularer Ebene beitragen. Gleichzeitig weisen die erhaltenen Ergebnisse den Weg zu neuen therapeutischen Ansätzen. Naheliegend wären Studien, die das Stabilisierungspotential von pharmakologischen Chaperonen für instabile ASL Mutanten untersuchen.

2 Introduction

2.1 Nitrogen metabolism and urea cycle

2.1.1 Overview

All living organisms depend on nitrogen as essential component of proteins, nucleic acids and several other important compounds. During catabolism of any of the numerous nitrogenous compounds, waste nitrogen in the form of ammonia is formed. Surplus ammonia cannot be stored and has to be removed fast to avoid its (neuro)toxicity.

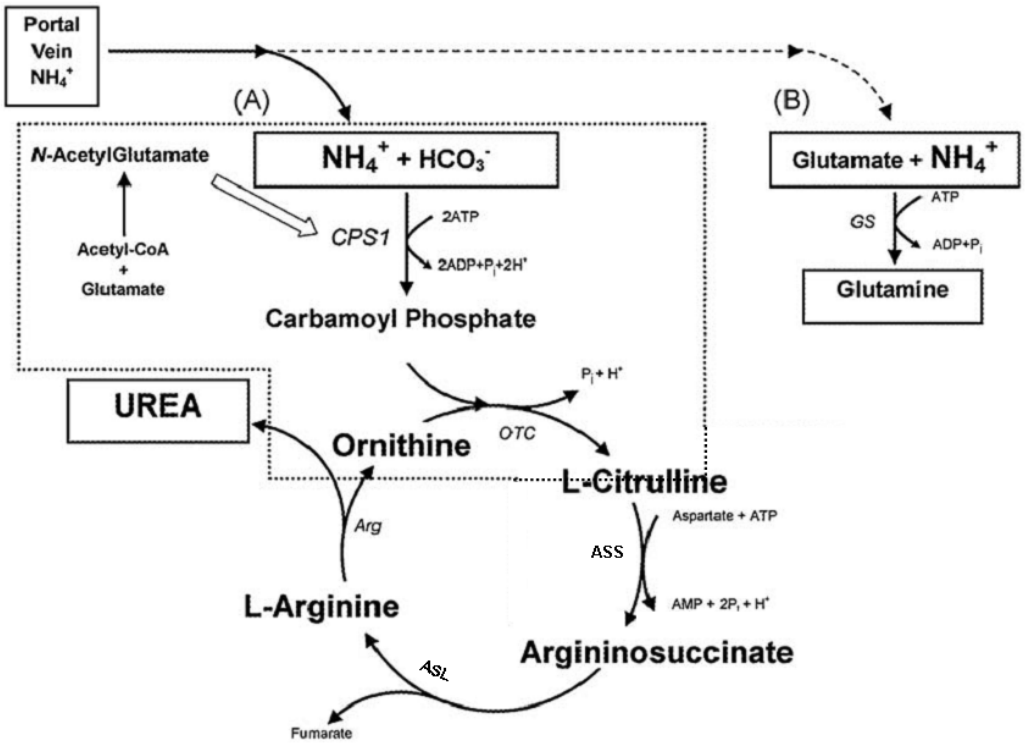

Fig.1: Pathways for ammonia detoxification within the liver.

(A): Primary pathway for ammonia removal: ureagenesis within the periportal hepatocytes. Sections within dotted line occur within the cell mitochondria. (B) Glutamine synthesis within the perivenous hepatocytes. ASL, argininosuccinate lyase; Arg, arginine; ASS, argininosuccinate synthetase; CPS1, carbamoyl phosphate synthetase 1; GS, glutamine synthetase; HCO_3^-, bicarbonate; OTC, ornithine transcarbamoylase (adapted from [1]).

In mammals, the major metabolic pathway for the metabolism of waste nitrogen is the urea cycle. In other words, the urea cycle functions as the primary pathway of ammonia detoxification in the liver. Ammonia in the hepatic portal vein is delivered to the liver, where it is incorporated into either urea via ureagenesis within the periportal hepatocytes (hepatocytes present around the portal vein) (Fig. 1(A)), or glutamine via

the glutamine synthetase (GS) reaction within the perivenous hepatocytes (hepatocytes present around the hepatic vein) (Fig. 1(B)) [1-4]. Ammonia at low concentrations is effectively removed by GS, not by ureagenesis. The two pathways of ammonia detoxification in the liver represent a low-affinity but high-capacity system for ureagenesis and a high-affinity system for glutamine synthesis [5].

2.1.2 Nitrogen metabolism

2.1.2.1 Nitrogen cycle

Nitrogen exists abundantly (80%) as a gaseous form (N_2) in the atmosphere, in organic form in the soil, and as an ion such as ammonium (NH_4^+) or nitrate (NO_3^-) in plants and microbes [6]. Continuous cycling of nitrogen occurs between the soil, plants, animal and the atmosphere including the following steps: (1) formation of ammonia by bacterial fixation of N2; (2) nitrification of ammonia to nitrate by soil organisms; (3) conversion of nitrate to ammonia by higher plants; (4) synthesis of amino acids from ammonia by all organisms, and conversion of nitrate to N_2 by denitrifying soil bacteria (Fig. 2) [7]. Thus, the nitrogen cycle is also a process in which nitrogen is converted between its various chemical forms. All metabolic pathways including nitrogen are based on a recycling of ammonia in its neutral or charged form ammonium. In living organisms, nonprotein nitrogen occurs primarily as ammonia and ammonium, which is a major constitute of the protein and nucleic acid pools [6]. Further, approximately 99% of the ammonia-ammonium pool is in the ionized (NH_4^+) form during physiological conditions [8].

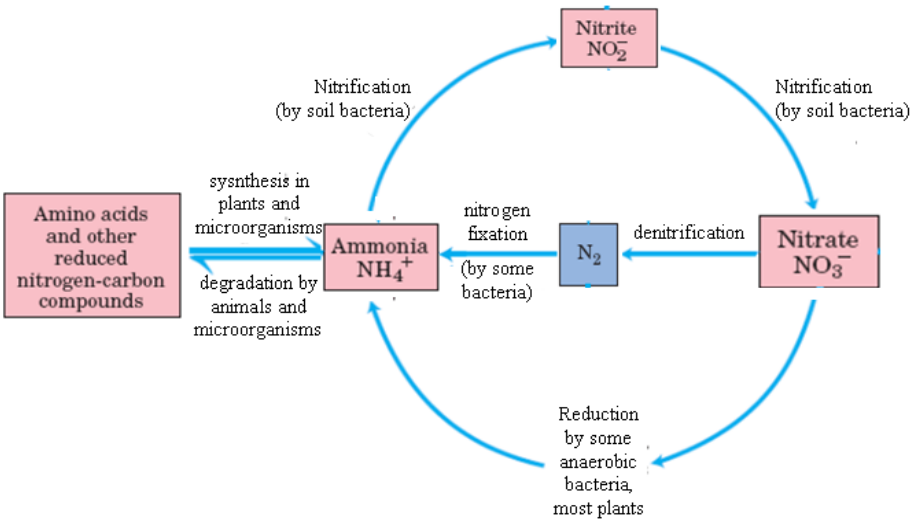

Fig. 2: The nitrogen cycle.

Details of the cycle are described in the text (taken from [7]).

2.1.2.2 Protein turnover and nitrogen balance

Cells continually turn over body proteins to supply amino acids for various purposes such as the synthesis of essential protein and other nitrogenous compounds (purines, pyrimidines, creatine, porphyrins) [9]. When proteins break down, they release amino acids, which form an “amino acid pool” within the cells and circulating blood, together with other amino acids from dietary protein. The rate of protein degradation and the amount of protein intake may vary, but the pattern of amino acids within the pool maintains fairly constant [10]. In healthy adults, protein synthesis balances with degradation, and dietary protein intake balances with nitrogen excretion in the urine, feces and sweat.

Quantitatively, liver and muscle are the most important organs in the protein turnover. Nutritional control of muscle and liver protein turnover is mediated by certain amino acids and hormones such as insulin, corticosteroids and thyroid hormone for muscle, and insulin and glucagon mainly for liver [9, 11, 12].

Usually, protein requirement is estimated by nitrogen balance, which refers to the nitrogen equilibrium between anabolism and catabolism. It can be measured by assessing dietary nitrogen intake versus urinary nitrogen output as urea and controlled by the amounts and composition of the diet as well as by changes in protein turnover. There is positive and negative nitrogen balance. The former status is the net storage of nitrogenous compounds, which occurs when the nitrogen intake is greater than its excretion, implies tissue formation and growth. The latter status is the net breakdown of stored nitrogenous compounds, which occurs when nitrogen output exceeds its intake, indicates wasting or destruction of tissue [10].

2.1.2.3 Removal of nitrogen from amino acids

Amino acids derived from the dietary protein are the source of most amino groups. The first step in amino acids degradation is the removal of nitrogen from the carbon skeleton. In the cytosol of hepatocytes, the amino group from most amino acids is transferred to α-ketoglutarate to form glutamate, which enters mitochondria and is then oxidatively deaminated to produce ammonium ion (NH_4^+) (Fig. 3) [7] [13]. The reactions involved in removing nitrogen from amino acids are known as transamination, which is catalyzed by aminotransferases or transaminases at the presence of pyridoxal phosphate as a cofactor. Some of the ammonia generated in

this process is recycled for a variety of biosynthetic pathways. In skeletal muscle, excess amino groups are generally transferred to pyruvate to form alanine, which transports amino groups to the liver. Depending on the organism, the amino nitrogen excess is either excreted directly as ammonia in most aquatic species such as bony fishes, or converted into urea in ureotelic animals or uric acid in birds and reptiles for excretion.

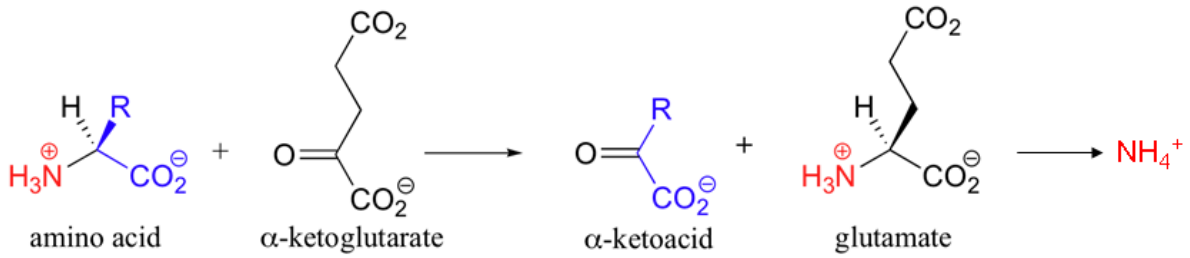

Fig. 3: Schematic reaction for removal of nitrogen from amino acid.
Details of the reaction are described in the text (modified from [13]).

2.1.2.4 Role of glutamate and glutamine

In living systems, reduced nitrogen in the form of NH_4^+ is incorporated first into amino acids and then into other nitrogen-containing bimolecules. The amino acids glutamate and glutamine play a key role in the nitrogen metabolism, acting as main storage pool for amino groups. In other words, glutamate und glutamine are important nitrogen donors in a wide variety of biosynthetic reactions. Glutamate is the most important excitatory neurotransmitter in the brain [14] and the precursor of glutamine. The ubiquitously expressed GS, which catalyzes the synthesis of glutamine from glutamate, is a main regulatory enzyme in nitrogen metabolism. On the other hand, at least six end products of glutamine metabolism are allosteric inhibitors of GS, resulting in a constant adjustment of glutamine metabolism to match immediate physiological requirements [7].

In brain, there is also an intercellular glutamine cycle, releasing glutamine to the extracellular space to be taken up into neurons, where it is converted back to glutamate by the action of glutaminase [5, 15, 16]. Moreover, glutamine appears to represent a temporary storage form of waste nitrogen for most extra-hepatic organs lacking a complete urea cycle [16]. In liver, periportal glutaminase and perivenous GS are simultaneously active leading to an intercellular glutamine cycle with periportal degradation and perivenous resynthesis of glutamine at the expense of energy [5, 17, 18].

2.1.2.5 Pathophysiology of hyperammonemia

Despite ammonia has an important role in nitrogen homeostasis, endogenous amino acid synthesis and acid-base balance, it is (neuro)toxic when present at high concentrations (> 50 µmol/L in plasma) [9]. Hyperammonemia refers to a clinical condition characterized by elevated ammonia levels in blood and tissues by its increased production and/or decreased detoxification indicating abnormal nitrogen homeostasis [19]. It increases the risk of irreversible brain damage, of neurodevelopmental retardation or even death, when ammonia has already reached above 400-500 µmol/L [19]. In urea cycle disorders (UCDs), organic acidemias, fatty acid oxidation defects, bypass of the major site of detoxification such as hepatic cirrhosis, Reye syndrome, postchemotherapy, or exposure to various toxins and drugs, patients can present with severe hyperammonemia [20]. The urea cycle is the major part of ammonia detoxification in the mammalian organisms (Fig. 1). Primary hyperammonemia is therefore caused by inherited defects of the urea cycle enzymes or transporters, while inborn or acquired defects outside the urea cycle can lead to secondary hyperammonemia [19].

Under conditions of hyperammonemia, there are several pathophysiological alterations but the entire neurotoxicity is still not yet fully understood [21]: (1) pathologic brain changes like brain edema, brainstem herniation, astrocytic swelling, white-matter damage and neural loss [22]; (2) amino acid disturbances including increased glutamine concentrations in the brain leading to astrocytic damage, swelling and cell death of the glutamatergic neurons as well as decreased arginine levels [20]; (3) alterations in neurotransmission systems such as accumulated extracellular glutamate in the glutamatergic system [23, 24], loss of cholinergic neurons leading to decreased choline acetyltransferase activity levels in cholinergic system [23, 25], elevated tryptophan (precursor for serotonin) and 5-hydroxyindoleacetic acid (metabolite of serotonin) in cerebrospinal fluid [26-28], cerebral energy deficit [29-31], cerebral exposure [23], altered potassium ion and water channels contributing to brain edema formation [32, 33].

Clinical signs and symptoms in hyperammonemia are unspecific but most affect cerebral function. The duration of the hyperammonemic coma and the maximum ammonia level are negatively correlated with the patient’s neurological outcome. Delayed diagnosis or treatment of hyperammonemia can lead to neurologic damage and death.

2.1.3 Urea cycle

2.1.3.1 Urea cycle pathway

The urea cycle is a complex series of biochemical reactions that converts the waste nitrogen in the form of ammonia into urea ($(NH_2)_2CO$) and is fully expressed only in the liver. This cycle was first described by Krebs and Henseleit in 1932 [34]. It is highly conserved in all mammalian species and spans two cellular compartments: the first two steps take place in the mitochondria and the subsequent three steps in the cytosol (Fig. 4). The urea cycle has three functions: (1) detoxification of nitrogen in the form of ammonia; (2) *de novo* biosynthesis of endogenous arginine; (3) maintenance of the acid-base homeostasis.

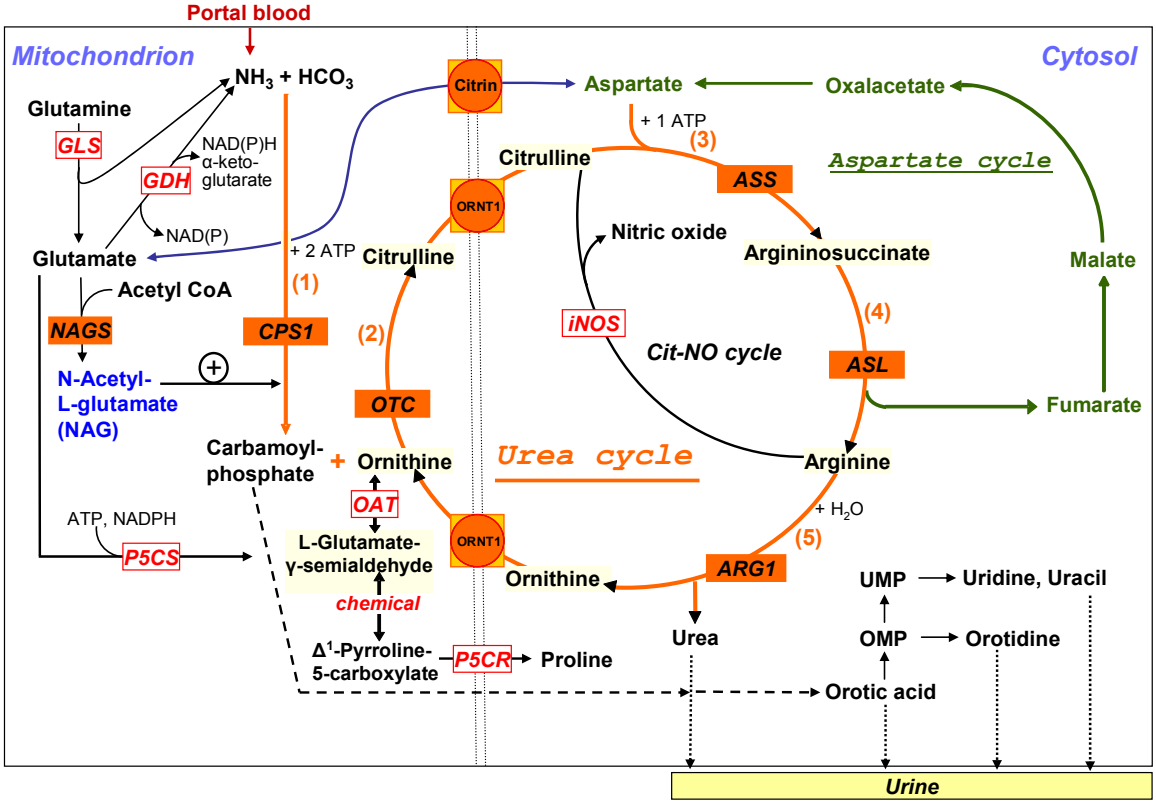

Fig. 4: The urea cycle and associated metabolic pathways.

The urea cycle takes place in five steps in the liver. The involved six enzymes and two transporters are marked in orange rectangle and circle, respectively. ARG1, arginase 1; ASL, argininosuccinate lyase; ASS, argininosuccinate synthetase; Cit-NO cycle, citrulline-nitric oxide cycle; CPS1, carbamoyl phosphate synthetase; GDH, glutamate dehydrogenase; GLS, glutaminase; iNOS, inducible nitric oxide synthase; NAD(P), nicotinamide adenine dinucleotide (phosphate); NAGS, N-acetylglutamate synthase; OAT, ornithine aminotransferase; OMP, orotidine monophosphate; OTC, ornithine transcarbamylase; P5CR, pyrroline-5-carboxylate reductase; P5CS, Δ^1-pyrroline-5-carboxylate synthetase; UMP, uridine monophosphate (modified from [35]).

The net effect of the urea cycle is to convert two nitrogen atoms derived from ammonia and aspartate to produce urea. The individual reactions are shown in Fig. 4: (1) Production of carbamoyl phosphate (CP) from ammonia and bicarbonate: $2ATP + NH_3 + HCO3^- \rightarrow 2ADP + P_i + CP$, this reaction takes place in mitochondria and is catalyzed by carbamoyl phosphate synthetase 1 (CPS1) in the presence of the essential allosteric activator N-acetyl-L-glutamate (NAG) [36-52]; (2) Formation of citrulline from CP and ornithine catalyzed by ornithine transcarbamylase (OTC) in the mitochondria with the release of P_i: ornithine + CP $\rightarrow$ citrulline + P_i + H^+, the produced citrulline is transported from mitochondria into the cytosol by the mitochondrial ornithine/citrulline transporter ORNT1; (3) Entering of the second amino group from aspartate by a condensation reaction between the amino group of aspartate and the carbonyl group of citrulline to form argininosuccinate: citrulline + aspartate + ATP $\rightarrow$ argininosuccinate + AMP + pyrophosphate (PP_i) + H^+, this cytosolic reaction is catalyzed by argininosuccinate synthetase (ASS); (4) The argininosuccinate is then cleaved by argininosuccinate lyase to form arginine and fumarate: argininosuccinate $\rightarrow$ arginine + fumarate, fumarate returns to the urea cycle through the aspartate cycle; (5) The produced endogenous arginine is further cleaved by arginase to yield urea and ornithine: arginine $\rightarrow$ urea + ornithine, ornithine is transported by the transporter ORNT1 into the mitochondria to initiate another round of the urea cycle [7, 9]. The biochemical reactions of the urea cycle also produce three physiological important metabolites: ornithine, citrulline and arginine.

2.1.3.2 Properties of individual urea cycle enzymes

The complete urea cycle requires the activity of six enzymes including NAGS, CPS1, OTC, ASS, ASL, ARG1 and two transporters, citrin and ORTN1. An overview on the molecular genetic characteristics in this pathway is summarized in Table 1. The first three urea cycle enzymes are mitochondrial and the other three are cyctosolic. Although some urea cycle enzymes are present in several tissues, the full set of urea cycle enzymes is only expressed in periportal hepatocytes. This section will only describe the six enzymes and mainly focus on the mitochondrial CPS1 and the cytosolic ASL enzymes.

Table 1: Overview on molecular genetics in urea cycle

Enzymes / transporters	EC #	Gene	Gene/ locus OMIM *	Protein location	Gene location	Exons (coding)	Amino acids	MW $ (kDa)
N-acetylglutamate synthase	2.3.1.1	*NAGS*	608300	Mitochondria	17q21.31	7	534	58
Carbamoylphosphate synthetase 1	6.3.4.16	*CPS1*	608307	Mitochondria	2p35	38	1500	160
Ornithine transcarbamylase	2.1.3.3	*OTC*	300461	Mitochondria	Xp21.1	10	354	40
Argininosuccinate synthetase	6.3.4.5	*ASS1*	603470	Cytosol	9q34.1	14	412	45
Argininosuccinate lyase	4.3.2.1	*ASL*	608310	Cytosol	7q11.21	16	464	52
Arginase 1	3.5.3.1	*ARG1*	608313	Cytosol	6q23	8	330	35
Ornithine/citrulline transporter ORNT1	-	*SLC25A15*	603861	Inner mitochondrial membrane	13q14	6	301	33
aspartate/glutamate carrier Citrin	-	*SLC25A13*	603859	Inner mitochondrial membrane	7q21.3	18	675	74

EC #: enzyme commission number; OMIM *: Online Mendelian Inheritance in Man number;

$ indicates the molecular weight for monomer

2.1.3.2.1 N-acetylglutamate synthase (NAGS)

NAGS (EC 2.3.1.1), a member of the N-acetyltransferase family of enzymes, catalyzes the formation of N-acetylglutamate (NAG) from glutamate and acetyl coenzyme A in the mitochondrial matrix. The produced NAG is the essential allosteric activator for CPS1 in mammals indicating that NAGS may have a key role as a regulator of ureagenesis by modulating the activity of CPS1 through NAG [53]. NAGS is expressed primarily in the liver and small intestine; the intestinal transcript is smaller in size than the liver transcript [54]. The human *NAGS* gene is located on chromosome 17q21.31 [55]. It consists of 7 exons spanning about 4 kb and encodes a preprotein of 534 amino acids with a molecular weight of 58 kDa [54]. Based on sequence similarity to mouse NAGS, the human NAGS cDNA was isolated from a liver library. Three regions with different degrees of sequence conservation were

identified: N-terminal mitochondrial targeting signal of 49 amino acids (63% identity with mouse NAGS), the variable domain of 45 amino acids (35% identity) and the conserved domain of 440 amino acids (92% identity) [54]. When the NAGS protein is transported into mitochondria, its N-terminal mitochondrial targeting peptide is subsequently cleaved at positions 31 and 49 amino acids resulting in the “long mature” and “short mature” protein, respectively [56]. The “short mature” NAGS exhibits the highest enzymatic activity. Mammalian NAGS activity increases in the presence of arginine and is also stimulated by protamines and other cationic polypeptides [57].

2.1.3.2.2 Carbamoyl phosphate synthetase 1 (CPS1)

2.1.3.2.2.1 Reactions catalyzed by CPS1

CPS1 (EC 6.3.4.16) is the first rate-limiting enzyme of the urea cycle, which catalyzes the synthesis of CP from ammonia, bicarbonate and two molecules of ATP in a global reaction ($2ATP + HCO_3^- + NH_3 \rightarrow NH_2CO_2PO_3^{2-} + ADP + P_i$) with three steps (Fig. 5) [36, 38, 40, 58]. In the first step, bicarbonate (HCO_3^-) is phosphorylated by ATP to form carboxyphosphate ($HCO_3PO_3^{2-}$). In the second step, carboxyphosphate reacts with ammonia to produce carbamate ($H_2NCO_2^-$). In the third step, the resulting carbamate is phosphorylated by another ATP yielding final product CP ($H_2NCO_2PO_3^{2-}$). In principal, these reactions can independently take place at the two catalytic centres of bicarbonate (step 1) and carbamate (step 3) phosphorylations reflecting partial reactions of bicarbonate-dependent ATP hydrolysis (ATPase) in the absence of ammonia and ATP synthesis from ADP and CP, respectively [59-63]. However, the stoichiometry of the CPS1 global reaction requires a coupling of the partial reactions at the two phosphorylation sites via conformational changes as shown in *E. coli* [64-67]. Moreover, the reaction requires the allosteric activator NAG without which CPS1 is inactive. In other words, the CPS1 activity is regulated by the allosteric effector which triggers the signals that are transmitted to the active sites thereby changing the affinity for ATP binding [68, 69].

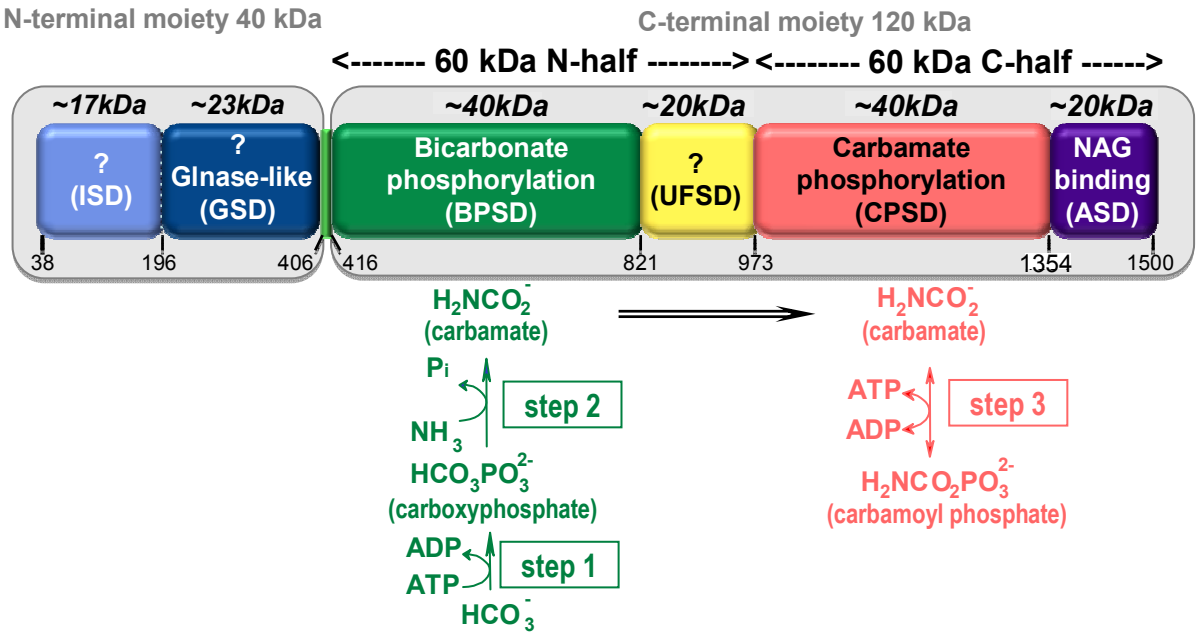

Fig. 5: Linear scheme of multidomain organization and reaction steps of mature human CPS1.

CPS1 consists of 40-kDa N-terminal and 120-kDa C-terminal moieties marked with grey-shaded background bars corresponding to the small and large subunits of *E. coli* CPS, respectively. The colored bars represent the different CPS1 domains with indicated specific functions as defined in [50]. Their approximate molecular weights (kDa) and the domain start/end residue numbers are given above and below each domain, respectively. Biochemical partial reactions are indicated below the domain that catalyzes them. ISD, intersubunit interaction domain; GSD, glutaminase domain; BPSD, bicarbonate phosphorylation domain; UFSD, unknown function domain; CPSD, carbamate phosphorylation domain; CPSD, carbamate phosphorylation domain; ASD, allosteric domain which binds NAG (modified from [63]).

2.1.3.2.2.2 Organization and function of CPS1 multidomain

The CPS1 enzyme has been purified from mammalian species such as human, rat and bovine [51, 70, 71]. The precursor form of CPS1 synthesized on free polysomes in the cytosol is transported to the mitochondria and then further converted to the mature form by proteolytic cleavage of its N-terminal mitochondria targeting sequence of 38 residues [40, 72-74]. The mature CPS1 is a large enzyme with complex multidomain. The N-terminal and C-terminal moieties of 40 and 120 kDa CPS1 corresponding to the small and large subunits of *E. coli* CPS, respectively (Fig. 5) [75], are fused by a short protease-sensitive peptidic bridge [63]. Unlike the small subunit of bacterial CPSs, the 40-kDa N-terminal moiety of CPS1 is unable to

hydrolyze glutamine [63]. Studies suggest that this domain might have a role in structural organization as well as in mediating the conformation of the active catalytic centres revealed by the existence of missense mutations affecting this region and the abolition of CPS activity upon deletion of the N-terminal domain of CPS1 [76, 77]. It has also been shown internal homology between the N- and C-terminal halves (each 60 kDa) of the 120 kDa moiety [38, 40, 43, 78]. The 120 kDa synthetase domain with two homologous halves has likely arisen by duplication and tandem fusion of an ancestral gene [79]. Moreover, each homologous half of this 120-kDa moiety is composed of N- and C-terminal domains of ~40 and ~20 kDa [78, 80-82]. The 40-kDa domains of the N- (BPSD in Fig. 5) and of the C-half (CPSD in Fig. 5) of the 120-kDa moiety catalyze the phosphorylation of bicarbonate and of carbamate, respectively. The C-terminal 20-kDa domain of the N-half (UFSD in Fig. 5) has been suggested to play a key integrating role for creating the CPS1 multidomain architecture and proposed as “integrating domain” [83]. The C-terminal 20-kDa domain of the C-half (ASD in Fig. 5) is the NAG binding site involved in regulation of CPS1 [52, 75, 82, 84-88].

2.1.3.2.2.3 E. coli CPS

There is only one form of CPS in prokaryotes which uses glutamine as the source of nitrogen. The *E. coli* CPS is an $(\alpha,\beta)_4$-heterotetramer [84] and exists as the α,β-heterodimer in the presence of uridine monophosphate (UMP) [89]. The α- and β-subunits also referred to as the small and large subunits are encoded by the *carA* and *carB* genes, respectively [90, 91]. The small subunit of CPS shows a distinctly bilobal in appearance with the N- (corresponding to ISD in Fig. 5) and C-terminal domains (corresponding to GSD in Fig. 5); the former delineated by Leu 1 to Leu 153 has not been crystallographically depicted in other proteins so far and the latter delinated by Asn 154 to Lys 382 matches with glutamine amidotransferase which hydrolyzes the glutamine used as the source as ammonia [75, 89]. The large subunit consists of four major components including the carboxyphosphate domain (corresponding to BPSD in Fig. 5), oligomerization domain (corresponding to UFSD in Fig. 5), carbamoyl phosphate domain (corresponding to CPSD in Fig. 5) and the allosteric domain (corresponding to ASD in Fig. 5). Structural investigation by X-ray crystallographic analysis of *E. coli* CPS revealed that the three active sites (one in small subunit and two in large subunit) on the protein widely separated from each

other are connected by a molecular tunnel with a total length of approximately 100 Å, suggesting that CPS utilizes this channel to facilitate the translocation of reaction intermediates from one side to another [89, 92]. The *E. coli* CPS is activated by the arginine precursor ornithine and by IMP, and inhibited by UMP [75].

2.1.3.2.2.4 Eukaryotic CPSs and human CPS1

In eukaryotic systems three different types of CPS have been identified so far: (1) mitochondrial CPS I (referred to as CPS1) functions in the production of arginine and urea and employs free ammonia as the source of nitrogen; (2) cytosolic CPS II is involved in pyrimidine biosynthesis and hydrolyzes glutamine for the production of the required ammonia; (3) CPS III (a urea-specific CPS in certain invertebrates and fishes) utilizes glutaminase as the nitrogen source but functions in the arginine and urea cycles [89]. Like CPS I, CPS III is a fused monofunctional enzyme, whereas CPS II exists as a fused multifunctional protein. Moreover, a residue substitution at the active site of the small subunit from cysteine in *E. coli* CPS to serine in rat CPS I cause the inability of CPS I to hydrolyze glutamine, while this active site cysteine residue is conserved in CPS III [89].

The human *CPS1* gene (Mendelian Inheritance of Man (MIM) *608307) has been cloned and characterized [74] and mapped to chromosome 2q35 [93, 94]. It consists of 37 introns and 38 exons spanning >120 kb of genomic DNA [44, 95, 96]. The full-length *CPS1* cDNA encodes a polypeptide of 1500 amino acids with a calculated molecular mass of approximately 160 kDa. Human CPS1 is activated by NAG and cannot use glutamine as the source of nitrogen [36]. Evidence in the frog enzyme showed that the GSD domain of CPS1 still remains the entry site for the ammonia substrate probably contributing to the lower K_m for ammonia observed in CPS I relative to other CPSs [97].

Human CPS1 is encoded by a single gene which resulted from an ancient gene fusion event [79]. CPS1 is located in the mitochondrial matrix and mainly expressed in hepatocytes and in epithelia cells of the intestinal mucosa as well as at low levels in kidney tissue and pancreas [42, 98-100]. Up to date, no crystal structure of the entire human CPS1 is available except for the allosteric regulatory domain. The best studied human CPS1 exhibited very similar properties with the rat CPS I because of the high sequence similarity (95% identity) [37]. Although the rat CPS I has been used as a model for human CPS1 [101], the structure of the rat or any

other CPS I has not yet been determined. Nevertheless, *E. coli* CPS can be used to model human CPS1 in studying the impact of mutations affecting the catalytic domains which are homologous in the both enzymes [102]. Recently, recombinant production of CPS1 in insect and yeast cell systems provided useful tools to rationalize the effects of disease-causing CPS1 mutations on enzyme stability and functionality [52, 76, 103].

2.1.3.2.3 Ornithine transcarbamylase (OTC)

OTC (EC 2.1.3.3), localized in the mitochondria of mammalian liver, is the second urea cycle enzyme that catalyzes the synthesis of citrulline from ornithine and CP. It has been highly purified from the bovine, human and rat livers and well characterized [104-109]. The *OTC* gene (MIM *311250) is mapped to the short arm of X chromosome within band Xp21.1 [110]. It consists of 10 exons spanning a region of 73 kb and has an open reading frame of 1062 nucleotides encoding a precursor protein of 354 amino acids with a molecular weight of 40 kDa [111-113]. The precursor OTC containing a 32-residue leader peptide is synthesized in the cytosol of hepatocytes and then translocated through both mitochondria membranes in an energy-dependent manner [114, 115], after which the leader peptide is proteolytically cleaved in two distinct steps to produce mature 36-kDa OTC monomer [113, 116]. The functional enzyme exists as a homotrimer and its crystal structure has been solved [117, 118]. The active sites are located at the interface between the protein monomers and each active site has two residues from an adjacent monomer contributing to substrate binding [119].

OTC is expressed mainly in the liver, but it can also be detected in the intestinal epithelial cells. Its gene can be regulated by glucocorticoids and other transcriptional factors such as C/EBP and HNF-4 [119]. Recently, evidence suggests that OTC could possibly also function as a signaling molecule during active cell proliferation (e.g., during liver regeneration) [119].

2.1.3.2.4 Argininosuccinate synthetase (ASS1)

ASS1 (EC 6.3.4.5; common gene symbol alias: ASS) [120] is a cytosolic urea cycle enzyme which is involved in the synthesis of arginine [121] and catalyzes the synthesis of argininosuccinate from citrulline and aspartate consuming one ATP

[122]. Besides its key role in liver urea synthesis, it may play a limiting role in arginine synthesis for NO production [123, 124]. There are multiple processed ASS pseudogenes localized on 11 chromosomes [125, 126], however none of them is expressed [127, 128]. The *ASS1* gene (MIM *603470) is located on the long arm of chromosome 9 at band 9q.34 [120, 125]. It spans 63 kb and consists of 16 exons (of which 14 are coding and the start codon is in exon 3) with an open reading frame of 1236 bp encoding a peptide of 412 amino acid residues which are highly conserved in human, bovine, rat and mouse [123, 129, 130]. Within the *ASS1* gene, the translational initiation codon is located in exon 3, because the first two exons encode 5' untranslated sequence [131]. It has been observed that there is tissue-specific alternative splicing in ASS exon 2 [132].

ASS is a homotetrameric protein composed of approximately 45-kDa monomers [120]. It is a ubiquitously expressed enzyme, but mainly found in periportal hepatocytes of the liver and in kidney [133]. The localization and regulation of ASS are quite different depending on arginine utilization. Hormones including glucocorticoids, glucagon and insulin, and nutrients constitute the major regulating factors [123]. An increase in specific ASS mRNA level was shown in rats induced by feeding with high protein diet [134, 135]. Moreover, glutamine was also found to induce the increase of ASS mRNA level in rat hepatocytes leading to increase in ASS activity [136]. On the other hand, ASS is repressed by the concentration of arginine in the medium in some cultured cell lines [137-139]. Recently, the crystal structure revealed three domains, namely, nucleotide-binding domain containing an "N-type" ATP pyrophosphatase consensus sequence, synthetase domain and C-terminal oligomerization domain in human ASS enzyme [140].

2.1.3.2.5 Argininosuccinate lyase (ASL)

2.1.3.2.5.1 ASL function and gene structure

ASL (EC 4.3.2.1) is the second cytosolic urea cycle enzyme which catalyzes the cleavage of argininosuccinate into arginine and fumarate. In human, ASL is essential for ammonia detoxification via the urea cycle, whereas in lower organisms it is required for the biosynthesis of arginine [141]. Recently, it has been shown that ASL is also required for systemic NO production [124]. ASL belongs to a superfamily of metabolic enzymes including aspartase [142], adenylosuccinate lyase [143], class II

fumarase [144] and 3-carboxyl-cis,cis-muconate lactonizing enzyme [145] that possess three highly conserved regions and catalyze similar cleavages [146]. The active enzyme is a homotetramer composed of four identical subunits each with a molecular weight of about 52 kDa [147]. ASL protein is predominantly expressed in the liver, but can also be found in other tissues such as fibroblasts, kidney, heart, small intestine, brain, muscle, pancreas and red blood cells [99, 147-153].

The *ASL* gene has now been identified in a variety of species including *E. coli*, yeast, algae, rat and human [154]. ASL cDNA clone containing an open reading frame of 464 amino acids has been isolated from human liver cDNA library [147]. The human *ASL* gene (MIM *603810) is located at chromosome 7q11.21 [155, 156] spanning approximately 25 kb composed of 16 exons [147]. One region on human chromosome 22 cross-hybridising to 5'-ASL-cDNA was assumed to be a pseudogene but late found to code for Ig-λ like mRNA [147, 155, 157]. Recently, a partial sequence on chromosome 7, about 3 million bases (Mb) upstream of the *ASL* gene was identified as a novel ASL pseudogene [158]. Additionally, it has been observed in different tissues that alternative splicing events occur frequently at the *ASL* locus leading to exon deletions. Amongst them, deletions of exons 2 or 7 are the most common [159].

2.1.3.2.5.2 Relationship to crystallins

Crystallins are diverse group of water soluble and highly stable structural proteins which accumulate in the eye lens and contribute to its refractive properties [160-162]. There are two categories in crystallins: (1) the ubiquitous crystallins including α, β and γ-crystallin are distributed in all vertebrate lenses; (2) the taxon-specific crystallins such as δ-crystallins are only present in certain species [163, 164]. α-crystallin, a small heat shock protein, exists as a large hetero-oligomeric complex with an average molecular weight of about 800 kDa [165, 166]. It is composed of two highly homologous subunits αA- and αB-crystallins which share about 55-60% sequence similarity and serve as molecular chaperone by preventing the aggregation of partly unfolded proteins [167-169]. αA-crystallin, only found in the lens, can increase thermal stability of both δ-crystallin and ASL by interaction with partly unfolded ASL and δ-crystallin to form high molecular weight hetero-oligomers [164]. Moreover, it has been shown that α-crystallin can protect ASL activity during freezing and thawing by hydrophobic interactions [170].

The human ASL enzyme and δ-crystallin were evolutionally related proteins. They share about 68.5% and 86.9% amino acid sequence identity and similarity, respectively [171]. Gene sharing of ASL and δ-crystallin has also been demonstrated for birds and reptiles [171]. δ-crystallin is the dominant structural protein in lenses of birds and reptiles but apparently is absent in mammals [161]. Gene duplication has resulted in two tandemly arranged, extremely similar δ-crystallin genes, δ1 and δ2-crystallin. The δ1 and δ2 genes express approximately equal amounts of δ-crystallin mRNA in the lens of duck [172], while δ1 produces most mRNA (90-99%) in lens of chicken that is specialized for its refractive role [173, 174]. ASL activity is only shown in δ2-crystallin but lacking in δ1-crystallin in chicken [175] and duck [176]. The δ2 gene encoding the ASL activity is preferentially expressed in non-eye tissues of chicken and duck. Despite δ1 gene encodes the crystallin protein lacking ASL activity, it is also found in non-transparent tissues outside of the eye in both species [177]. ASL/δ-crystallin, a major soluble protein of transparent eye lens of birds and reptiles, is a mixture of tetramers comprising all possible combinations of two δ1 and δ2 crystallins [177]. It is an enzyme-crystallin with little ASL activity in chicken [171] and pigeon [178] lenses but high enzymatic activity in duck [171, 178, 179], ostrich [180] and goose [181]. Native δ-crystallin is a tetrameric protein with a molecular mass about 200 kDa [160] as is mammalian ASL. The relative amount of ASL activity of the tetramers was related to the relative amount of their δ2 polypeptides. Taken together, ASL plays a dual role both as a catalyst and a structural component [131].

2.1.3.2.5.3 Intragenic complementation at the ASL locus

Intragenic complementation has been observed at the *ASL* gene locus in ASL-deficient cell strains [182-184]. The tetrameric structure of ASL accounts for this phenomenon. On complementation, a hybrid protein produced from the two distinct types of mutant subunits obtains an increase in functional activity that is greater than observed in either mutant alone. As suggested by the crystal structure of ASL, the recovered partial ASL activity may be due to the formation of one or more “native-like” active sites rather than the conformational correction of one mutant monomer by the other [182].

2.1.3.2.5.4 ASL crystal structure

The structures of human ASL [185] and the homologous δ2-crystallin of duck eye lens protein [186] have been determined using X-ray crystallographic techniques. Each monomer, composed of three structural domains, is predominately α helical. Domains 1 and 3 have similar topologies consisting of two helix-turn-helix motifs stacked perpendicularly to each other, whereas the central domain 2 is composed of one small β sheet and nine α helices [154]. Five helices form a helical bundle arranged coaxially in an up-down-up-down-up topology, and three of these five helices from two monomers forming a closely associated dimer are held together by mainly hydrophobic interactions. A tetramer is consisted of two such dimers with one helix of each monomer interacting at the core to form a four-helix bundle.

The three regions of highly conserved residues across the superfamily are spatially removed from one another in the monomer, but they meet together at each of the four “corners” of the tetramer to form four ASL active sites. Each active site of ASL contains residues from three different monomers.

2.1.3.2.6 Arginase1 (ARG1)

Arginase, the terminal enzyme of urea cycle, catalyzes the hydrolysis of arginine to ornithine and urea. The produced ornithine is then transported from cytosol into mitochondria by the ornithine/citrulline transporter (ORNT1). In mammals, it exists as two distinct isoenzymes, arginase1 (ARG1) and arginase2 (ARG2), which are encoded by different genes [187]. Although ARG1 and ARG2 catalyse the same biochemical reaction, they differ in cellular expression, regulation and subcellular localization. The isoform ARG1 (EC 3.5.3.1), known as liver-type arginase, is highly expressed in the liver as one of the cytosolic urea cycle enzymes, whereas ARG2 (kidney-type arginase) is a mitochondrial protein found in a variety of tissues, most prominently in kidney. Human *ARG1* gene, localized on chromosome 6q23 [188], consists of 8 exons encoding a polypeptide of 322 amino acids which demonstrates 58% sequence identity to human ARG2. Recently, it has been found that ARG1 can be highly induced in many tissues and cell types following exposure to a variety of cytokines and other agents [189]. ARG1 is a homotrimer with a molecular weight of 105 kDa. Each 35 kDa subunit contains a binuclear Mn(II) center that is critical for catalytic activity. The overall fold of each subunit belongs to the α/β family, consisting of a parallel, 8 stranded β-sheet flanked on both sides by numerous α-helices [190].

2.1.3.3 Involvement of urea cycle in other pathways

The complete urea cycle occurs only in liver. However some urea cycle enzymes such as ASS and ASL are also expressed in other tissues, where they function to generate important metabolites such as ornithine, citrulline and arginine, which are precursors important for other pathways. As shown in the Fig. 4, the urea cycle is linked with the citrulline-NO cycle by sharing the use of two enzymes ASS and ASL. Arginine, an intermediate of urea cycle, serves also as precursor for synthesis of NO, polyamines, proline, glutamate, creatine and agmatin in arginine metabolism [191]. NO is a short-lived signal molecule which plays diverse roles in cardiovascular, immune and neurological systems involving regulation of smooth muscle contraction, gene transcription, metabolism, and neurotransmission. Polyamines (putrescine, spermidine, and spermine) are ubiquitous small basic molecules with diverse roles in cell growth and proliferation. Polyamines are synthesized from arginine, first converted into agamatine, or from ornithine catalyzed by arginine decarboxylase (ADC) or ornithine decarboxylase (ODC), respectively. Ornithine can also be metabolized by ornithine aminotransferase (OAT) to generate proline, which is an important component of collagen. Creatine, mostly found in muscle, is synthesized from arginine catalyzed by arginine:glycine amidinotransferase (AGAT) and guanidinoacetate methyltransferase (GAMT). Arginine can be recycled from citrulline via ASS and ASL in the citrulline-NO cycle [189].

2.1.3.4 Regulation of the urea cycle

Since the urea cycle enzymes are localized within two distinct subcellular compartments (mitochondria and cytosol) and their genes are divided into different linkage groups, it appears that different mechanisms regulate gene expression (e.g., translational, pre/post-translational, transcriptional) of individual urea cycle genes. It has been demonstrated that the activities of all urea cycle enzymes in rat liver exhibited adaptive responses to changes in dietary protein and hormones [192]. Moreover, it has been shown that changes in mRNA levels for the urea cycle enzymes induced by diet are largely coordinated but these mRNAs differ in their responses to specific hormones [135]. This suggests that regulatory mechanisms for modulating each of the urea cycle enzymes are not identical. In addition, three different mechanisms have been demonstrated for the action of glucagon and

dexamethasone on urea cycle enzymes: stabilization of mRNA with increased transcription for CPS1 and ARG1, increased transcription primarily for ASS and ASL, and enzyme stabilization for OTC [193].

Long-term changes in enzymatic activity are largely due to changes in enzyme mass reflecting alterations in enzyme synthesis rates [135]. In the short term regulation of ureagenesis, it mainly refers to the activation of CPS1, since CPS1 is the first rate-limiting enzyme in urea cycle and is allosterically regulated by NAG. NAG is synthesized from acetyl-CoA and glutamate by NAGS. An autoregulatory control of ureagenesis was observed only at moderate loads of amino acids, and mediated by glutamate effects on NAG synthesis [194]. The remaining urea cycle enzymes are controlled by the concentrations of their substrates.

Hormones such as glucagon, glucocorticoids, and insulin are major regulators of the expression of urea cycle enzymes in liver [189]. Glucagon and glucocorticoids elevate the activities and the mRNA levels in urea cycle enzymes except for OTC, whereas insulin represses CPS1 and ASL [195]. In contrast, the “urea cycle” enzymes expressed in non-hepatic cells are regulated by a wide range of pro- and anti-inflammatory cytokines and other agents [189]. Actually, regulation of these enzymes is mainly transcriptional in all cell types.

To date, the molecular bases for transcriptional regulation such as DNA regulatory elements involved in hormonal regulation of gene expression in hepatic urea cycle enzymes is mainly based on data already described in 1995 [195]. For instance, studies on transcriptional regulation of CPS1 expression revealed that a far upstream -6.3 kb enhance region [196] is necessary and largely sufficient for liver-specific, developmental and hormonal regulation of CPS1 expression [197, 198].

2.2 Urea cycle disorders (UCDs)

2.2.1 UCDs overview

UCDs are a group of inherited inborn errors of nitrogen metabolism resulting in accumulation of ammonia with a high mortality and morbidity. The estimated overall incidence in UCDs is about 1 in 35’000 live births in the United States [199], which may be in fact higher due to underdiagnosis of deceased cases. Hence, UCDs belong to the most common liver-based inborn errors of metabolism (IEMs).

Table 2: Overview on clinical characteristics in urea cycle disorders

Urea cycle Disorder	Phenotype OMIM #	Incidence [199, 200]	Inheritance	Abnormalitities of metabolites	Specific clinical features
NAGS deficiency	237310	< 1:2,000,000	Autosomal recessive	+ Ammonia, - citrulline, - orotic acid in urine	None
CPS1 deficiency	237300	1:62,000	Autosomal recessive	+ Ammonia, + glutamine, - citrulline, - orotic acid in urine	None
OTC deficiency	311250	1:14,000	X-linked	+ Ammonia, + glutamine, + ornithine, - citrulline, + uracil, + orotic acid in urine	None
ASS deficiency = citrullinemia type 1 or classical citrullinemia	215700	1:57,000	Autosomal recessive	+ Ammonium, + citrulline, - arginine, + orotic acid in urine	None
ASL deficiency = argininosuccinic aciduria	207900	1:70,000	Autosomal recessive	+ Ammonia, + citrulline, + argininosuccinate - arginine	Liver disease, fragile hair, hypertension
ARG1 deficiency = hyperargininemia	207800	1:350,000	Autosomal recessive	+ Arginine	Spastic paraplegia
HHH syndrome = hyperornithinemia-hyperammonemia-homocitrullinuria syndrome	238970	< 1:2,000,000	Autosomal recessive	+ Ammonia, + ornithine, + homocitrulline in urine	None
Citrullinemia type 2	603471[a] 605814[b]	1:21,000 (in Japan)	Autosomal recessive	+ Ammonia, + citrulline, - arginine	Cholestasis in neonates

OMIM: Online Mendelian Inheritance in Man; +/- indicates elevated/decreased level in plasma; [a] indicates adult-onset; [b] indicated neonatal-onset

UCDs affect the detoxification of surplus nitrogen leading to hyperammonemia. Six enzymes (NAGS, CPS1, OTC, ASS1, ASL and ARG1) and two mitochondrial transporters (citrin and ORNT1) are involved in the urea cycle. Deficiency caused by gene mutation in any of the enzymes or transporters in this pathway can lead to a UCD corresponding to NAGS deficiency (NAGSD, OMIM #237310), CPS1 deficiency (CPS1, OMIM #237300), OTC deficiency (OTCD, OMIM #311250), ASS1 deficiency (ASS1D or classical citrullinemia or citrullinemia type 1, OMIM #215700), ASL deficiency (ASLD or argininosuccinic aciduria (ASA), OMIM #207900), ARG1 deficiency (ARG1D or hyperargininemia, OMIM #207800), citrullinemia type 2 (OMIM #605814 for late-onset and OMIM #603471 for neonatal-

onset) and the hyperornithinemia-hyperammonemia-homocitrullinuria syndrome (HHH syndrome, OMIM #238970), respectively. All of them are inherited as autosomal recessive disorders except for the X-linked OTC deficiency. An overview on clinical characteristics in UCDs is summarized in Table 2. Although a pedigree with evidence of X-linked transmission suggests a diagnosis of OTCD, these diseases can be distinguished from one another only by appropriate laboratory measurements [131].

Most affected patients present as neonates. But UCDs can manifest at any age with a broad phenotypic variability ranging from asymptomatic to severe life-threatening courses. However the molecular basis and pathology of this variability is not yet fully understood. In addition, the urea cycle is the *de novo* pathway for synthesis of endogenous arginine. Defects in the urea cycle can cause various disorders in other related downstream metabolic pathways. This section will describe the general clinical picture, diagnosis, treatment, and animal models in UCDs as well as the specific disorders with a particular focus on CPS1D and ASLD.

2.2.2 Classification of UCDs

The clinical presentations of patients with UCDs are virtually similar and mainly related to hyperammonemia. The severity of the disease is dependent on the age at onset. Therefore, UCDs are classified as either presenting in the neonatal period (=early onset) or as late onset. However, it should be noted that this classification is an arbitrary division of a continuous spectrum of phenotypic expression.

2.2.2.1 Neonatal UCDs

Neonatal onset UCDs are caused by genetic defects resulting in severe impairment of urea cycle function. Hyperammonemia is the primary cause of neonatal UCDs leading to rapid accumulation of ammonia and other precursor metabolites. Since no effective alternative detoxification pathway for ammonia exists in the newborn period (<30 days of age), disruption of the urea cycle can result in the rapid development of symptoms such as acute cerebral edema with severe neurologic compromise [201, 202]. If undiagnosed and untreated, the neonatal UCDs will cause mental retardation or even early death.

2.2.2.2 Late-onset UCDs

Late-onset UCDs are caused by genetic defects allowing for some partial enzyme or transporter function. Individual UCDs may vary regarding their onset from childhood to adult, and regarding severity from asymptomatic to mild or severe. Often, symptoms in late-onset UCDs occur episodic and related to high protein intake.

2.2.3 Pathogenesis of UCDs

A defect caused by a mutation in any one of the six enzymes and two transporters involved in the urea cycle can result in UCD. The common feature of a UCD is a defect in ammonia elimination in liver, leading to a toxic accumulation of ammonia (hyperammonemia). The toxic effects of ammonia mainly occur in the central nervous system (CNS). Depending on the age of onset as well as the duration and the level of ammonia exposure, these effects can be reversible or irreversible [23]. The pathophysiology of hyperammonemia has been already described above (in section 2.2.1.3). Better understanding the pathophysiology of ammonia toxicity to the brain will allow the development of new strategies for neuroprotection in UCD patients.

Enzymatic defects can occur at all steps of the urea cycle. Patients with residual activity of urea cycle enzyme < 2-5% of normal show an early onset acute clinical course leading to death if not treated [9]. In patients with higher residual activities (5-15% of normal), episodic hyperammonemia may occur at any time during childhood or later. It has been shown that less severe hyperammonemia occurs in ARG1D than in other UCDs [203].

2.2.4 Diagnostic aspects

The UCDs patients are still affected by a poor outcome. To improve both the survival rates as well as the quality of life in surviving patients, the early diagnosis is required. The diagnosis of a UCD is mainly based on evaluation of clinical, biochemical, and molecular genetic data. In other words, diagnosis is made by quantitative plasma and urine amino acids, measurement of orotic acid in urine, enzyme assays and genetic analysis.

2.2.4.1 Clinical features

UCDs can manifest at any age. Infants with UCDs always had a normal pregnancy and postnatal adaption. Typically, they develop the symptoms rapidly after the first 24 hours (h) of life. About the half of affected patients present in the neonatal period. The median age at presentation was two years in a large cohort of UCD patients [204]. Clinical symptoms of UCD patients are mostly associated with hyperammonemia leading to neurological impairments due to the toxicity of ammonia primarily to the CNS. The most common symptoms are unspecific such as decreased level of consciousness, mental retardation, abnormal motor function, and seizures or gastrointestinal such as vomiting, poor feeding, diarrhea, nausea, and failure to thrive. While signs and symptoms of hyperammonemia are highly unspecific, the manifestation can be acute or chronic.

In acute hyperammonemia, the induced cerebral edema can lead to vomiting, seizures, and hyperventilation causing respiratory alkalosis. The neurological impairment can range from mild lethargy to deep coma. Patients with acute liver and multiorgan failure are also reported [205]. Notably, the clinical features in neonatal UCDs resemble a sepsis-like picture, thus bacterial sepsis is a common initial misdiagnosis. Concerning differential diagnosis, neonatal hyperammonemia can also be caused by other inborn errors such as organic acidemias and fatty acid oxidation defects that result in secondary hyperammonemia, or by liver failure or congenital infection [35].

In chronic presentation, hyperammonemia is often less severe. The associated symptoms include confusion, lethargy, dizziness, migraine-like headaches, tremor, ataxia, dysarthria, learning disabilities, neurodevelopmental delay, mental retardation, behavioural changes, vomiting, failure to thrive, protein aversion, hepatomegaly [35]. Symptoms are often triggered by infection, fever, vomiting, high-protein load, trauma, surgery, and several drugs. Some of the patients tend to self-select a vegetarian diet due to protein aversion.

2.2.4.2 Biochemical diagnosis

The laboratory hallmark of a UCD is an elevated concentration of plasma ammonia (> 100-150 µM). Hyperammonemia is always present in neonatal UCD patients. Additionally, respiratory alkalosis is present in about 50% of acute UCDs [206]. However, hyperammonemia may not be as severe in late-onset UCD patients. In the

case of an unexplained change in consciousness, unusual or unexplained neurological impairment, liver failure, or suspected intoxication, ammonia should be measured [35].

Besides ammonia determination, routine laboratory investigations including plasma amino acids, blood acylcarnitines, urinary organic acids and orotic acid are essential [35]. Quantitative plasma amino acid analysis is useful to differentiate among UCDs [202]. For instance, finding of a specific amino acid profile such as argininosuccinate allows the diagnosis of ASLD. In ASS1D and ASLD, citrulline concentration is increased, but absent or decreased in CPS1D, OTCD, or NAGSD. Orotic acid in urine is increased in OTCD but low in CPS1D or NAGSD. Arginine is elevated in ARG1D. Ornithine and urinary homocitrulline are elevated in HHH syndrome. In some UCDs, hepatic dysfunction may be found including elevated liver enzymes, coagulopathy, and histologic changes [207, 208].

2.2.4.3 Enzyme activity assay

When the metabolite profile is not clear-cut, the diagnosis of a specific UCD can still be achieved by enzyme activity analysis for all UCD enzymes by using liver tissue, for ASLD and ARG1D with erythrocytes, for CPS1D and OTCD with intestinal mucosa, and for ASSD and ASLD with fibroblasts [35]. It should be noted that the found enzyme activity does not always correlate with residual activity *in vivo* or with the clinical phenotype due to the excess substrate used in most *in vitro* assays. Moreover, the required invasive sampling such as liver biopsy for mitochondrial UCDs limits its application. Enzymatic testing is regarded as an alternative in patients with negative genetic analysis.

2.2.4.4 Genetic analysis

DNA-sequencing-based genetic analysis provides a confirmatory mean for the diagnosis in all UCDs. The used DNA is generally extracted from blood cells. This is mostly performed by polymerase chain reaction (PCR)-based DNA-sequencing to detect mutations. The sensitivity of DNA-based OTC mutation analysis is only about 80% [209] possibly due to changes in the large intronic sequences of the *OTC* gene. Therefore, array comparative genomic hybridization (aCGH) [210] should be considered if initial DNA sequencing was inconclusive. Recently, it was shown in our

lab that RNA-based gene testing facilitates identification of CPS1 mutations when cultured lymphocytes are stimulated by phytohaemagglutinin [211].

In addition, other effective alternative techniques such as next generation DNA sequencing [212] become available, which may revolutionize future sequencing analysis. Mutation detection in UCDs allows carrier identification, prenatal diagnosis, facilitating pedigree analysis, genetic counselling, and defining genotype-phenotype correlations at least for some cases, which may provide a benefit for future therapies [35] as well as for understanding of their disease-causing role.

2.2.4.5 Prenatal testing

Prenatal testing can be done by molecular genetic studies or by biochemical testing, and it is available for all UCDs. DNA isolated from chorionic villi can be used for prenatal mutation analysis. The carrier status of both parents should be confirmed prior to the prenatal DNA testing. This provides an early, fast and safe method to detect affected fetuses. In the case of no mutation detected in the index patient, biochemical testing for the determination of citrulline and argininosuccinate in the amniotic fluid can be performed for prenatal diagnosis of ASS1D and ASLD, respectively [213]. Additionally, cultured chorionic villus or amniotic fluid cells can also be used by the enzyme analysis for ASS and ASL, respectively [214].

2.2.4.6 Newborn screening (NBS)

Since the early 1960's, newborn screening (NBS) has been applied for metabolic disorders. Initially, it was applied to screen for a single disorder, phenylketonuria (PKU), using a simple bacterial inhibition assays ("Guthrie test"). Usually, the whole blood spots from neonatal heel (between 24h and 72h after birth) are collected on specially designed filter paper (known as Guthrie cards) for NBS tests. In the early 1990's, the development of tandem mass spectrometry (TMS=MS/MS) allowed the additional detection of a variety of disorders of amino acid, organic acid and fatty acid oxidation metabolism by analyzing amino acids and acylcarnitines. TMS provides a powerful technology for the rapid and sensitive measurement in NBS. It becomes an exciting area of preventive medicine.

Some of the expanded NBS programs using TMS in most US states, Europe, Australia, and Taiwan, included the distal UCDs (ASS1D, ASLD and ARG1D) by identifying citrulline, argininosuccinate and arginine, respectively [35]. Proximal UCDs

such as NAGSD, CPS1D and OTCD are not included in NBS panels due to the unreliable results of low citrulline [215]. Moreover, ASLD screening was cancelled in Austria due to the high rate of asymptomatic cases in positive newborns [216], although NBS shows its high sensitivity for ASLD. Thus, it still remains open for the benefit of UCDs from NBS to obtain a rapid diagnosis allowing proper counselling and prospective treatment for the patients' parents [217].

2.2.5 Treatment of UCDs

UCDs patients except for asymptomatic patients need a lifelong treatment when the diagnosis is made. The overall goal of treatment of UCDs is to correct the biochemical abnormalities, and at the same time to maintain the balance between protein restriction and nutritional requirements. The outcome is particularly dependent on the neurological status caused by hyperammonemia at the time of diagnosis and the response to treatment.

2.2.5.1 Acute treatment

The acute treatment of UCDs refers to the emergency management of patients in hyperammonemic crisis. Since the duration of hyperammonemic coma and peak ammonia levels have a strong impact on the neurodevelopmental prognosis, therapy should start immediately. In general, it is based on three interdependent principles [35, 202, 214]: (1) removal of ammonia by dialysis or continuous hemofiltration; (2) reversal of catabolism through caloric supplementation such as infusion of high dose glucose with the use of insulin; (3) alternative detoxification by pharmacologic scavenging of excess nitrogen. These should be carried out in parallel as quickly as possible.

2.2.5.2 Long term therapy

The current strategy for long term therapy of UCDs is a multidisciplinary combination consisting of dietary protein restriction, alternative pathways of nitrogen excretion using nitrogen scavenging drugs, and substitution of essential amino acids and vitamins [35]. In general, severe UCDs patients need to be treated with all above three options, whereas the mild forms of UCDs might not.

Dietary treatment of UCDs aims primarily to avoid the endogenous protein degradation. To keep the balance between the dietary protein intake and

overrestriction in patients is a big challenge. Therefore, supplementation of essential amino acids as well as vitamins is required. Long-term diet adjustment with nutritional monitoring is often necessary in patients with chronic episodes of hyperammonemia. In many chronic UCDs patients, diet alone is not sufficient to maintain the nitrogen homeostasis. Hence, an alternative detoxification [218] is necessary to increase the removal of waste nitrogen by using some compounds such as sodium benzoate, phenylacetate and phenylbutyrate. Benzoate or phenylacetate conjugate with glycine or glutamine in the liver, respectively, and are excreted as a glycine- or glutamine-conjugated form resulting in excretion of one or two molecule(s) of nitrogen [219].

Since the urea cycle is the only pathway for endogenous biosynthesis of arginine, UCDs except for ARG1D cause arginine deficiency. Arginine is the precursor for several other pathways. Deficiency in arginine leads to a catabolic state that stimulates further nitrogen metabolism from protein breakdown. Hence, arginine administration is required in most UCD patients. Alternatively, citrulline supplementation can be used in ASSD patients [220] and is also provided in NAGSD, CPS1D, OTCD, and HHH syndrome [35].

2.2.5.3 Liver transplantation

Liver transplantation has been used in treatment of most UCDs [221] and considered the only available curative therapy for UCDs. Since the long term prognosis of UCD patients is generally poor, liver transplantation becomes an important cure for severe enzyme deficiency. However, the neurological impairment caused by the initial hyperammonemia can not be reserved by this treatment [222]. It is now widely considered first line treatment for newborns with CPS1D or OTCD, in patients who have no response to medical therapy, and in ASLD associated with cirrhosis. It was suggested that liver transplantation should be done in all severe neonatal UCD patients except for NAGSD and ideally performed between 3 and 12 months of age in stable metabolic condition without severe neurological damage and/or recurrent episodes [35]. Additionally, patients with progressive liver disease such as ASLD, with recurrent metabolic decompensations threatening the neurological development, or with poor quality of life are also recommended for liver transplantation [35]. The overall post-transplant UCD patients show similar survival as non-UCD patients. Compared to auxiliary liver transplantation, standard orthotopic liver transplantation is advantageous with fewer complications in most cases [221].

2.2.5.4 Hepatocyte transplantation

Hepatocyte transplantation has been recently proposed as alternative therapeutic option to orthotopic liver transplantation, because the limited availability of donor organs [223-225]. Until 2011, a total of 10 patients with UCDs (6 OTCD, 2 ASS1D, 1 ASLD and 1 CPS1) have been treated with hepatocyte transplantation [225]. Metabolic stabilization was achieved with decreased ammonia levels and increased urea production in most cases. Although hepatocyte transplantation provided a successful bridge to liver transplantation in six patients, metabolic decompensation causing death occurred in two patients after hepatocyte transplantation. Thus, this new therapeutic technique and its efficacy still remain to be investigated in studies before it becomes to a routine treatment.

2.2.5.5 Gene therapy

Many metabolic diseases including UCDs, caused by mutations resulting in the deficiency of a particular enzyme, are compelling candidates for gene therapy. Gene delivery, referred to as “the Achilles heel”, is one of the key challenging in gene therapy. There are several different gene delivery methods to introduce the genetic material into the cells including physical methods (such as electroporation, ultrasound and gene gun), viral vectors (such as adenovirus, retrovirus, and adeno-associated virus (AVV)) and non-viral methods (such as liposomes or nanoparticles as gene carrier). Amongst them, adenoviruses are currently the most promising gene delivery vectors in gene therapy [226].

OCTD is the most common UCD providing an ideal model disease to treat genetic metabolic liver disease including UCDs by liver-targeted gene therapy based on phenotype correction. To date, few gene therapy studies have investigated in OTC-deficient mouse models the use of adenoviral [227], helper-dependent adenoviral [228, 229], AVV [230], recombinant AAV (rAAV) [231, 232], and, more recently, shRNA and rAAV-mediated vectors [233]. Although phenotype correction was reported in OTC-deficient mice [227], ASS-deficient bovine [234] and mice [235] using first generation adenoviral vectors, the rescue is transient due to the cellular immunity to viral antigens [236]. Further studies showed prolonged metabolic correction in OTC- [227, 228] and ASL-deficient [237] mice, but only short-term correction in neonatal ARG1-deficient mice [238] using helper-dependent adenoviral vectors. However, the gene therapy using adenoviral gene transfer was not

successful in a clinical trial of OTC-deficient patients leading to fatal systemic inflammatory response syndrome [239]. Notably, liver targeted gene transfer using AAV-based vectors provide promising efficacy for phenotype correction not only in mouse models [230] but more importantly in human clinical trials [240, 241]. Recently, improved and optimized AAV vectors including self-complementary AAV2/8 vectors expressing mouse Otc or a codon-optimized human OTC showed greatly increased efficacy in treating OTC-deficient mice indicating potential therapeutic effects in OCTD patients [232, 242, 243]. However, the OTC-deficient *spf*^{ash} mouse model has a limitation for gene therapy due to its absence of hyperammonemia, which is the therapeutic goal. Very recently, a shRNA-based rAAV-mediated gene delivery was successfully applied to control severe hyperammonemia in OTC-deficient *spf*^{ash} mouse model, even using vector dosages 5-fold lower than those required to control orotic aciduria [233]. Additionally, AVV-base gene therapy also provides long-term survival of the juvenile lethal ARG1-deficient mouse model [244] and normal cognitive development in hyperargininemic mouse [245]. Although gene therapy has experienced several “ups and downs”, with the development in technology, it will overcome the translational challenges involved in human therapy and might become a standard treatment for genetic disease in the near feature.

2.2.6 Mouse models of UCDs

Mouse models have been established for all six urea cycle enzyme defects [246, 247]. These include OTC-deficient *spf* and *spf*^{ash} mouse models, knockout models for CPS1, ASS, ASL and ARG1, and a salvageable knockout mouse model for NAGS. However, all knockout mouse models of UCDs die in the neonatal period or shortly thereafter without treatment.

2.2.6.1 Salvageable NAGS knockout mouse model

Recently, a biochemically salvageable NAGS knockout mouse model [247] was established. Use of N-carbamyl-L-glutamate (NCG) and citrulline allow rescuing the animals and normal development, apparent health, and reproduction. However, the knockout mice develop severe hyperammonemia and die within 48 h when this rescue intervention interrupts. Moreover, the animals also display elevated plasma glutamine, glutamate, and lysine, and reduced citrulline, arginine, ornithine and proline levels.

2.2.6.2 CPS1 knockout mouse model

In the CPS1-deficient mouse model [248], exon 17 of CPS1 was disrupted because it contains the sequences encoding the most 5'-nucleotide binding domain. CPS1 activity in liver is completely abolished in all knockout mice which die within 36 h of birth due to hyperammonemia.

2.2.6.3 OTC-deficient mouse models

In two available OTC-deficient mouse models, spf (sparse fur) [249] and spf^{ash} (abnormal skin and hair) [250] mice, both affected by a missense mutation, with 5-10% residual OTC activity display several characteristic biochemical hallmarks of OTCD including elevated plasma ammonia and glutamine, decreased plasma arginine and citrulline, and increased urinary orotic acid.

2.2.6.4 ASS1 knockout mouse model

For ASSD (citrullinemia type 1), a naturally occurring bovine model [251] and a knockout mouse model [252] are available. Exon 4 was interrupted in the ASS knockout mouse resulting in death within a few days after birth exhibiting highly elevated plasma citrulline and decreased arginine. Additionally, two spontaneous hypomorphic alleles of the mouse *Ass1* gene was recently described as mouse model of ASSD [253]. Some mutant mice died within the first week after birth, others survived displaying similar symptoms as found in ASSD patients.

2.2.6.5 ASL knockout mouse model

ASL-deficient mouse model was generated by replacement of exons 8 and 9, creating a frameshift in the mRNA beginning with exon 10 [254]. All homozygote mice show deficiency in ASL and ARG1 activity and die within 48 h after birth with elevated plasma ammonia, argininosuccinate, glutamine and citrulline, and decreased plasma arginine. In addition, a conditional hypomorphic mouse model was generated for ASLD [124] by introducing a neomycin selection cassette into intron 9 in the mouse *Asl* gene resulting in 16% residual enzymatic activity. The normal born hypomorphic mice died within 3-4 weeks after birth from multiorgan failure showing similar plasma amino acid profiles as in ASLD patients with elevated citrulline and argininosuccinate,

and reduced arginine. A triple therapy with the combination of sodium benzoate, arginine and sodium nitrite increased the survival and weight gain in these hypomorphic mice.

2.2.6.6 ARG1 knockout mouse model

An ARG1 knockout mouse model is also available for ARG1D [255]. The mouse is born normally and develops hyperammonemia after 10-12 days with only moderate hyperargininemia and markedly reduced ornithine. Symptoms in these mice include decerebrate posture, encephalopathy, and tremors in the extremities all of which are more severe than in human ARG1D patients. This might be due to the decreased level of upregulated kidney ARG2 activity in the knockout mouse which is unable to compensate for a loss of liver ARG1 activity.

2.2.7 Individual disease-specific UCD

UCDs caused by deficiency of individual enzymes or transporters are summarized in Table 2. In this section, the specific enzyme deficiencies (NAGS, CPS1, OTC, ASS1, ASL and ARG1) are described with a focus on CPS1D and ASLD.

2.2.7.1 NAGS deficiency (NAGSD)

NAGSD (OMIM #237310) caused by a defect in NAGS, a very low abundant enzyme which catalyzes the synthesis of NAG from glutamate and acetyl-CoA, is the rarest and most-recently identified UCD [256]. NAGSD manifests similar clinical symptoms and laboratory findings as CPS1D including elevated plasma glutamine, reduced citrulline, and normal urinary orotic acid. Liver enzymatic studies [257] and molecular genetic diagnostics [258] can distinguish these two proximal UCDs. NAGSD presents variable clinical symptoms ranging from early neonatal hyperammonemia to late-onset. The majority of neonatal NAGSD shows < 5% residual enzymatic activity with frequent frameshift or nonsense mutations [258, 259]. It was suggested that the few reported NAGSD patients without detectable deleterious mutations having reduced NAGS activity may not have primary NAGSD, but have a secondary deficiency of NAG due to lacking coenzyme A, acetyl-CoA, L-glutamate, or inhibition of the NAGS reaction [256]. Additionally, the neonatal hyperammonemia in NAGSD can also result from secondary CPS1D, since NAG is the allosteric activator for CPS1. Furthermore, a specific treatment for NAGSD using NCG, a NAG structural analogue, to activate

CPSI is available and approved for use in Europe and the US (Carbaglu®, Orphan Europe) [55, 258-260]. Hence, NAGSD is the only UCD that can be specifically and effectively treated by a drug. Understanding NAGSD may help to better understand the regulation of ureagenesis.

2.2.7.2 CPS1 deficiency (CPS1D)

2.2.7.2.1 Clinical and biochemical findings

CPS1D (OMIM #237300) results from a genetic defect of CPS1 leading to hyperammonemia, which is primary due to mutations in the *CPS1* gene or secondary due to the lack of its allosteric activator NAG caused by mutations in the *NAGS* gene. The estimated incidence of CPS1D is approximately 1 in 62,000 live births [200]. Because CPS1 catalyzes the initial step in the urea cycle, CPS1D manifests with the most severe symptoms of all UCDs. The clinical and biochemical features of CPS1D are indistinguishable from NAGS with identical biochemical alterations: increased plasma ammonia and glutamine, reduced citrulline, and normal urinary orotic acid levels. Thus, enzyme activity or genetic mutation analysis are required for a correct diagnosis of CPS1D. Its clinical symptoms are variable from severe to asymptomatic forms depending on the patients' age at onset and severity of the enzymatic impairment. Like the other neonatal onset forms of UCDs, CPS1D exhibits most severe life-threatening hyperammonemia with a residual enzymatic activity < 5% in newborn infants [131]. A less severe and late-onset form also exists in CPS1D with partial enzymatic activity.

2.2.7.2.2 Treatment

In general, CPS1D patients are treated in the same way as other UCDs including nutritional restriction of protein intake, administration of arginine/citrulline and benzoate/sodium phenylacetate. Liver transplantation is used to treat the severe life-threatening CPS1D patients. Additionally, evidence showed that NCG, an analogue of NAG, with therapeutic effect in NAGSD can also improve metabolic correction in some anecdotal CPS1D patients. Particularly, NCG treatment might be beneficial for CPS1D patients with mutations affecting the affinity for NAG binding [101].

2.2.7.2.3 Mutations and affected functional domains

A total of 222 clinical mutations including missense, nonsense, insertions/deletions (indels), and splice are reported in the *CPS1* gene so far [50] and distributed along the entire coding region. Most mutations are “private” to individual families with little recurrence. Amongst them, single-nucleotide substitutions with missense changes are the vast majority of the mutations followed by small deletions and insertions or duplications, indels, and large deletions. Nonsense mutations generating truncated proteins that lack one or more domains and mutations leading to aberrant proteins are necessarily disease-causing. Findings of the majority of the missense mutations but corresponding to a smaller fraction compared to that of nonsense changes indicate that only a fraction of the missense changes would probably be disease-causing for CPS1D [50]. In addition, the missense mutations are highly unevenly distributed in some *CPS1* exons than in others even after removal of the mutations affecting the CpG islands. This heterogeneous distribution of missense mutations indicates that some enzyme regions are more important than others for enzyme stability, folding and functionality [50]. Thus, mutations affecting these regions would be expected to have disease-causing potential.

Generally, missense mutations are found more frequently in the large subunit-like region of 120 kDa C-terminal moiety including BPSD, CPSD, UFSD and ASD, which performs the functions such as substrate binding, catalysis, and NAG regulation, than in the small subunit-like region of 40 kDa N-terminal moiety including ISD and GSD (see the domain organization in the Fig. 5). Amongst them, BPSD, a key catalytic and substrate binding domain is the most frequent localization of clinical missense mutations (normalized per 100 amino acids) then followed by UFSD. Additionally, three consecutive structural subdomains (A, B, C) in both phosphorylation domains exhibit the highest frequency of missense mutations for the entire proteins. Studies have also been shown the impact of clinical missense mutations affecting BPSD and CPSD on enzyme stability, folding and functionality, and disease-causing nature [101-103].

Interestingly, the peak of highest density of missense mutations is observed at exon 24 and the surrounding exons in the UFSD [50] which connects BPSD and CPSD. Expression studies of the clinical mutations affecting UFSD suggests that this domain has a key integrating role for creating the CPS1 multidomain architecture and is proposed as “integrating domain” [83]. Taken together, these findings indicate that

subdomains including BPSD, UFSD and CPSD occupy a central position in constituting a continuous highly profound region for missense mutations. Moreover, peaks of frequent occurrence of missense mutations found in the regulatory C-terminal ASD reveal the functional importance of CPS1 activity by NAG [50, 101]. There are also clinical mutations observed in the small subunit-like region supporting its functional importance as well [76].

2.2.7.2.4 Recombinant CPS1 expression systems

The main aim of employing expression studies is to determine the enzyme functionality thus to establish the causality of clinical mutations based on the biochemical and structural basis of CPS1D. In other words, establishment of expression systems for functional analysis of CPS1 mutant proteins is required for establishing structural genotype-phenotype relationships. The large size of CPS1 gene, the complex multidomain organization of the enzyme and the lack of a human CPS1 crystal structure all contribute to the difficulty in establishing such relationship. Moreover, it is quite difficult to get an *in vitro-in vivo* correction in those mutant proteins with partial enzymatic activity due to the external and intrinsic factors that can influence the *in vivo* enzyme activity [63]. Further, allelic imbalance may also affect the prognosis of CPS1D [261].

Several expression studies have been shown that the clinical missense mutations associated with CPS1D expressed in bacteria [102] and in insect cells [83, 101, 103], as well as a common single nucleotide polymorphism expressed in yeast (*Schizosaccharomyces pombe*) [76] could provide an effective approach to define the nature of specific amino acid changes. However, the differences between the C-terminal regulatory and N-terminal domains of the bacterial CPS and human CPS1 have limited the application of this model in the investigation of clinical mutations affecting those domains. Furthermore, the recombinant human CPS1 expressed in the baculovirus/insect system show essentially the same kinetic and molecular properties for the natural human enzyme and thus provides a valuable tool to identify disease-causing mutations [83, 103], which might be helpful for diagnosis and prognosis of CPS1D.

There is another powerful tool to study the contributions of CPS1 genetic variants to the wide range of CPS1D phenotypes. This expression system is based on modified BACs (bacterial artificial chromosomes) for eukaryotic episomal

replication, marker expression, and selection [262]. It allows to analyse the mutations located in non-coding regions as well as to test potential splicing and RNA-processing defects. Thus, this expression system appears to provide advantages of using whole-gene constructs to study the effects of sequence variation on gene expression and function.

2.2.7.3 OTC deficiency (OTCD)

OTCD (OMIM #311250) is caused by genetic defect of OTC that catalyzes the formation of citrulline from CP and ornithine. OTCD is the most common of UCDs with an estimated incidence of 1 in 14,000 live births [263]. In contrast to other UCDs, OTCD is the only X-linked UCD with extreme heterogeneity ranging from acute neonatal hyperammonemic coma to asymptomatic adult hemizygous males [113]. Even the late-onset patients affected by the same mutation can present at different ages with diverse clinical courses [264]. This phenotypic heterogeneity might partly be due to the variability in the concentration of a substrate or the ability of the liver to compensate for enhanced degradation of the OTC protein [113]. In general, hemizygous males display the most severe symptoms, while female heterozygotes can have quite variable clinical course [131, 209, 265, 266], which is mostly due to the X-chromosome inactivation in liver [267]. Up to date, more than 400 “private” mutations are identified in OTCD [209]. A “hot spots” of mutation is found in CpG dinucleotides in the *OTC* gene. Approximately 50% of OTCD patients are late-onset with partial OTC activity, while the neonatal patients harbouring no significant residual activity. Besides hyperammonemia as in other UCDs, reduced citrulline and arginine and elevated urinary orotic acid are typical biochemical features in OTCD.

2.2.7.4 ASS deficiency (ASSD, Citrullinemia type 1)

ASSD (OMIM #215700) is caused by a defect in ASS, which catalyzes citrulline and aspartate to form argininosuccinate [121], the immediate precursor of arginine. It is biochemically characterized by an increase of plasma citrulline and urine orotic acid and a decrease of plasma arginine [268]. The clinical manifestation is very heterogeneous from severe to asymptomatic courses. There is no firm correlation between genotypes and phenotypes, neither in biochemical metabolites nor in enzymatic activities. To date, more than 93 mutations including gross

deletions/duplications, have been identified in citrullinemia patients [269]. Amongst them, missense mutations are the most common. Mutations are clustered in the exons and exon-intron boundaries of the *ASS1* gene due to the high rates of mutation detection found in various ethnic groups (>90%) [269-271]. Depending on the ethnic background, highly frequent mutations have been accordingly detected in certain ethnic groups such as Japanese, Korean and Turkish. The treatment strategy for citrullinemia is a combination with nutritional restriction of protein intake and administration of arginine. Generally, the prognosis for classical citrullinemia patients is better than for those with OTCD or CPS1D.

2.2.7.5 ASL deficiency (ASLD, Argininosuccinic aciduria (ASA))

2.2.7.5.1 Clinical and biochemical characteristics

ASA (OMIM #207900) is caused by mutations in the gene encoding ASL, a cytosolic urea cycle enzyme that cleaves argininosuccinate into arginine and fumarate, leading to deficiency of ASL (ASLD). It is the second most common UCD after OTCD with an estimated incidence of 1 in 70,000 live births [200]. The first case of this disease was described by Dr. Allan in 1958 [272].

The clinical presentation of ASA is very variable ranging from severe neonatal-onset to asymptomatic late-onset forms. Patients with severe neonatal-onset ASA typically present hyperammonemia within the first few days of life as in other UCDs, whereas those with late-onset forms can have milder or asymptomatic manifestations with few or no episodic hyperammonemia. Biochemically, it is characterized by elevated plasma ammonia, citrulline and argininosuccinate (the hallmark of ASLD), and reduced arginine levels. Clinical symptoms of ASLD are milder compared to those presented in CPS1D or OTCD, which is mostly due to the excretion of significant amounts of argininosuccinate, a nitrogen rich compound [201, 273]. Surprisingly, the neurocognitive deficits such as mental retardation, behavioural abnormalities, learning disability, intellectual disability, developmental delay etc. are more common in ASLD than in other UCDs [274]. It is also reported that ASLD patients detected by NBS have only biochemical phenotype such as elevated argininosuccinate level in urine or blood, but without any clinical symptoms [216, 275]. There are several unique clinical phenotypes including hepatic disease, trichorrhexis nodosa (coarse and fragile hair) and systemic hypertension in ASA patients.

2.2.7.5.2 Molecular pathogenesis of phenotypic variability

Mutations in the *ASL* gene results in ASLD with wide phenotypic variability, which might be explained by tissue-specific ASL expression [276, 277], genetic heterogeneity at the *ASL* locus [278], intragenic complementation [182-185], residual enzyme activity [141, 279], developmental control of *ASL* gene by DNA methylation [280], and frequent alternative splicing at *ASL* locus [281-283]. In general, there is a poor correlation between enzymatic activity and clinical phenotype in ASA patients. This might partly be due to the instability of the mutant ASL protein in the cell homogenate [157].

As stated above, the complex clinical phenotype observed in ASA patients indicates that the involved mechanisms are beyond the defect in ureagenesis. Very recently, it was shown that ASLD leads to a decrease in NO synthesis in both mice and humans [124]. Interestingly, treatment with liver-targeted gene therapy could not correct the hypertension in ASA mice with decreased NO production [237]. These findings suggest that the tissue specific requirement of ASL for NO production, but not the blockade of ureagenesis, is responsible for some clinical presentations not caused by hyperammonemia such as hypertension in ASA [273].

Moreover, arginine is the precursor not only for urea but also for NO production catalyzed by NOS. Free radicals generated by “uncoupling” of NOS are increased in low arginine substrate availability [284-286]. Indeed, ASA mice show increased free radicals of NOS_3 suggesting the contribution to tissue damage in ASA, since argininosuccinate could be converted into guanidinosuccinic acid, a known cellular and neuronal toxin [287-289].

2.2.7.5.3 Mutations and polymorphisms

To date, 134 mutations spread over the entire *ASL* gene including nonsense, missense, insertions, deletions, and splice are known as well as 160 different genotypes in 223 ASLD patients [290]. Many heterogeneous mutations are associated with ASLD. Most mutations are “private” in individual families with little recurrence. There are three mutations, c.299T>C [290] and c.1153C>T [291] reported only in Finnish patients, while c.1060C>T [290] only identified in Arab patients, indicating a founder effect.

The majority of known mutations are missense changes. Mutations can be found in the entire *ASL* coding region except for exon 1, which comprises only 9 nucleotides. However, exons 3, 4, 6, 7 and 9 carrying 41% of the mutations [290] appear to be mutational hotspots, since they only occupy 25% of the total ASL *cDNA* sequence, while exons 4, 6 and 12 contain functional important residues close to the active site and seem not to be a prefered location for mutation occurrence.

More than 350 polymorphisms have been identified so far across the entire *ASL* gene [290]. Of these, 18 missense changes located in the coding region are considered benign. In addition, more than 280 polymorphisms found in the *ASL* intronic regions allowing for allele tracking which might provide a tool for prenatal diagnostics in the cases of only one known parental mutation [290].

2.2.7.5.4 Treatment

The current therapeutic strategies used in the chronic treatment of ASA are the same as those for other UCDs including dietary restriction and arginine supplementation, which aim to control hyperammonemia, but which are not effective to prevent the neurocognitive deficits, hepatic disease or hypertension in ASA [216, 275]. Recently, high-dose arginine, a hitherto commonly used strategy, was shown to impair the prognosis [292]. As mentioned above, decreased NO production in NOS deficiency is partly responsible for the some clinical manifestations of ASA indicating that NOS-independent NO donor therapy could be beneficial. Treatment with sodium nitrite in ASA mice showed comparable survival to traditional treatment including arginine and sodium benzoate [124]. Further, NO supplementation was successfully used to treat the hypertension in an ASA patient [237]. Although the limited preliminary data in humans, these findings imply NO supplementation therapy in ASA may be beneficial beyond the vascular complications [273].

2.2.7.5.5 Recombinant ASL expression systems

The main goal of employing expression studies is to determine the functional role of *ASL* mutations combined to the structural modelling. Different ASL expression systems have been established in *E. coli* [279, 293, 294], yeast [141, 278], and eukaryotic cells including COS-1 cells [182, 283] and HEK 293T cells [159]. They all provide a useful tool to better understand the molecular basis of ASLD. The existing

expression systems except for HEK 293T cells are mostly used for ASL intragenic complementation analysis between missense mutations. Although ASL mutants were successfully expressed in the bacterial expression system, this system revealed an imperfect correlation of *in-vitro* enzyme activity with clinical phenotype in ASA [279]. HEK 293T cells were used for (co)-expression of truncated ASL transcript variants [159] as well as for expression of clinical variant ASL mutants associated with late-onset and/or mild clinical and biochemical courses (See chapter 2 in manuscripts) to study the role of transcript variants and of the residual activity in the phenotypic variability of ASA. However, none of the presented expression systems can be convincingly used to predict the genotype-phenotype relationships in ASA due to lack of understanding of the mechanisms. Moreover, the catalytic function of ASL depending on its tetrameric confirmation and thus intragenic complementation among specific mutations allowing for residual activity add to the difficulty and complexity for the prediction based on the genotype.

2.2.7.6 ARG1 deficiency (ARG1D, Argininemia)

Argininemia (OMIM #207800) is caused by mutations in the *ARG1* gene leading to deficiency of ARG1 (ARG1D), a liver-type arginase, which hydrolyses arginine into ornithine and urea. ARG1D is the one of the least frequent UCDs with an estimated incidence of 1 in 350,000 live births [200]. Many missense mutations found in ARG1D patients occur in highly conserved regions of the gene [295, 296]. ARG1D is characterized by progressive neurological and intellectual impairment, spasticity, and persistent growth retardation [297]. Additionally, the episodic hyperammonemia occurs less frequently with lower ammonia levels than those observed in other UCDs, which appears to be due to intestinal ureagenesis by ARG2 (kidney-type), encoded by a second arginase locus, to compensate in part for the liver-type ARG1D [298]. Because of the neurotoxicity of hyperargininemia of unknown mechanism in ARG1D, its clinical symptoms are distinct from other UCDs with low plasma arginine levels. Accordingly, long-term investigations on ARG1D patients reveal a correlation between the plasma arginine levels and the severity of the neurological damage [299]. Therefore, dietary supplementation with all essential amino acids other than arginine is a necessary therapy for ARG1D.

2.3 Aims of the study

UCDs manifest at any age with broad clinical spectrum from asymptomatic to severe neonatal courses. This phenomenon exists particularly in ASLD, since an increasing number of ASLD patients with variable and often milder clinical courses are detected by extended NBS. The molecular basis and pathology of this phenotypic variability in UCDs remains to be clarified. It was reported that different tissues exhibited different levels of ASL activity in ASA patients indicating tissue-dependent ASL expression [276, 277]. Moreover, it has been shown that alternative ASL splicing occurs frequently within the *ASL* gene [281-283]. Based on these findings, we hypothesized that ASL transcription expression is tissue-specific and ASL transcript variants contribute to the phenotypic variability in ASA in the first project described below. Further, we hypothesized that relevant residual ASL activity contributes to the phenotypic variability in late-onset ASA in the second project.

In the third project, we wanted to characterize the molecular basis for the only known frequently recurrent *CPS1* mutation, p.Val1013del, found in nine unrelated patients of Turkish descent. The reason to study this was that almost all CPS1 mutations found in CPS1D patients are “private” to individual families, with only very little recurrence [50].

The aims of the first project describing the role of ASL transcript variants in ASA are:

(1) to investigate whether ASL transcription expression is tissue-specific
(2) to identify the most common ASL transcript variants
(3) to illustrate the physiological relevance of transcript variants in ASA
(4) to establish an ASL expression system lacking endogenous ASL activity but allowing for high ectopic ASL expression
(5) to (co)-express diverse recombinant proteins for ASL WT, transcript variants and/or mutant p.E189G
(6) to determine the residual enzyme activity
(7) to predict the effect of single exon deletions on ASL homotetrameric structure

The aims of the second project for the residual ASL activity of variant mutants are:

(1) to express all known variant *ASL* mutants identified in patients associated with late-onset and/or mild clinical and biochemical courses
(2) to determine the residual enzyme activity, kinetic parameters and protein thermostability
(3) to predict the effect of single amino acid substitutions for ASL mutation

The aims of the third project for the only known recurrent CPS1 mutant p.Val1013del:

(1) to establish the CPS1 expression system in baculovirus/insect cells in our lab
(2) to express and purify the recombinant proteins for CPS1 WT and mutant p.V1013del
(3) to determine the global and partial enzyme activities
(4) to determine the protein thermostability
(5) to rationalize the effect of deletion of the Val1013 residue

3 Manuscripts

3.1 Chapter 1

Understanding the Role of Argininosuccinate Lyase Transcript Variants in the Clinical and Biochemical Variability of the Urea Cycle Disorder Argininosuccinic Aciduria

Molecular Bases of Disease:
Understanding the Role of Argininosuccinate Lyase Transcript Variants in the Clinical and Biochemical Variability of the Urea Cycle Disorder Argininosuccinic Aciduria

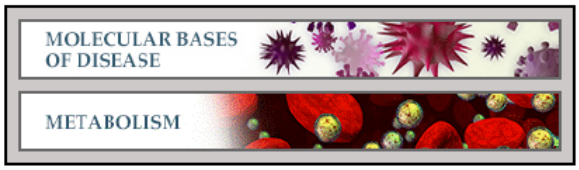

Liyan Hu, Amit V. Pandey, Sandra Eggimann, Véronique Rüfenacht, Dorothea Möslinger, Jean-Marc Nuoffer and Johannes Häberle
J. Biol. Chem. 2013, 288:34599-34611.
doi: 10.1074/jbc.M113.503128 originally published online October 17, 2013

THE JOURNAL OF BIOLOGICAL CHEMISTRY VOL. 288, NO. 48, pp. 34599–34611, November 29, 2013

Understanding the Role of Argininosuccinate Lyase Transcript Variants in the Clinical and Biochemical Variability of the Urea Cycle Disorder Argininosuccinic Aciduria*

Received for publication, July 22, 2013, and in revised form, September 26, 2013 Published, JBC Papers in Press, October 17, 2013, DOI 10.1074/jbc.M113.503128

Liyan Hu[‡§], Amit V. Pandey[¶], Sandra Eggimann[‖], Véronique Rüfenacht[‡§], Dorothea Möslinger[‡‡], Jean-Marc Nuoffer[‖**], and Johannes Häberle[‡§1]**

*From the [‡]Division of Metabolism, University Children's Hospital, 8032 Zurich, Switzerland, [§]Children's Research Center, 8032 Zurich, Switzerland, [¶]Pediatric Endocrinology, Department of Clinical Research, University of Bern, 3010 Bern, Switzerland, the [‖]University Institute of Clinical Chemistry, University of Bern, 3010 Bern, Switzerland, **University Children's Hospital, University of Bern, 3010 Bern, Switzerland, and the [‡‡]Department of Pediatrics and Adolescent Medicine, Medical University of Vienna, 1090 Vienna, Austria*

Background: The role of argininosuccinate lyase (ASL) transcripts in disease variability is unclear.
Results: The most common ASL transcript variants decrease the functional enzymatic activity after co-expression with wild type or mutant ASL.
Conclusion: ASL transcripts expressed at high levels can contribute to the variable phenotype in ASL-deficient patients.
Significance: A new explanation of the molecular basis adds to our understanding of the clinical variability in patients.

Argininosuccinic aciduria (ASA) is an autosomal recessive urea cycle disorder caused by deficiency of argininosuccinate lyase (ASL) with a wide clinical spectrum from asymptomatic to severe hyperammonemic neonatal onset life-threatening courses. We investigated the role of ASL transcript variants in the clinical and biochemical variability of ASA. Recombinant proteins for ASL wild type, mutant p.E189G, and the frequently occurring transcript variants with exon 2 or 7 deletions were (co-)expressed in human embryonic kidney 293T cells. We found that exon 2-deleted ASL forms a stable truncated protein with no relevant activity but a dose-dependent dominant negative effect on enzymatic activity after co-expression with wild type or mutant ASL, whereas exon 7-deleted ASL is unstable but seems to have, nevertheless, a dominant negative effect on mutant ASL. These findings were supported by structural modeling predictions for ASL heterotetramer/homotetramer formation. Illustrating the physiological relevance, the predominant occurrence of exon 7-deleted ASL was found in two patients who were both heterozygous for the ASL mutant p.E189G. Our results suggest that ASL transcripts can contribute to the highly variable phenotype in ASA patients if expressed at high levels. Especially, the exon 2-deleted ASL variant may form a heterotetramer with wild type or mutant ASL, causing markedly reduced ASL activity.

Argininosuccinate lyase (ASL[2]; EC 4.3.2.1; OMIM *608310) catalyzes the reversible hydrolytic cleavage of argininosuccinate into arginine and fumarate and contributes to the removal of waste nitrogen and biosynthesis of arginine within the urea cycle in ureotelic species (1). ASL is also involved in the arginine-citrulline cycle as part of a multiprotein complex required for production of nitric oxide (2) as well as in other pathways (Fig. 1).

The human *ASL* gene is located on chromosome 7q11.21 (3, 4) and comprises 16 exons encoding 464 amino acids (5, 6). The resulting monomers have a predicted molecular mass of ~52 kDa and form a homotetrameric functional enzyme with four active sites (7). ASL has significant homology to δ-crystallin with an amino acid sequence identity of 64–71% between human ASL and various δ-crystallins (8, 9). The δ-crystallins are major structural components of avian and reptilian eye lenses and show significant ASL enzyme activity in duck and chicken (9, 10). Human ASL is expressed predominantly in liver (11) but is also detected in many other tissues, including kidney (12), small intestine (13, 14), pancreas and muscle (15), heart (16), brain (17, 18), skin fibroblasts (19), and erythrocytes (20).

Mutations in the *ASL* gene result in an autosomal recessive disorder known as argininosuccinic aciduria (ASA; synonymous ASL deficiency, ASLD; OMIM number 207900) (21), which is the second most common disorder in the urea cycle, with an estimated incidence of ~1 per 70,000 live births (22). The clinical and biochemical phenotype of ASA is highly variable ranging from asymptomatic cases with only a biochemical phenotype (23–25), some of them diagnosed through newborn screening, to severe neonatal-onset hyperammonemic encephalopathy (26, 27). The molecular basis for the diversity of ASA is not fully understood, and several explanations have been suggested, including tissue-specific ASL expression (27, 28), genetic heterogeneity at the *ASL* locus (29), intragenic comple-

* This work was supported by Swiss National Science Foundation Grants 310030_127184/1 (to J. H.) and 31003A-134926 (to A. V. P.) and a grant from Schweizerische Mobiliar Genossenschaft Jubiläumsstiftung (to A. V. P.).
[1] To whom correspondence should be addressed: University Children's Hospital Zurich, Division of Metabolism, Steinwiesstrasse 75, 8032 Zurich, Switzerland. Tel.: 41-44-266-7342; Fax: 41-44-266-7167; E-mail: Johannes.Haeberle@kispi.uzh.ch.
[2] The abbreviations used are: ASL, argininosuccinate lyase; ASA, argininosuccinic aciduria; EV, empty vector pcDNA3; P-E189G, pcDNA3-ASL-E189G; P-WT, pcDNA3-ASL-WT; ex2del, exon 2-deleted; P-ex2del, pcDNA3-ASL-ex2del; ex7del, exon 7-deleted; P-ex7del, pcDNA3-ASL-ex7del; MD, molecular dynamics; PDB, Protein Data Bank.

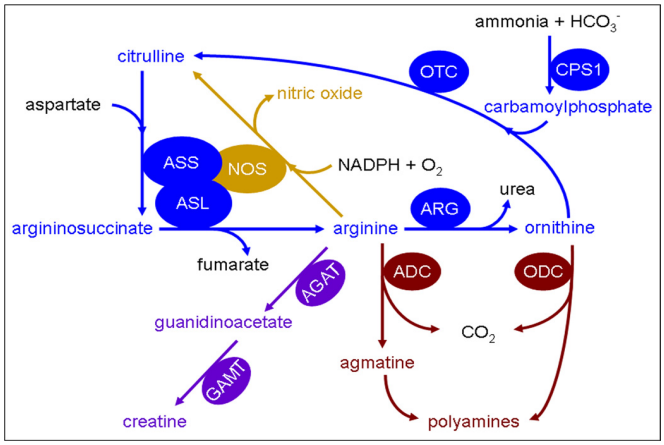

FIGURE 1. **Involvement of argininosuccinate lyase in various metabolic and biochemical pathways.** Shown is a schematic illustration of the involvement of ASL in various metabolic and biochemical reactions. *Colors* are used to show the affiliation of metabolites and enzymes to different pathways: urea cycle (*blue*), nitric oxide synthesis (*gold*), polyamine synthesis (*maroon*), and creatine synthesis (*purple*). Enzymes are depicted in *ovals*: arginine decarboxylase (*ADC*), arginine:glycine amidinotransferase (*AGAT*), arginase (*ARG*); argininosuccinate lyase (*ASL*), argininosuccinate synthetase (*ASS*), carbamoylphosphate synthetase 1 (*CPS1*), guanidinoacetate methyltransferase (*GAMT*), nitric-oxide synthase (*NOS*), ornithine decarboxylase (*ODC*), and ornithine transcarbamylase (*OTC*).

mentation (7, 30–32), different levels of residual ASL activity (33, 34), the developmental control of the *ASL* gene by DNA methylation (35), and alternative splicing events at the *ASL* locus leading to frequent exon deletions (5, 36, 37).

In this study, we explored the role of naturally occurring ASL transcript variants in the formation and function of the ASL homotetramer to better understand the phenotypic variability of ASA. By combining computational structural analysis using molecular dynamic (MD) simulations and eukaryotic (co-)expression of wild type (WT) with the most common transcript variants formed by deletions of exon 2 or 7, we could show that exon 2-deleted (ex2del) or exon 7-deleted (ex7del) ASL has a dominant negative effect on the ASL activity after co-expression with wild type or mutant ASL, respectively. Suggesting a physiological role of transcript variants, RNA analysis revealed a predominant expression of ex7del ASL in two ASA patients identified with heterozygosity for the ASL mutant p.E189G. Taken together, these findings suggest that the frequent occurrence of ASL transcript variants, when they are expressed at high levels, can be a factor contributing to the highly variable clinical and biochemical phenotype of ASA. In particular, the effect may be even more striking in a stable mutant, such as the ex2del ASL variant, because it may form a heterotetramer with ASL wild type or naturally occurring missense mutations (*i.e.* sequence alterations with a disease-causing role found in ASL-deficient patients), contributing to reduced ASL activity.

EXPERIMENTAL PROCEDURES

ASL Transcript Expression in Different Tissues

A panel of cDNAs from 17 different human tissues comprising ASL patient fibroblasts and 16 other tissues (Multiple Tissue cDNA Panel Human I and II, Clontech, Mountain View CA) was used for the amplification of full-length ASL as well as shorter RNA fragments. In addition, short *ASL* cDNA fragments derived from skin fibroblasts of 24 ASA patients with 10 different genotypes were amplified. Specific oligonucleotides ASL-FL-F (5′-acgaggaaccgcccaacat-3′) (forward) and ASL-FL-R (5′-tgcctctccagtccctgactgt-3′) (reverse) were used for amplification of full-length *ASL*; primers ASL-SF-F (5′-acactatccgtgcggccagg-3′) (forward, derived from ASL 5′-UTR sequence) and ASL-SF-R (5′-tgagatgggtcatgcacagcg-3′) (reverse, derived from ASL exon 10 sequence) were used for amplification of a short fragment containing exons 1–9 with a fragment size of 864 bp. Hot start PCR was performed at an annealing temperature of 60 °C (62 °C for primer ASL-SF-F with ASL-SF-R) for 38 cycles (42 cycles for primer ASL-SF-F with ASL-SF-R) using HOT FIREPol® DNA polymerase (Solis Biodyne, Tartu, Estonia) or HotStarTaq DNA Polymerase (Qiagen GmbH, Hilden, Germany) prior to gel electrophoresis. PCR products representing probable splice variants were confirmed by sequencing using the BigDye Terminator cycle sequencing kit version 1.1 (ABI sequence, Applied Biosystems). Patients or their legal guardians had consented to the use of the cultured skin fibroblasts for research purposes when the skin biopsy was taken, and cDNA samples were anonymized prior to their use in this study.

Patient Characteristics and RNA Studies

The 19-year-old male patient, offspring of non-consanguineous parents, was first identified at the age of 13 years with mild hyperammonemia (250 μmol/liter, normal <50), confusion, and irritability during an episode of gastroenteritis. The diagnosis of ASA was made based on characteristic urine metabolites and underlined by typical signs and symptoms such as mild hepatomegaly but normal liver function, trichorrhexis nodosa, cognitive impairment (IQ 67), and a natural avoidance of protein-rich food since early childhood. In addition, there was persistent mild elevation of plasma citrulline (between 80 and 150 μmol/liter, normal <60). Under treatment with L-arginine (150 mg/kg/day) and mild protein restriction, he had been stable since age 13 apart from a single mild metabolic decompensation at age 17 years, again during gastroenteritis with maximum ammonia (230 μmol/liter).

To confirm the diagnosis, DNA sequencing of the *ASL* gene by standard methods (6) as well as array comparative genomic hybridization (38) for exclusion of a deletion on the second allele revealed only a single heterozygous mutation in exon 7 (c.566A→G, p.E189G), which was not present on the maternal allele (also, no other mutation was found in the mother in DNA or RNA), whereas the mutation was found in a heterozygous state in paternal DNA. To identify the second mutant allele, RT-PCR was performed using RNA (PrimeScript II 1st Strand cDNA Synthesis kit, TaKaRa Bio) derived from a 3-day full blood culture treated with phytohemagglutinin and cycloheximide (39). For control RT-PCR, cDNAs derived from lymphocytes, liver, and fibroblasts were used. The patient's cDNA was amplified in full-length ASL as well as in a short fragment comprising exons 1–9, as described above. In addition, primers ASL-SF-F and ASL-SF-R7 (5′-ctccccaggggcaggacattg-3′) (reverse, derived from ASL exon 7 sequence) were used for amplification of a short fragment containing exons 1–7 (fragment size of 670 bp)

to confirm mutation c.566A→G in this transcript. PCR products were sequenced as described above.

In another patient (aged 12 years) with late onset ASA and a similar clinical and biochemical situation, the mutation p.E189G was found in a heterozygous state, and the same DNA and RNA investigations were performed as above. To estimate expression levels of transcripts, densitometry analysis of RT-PCR products on gel electrophoresis and of bands detected by Western blotting was performed by using Carestream Molecular Imaging software (Carestream Health). The genetic studies were done after written informed consent of the patient and his legal guardians was obtained.

Generation of Wild Type, Mutant ASL p.E189G, and Exon 2- or 7-deleted Splice Variant Constructs

Full-length *ASL* cDNA (1395 bp) and ex7del ASL transcript variant (1317 bp) were cut from pCR2.1 carrying the WT *ASL* (33) and pCMV6-XL4 carrying the ex7del ASL cDNA (OriGene, Rockville, MD) using restriction enzymes BamHI and NotI (both from New England Biolabs (Beverly, MA)), respectively. Restriction products were cloned into the expression vector pcDNA3 (Invitrogen), yielding pcDNA3-ASL-WT (P-WT) and pcDNA3-ASL-ex7del (P-ex7del), respectively. Oligonucleotides ASL-ex2del-F (5′-atccggatccatggcctcggaggtggctgaggagtgggcc-3′) (forward, consisting of a BamHI site, the 12 nucleotides of *ASL* exon 1, and 18 nucleotides from 5′ exon 3) and ASL-ex2del-R (5′-cctctagatgcatgctcgagcggccgctatatctaggc-3′) (reverse, with a NotI site added to an ASL 3′-UTR sequence) were used to amplify the exon 2-deleted *ASL* cDNA from P-WT. The obtained PCR product was gel-purified and cloned into the above expression vector, yielding pcDNA3-ASL-ex2del (P-ex2del). The mutant p.E189G (c.566A→G) was constructed as pcDNA3-ASL-E189G (P-E189G) based on P-WT by site-directed mutagenesis (Phusion Site-directed Mutagenesis Kit, Finnzymes (Espoo, Finland)) according to the manufacturer's protocol. All established constructs were confirmed by sequencing as above.

Expression and Co-expression of ASL Constructs in Human Embryonic Kidney 293T Cells

Three different mammalian cell lines (COS-1, HeLa, and 293T) were tested for their background ASL activity before establishing the eukaryotic ASL expression system. ASL expression levels after transfection with P-WT were determined by Western blot. Cells were grown in Dulbecco's modified Eagle's medium + GlutaMAX (DMEM, Invitrogen) supplemented with 10% fetal bovine serum (FBS) and 1% antibiotic/antimycotic solution (both from PAA (Pasching, Austria)) and maintained in an incubator containing 5% CO_2 at 37 °C in a humidified atmosphere.

Based on the lowest ASL background activity, 293T cells were considered as ideal for the ASL expression system in this study. The cells were transiently (48 h) transfected with a total of 7 μg of the construct P-WT, P-ex2del, or P-ex7del in 60-mm dishes using Lipofectamine™ LTX and PLUS™ reagents according to the manufacturer's instructions (Invitrogen). A total of 7 or 10.5 μg of plasmids was used for co-transfection with two or three plasmids; if not indicated otherwise, we used the same amount of the respective constructs (3.5 μg each) in co-transfectants. For the co-transfection of P-WT and P-ex2del at different ratios, 1.75 μg of P-WT and 1.75 μg of P-ex2del was used for the ratio 1:1; 1.75 μg of P-WT and 3.5 of μg P-ex2del for 1:2; 1.75 μg of P-WT and 8.75 μg of P-ex2del for 1:5; 3.5 μg of P-WT and 1.75 μg of P-ex2del for 2:1; and 8.75 μg of P-WT and 1.75 μg of P-ex2del for 5:1. The empty vector (EV) pcDNA3 was used either as negative control or to set up the same amounts of total plasmids for co-transfection.

RNA was isolated from the cells transiently transfected with P-WT, P-ex2del, or P-ex7del, respectively, using the QIAamp RNA blood minikit according to the manufacturer's protocol (Qiagen GmbH, Hilden, Germany). The concentration of nucleic acids was determined by a NanoDrop spectrophotometer. RT-PCR was performed as a standard protocol using primers ASL-SF-F3 (5′-atccacacagccaatgagcgc-3′) (forward, derived from ASL exon 3 sequence) and ASL-SF-R for amplification of a short fragment containing exons 4–9 with a fragment size of 535 bp.

Protein Extraction, Western Blot Analysis, and Immunoprecipitation

Cells were harvested and lysed in Lubrol WX lysis buffer containing 0.15% (w/v) of Lubrol WX (Sigma) and 10 mM Tris-HCl (pH 8.6). Human liver tissue (n = 3, shock-frozen needle biopsy samples for diagnostic purposes in non-ASLD patients after informed consent for scientific use was obtained) was homogenized in complete Nonidet P-40 (Roche Applied Science) lysis buffer containing 1% Nonidet P-40, 50 mM Tris-HCl (pH 8), 125 mM NaCl, 1 mM EDTA, and protease inhibitors (1× Complete EDTA-free + 1 mM of PMSF) (Roche Applied Science) in a prechilled glass grinder by quickly grinding on ice. Cell lysates and liver homogenates were then centrifuged at maximum speed at 4 °C for 15 min. Protein concentrations in the supernatants (equivalent to cell extracts) were determined by the method of Lowry (40) using bovine serum albumin (BSA) as a standard.

Western blotting was performed as described previously (41). 30 μg of total protein of cell extracts was separated by 10% denaturing SDS-PAGE or native PAGE (without SDS in the Laemmli loading buffer and electrophoresis buffer), and subsequently transferred to nitrocellulose transfer membranes (Whatman GmbH, Dassel, Germany). The primary polyclonal antibody anti-ASL (GeneTex, Irvine, CA), recognizing ASL residues 13–261 according to the manufacturer, was used at a dilution of 1:1000, and the horseradish peroxidase (HRP)-conjugated secondary antibody anti-rabbit (Santa Cruz Biotechnology, Inc.) was used at a dilution of 1:5000. Antibodies against β-actin or glyceraldehyde-3-phosphate dehydrogenase (GAPDH) (both from Santa Cruz Biotechnology) served as loading controls. Protein detection was done using ECL reagents (GE Healthcare) for chemiluminescent labeling.

Fibroblasts derived from three ASA patients as well as one control were cultured under the same conditions as for 293T cells. Immunoprecipitation analysis was done as a standard protocol using 5 mg of total protein of fibroblasts, followed by Western blot analysis as described above. HRP-conjugated mouse anti-rabbit IgG (L27A9, Cell Signaling Technology, Inc.

(Danvers, MA)), which does not recognize the denatured and reduced rabbit IgG heavy or light chains on Western blot, was used as secondary antibody at a working dilution of 1:2000.

Measurement of ASL Enzymatic Activity

The ASL enzyme activity was determined spectrophotometrically in cell extracts after transient transfection or co-transfection of P-WT, P-ex2del, and/or P-ex7del, using a coupled assay with arginase and measuring urea production as described before (33). Briefly, 100 μl of 34 mM argininosuccinate (argininosuccinic acid disodium salt hydrate) in water and 100 μl of arginase (50 units) (both from Sigma-Aldrich) in 66.7 mM phosphate buffer (11.1 mM potassium dihydrogenphosphate and 55.6 mM disodium hydrogenphosphate, pH 7.5) were incubated at 37 °C for 5 min. Then 40 μl of cell extract (3–14 μg of total protein) and 10 μl of phosphate buffer were incubated with the above reagents at 37 °C for 30 min. The reaction was stopped by adding perchloric acid at a final concentration of 2%. The ASL enzyme activities are given as mIU/mg total protein. The residual ASL activities of splicing variants were determined as a percentage of ASL-WT or ASL-WT with EV activity (percentage) in each (co-)transfection under the same conditions, respectively. All assays were carried out in triplicate for at least three independent co-transfection experiments.

Structure Modeling

Three-dimensional Protein Model and in Silico Mutagenesis of ASL—The tetrameric three-dimensional structural model of ASL (NCBI NP_000039.2, Uniprot P04424) sequence (amino acids 1–464) was built using the ASL structure (PDB entry 1K62) as template. Model building was performed with the programs YASARA (42) and WHATIF (43). Side chains in newly built parts were optimized by MD simulations. The geometry information for the tetramer was extracted from the original crystallographic data. The final model was refined by a 1000-ps (MD) simulation using an AMBER 2003 force field and checked with the programs WHAT_CHECK (44), WHATIF (43), and Verify3D (45, 46) and Ramachandran plot analysis (47, 48). To create the exon 2 and exon 7 deletions, we first made the FASTA sequence files of modified proteins and performed model building using both the monomer and tetramer structures and performed refinements as described for WT protein. Structures were depicted with PyMOL (Schrödinger, LLC, New York). Structural properties of the proteins were calculated by YASARA and WHATIF, and general protein parameters were calculated with ExPASy protein tools (available from the ExPASy Web site).

Molecular Dynamics Simulation for Model Refinement—The MD simulations were performed using an AMBER03 force field (42). The simulation cell was filled with water, pH was fixed to 7.4, and the AMBER03 (49) electrostatic potentials were evaluated for water molecules in the simulation cell and adjusted by the addition of sodium and chloride ions. The final MD simulations were then run with the AMBER03 force field at 298 K, 0.9% NaCl, and pH 7.4 for 1000 ps to refine the models. The best models were selected for analysis and evaluation of the effect of exon deletions on monomer and tetramer structures.

Statistics

Statistical analyses were done using percentages of ASL-WT activities by one-way analysis of variance with the program GraphPad Prism 4 (GraphPad Software, San Diego, CA) to describe the differences of ASL activities between cells co-expressing ASL-WT with EV and cells co-expressing ASL-WT with the transcript variants. Differences were considered as significant if the p value was <0.05.

RESULTS

Expression of Wild Type ASL and of Transcript Variants in Different Tissues—To investigate whether the expression of *ASL* transcript variants is tissue-dependent and to confirm the reported occurrence of transcripts with deletions of exon 2 or 7 (5, 36, 37), we amplified *ASL* cDNA either in full-length cDNA (data not shown) or in short cDNA fragments comprising exons 1–9 from 17 different human tissues (only 16 tissues shown in Fig. 2*A*) and a series of 24 skin fibroblast cell lines from ASA patients representing 10 different genotypes (Fig. 2*B*). In all tissues, WT *ASL* cDNA (short fragment with 864 bp) could be detected, and in addition, in most tissues shorter transcript variants (786 and 669 bp) could be detected (Fig. 2, *A* and *B*). *ASL*-WT cDNA was predominantly found in liver (Fig. 2*A*, *lane 5*) and kidney (Fig. 2*A*, *lane 7*), but expression was detected in all tissues. Furthermore, a similar expression pattern of ASL transcript variants was detected at a low level in all cDNAs investigated for short fragments (Fig. 2, *A* and *B*). Sequencing analysis of the shorter fragments identified them as exon 2-deleted (669 bp) or exon 7-deleted (786 bp) transcripts.

RNA Studies Reveal Predominant Expression of Exon 7-deleted ASL Transcript Variant in ASA Patients—In RNA from both patients, ASL-ex7del variant (786 bp) was predominantly expressed (Fig. 2, *C* (*lanes 2* and *3*) and *D* (*lane 16*)). Estimation of expression levels by densitometry yielded similar levels of the mutant variant (114% for Fig. 2*C* (*lane 2*) and 83% for Fig. 2*C* (*lane 3*)) when compared with WT ASL (864 bp) in lymphocyte control (Fig. 2*C* (*lane 4*), set to 100%) but much higher levels (330% for Fig. 2*C* (*lane 2*) and 182% for Fig. 2*C* (*lane 3*)) if compared with the full-length band in the same patients (Fig. 2*C* (*lanes 2* and *3*), set to 100%). Notably, the full-length band was expressed much less (34% for Fig. 2*C* (*lane 2*) and 46% for Fig. 2*C* (*lane 3*)) compared with WT in lymphocyte control (Fig. 2*C* (*lane 4*), set to 100%). Expression levels of transcript variants in controls (Fig. 2, *C* (*lane 4*) and *D* (*lanes 1–15*)) and also in the patient's mother (Fig. 2, *C* (*lane 1*) and *D* (*lane 17*)) were much lower in all tissues compared with WT (lymphocytes 9%, liver 6%, and fibroblasts 10%, as shown in Fig. 2*D*, *lanes 1–5*, *6–10*, and *11–15*, respectively). Sequencing confirmed that the variants represented ex2del or ex7del transcripts. To facilitate further sequencing, only a small fragment comprising exons 1–7 was amplified using a reverse primer derived from exon 7. Hereby, the mutation c.566A→G was confirmed in a hemizygous state in one patient (Fig. 2, *C* (*lane 2*) and *E*) and in a heterozygous state in the other patient (Fig. 2, *C* (*lane 3*) and *F*).

Endogenous ASL Expression in Mammalian Cell Lines and in Human Liver—To establish an ASL expression system in mammalian cells lacking endogenous but allowing for high ectopic

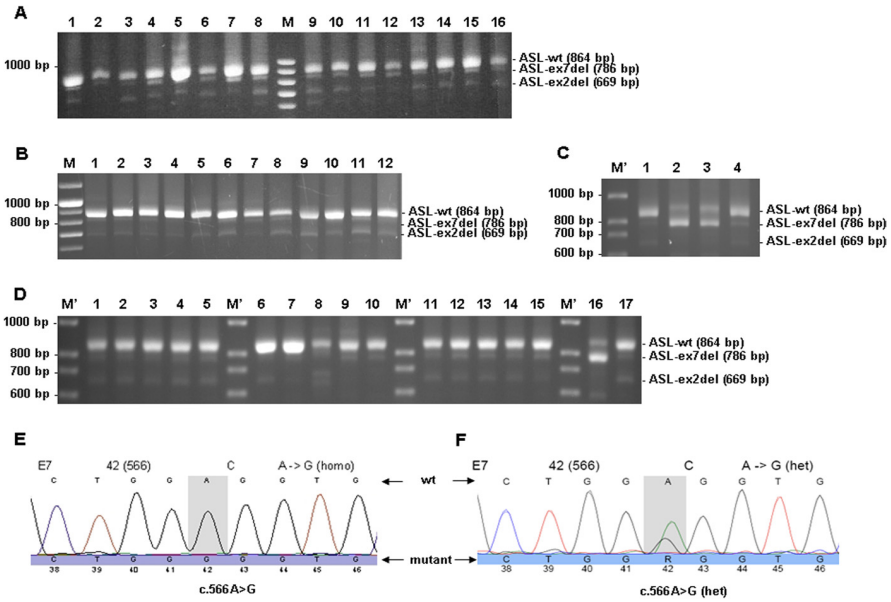

FIGURE 2. **Occurrence of transcript variants of the *ASL* gene in different tissues.** PCR products representing short fragments of *ASL* cDNA from 16 different tissues (*A*), from cultured skin fibroblasts derived from 12 ASA patients (*B*), from lymphocytes derived from two ASA patients and one patient's mother (*C*), and from controls' lymphocytes, livers, and fibroblasts as well as lymphocytes derived from one ASA patient and his mother (*D*). *A*, *lane 1*, skin fibroblast; *lane 2*, brain; *lane 3*, placenta; *lane 4*, lung; *lane 5*, liver; *lane 6*, skeletal muscle; *lane 7*, kidney; *lane 8*, pancreas; *lane 9*, spleen; *lane 10*, thymus; *lane 11*, prostate; *lane 12*, testis; *lane 13*, ovary; *lane 14*, small intestine; *lane 15*, colon; *lane 16*, peripheral leukocytes. *B*, *lanes 1–12* (obtained from three different investigations), skin fibroblasts from 12 ASA patients with 10 different genotypes. *C*, *lane 1*, mother of patient in *lane 2*; *lanes 2* and *3*, two ASA patients; *lane 4*, control. *D*, *lanes 1–15*, five controls' lymphocytes (*lanes 1–5*), livers (*lane 6–10*), and fibroblasts (*lanes 11–15*); *lane 16*, lymphocytes from one patient (same patient as in Fig. 2*C*, *lane 2*); *lane 17*, lymphocytes from mother of patient in *lane 16* (same as in Fig. 2*C*, *lane 1*). *E*, sequencing chromatogram of PCR product from *lane 2* in Fig. 2*C*. *F*, sequencing chromatogram of PCR product from *lane 3* in *C*. *M*, peqGOLD 100-bp DNA ladder plus (Peqlab, Erlangen, Germany); *M'*, 100-bp DNA ladder (Solis BioDyne, Tartu, Estonia). Gel electrophoresis was done in 1% agarose.

ASL expression, we transiently transfected P-WT as well as EV pcDNA3 into COS-1, 293T, and HeLa cells, respectively. Western blot analysis indicated that 293T cells fulfilled the above criteria in an optimal way, whereas COS-1 cells showed endogenous ASL expression and HeLa cells failed to express ASL after transfection (Fig. 3*A*). These results were further confirmed by analysis of ASL activity (ASL endogenous activity in 293T cells shown in Table 1).

Although ASL splice variants (ASL-ex7del and ASL-ex2del) were present in all cDNAs from various tissues (Fig. 2, *A–D*), there was no corresponding signal detected when human liver homogenates from controls were investigated by Western blot analysis (Fig. 3*B*). Likewise, immunoprecipitation did not yield a detectable WT signal when patient and control fibroblasts were used (data not shown). This points toward and is probably explained by the low level of ASL expression in this cell type, which is obviously not suited for further investigation of ASL wild type and mutants on the protein level.

Expression and Co-expression of ASL Wild Type, Mutant, and Transcript Variants in 293T Cells—To study the role of naturally occurring ASL splice variants in wild type as well as in mutant p.E189G, we first introduced diverse ASL recombinant constructs P-WT, P-E189G, P-ex2del, and P-ex7del into 293T cells to (co-)express ASL WT or mutant p.E189G, ex2del, or ex7del ASL, respectively. At the protein level, expression of ASL-WT or ASL-ex2del was detected either as monomers (Fig. 3, *C* (*top*, *lanes 3* and *4*) and *D* (*top*, *lanes 1* and *5*), respectively) or as homotetramer (Fig. 3, *C* (*middle*, *lanes 3* and *4*) and *E* (*top*, *lanes 1* and *5*), respectively). Moreover, ASL-ex2del could also be co-expressed with ASL-WT as well as with mutant p.E189G (Fig. 3, *D–G*). Densitometry analysis of the detectable bands by Western blotting showed that ASL-WT was less expressed in cells co-expressed with transcript variants (71.7% in co-transfectant with ASL-ex2del (Fig. 3*D*, *lane 2*), 88.7% in co-transfectant with ASL-ex7del (Fig. 3*D*, *lane 3*), and 71.2% in co-transfectant with ASL-ex2del and ASL-ex7del in Fig. 3*D* (*lane 4*); all done after normalization according to expressed loading control GAPDH, respectively) compared with co-expression with EV (Fig. 3*D* (*lane 1*), set to 100%). Additionally, ASL-ex2del was expressed at higher levels (55.4, 53.6, 60, or 61%) than ASL-WT (44.6, 46.4, or 40%) or mutant p.E189G (39%) (cells co-transfected with ASL-ex2del and ASL-WT (Fig. 3, *A* (*lanes 2* and *4*) and *G* (*lane 4*)) and cells co-transfected with ASL-ex2del and p.E189G in Fig. 3*G* (*lane 6*)). However, ASL-ex7del was not found (Fig. 3, *C* (*lane 5*), *D*, *E* (*top*, *lane* 6), and *G* (*lane 9*), respectively), although ASL-ex7del-RNA derived from cells transfected with P-ex7del could be detected by RT-PCR (data not shown). These results suggest that deletion of *ASL* exon 2 results in a truncated but stable ASL protein, whereas deletion of *ASL* exon 7 probably leads to an unstable protein.

Structure of ASL Monomers and Homotetramer—To study the structural implications of exon 2 and 7 deletions, we made computational structural models of exon-deleted ASL variants based on known structures of ASL available from the RCSB database. We first performed a PhiBlast search of the PDB database with the modified amino acid sequences to create a custom position-specific scoring matrix that was then used in further runs of PhiBlast searches to identify structurally similar

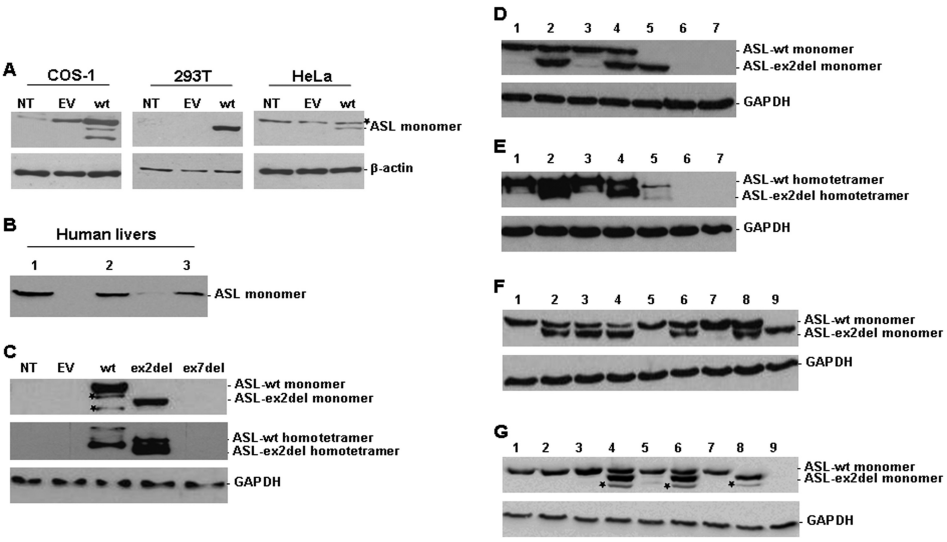

FIGURE 3. **Expression or co-expression of ASL wild type and transcript variants in different mammalian cell lines and human livers.** Western blot analysis of ASL expression in cell extracts of COS-1, 293T, and HeLa cells (*A*); in human livers (*B*); or in transfected 293T cells (*C–G*). 30 μg of total protein was separated by 10% SDS-PAGE (*A*, *B*, *D*, *F*, *G*, and *top panel* in *C*) or by native PAGE (*E* and *middle panel* in *C*) for analyzing ASL expression. *A*, *NT*, non-transfected; *wt*, pcDNA3-ASL-WT (P-WT). *B*, *lanes 1–3*, human liver samples from three controls. *C*, ASL expression in 293T cells non-transfected (*NT*) or transfected with EV, P-WT, pcDNA3-ASL-ex2del (P-ex2del), or pcDNA3-ASL-ex7del (P-ex7del), respectively. *D*, (co-)expression of ASL monomers in 10% SDS-PAGE (ASL-WT, 52 kDa; ASL-ex2del, 45 kDa). *Lane 1*, P-WT with EV; *lane 2*, P-WT with P-ex2del and EV; *lane 3*, P-WT with P-ex7del and EV; *lane 4*, P-WT with P-ex2del and P-ex7del; *lane 5*, P-ex2del; *lane 6*, P-ex7del; *lane 7*, EV. *E*, (co-)expression of ASL homotetramers in 10% native PAGE (ASL-WT, ~200 kDa; ASL-ex2del, ~180 kDa). *Lanes 1–7*, same as in *D*. *Asterisks*, nonspecific bands. *F*, ASL expression in 293T cells co-transfected with P-WT and P-ex2del at different ratios. *Lane 1*, P-WT (1.75 μg); *lane 2*, 1:1; *lane 3*, 1:2; *lane 4*, 1:5; *lane 5*, P-WT (3.5 μg); *lane 6*, 2:1; *lane 7*, P-WT (8.75 μg); *lane 8*, 5:1; *lane 9*, ASl-ex2del (3.5 μg). *G*, (co-)expression of ASL mutant p.E189G (P-E189G) with transcript variants. *Lane 1*, P-WT with EV; *lane 2*, P-E189G with EV; *lane 3*, P-WT with P-E189G; *lane 4*, P-WT with P-ex2del; *lane 5*, P-WT with P-ex7del; *lane 6*, P-E189G with P-ex2del; *lane 7*, P-E189G with P-ex7del; *lane 8*, P-ex2del; *lane 9*, P-ex7del. *Asterisks*, nonspecific bands. β-Actin (42 kDa) and GAPDH (37 kDa) served as loading control.

TABLE 1

Residual ASL activities in 293T cells (co-)transfected with recombinant ASL-WT and transcript variants

Data were obtained under standard conditions (13.6 mM argininosuccinate) after at least three independent experiments. ASL activity in cells (co-)expressing ASL-WT or ASL-WT with EV is set to 100% in each transfection (7 μg of plasmid) or co-transfection (total 10.5 μg of plasmids, each 3.5 μg) under the same condition, respectively. NT, non-transfected cells; EV: empty vector.

293T whole cell extracts	NT	EV	ex2del	ex7del	WT	WT + EV	WT + EV + ex2del	WT + EV + ex7del	WT + ex2del + ex7del	ex2del + ex7del + EV
ASL activity in mIU/mg total protein[a]	1.2 ± 1.9	1.6 ± 2.2	3.2 ± 3.0	1.9 ± 1.4	830.2 ± 78.8	520.1 ± 297.5	307.5 ± 151.4	466.1 ± 232.7	305.3 ± 201.7	3.2 ± 1.5
ASL activity in % of ASL-WT[a]	0.4 ± 0.4	0.3 ± 0.2	0.5 ± 0.4	0.4 ± 0.2	100.0 ± 7.8	100.0 ± 2.6	62.5[b] ± 7.2	94.2 ± 9.4	55.5[b] ± 7.2	0.7 ± 0.3

[a] Mean S.D. (in triplicate).
[b] Significant difference compared with ASL-WT activity ($p < 0.05$).

sequences. Then a secondary structure prediction of the original WT sequence was used to perform the structure-based alignment of the sequences (Fig. 4). Aligned sequences were loaded in the programs YASARA and WHATIF for generating structural models. Some of the loops in exon-deleted sequences were modeled separately by scanning a library of loop databases. For our model building, we used the information available in the PDB_REDO database, which re-refines the old structures in the PDB database using the latest methods based on original structural data deposited in the PDB and corrects the errors in structures found in the PDB database. This is achieved by employing current state of the art refinement methods and software to the older crystallographic data. For the ASL structure (PDB code 1K62), the overall Ramachandran plot appearance improved from −2.514 to −0.803 for the optimized entry, and the total number of bumps/structural clashes was reduced from 150 in the original entry to 54 in the optimized structure, χ-1/χ-2 rotamer normality improved from −2.186 to −0.576, first generation packing quality improved from 0.148 to 0.466, backbone conformation improved from −0.369 to −0.168, and the *R*-free value changed from 0.2290 to 0.1909 in the fully optimized version used by us.

The ASL structure is composed of residues 5–464 of the ASL protein. The enzymatically active ASL tetramer is formed by four identical subunits of ASL, comprising mainly α helices, and contains three structurally distinct domains. Domains 1 and 3 have similar topology and contain two helix-turn-helix motifs, whereas domain 2 has nine helices, of which five helices form the core monomer structure in an up-down-up-down-up sequence (Fig. 5*A*). Two sets of dimers come together in an antiparallel manner to form the tetramer (Figs. 5*A* and 6A). The core of the homotetramer is composed of a four-helix bundle, with each monomeric subunit contributing one helix to the central core, and the tetramer is held together by hydrophobic

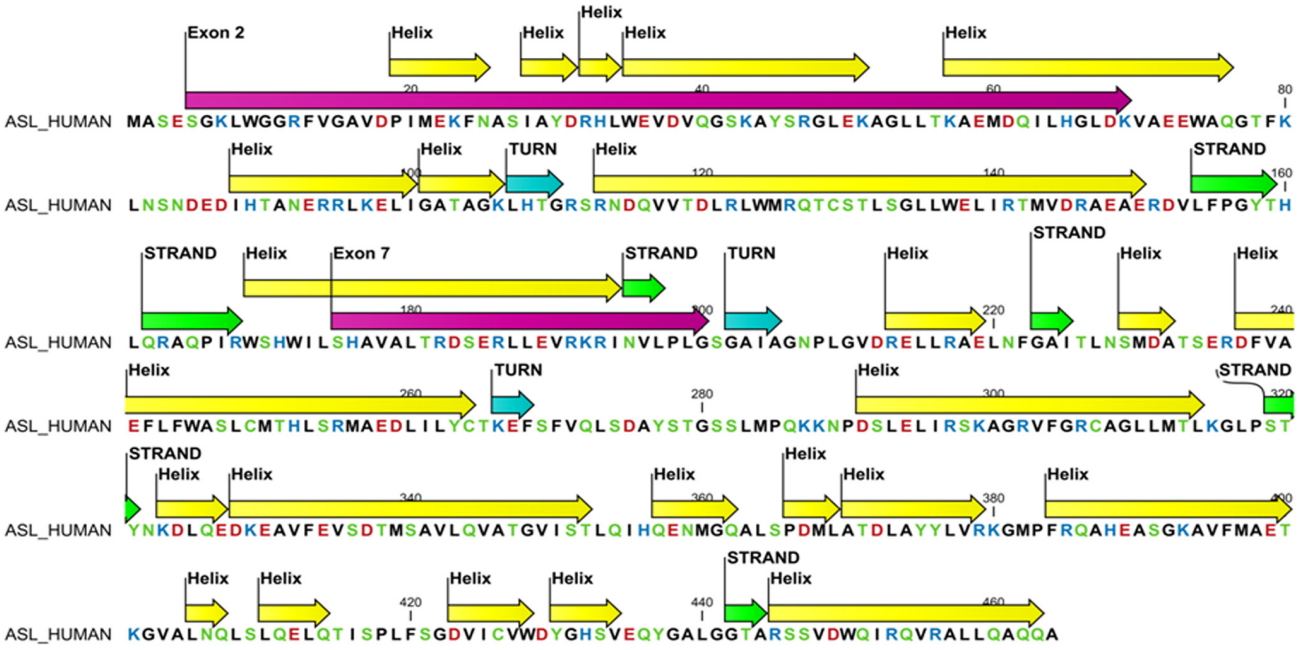

FIGURE 4. **Positions of exons 2 and 7 in secondary structure of the ASL protein.** The helices are in *yellow*, sheets in *green*, and turns in *cyan*; exons 2 and 7 are depicted in *magenta*. Amino acids are *colored* based on their chemical properties with aspartic and glutamic acid in red, arginines and lysines in *blue*, and aromatic amino acids in *green*.

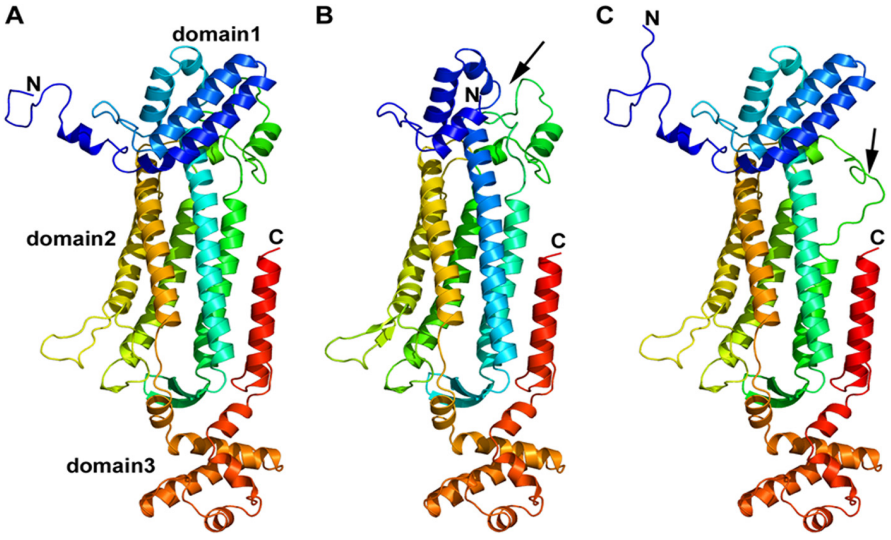

FIGURE 5. **Monomeric structure of wild type and models of ASL exon 2- or exon 7-deleted transcript variant.** *A*, monomeric structure of WT ASL. ASL monomer has three distinct subdomains, domains 1 and 3 have similar structure and topology with two helix-turn-helix motifs in a perpendicular arrangement. Domain 2 has nine helices, and five of them form the central five-helix bundle with up-down-up-down-up topology. *B*, monomeric structural model of ex2del ASL. Two critical helices that are part of domain 1 (indicated by a *black arrow*) and contribute to the active site are missing in the ex2del variant of ASL. *C*, monomeric structural model of ex7del ASL. Exon 7 residues are part of domain 2 in the ASL monomer comprising the central five-helix bundle. Deletion of exon 7 results in a disordered central core with one of the five central helices partially replaced by an unstructured loop (indicated by a *black arrow*). *N*, N terminus; *C*, C terminus.

interactions between the four central helices as well as ionic interactions between arginines and glutamic acid residues on two distinct dimeric structures.

Role of Exon 2 Residues—The amino acid residues contributed by exon 2 (residues 5–69) form the N terminus of the ASL protein (Figs. 4 and 5*A*) and are needed for the enzymatic activity because the previously described R12Q mutation in exon 2 has been shown to result in loss of activity. Two of the helices in domain 2 of ASL monomeric structure are formed by residues from exon 2 and are missing in the ex2del variant of ASL (Fig. 5*B*). Most of the N-terminal chain in the ASL monomer is flexible, and during molecular dynamic simulations, it was found to fluctuate during the whole run, indicating a dynamic arrangement in both the monomeric and tetrameric form. There were

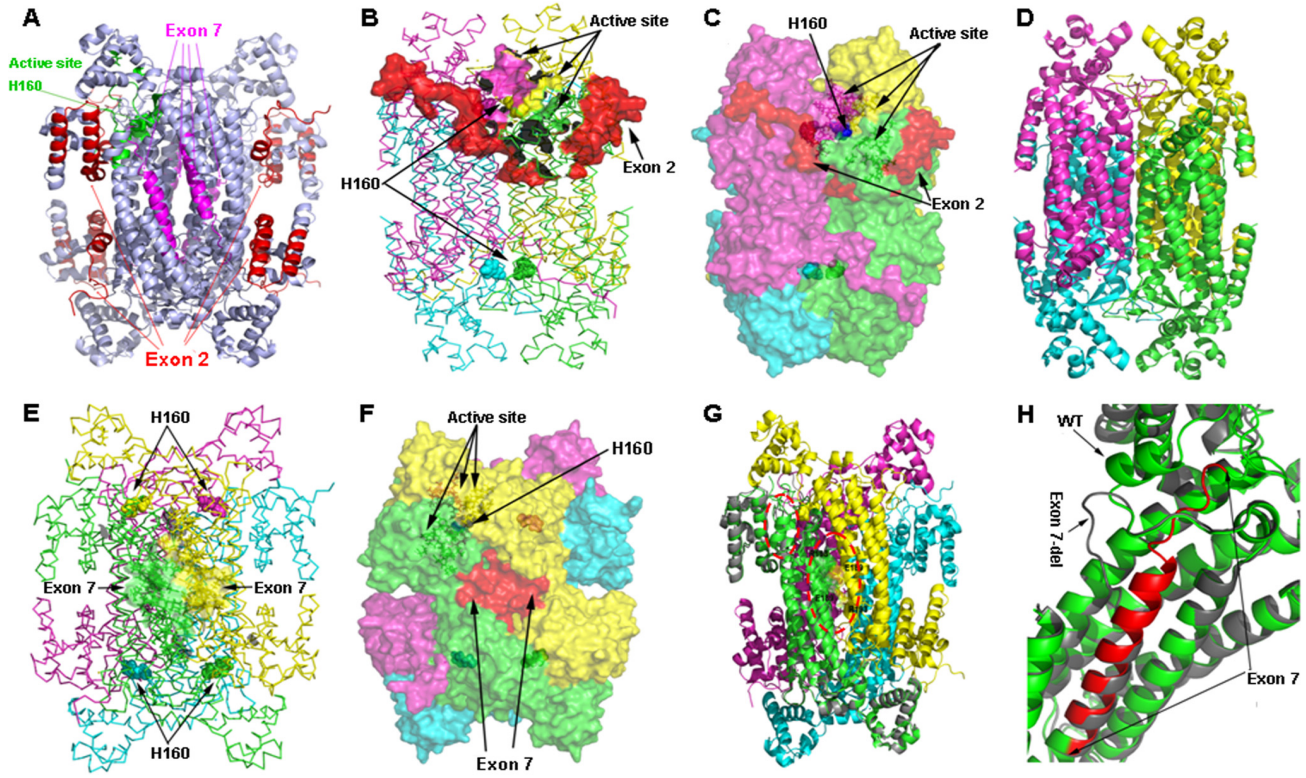

FIGURE 6. **Tetrameric structure of wild type and models of ASL exon 2- or exon 7-deleted transcript variant.** *A*, tetrameric structure of WT ASL showing the positions of active site histidine 160 and exons 2 and 7. The structure is shown as a *ribbon model* in *light blue*; amino acids contributed by exon 2 are *colored* in *red*, whereas amino acids contributed by exon 7 are *colored* in *magenta*. The active site residues are colored in *green* with His-160 at the catalytic center shown a *sphere model*. *B*, location of exon 2 in relation to the active site. In the ASL homotetramer, active site residues are contributed by three different subunits. The ASL structure is shown as a *ribbon model* with different subunits colored in *green*, *cyan*, *magenta*, and *yellow*. The *green* and *cyan* subunits form a dimer and join with another dimer formed by *magenta* and *yellow* subunits to form the tetramer. Active site residues from one of the sites are shown as *solid surfaces*, whereas the catalytic center (His-160) is shown as *spheres*. Residues contributed by exon 2 are shown in *red*. *C*, role of the N terminus tail in stabilizing the active site. The ASL homotetramer is shown as a *solid surface model* with different subunits *colored* in *green*, *cyan*, *magenta*, and *yellow*. Residues contributed by exon 2 are shown in *red*. The N terminus tail surrounds the active site and provides the stability required for binding of substrate. *D*, conjectural prediction of exon 2-deleted ASL based on homology modeling. The core structure of the ASL homotetramer can still be formed in the absence of N terminus residues contributed by exon 2. The model of the ex2del tetrameric complex is similar to the WT ASL, and the central four-helix bundle comprising the tetramer remains intact, resulting in a stable structure. However, the loss of the N terminus required for substrate binding will result in an enzymatically inactive protein. *E*, the WT ASL tetramer structure showing the locations of residues contributed by exon 7. The homotetramer structure is shown as a *ribbon model* with different subunits *colored* in *green*, *cyan*, *magenta*, and *yellow*. The amino acids contributed by exon 7 are shown as *surface models* in two of the adjacent dimeric structures that form the tetramer. Chains shown in *green* and *yellow* are from two different dimers that join together to form the tetramer. The His-160 residue at the catalytic center is shown as *spheres*. *F*, a space-filled surface model of homotetrameric ASL structure showing the role of exon 7 in tetramer formation. Interactions between charged residues on adjacent dimeric ASL subunits stabilize the tetrameric structure. *G*, a structural model of exon 7 deleted variant of ASL transcript. One subunit of the exon 7-deleted variant is superimposed on the WT ASL homotetramer to show the structural differences. The protein is shown as a *ribbon model* with the exon 7-deleted variant *colored* in *gray*, whereas WT subunits in the tetramer are *colored* in *green*, *cyan*, *magenta*, and *yellow*. The residues involved in charge-based interaction located on two adjacent subunits in the WT protein are shown as *sticks* in the *larger oval red dotted box*. The secondary structure elements altered in the exon 7-deleted variant are marked in a *smaller oval box*. *H*, a close-up of the structural changes resulting from the exon 7 deletion. The exon 7-deleted variant (*gray*) and WT (*green*) are superimposed, and residues contributed by exon 7 in the WT protein are shown in *red*. Two of the central helices in the WT protein are altered to flexible loops in the exon 7-deleted variants, resulting in an unstable protein due to the requirement of core helices in domain 2 of the ASL monomers for overall stability. The resultant protein was found to be highly unstable and unlikely to participate in tetramer formation.

few contacts between the N-terminal loops of any individual subunit and other subunits in the tetrameric structure, indicating that it probably does not influence tetramer formation. The role of N terminus residues on the catalytic activity is not clear, but one side of the active site is covered by these residues (Fig. 6, *B* and *C*). The flexible nature of amino acids 5–18 suggests that although exact conformation of the N terminus does not influence the overall tetrameric structure or active site of the enzyme (Fig. 6, *B* and *C*), the structural requirements for substrate binding and retention in the active site may depend on an intact N terminus. Residues 23–32 of the ASL have been proposed to be important for substrate binding (50, 51).

From our computational analysis, we found that exon 2-deleted protein can form a stable monomer (Fig. 5*B*) and homotetramer (Fig. 6*D*), which was confirmed by Western blots showing a smaller sized complex from the cell-based assays (Fig. 3, *C*–*G*). However, such a homotetramer will be devoid of activity due to loss of N-terminal residues needed for substrate binding. Therefore, although an exon 2-deleted transcript of ASL is still capable of expressing a stable monomer that can form a tetrameric complex, the loss of residues involved in catalysis means that such a complex cannot be enzymatically active. It is possible that ASL-WT and ex2del monomers can form heterotetramers with different combinations of the two

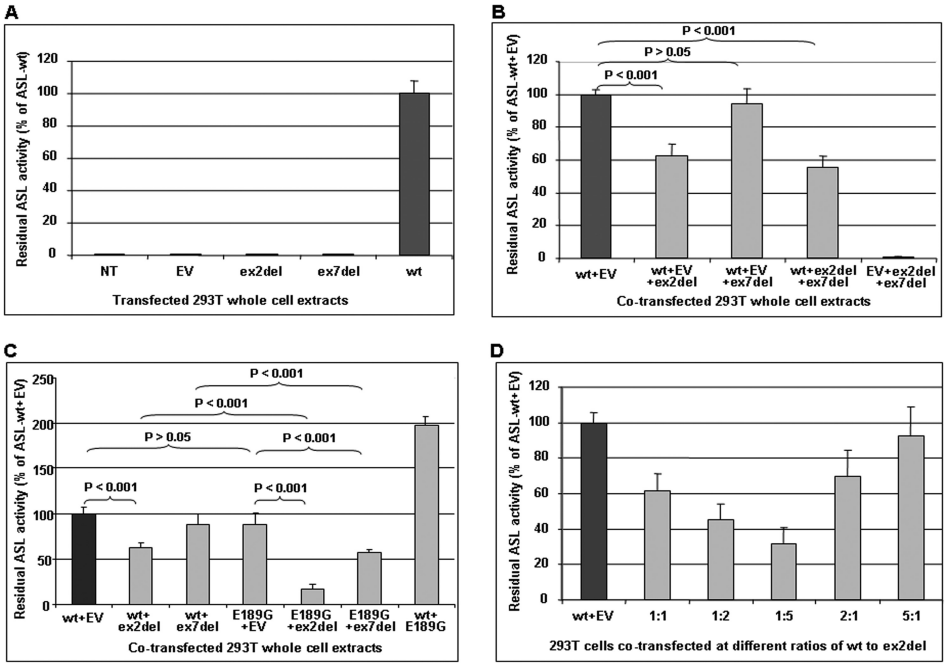

FIGURE 7. **Analysis of recombinant ASL activities.** Shown is ASL enzymatic activity analysis in non-transfected or (co-)transfected 293T cell extracts. Each 4.8–14 μg of total protein of cell extracts was used for the enzyme assay. The residual ASL activities are represented as a percentage of ASL-WT activity (percentage of ASL-WT or of ASL-WT with EV). *A*, 293T cells were transiently transfected with 7 μg of P-WT (*wt*), P-ex2del (ex2del), or P-ex7del (ex7del), respectively. *NT*, non-transfected. Non-transfected cells and those transfected with EV served as negative control. *B*, 293T cells were transiently co-transfected with 10.5 μg of total plasmids at a ratio of 1:1 (each 3.5 μg) of P-WT to P-ex2del or P-ex7del plasmid, respectively. *C*, 293T cells were transiently co-transfected with 7 μg of total plasmids at a ratio of 1:1 (each 3.5 μg) of P-WT to P-ex2del or P-ex7del and of P-E189G to P-ex2del or P-ex7del plasmid, respectively. *D*, ASL enzymatic activity in 293T cell extracts co-transfected with P-WT and P-ex2del at different ratios. 3–12 μg of cell extracts was used for ASL enzyme analysis depending on the amount of P-WT used for the co-transfections. For co-transfections, different ratios of ASL-WT to ex2del splice variant (1:1, 1:2, 1:5, 2:1, or 5:1) were used, respectively. The residual activity of each co-transfectant compared with ASL-WT under the same condition is indicated as a percentage of ASL-WT activity (percentage of ASL-WT co-transfected with EV to use identical amounts of total plasmids and of P-WT for all experiments). EV was used to set up the same amount of total plasmids for the co-transfections. Levels of significance are given as *p* values obtained by one-way analysis of variance using GraphPad software from triplicate measurements of at least three independent experiments, respectively. Differences were considered as significant if the *p* value was <0.05. *Error bars*, S.D.

transcript variants. Because the active site of the ASL protein is formed by contributions from three different monomeric subunits, each unit of exon 2-deleted transcript variants in the heterotetramer will result in loss of one active site, without compromising the overall structure. Because the N-terminal residues affected by deletion of exon 2 do not participate in the formation of ASL dimers, we propose that a combination of WT, ex2del, and WT-ex2del versions of the dimers is generated, which will then further oligomerize to form the tetrameric structures. WT and ex2del variants of the monomers may have a preference for similar sized proteins and only form homodimers, which will result in at least two functional active sites in a 2:2 heterotetramer. Functional data from cell-based assays that show that even a 1:5 combination of WT-ex2del ASL retained about 30% activity (Fig. 7*C*) seem to support this model. A combination of WT-ex2del dimers may also give similar activities.

Role of Exon 7 Residues—Residues 175–200 are contributed by exon 7 in the WT ASL transcript. Exon 7-deleted variant was found to be capable of forming a monomeric structure still composed of three distinct domains, similar to that of WT ASL (Fig. 5*C*). Although the core of the homotetramer of ASL is formed by α helices of monomers formed by residues 291–314, we found ionic interactions between adjacent dimeric subunits in the tetramer to stabilize the structure (Fig. 6, *E* and *F*). From the molecular dynamic simulations and structural analysis, we found that charge pair interactions between Arg-193 on one subunit and Glu-189 and Glu-185 of another adjacent subunit in the tetramer stabilize the structure (Fig. 6*G*). The loss of ionic interactions contributed by exon 7 residues will result in an unstable tetramer. Computational potential energy of WT and ex7del tetramers supported this theory with an increase in potential energy for the ex7del tetramer (−76,378 kJ/mol for ex7del compared with −95,229 kJ/mol for WT) (Table 2). Moreover, a change in core structure of the monomers was also observed with the loss of two central helices and formation of a structurally unstable loop in the middle of the helical core (Figs. 5*C* and 6, *G* and *H*). Such a change is likely to impact the stability of the monomers and may result in an unstable protein that will probably be degraded, especially in the absence of a stable tetrameric complex. Significantly, due to this unstructured loop formation, the accessible surface area of the ex7del variant increased significantly (65,259 Å^2 compared with 53,534 Å^2 for the WT), whereas the solvent-accessible surface remained similar (326,476 Å^3 compared with 322,934 Å^3 for the WT), which further points toward structural instability of ex7del variant (Table 2). This was also further supported by Western blots showing no detectable ASL-ex7del expression (Fig. 3, *C–E* and *G*).

TABLE 2
Computational determination of structural properties of ASL-WT, ASL-ex2del, and ASL-ex7del proteins
Computational parameters were determined with WHATIF and YASARA.

	ASL-WT	ASL-ex2del	ASL-ex7del
Molecular mass	51,658 Da	44,471 Da	48,733 Da
Theoretical pI	6.04	5.90	5.76
Solvent-accessible surface	322,934 Å^3	296,898 Å^3	326,476 Å^3
Accessible surface area	53,534 Å^2	55,904 Å^2	65,259 Å^2
Potential energy	−95,229 kJ/mol	−77,219 kJ/mol	−76,378 kJ/mol
Radius of gyration	36.3 Å	36.1 Å	36.9 Å
Electrostatic solvation energy	−29,769 kJ/mol	−24,454 kJ/mol	−27,781 kJ/mol
Electrostatic potential	−14.89 kJ/mol	−20.4 kJ/mol	−43.07 kJ/mol

Residual ASL Enzymatic Activities in (Co-)transfected 293T Cell Extracts—To determine whether the expressed ASL splice variants have any residual enzyme activity, we performed ASL enzyme activity assays with the cell extracts used for Western blot analysis (summary of data in Table 1, Table 3, and Fig. 7). There was no relevant background activity in cells transfected with the empty vector or non-transfected cells (Fig. 7*A*, *columns 1* and *2*, respectively). No significant residual activity was detected in exon 2- and exon 7-deleted ASL splice variants (Fig. 7*A*, *columns 3* and *4*, respectively), whereas ASL-WT transfection yielded high enzymatic activity (Fig. 7*A*, *column 5*).

To study the effect of ASL splice variants on the function of the ASL homotetramer and the possibility of a heterotetramer formation with reduced ASL activity that may contribute to the biochemical and clinical variability in ASA patients, we measured the ASL activity after co-transfections. The residual ASL activities in cells co-expressing P-WT and P-ex2del (Fig. 7, *B* and *C*, *column 2*) or co-expressing P-WT, P-ex2del, and P-ex7del (Fig. 7*B*, *column 4*) showed a significant decrease to 62.5 ± 7.2 or 55.5 ± 7.2% (mean ± S.D.), respectively, of cells co-transfected with P-WT and EV (Fig. 7, *B* and *C* (*column 1*), and Table 1). Cells co-transfected with P-WT and P-ex7del (Fig. 7, *B* and *C*, *column 3*) displayed no decrease of ASL activity (94.2 ± 9.4% of ASL WT). Cells co-transfected with P-ex2del and P-ex7del (Fig. 7*B*, *column 5*) showed no relevant residual ASL activity. Furthermore, the reduced level of residual ASL activities exhibited no significant difference between cells co-expressing P-WT and P-ex2del and cells co-expressing P-WT, P-ex2del, and P-ex7del (Fig. 7*B*, *column 4*). Interestingly, cells expressing only the ASL mutant P-E189G had a similar level of ASL-WT activity (Fig. 7*C*, *column 4*), but cells co-expressing P-WT and P-E189G showed 2-fold levels of WT activity (Fig. 7*C*, *column 7*). However, the residual activity in cells co-transfected with P-E189G and P-ex2del or co-transfected with P-E189G and P-ex7del (Fig. 7*D*, *column 5* or *6*) exhibited a significant decrease to 16.6 ± 5.3 or 57.5 ± 3.2% (mean ± S.D.), respectively, of cells co-transfected with P-WT and EV (Table 3). These findings indicate that the truncated protein caused by deletion of *ASL* exon 2, although showing no relevant residual activity, has a dominant negative effect on the ASL activity after co-expression with P-WT or P-E189G. In contrast, deletion of exon 7 seems to have no significant effect on ASL-WT activity after co-expression with P-WT, because it probably forms an unstable protein according to Western blot analysis (Fig. 3, *C–E* and *G*) and computational predictions (Figs. 5*C* and 6 (*G* and *H*)), but it nevertheless has a potential dominant negative effect on ASL mutant activity after co-expression with P-E189G (Fig. 7*C*, *column 6*).

In order to further assess whether the negative effect of the simultaneous expression of ex2del mutant on ASL-WT is dose-dependent in *vitro*, we performed transient co-transfections with P-WT and P-ex2del at different ratios (1:1, 1:2, 1:5, 2:1, or 5:1). The co-expression of ASL-WT and ASL-ex2del at the different ratios above could be detected by Western blot analysis (Fig. 3*F*). In cells co-expressing ASL-WT and ASL-ex2del with a higher proportion of mutant DNA, we observed a significant gradual decrease of ASL activity when compared with cells co-expressing WT and EV (Fig. 7*D*). Moreover, cells co-expressing ASL-WT and ASL-ex2del with a higher proportion of WT DNA showed a significant gradual increase of ASL activity (Fig. 7*D*). These findings indicate that the negative effect of ASL-ex2del on the WT activity is dose-dependent.

DISCUSSION

To date, the mechanism of the broad biochemical and clinical heterogeneity in ASA patients still remains to be fully explained because it is not just the result of different genotypes. Possible hypotheses include ASL tissue-specific expression (27, 28), genetic variability (29), intragenic complementation (7, 30–32), the DNA methylation status (35), and the frequent occurrence of alternative splicing variants at the *ASL* locus (5, 36, 37). In addition, several hormones, such as glucocorticosteroids and insulin, influence the regulation of *ASL* mRNA (52). Recently, a complex formation with the enzymes argininosuccinate synthetase and nitric-oxide synthase required for nitric oxide synthesis was described (2), adding further to the complexity of this, obviously not only, urea cycle enzyme. In the present study, we were interested in the tissue dependence of *ASL* transcript variants and their role for the clinical and biochemical phenotype in ASA.

RT-PCR yielded comparable expression levels for the detected transcript variants in 17 different human tissues (Fig. 2), suggesting that the expression of transcript variants is not tissue-dependent. These findings are consistent with earlier reports, in which full-length *ASL* expression was studied in 11 different human tissues (53) and with previous reports on the frequent skipping of exons 2 or 7 (5, 36).

However, it remains pivotal to understand whether the frequent transcript variants in this gene indeed play a role in ASA patients at physiological levels or if they are present at higher concentrations. To do so, we further investigated the expression levels of transcript variants as well as their enzymatic characteristics *in vitro*. Establishment of an ASL expression system in 293T cells (Fig. 3*A*) allowed us to investigate the ASL activities after ectopically expressing or co-expressing ASL-WT and one ASL mutant (p.E189G) and/or splicing variants. Immunoblotting showed non-detectable ASL expression in cells transfected with the ex7del construct (Fig. 3, *C–E* and G), yielding unchanged ASL activity levels after co-expression of ASL-WT and ASL-ex7del (Fig. 7, *B* and *C*, and Table 1) but having a potential dominant negative effect on the ASL mutant activity after co-expression of ASL mutant p.E189G and ASL-ex7del (Fig. 7*C* and Table 3). Moreover, the observation of a 2-fold increase in the ASL activity after co-expressing P-WT and

TABLE 3

Residual ASL activities in 293T cells co-transfected with recombinant ASL-WT, mutant p.E189G, and transcript variants

Data were obtained under standard conditions (13.6 mM argininosuccinate) after three independent experiments. ASL activity in cells co-expressing ASL-WT with EV is set to 100% in each co-transfection (total 7 μg of plasmids, each 3.5 μg) under the same conditions. All measurements were in triplicate.

293T whole cell extracts	WT + EV	WT + ex2del	WT + ex7del	E189G + EV	E189G + ex2del	E189G + ex7del	WT + E189G
Mean ASL activity in mIU/mg total protein (mean ± S.D.)	450.2 ± 38.3	286.1 ± 5.5	363.5 ± 15.0	389.1 ± 30.8	78.4 ± 26.4	257.2 ± 10.5	883.8 ± 80.0
Mean ASL activity in % of ASL-WT + EV (mean ± S.D.)	100.0 ± 7.1	61.9[a] ± 5.8	88.5 ± 11.5	88.4 ± 11.9	16.6[a] ± 5.3	57.5[a] ± 3.2	197.6 ± 8.9

[a] Significant differences compared with ASL-WT activity ($p < 0.05$).

P-E189G (Fig. 7*C*, *column 7*) further supports the view that the negative effect on ASL mutant activity in cells co-transfected with P-E189G and P-ex7del is not caused by the mutant itself. Computational structure modeling revealed that the ex7del variant was capable of forming a monomeric structure with three distinct domains, similar to that of ASL-WT (Fig. 5*C*). As predicted by structural analysis, ex7del may interfere with tetramer formation and seriously impact the stability of the core monomeric structure (Fig. 5), leading to premature degradation of the monomers. This may explain the undetectable ASL-exdel7 monomers after co-expression with ASL-WT or with p.E189G (Fig. 3, *D* and *G*). Nevertheless, the ex7del ASL monomer may still form a heterotetramer with other monomers before degradation occurs, especially with easily accessible mutants, such as p.E189G, which then would result in reduced ASL activity. It should be noted that exon 7 contains 78 bases, allowing formation of an in-frame mutant ASL protein (5). This finding is somewhat different from that of an earlier study (54), in which a small amount of a 49 kDa band in addition to the expected ASL-WT band on Western blots was speculated to be an exon 7 skipping product that may be due to proteolysis (5). However, the details of the possible degradation of ex7del ASL were not investigated in this study.

Although exon 2 skipping was observed in previous studies (29, 36), these authors did not determine the molecular basis and impact of this deletion. As one of the main findings of our investigations, we could show that exon 2-spliced ASL can form a stable truncated protein (Fig. 3, *C–G*), but it lacks any relevant activity (Fig. 7*A* and Table 1). This finding is consistent with our prediction explored by computational structure modeling that exon 2 is in close vicinity to the active site (Fig. 6, *B* and *C*), and its deletion is probably deleterious. Surprisingly, this stable truncated mutant protein has a dominant negative effect on the ASL activity after co-expressing ASL-WT as well as ASL-p.E189G with ASL-ex2del (Fig. 7, *B* and *C*); in the latter case, this was even more relevant. Furthermore, this negative effect is ASL-ex2del DNA dose-dependent (Fig. 7*D*). The reduced ASL activity may result from the formation of a heterotetramic structure between ASL-WT and ASL-ex2del mutant protein as well as homotetrameric ex2del variants that are enzymatically inactive, competing for the substrate, depending on their proportions. Because three different subunits of ASL contribute to the active site in the tetrameric structures, different combinations of WT and ex2del variant subunits may combine to form tetramers with three, two, one, or zero active sites. It is possible that proteins of different size resulting from WT or exon 2-deleted transcripts may have a preference for each other when forming the dimeric units before joining to form tetramers. In such a scenario, only 2:2 versions of the heterotetramers may be the preferred assembly in addition to the fully functional and non-functional molecules with four or zero active sites. Due to a lack of liver samples derived from ASA patients, we could not show whether a different amount of ASL-ex2del mutant protein is expressed in the ASA patients, which may interact with ASL-WT to form a heterotetramer, leading to a different level of residual ASL activity.

Although this study clearly shows that transcript variants under physiological conditions are only present at low concentrations (Fig. 2, *A–D*), the situation was found to be different in two patients affected by late onset ASA (Figs. 1*D* (*lane 16*) and 2*C* (*lanes 2* and *3*)). Both patients were shown to carry the same known *ASL* missense mutation (p.E189G) with low residual ASL activity in red blood cells found in one of the patients (25) and absent activity after bacterial overexpression (33) but significant residual activity in yeast experiments (55). Although the mutation was found in a heterozygous state by genomic DNA sequencing, the level of the ASL-ex7del transcript variant observed by RNA studies was much higher (Fig. 2, *C* (*lanes 2* and *3*) and *D* (*lane 16*)). Under standard PCR conditions (38 cycles), no full-length ASL transcript was amplified, but a faint full-length band was detected after 42 PCR cycles, indicating the low expression of this transcript. Sequencing confirmed the mutation c.566A→G in a hemizygous state in one patient (Fig. 2*E*), suggesting that the ASL WT allele in this particular patient is completely subject to alternative splicing, and hence, no WT transcript is expressed, whereas in the other patient heterozygosity was found (Fig. 2*F*). We suggest here that the high expression level of the ASL-ex7del variant contributed to the ASA phenotype in the patients in addition to the missense mutation. From the finding in these patients, we deduce that the same phenomenon may also play a role in other patients possibly affected by any of the transcript variants (such as patient 16 in Ref. 25 with no mutation found but skipping of exon 5).

In conclusion, this study suggests that transcript variants of *ASL* exist at high frequency in different tissues and play a role in the clinical and biochemical variability in ASA patients in whom they are expressed at high levels. If this occurs with an increased expression level of a stable expressed truncated variant, such as the ASL-ex2del variant, the effect may be even more prominent because the likelihood of stable mutant homo- or heterotetramer formation increases, impairing overall ASL activity. Although the unstable splice variant ASL-ex7del has no effect on ASL-WT activity, it probably shows a dominant negative effect on ASL mutant activity. The findings from this study expand our knowledge of the molecular background in

Role of ASL Transcript Variants in ASA

ASA patients, rendering further studies into transcript variants necessary, especially in patients with no or only single mutations.

Acknowledgments—We acknowledge the technical assistance provided by Dana Leiteritz (Zurich, Switzerland). We thank Drs. C. Giunta and D. Coelho (Zurich, Switzerland) for helpful suggestions during planning of experiments. We also acknowledge Dr. Lee-Jun C. Wong (Baylor College of Medicine, Houston, TX) for performing array comparative genomic hybridization.

REFERENCES

1. Brusilow, S., and Horwich, A. (2001) Urea cycle enzymes. in *The metabolic and molecular bases of inherited disease* (Scriver, C., Beaudet, A., Sly, W., and Valle, D., eds) pp. 1909–1963, 8th Ed., McGraw-Hill, New York
2. Erez, A., Nagamani, S. C., Shchelochkov, O. A., Premkumar, M. H., Campeau, P. M., Chen, Y., Garg, H. K., Li, L., Mian, A., Bertin, T. K., Black, J. O., Zeng, H., Tang, Y., Reddy, A. K., Summar, M., O'Brien, W. E., Harrison, D. G., Mitch, W. E., Marini, J. C., Aschner, J. L., Bryan, N. S., and Lee, B. (2011) Requirement of argininosuccinate lyase for systemic nitric oxide production. *Nat. Med.* **17,** 1619–1626
3. Todd, S., McGill, J. R., McCombs, J. L., Moore, C. M., Weider, I., and Naylor, S. L. (1989) cDNA sequence, interspecies comparison, and gene mapping analysis of argininosuccinate lyase. *Genomics* **4,** 53–59
4. Naylor, S. L., Klebe, R. J., and Shows, T. B. (1978) Argininosuccinic aciduria. Assignment of the argininosuccinate lyase gene to the pter to q22 region of human chromosome 7 by bioautography. *Proc. Natl. Acad. Sci. U.S.A.* **75,** 6159–6162
5. Abramson, R. D., Barbosa, P., Kalumuck, K., and O'Brien, W. E. (1991) Characterization of the human argininosuccinate lyase gene and analysis of exon skipping. *Genomics* **10,** 126–132
6. Linnebank, M., Tschiedel, E., Häberle, J., Linnebank, A., Willenbring, H., Kleijer, W. J., and Koch, H. G. (2002) Argininosuccinate lyase (ASL) deficiency. Mutation analysis in 27 patients and a completed structure of the human ASL gene. *Hum. Genet.* **111,** 350–359
7. Turner, M. A., Simpson, A., McInnes, R. R., and Howell, P. L. (1997) Human argininosuccinate lyase. A structural basis for intragenic complementation. *Proc. Natl. Acad. Sci. U.S.A.* **94,** 9063–9068
8. Matsubasa, T., Takiguchi, M., Amaya, Y., Matsuda, I., and Mori, M. (1989) Structure of the rat argininosuccinate lyase gene. Close similarity to chicken δ-crystallin genes. *Proc. Natl. Acad. Sci. U.S.A.* **86,** 592–596
9. Piatigorsky, J., O'Brien, W. E., Norman, B. L., Kalumuck, K., Wistow, G. J., Borras, T., Nickerson, J. M., and Wawrousek, E. F. (1988) Gene sharing by δ-crystallin and argininosuccinate lyase. *Proc. Natl. Acad. Sci. U.S.A.* **85,** 3479–3483
10. Piatigorsky, J., and Horwitz, J. (1996) Characterization and enzyme activity of argininosuccinate lyase/δ-crystallin of the embryonic duck lens. *Biochim. Biophys. Acta* **1295,** 158–164
11. Ratner, S. (1973) Enzymes of arginine and urea synthesis. *Adv. Enzymol. Relat. Areas Mol. Biol.* **39,** 1–90
12. Ratner, S., and Petrack, B. (1953) The mechanism of arginine synthesis from citrulline in kidney. *J. Biol. Chem.* **200,** 175–185
13. De Jonge, W. J., Dingemanse, M. A., de Boer, P. A., Lamers, W. H., and Moorman, A. F. (1998) Arginine-metabolizing enzymes in the developing rat small intestine. *Pediatr. Res.* **43,** 442–451
14. Flynn, N. E., Meininger, C. J., Kelly, K., Ing, N. H., Morris, S. M., Jr., and Wu, G. (1999) Glucocorticoids mediate the enhanced expression of intestinal type II arginase and argininosuccinate lyase in postweaning pigs. *J. Nutr.* **129,** 799–803
15. Walker, J. B. (1958) Role for pancreas in biosynthesis of creatine. *Proc. Soc. Exp. Biol. Med.* **98,** 7–9
16. Pisarenko, S. I., Minkovskiĭ, E. B., and Studneva, I. M. (1980) [Urea synthesis in the myocardium]. *Biull. Eksp. Biol. Med.* **89,** 165–168
17. Ratner, S., Morell, H., and Carvalho, E. (1960) Enzymes of arginine metabolism in brain. *Arch. Biochem. Biophys.* **91,** 280–289
18. Jones, M. E., Anderson, A. D., Anderson, C., and Hodes, S. (1961) Citrulline synthesis in rat tissues. *Arch. Biochem. Biophys.* **95,** 499–507
19. O'Brien, W. E., and Barr, R. H. (1981) Argininosuccinate lyase. Purification and characterization from human liver. *Biochemistry* **20,** 2056–2060
20. Tomlinson, S., and Westall, R. G. (1964) Argininosuccinic aciduria. Argininosuccinase and arginase in human blood cells. *Clin. Sci.* **26,** 261–269
21. Allan, J. D., Cusworth, D. C., Dent, C. E., and Wilson, V. K. (1958) A disease, probably hereditary characterised by severe mental deficiency and a constant gross abnormality of aminoacid metabolism. *Lancet* **1,** 182–187
22. Brusilow, S. W., and Maestri, N. E. (1996) Urea cycle disorders. Diagnosis, pathophysiology, and therapy. *Adv. Pediatr.* **43,** 127–170
23. Wong, L. T., Hardwick, D. F., Applegarth, D. A., and Davidson, A. G. (1979) Review of metabolic screening program of Children's Hospital, Vancouver, British Columbia. 1971–1977. *Clin. Biochem.* **12,** 167–172
24. Ficicioglu, C., Mandell, R., and Shih, V. E. (2009) Argininosuccinate lyase deficiency. Longterm outcome of 13 patients detected by newborn screening. *Mol. Genet. Metab.* **98,** 273–277
25. Mercimek-Mahmutoglu, S., Moeslinger, D., Häberle, J., Engel, K., Herle, M., Strobl, M. W., Scheibenreiter, S., Muehl, A., and Stöckler-Ipsiroglu, S. (2010) Long-term outcome of patients with argininosuccinate lyase deficiency diagnosed by newborn screening in Austria. *Mol. Genet. Metab.* **100,** 24–28
26. Erez, A., Nagamani, S. C., and Lee, B. (2011) Argininosuccinate lyase deficiency-argininosuccinic aciduria and beyond. *Am. J. Med. Genet. C Semin. Med. Genet.* **157C,** 45–53
27. Glick, N. R., Snodgrass, P. J., and Schafer, I. A. (1976) Neonatal argininosuccinic aciduria with normal brain and kidney but absent liver argininosuccinate lyase activity. *Am. J. Hum. Genet.* **28,** 22–30
28. Perry, T. L., Wirtz, M. L., Kennaway, N. G., Hsia, Y. E., Atienza, F. C., and Uemura, H. S. (1980) Amino acid and enzyme studies of brain and other tissues in an infant with argininosuccinic aciduria. *Clin. Chim. Acta* **105,** 257–267
29. Barbosa, P., Cialkowski, M., and O'Brien, W. E. (1991) Analysis of naturally occurring and site-directed mutations in the argininosuccinate lyase gene. *J. Biol. Chem.* **266,** 5286–5290
30. Howell, P. L., Turner, M. A., Christodoulou, J., Walker, D. C., Craig, H. J., Simard, L. R., Ploder, L., and McInnes, R. R. (1998) Intragenic complementation at the argininosuccinate lyase locus. Reconstruction of the active site. *J. Inherit. Metab. Dis.* **21,** Suppl. 1, 72–85
31. McInnes, R. R., Shih, V., and Chilton, S. (1984) Interallelic complementation in an inborn error of metabolism. Genetic heterogeneity in argininosuccinate lyase deficiency. *Proc. Natl. Acad. Sci. U.S.A.* **81,** 4480–4484
32. Walker, D. C., Christodoulou, J., Craig, H. J., Simard, L. R., Ploder, L., Howell, P. L., and McInnes, R. R. (1997) Intragenic complementation at the human argininosuccinate lyase locus. Identification of the major complementing alleles. *J. Biol. Chem.* **272,** 6777–6783
33. Engel, K., Vuissoz, J. M., Eggimann, S., Groux, M., Berning, C., Hu, L., Klaus, V., Moeslinger, D., Mercimek-Mahmutoglu, S., Stöckler, S., Wermuth, B., Häberle, J., and Nuoffer, J. M. (2012) Bacterial expression of mutant argininosuccinate lyase reveals imperfect correlation of *in-vitro* enzyme activity with clinical phenotype in argininosuccinic aciduria. *J. Inherit. Metab. Dis.* **35,** 133–140
34. Trevisson, E., Burlina, A., Doimo, M., Pertegato, V., Casarin, A., Cesaro, L., Navas, P., Basso, G., Sartori, G., and Salviati, L. (2009) Functional complementation in yeast allows molecular characterization of missense argininosuccinate lyase mutations. *J. Biol. Chem.* **284,** 28926–28934
35. Renouf, S., Fairand, A., and Husson, A. (1998) Developmental control of argininosuccinate lyase gene by methylation. *Biol. Neonate* **73,** 190–197
36. Linnebank, M., Homberger, A., Rapp, B., Winter, C., Marquardt, T., Harms, E., and Koch, H. G. (2000) Two novel mutations (E86A, R113W) in argininosuccinate lyase deficiency and evidence for highly variable splicing of the human argininosuccinate lyase gene. *J. Inherit. Metab. Dis.* **23,** 308–312
37. Walker, D. C., McCloskey, D. A., Simard, L. R., and McInnes, R. R. (1990) Molecular analysis of human argininosuccinate lyase. Mutant characterization and alternative splicing of the coding region. *Proc. Natl. Acad. Sci. U.S.A.* **87,** 9625–9629

38. Landsverk, M. L., Wang, J., Schmitt, E. S., Pursley, A. N., and Wong, L. J. (2011) Utilization of targeted array comparative genomic hybridization, MitoMet, in prenatal diagnosis of metabolic disorders. *Mol. Genet. Metab.* **103,** 148–152
39. Kretz, R., Hu, L., Wettstein, V., Leiteritz, D., and Häberle, J. (2012) Phytohemagglutinin stimulation of lymphocytes improves mutation analysis of carbamoylphosphate synthetase 1. *Mol. Genet. Metab.* **106,** 375–378
40. Lowry, O. H., Rosebrough, N. J., Farr, A. L., and Randall, R. J. (1951) Protein measurement with the Folin phenol reagent. *J. Biol. Chem.* **193,** 265–275
41. Laemmli, U. K. (1970) Cleavage of structural proteins during the assembly of the head of bacteriophage T4. *Nature* **227,** 680–685
42. Krieger, E., Darden, T., Nabuurs, S. B., Finkelstein, A., and Vriend, G. (2004) Making optimal use of empirical energy functions. Force-field parameterization in crystal space. *Proteins* **57,** 678–683
43. Vriend, G. (1990) WHAT IF. A molecular modeling and drug design program. *J. Mol. Graph.* **8,** 52–56, 29
44. Hooft, R. W., Vriend, G., Sander, C., and Abola, E. E. (1996) Errors in protein structures. *Nature* **381,** 272
45. Bowie, J. U., Lüthy, R., and Eisenberg, D. (1991) A method to identify protein sequences that fold into a known three-dimensional structure. *Science* **253,** 164–170
46. Lüthy, R., Bowie, J. U., and Eisenberg, D. (1992) Assessment of protein models with three-dimensional profiles. *Nature* **356,** 83–85
47. Ramachandran, G. N., Ramakrishnan, C., and Sasisekharan, V. (1963) Stereochemistry of polypeptide chain configurations. *J. Mol. Biol.* **7,** 95–99
48. Hooft, R. W., Sander, C., and Vriend, G. (1997) Objectively judging the quality of a protein structure from a Ramachandran plot. *Comput. Appl. Biosci.* **13,** 425–430
49. Liu, H., Elstner, M., Kaxiras, E., Frauenheim, T., Hermans, J., and Yang, W. (2001) Quantum mechanics simulation of protein dynamics on long timescale. *Proteins* **44,** 484–489
50. Vallée, F., Turner, M. A., Lindley, P. L., and Howell, P. L. (1999) Crystal structure of an inactive duck δ II crystallin mutant with bound argininosuccinate. *Biochemistry* **38,** 2425–2434
51. Sampaleanu, L. M., Yu, B., and Howell, P. L. (2002) Mutational analysis of duck δ2 crystallin and the structure of an inactive mutant with bound substrate provide insight into the enzymatic mechanism of argininosuccinate lyase. *J. Biol. Chem.* **277,** 4166–4175
52. Husson, A., Renouf, S., Fairand, A., Buquet, C., Benamar, M., and Vaillant, R. (1990) Expression of argininosuccinate lyase mRNA in foetal hepatocytes. Regulation by glucocorticoids and insulin. *Eur. J. Biochem.* **192,** 677–681
53. Neill, M. A., Aschner, J., Barr, F., and Summar, M. L. (2009) Quantitative RT-PCR comparison of the urea and nitric oxide cycle gene transcripts in adult human tissues. *Mol. Genet. Metab.* **97,** 121–127
54. Simard, L., O'Brien, W. E., and McInnes, R. R. (1986) Argininosuccinate lyase deficiency. Evidence for heterogeneous structural gene mutations by immunoblotting. *Am. J. Hum. Genet.* **39,** 38–51
55. Doimo, M., Trevisson, E., Sartori, G., Burlina, A., and Salviati, L. (2012) Yeast complementation is sufficiently sensitive to detect the residual activity of ASL alleles associated with mild forms of argininosuccinic aciduria. *J. Inherit. Metab. Dis.* **35,** 557–558

3.2 Chapter 2

Variant Forms of the Urea Cycle Disorder Argininosuccinic Aciduria are Caused by Folding Defects of Argininosuccinate Lyase

(Manuscript submitted to *Human Molecular Genetics*, *2014*)

Human Molecular Genetics

Variant forms of the urea cycle disorder argininosuccinic aciduria are caused by folding defects of argininosuccinate lyase

Liyan Hu[1,2], Amit V. Pandey[3], Cécile Balmer[1], Sandra Eggimann[4,5], Véronique Rüfenacht[1,2] Jean-Marc Nuoffer[4,5,*], Johannes Häberle[1,2,*]

[1]Division of Metabolism, University Children's Hospital, 8032 Zurich, Switzerland

[2]Children's Research Center, 8032 Zurich, Switzerland

[3]Pediatric Endocrinology, [5]University Children's Hospital and Department of Clinical Research, University of Bern, 3010 Bern, Switzerland

[4]University Institute of Clinical Chemistry, University of Bern, 3010 Bern, Switzerland

[5]University Children's Hospital, University of Bern, 3010 Bern, Switzerland

[*] These two authors contributed equally to this study.

Corresponding author:
Johannes Häberle, MD
University Children's Hospital Zurich
Division of Metabolism
8032 Zurich, Switzerland
Tel.: +41 44 266 7342
Fax: +41 44 266 7167
Email: Johannes.Haeberle@kispi.uzh.ch

Abstract

Loss of function of the urea cycle enzyme argininosuccinate lyase (ASL) is caused by mutations in the *ASL* gene leading to ASL deficiency (ASLD) with a broad clinical spectrum ranging from life-threatening severe neonatal to asymptomatic forms. Different levels of residual ASL activity probably contribute to the phenotypic variability but reliable expression systems allowing clinically useful conclusions are not yet available. In order to define the molecular characteristics underlying the phenotypic variability, we investigated all *ASL* mutants that were hitherto identified in patients with late onset or mild clinical and biochemical courses by ASL expression in human embryonic kidney 293T cells. We found residual activities >3% of ASL wild type (WT) in nine of eleven ASL mutants. Six ASL mutants (p.Arg95Cys, p.Ile100Thr, p.Val178Met, p.Glu189Gly, p.Val335Leu, and p.Arg379Cys) with residual activities ≥18% of ASL WT showed no significant or less than 2-fold reduced Km values, but displayed thermal instability. Computational structural analysis revealed a multitude of effects ranging from protein instability, disruption of ionic interactions and hydrogen bonds between residues in monomeric form of protein, to disruption of contacts between adjacent monomeric units in the ASL tetramer complex. These findings suggest that variations in residual levels of ASL activity as well as folding defects of mutant ASL proteins contribute to the clinical and biochemical variability of ASLD. Since at least 25% of known ASLD genotypes are affected by folding mutations, ASLD should be considered as a candidate for chaperone treatment to improve mutant protein stability.

Introduction

Argininosuccinate lyase deficiency (ASLD, MIM #207900) is a rare autosomal-recessive urea cycle defect caused by mutations in the *ASL* gene encoding argininosuccinate lyase (ASL, EC 4.3.2.1, MIM *608310). ASL catalyzes the hydrolytic cleavage of argininosuccinate into arginine and fumarate and is, as part of the urea cycle, essential for ammonia detoxification and L-arginine synthesis (1). ASLD is considered the second most common urea cycle disorder (UCD) with an estimated incidence of 1:70’000 live births (1-3).

Biochemically, ASLD is characterised by hyperammonemia, an unspecific finding, and accumulation of argininosuccinic acid in tissues and body fluids (hence the synonymous term argininosuccinic aciduria, ASA), the latter being a specific and

thus diagnostic biochemical marker (4-6). Levels of argininosuccinic acid in blood or urine vary between patients but there is no useful correlation between this marker and the severity of disease.

Clinically, patients with ASLD show a continuum from asymptomatic individuals over mild late onset forms to severe neonatal onset presentations with fatal hyperammonemic encephalopathy within the first few days of life (3). In contrast to most other UCDs, patients with ASLD seem to be affected by mental retardation independent from the occurrence of hyperammonemic decompensations. Other, for UCDs unusual and not fully understood complications of ASLD are the frequent findings of hepatic disease (7, 8) and of arterial hypertension (9) indicating to additional and possibly tissue-specific biological functions of ASL (10). The *ASL* gene is located on chromosome 7cen-q11.2 and comprises 16 coding exons (NM_000048) (11-13). The coding region of 1392 base pairs encodes a polypeptide of 464 amino acids (NP_000039), which forms as active enzyme a cytosolic homotetramer consisting of four subunits of identical molecular weight (~ 52kDa) (14, 15). ASL is ubiquitously expressed in the human body with highest levels in the liver. A sequence on chromosome 22 was previously considered as a pseudogene (11, 12) but later found to encode Ig-λ like mRNA (11). Recently, an *ASL* pseudogene, which includes sequences from intron two to in-tron three, was identified upstream of the human *ASL* gene on chromosome 7 (16). Mutations are spread almost all over the *ASL* gene and have recently been reviewed (17).

Several attempts have been made to accomplish a prognostic marker and improve our understanding of the biochemical and clinical variability of ASLD. Enzymatic assays in erythrocytes (18, 19) or in cultured skin fibroblasts by direct (5) or indirect ASL measurement (20, 21) have proven to be of some prognostic value for selected patients but lacked predictive reliability. Nevertheless, the indirect *ASL* assay by analysis of 14C-citrulline incorporation in intact fibroblasts yielded sufficient sensitivity for detection of residual activities in variant forms of ASLD (11, 21, 22) comprising patients with non-classical ASLD affected by only mild clinical symptoms, slight biochemical abnormalities, but no, or only mild, hyperammonemia.

In addition to measurements in patients' samples, there are some *in vitro* assays investigating naturally occurring *ASL* mutants in bacterial (*E. coli*) (23-25), yeast (26, 27) and eukaryotic (COS1-cells) (28, 29) expression systems. While identification of severely affected ASL proteins was feasible in all of these, there was

overall no satisfying sensitivity for residual ASL activities and hence the predictive value was limited. In order to achieve an improved eukaryotic expression system allowing more sensitive analysis of residual ASL activities, we recently established the measurement of ASL activity in human embryonic kidney 293T cell lysates after transient transfection of *ASL* wild type (WT) and mutants (30).

In the present study, we investigated all naturally occurring *ASL* mutants up till now identified in patients with a variant biochemical or clinical phenotype (17) and aimed to better understand the cause of the broad variation in ASLD phenotypes. We found evidence for thermal instability as well as low expression levels pointing towards a hampered stability due to a folding defect in these mutant ASL proteins. Besides contributing to our understanding of the underlying pathology in ASLD, this finding suggests that novel therapeutic approaches such as chaperone treatment aiming at stabilization of mutant ASL should be pursued with high priority in ASLD.

Material and methods

Patients and choice of *ASL* mutations

In this study, 13 known ASL sequence changes, including the severe mutants p.Gln286Arg (c.857A>G) and p.Arg385Leu (c.1154G>T) as negative controls, were investigated together with WT ASL (Figure 1). Of the total 13 mutations, eleven (p.Arg12Gln (c.35G>A), p.Asp31Asn (c.91G>A), p.Arg95Cys (c.283C>T), p.Ile100Thr (c.299T>C), p.Val178Met (c.532G>A), p.Glu189Gly (c.566A>G), p.Arg193Trp (c.577C>T), p.Val335Leu (c.1003G>T), p.Arg379Cys (c.1135C>T), p.Arg385Cys (c.1153C>T), and p.Arg445Pro (c.1334G>C)) are, according to literature (17), always associated with a variant clinical course, defined as late onset and/or mild clinical and biochemical phenotype. This list of eleven mutations comprises all known base pair substitutions meeting the criteria of a variant change (Table 1). The amino acid substitutions p.Ile100Thr and p.Arg379Cys belong to the two most frequent changes in ASLD that were initially described in Finish patients (11). Notably, the mutations c.1153C>T (p.Arg385Cys) and c.1154G>T (p.Arg385Leu) affect the same amino acid but are reported to result in variant and severe clinical courses, respectively (17).

Construction of recombinant ASL mutants Full-length *ASL* cDNA (1395 bp, RefSeq NM_000048.3) was cloned into the expression vector pcDNA3 (Invitrogen, Carlsbad, CA, USA) at *BamH*I and *Not*I restriction sites yielding pcDNA3-ASL-WT (P-

WT) as described previously (30). The mutant plasmids were constructed based on P-WT by site-directed mutagenesis (Phusion Site-directed mutagenesis Kit, Finnzymes, Espoo, Finland) according to manufacturer's protocol. Oligonucleotide primers designed to achieve the respective point mutations are listed in Supplemental Table 1. PCR products obtained after mutagenesis were subjected to *BamH*I (New England Biolabs, Beverly, MA, USA) digestion and their size compared to P-WT by gel electrophoresis. The PCR products with correct size were then transformed into chemically competent DH5αTM-T1R *E.coli* cells (Invitrogen, Carlsbad, CA, USA) by using the heat shock method and selected by growth on ampicillin-containing (100µg/ml) LB-agar. Screening-PCR with primers T7 forward [5'TAATACGACTCACTATAGGG3'] and Sp6 reverse [5'ATTTAGGTGACACTATAG3'] was used to identify positive clones. Then, mutant plasmids were isolated from *E. coli* and purified by using standard procedures (QIAprep spin column Miniprep Kit, Qiagen, Hombrechtikon, Switzerland). The yielded mutant plasmids (P-mutant) were named as P-R12Q, P-D31N, P-R95C, P-I100T, P-V178M, P-E189G, P-R193W, P-Q286R, P-V335L, P-R379C, P-R385C, P-R385L, and P-R445P. All established constructs were confirmed by sequencing using the BigDye Terminator cycle sequencing kit V.1.1 (Applied Biosystems, ABI sequence).

Expression of ASL constructs in human embryonic kidney 293T cells

We have previously shown that 293T cells were an ideal ASL expression system lacking endogenous ASL but allowing for high ectopic ASL expression (30). Cells were grown, maintained and transiently transfected as described before (30). In brief, 293T cells were grown in Dulbecco's modified Eagle's medium + GlutaMAX (DMEM, Gibco, Paisley, UK) supplemented with 10% fetal bovine serum (FBS) and 1% antibiotic/antimycotic solution (both PAA, Pasching, Austria) and maintained in an incubator containing 5% CO2 at 37oC in a humidified atmosphere. Total 7 µg of plasmid carrying ASL WT or the intended mutations was introduced into the cells in a 60 mm-dish format, using Lipofectamine™ LTX and PLUS™ Reagents (Invitrogen, Basel, Switzerland) according to manufacturer's instructions. The empty vector (EV) pcDNA3 was used as negative control.

Protein extraction and Western blot analysis

Cells were harvested 48 hours post-transfection and lysed in Lubrol WX lysis buffer containing 0.15% (w/v) of Lubrol WX (Sigma Chemical Co., Poole, Dorset, UK) and 10 mM of Tris-HCl (pH 8.6) for 1 hour on ice. Cell lysates were then centrifuged at maximum speed at 4^{o}C for 15 min. Protein concentrations in the supernatants (cell extracts) were determined by Bradford assay (31) using bovine serum albumin as standard. Western blotting was performed as previously described (32). Cell extracts (30 µg total protein) were separated by 10% denaturing sodium dodecyl sulfate-polyacrylamide gel electrophoresis (SDS-PAGE) and subsequently transferred to nitrocellulose transfer membranes (Whatman GmbH, Dassel, Germany). The primary polyclonal antibody anti-ASL (GeneTex, Irvine CA, USA), recognizing ASL residues 13 to 261 according to the manufacturer, was used at a dilution of 1:1000 and the horseradish peroxidase (HRP)-conjugated secondary antibody anti-rabbit (Santa Cruz Biotechnology, Santa Cruz CA, USA) was used at a dilution of 1:5000. Antibodies against glyceraldehyde-3-phosphate dehydrogenase (GAPDH) (Santa Cruz Biotechnology) served as loading control. ECL reagents (GE Healthcare, Glattbrugg, Switzerland) were used for chemiluminescent labelling to detect protein. To estimate expression levels of recombinant ASL mutants, densitometry analysis of bands detected by Western blotting was performed by using Carestream Molecular Imaging software (Carestream Health, Germany).

ASL enzymatic activity assay, kinetic study and thermal stability assay

The ASL enzymatic activity was determined spectrophotometrically in cell extracts after three independent transient transfections of P-WT or P-mutants, using a coupled assay with arginase and measuring urea production as described before (23). In short, 100 µl of 34 mM argininosuccinate (argininosuccinic acid disodium salt hydrate) in water and 100 µl arginase (50 units) (both Sigma-Aldrich, Buchs, Switzerland) in 66.7 mM phosphate buffer (11.1 mM potassium dihydrogenphosphate and 55.6 mM disodium hydrogenphosphate, pH 7.5) were incubated at 37oC for 5 min. Then 40 µl of cell extract (6 µg of total protein diluted in albumin buffer yielding 0.15 mg/ml of concentration for WT and all mutants except for p.Arg95Cys, in which we adapted protein quantity to 0.65 mg/ml according to low expression levels) and 10 µl phosphate buffer were incubated with the above reagents at 37oC for 30 min. The reaction was stopped by adding perchloric acid at a final concentration of 2%. In this assay, the measured extinctions are corrected with the extinctions of a blank

containing all the reagents and cells as well as perchloric acid before the reaction started. The ASL enzyme activities are given as mIU/mg total protein indicating nmol of urea production/min/mg total protein and normalized according to the expressed ASL protein levels by densitometry analysis using GAPDH as control. The residual activities of ASL mutants are determined as percentage of ASL WT under same conditions in triple measurements, respectively.

Kinetic studies and thermal stability assays were performed for ASL WT and mutants (p.Arg95Cys, p.Ile100Thr, p.Val178Met, p.Glu189Gly, p.Val335Leu and p.Arg379Cys) with residual ASL activities ≥18% of ASL WT. The measured enzymatic activities were normalized according to the expressed ASL protein levels by densitometry using GAPDH as control. The kinetic parameters were determined by Michaelis-Menten analysis at 10 different argininosuccinate concentrations (0.045, 0.068, 0.136, 0.272, 0.544, 0.907, 1.813, 3.4, 6.8 and 13.6 mM) after curve fitting using GraphPad Prism 4 (GraphPad Software, San Diego, CA, USA). For ASL thermal stability assay all ASL proteins were diluted at 0.15 mg/ml in albumin buffer (pH 7.4) and heated at different temperatures for 30 min in a PCR machine, and then immediately cooled down to 0oC on ice followed by measuring ASL enzymatic activity as above (incubation temperatures in °C for WT: 37, 42, 47, 52, 54, 56, 57; mutant p.Arg95Cys: 37, 40, 43, 45, 47, 49, 51; mutants p.Ile100Thr, p.Glu189Gly and p.Val178Met: 37, 42, 47, 48.5, 50, 51.5, 53; mutant p.Val335Leu: 37, 40, 42, 44, 46, 47, 48, 50; mutant p.Arg379Cys: 37, 42, 47, 48, 48.5, 50, 51, 51.5, 53). The mutant protein p.Arg95Cys, which is expressed less efficient and exhibited only low enzyme activity, was diluted at 0.65 mg/ml. The value V_{50} (^{o}C) indicating the temperature at which 50% of protein is inactivated, was determined by Boltzmann sigmoidal curve fitting of the data using GraphPad Prism 4 (GraphPad Software). All assays were carried out in triplicate using cell lysates from the same transfection experiment.

Structure Models of ASL mutants

3D protein model and in-silico mutagenesis of ASL

The tetrameric 3D structural model of ASL (NCBI NP_000039.2, Uniprot P04424) sequence (AA 1-464) was built using the ASL structure (PDB 1K62) as described previously (30). Model building was performed with programs YASARA (33) and WHATIF (34). Side chains were optimized by molecular dynamic (MD) simulations. The geometry information for the tetramer assembly was extracted from the original

crystallographic data. The final model was refined by a 1000 ps (MD) simulation using AMBER 2003 force field and checked with the programs WHAT_CHECK (35), WHATIF (34), Verify3D (36, 37), and Ramachandran plot analysis (38, 39). Information about the residues located at the argininosuccinic acid binding pocket was extracted from the duck crystallin structure (PDB 1DCN) (40) using the program SiteEngines (41, 42). Structures were depicted with Pymol (www.pymol.org) and rendered as ray-traced images using the program POV-RAY (www.povray.org). Structural properties of the proteins were calculated by YASARA and WHATIF and general protein parameters were calculated with Expasy protein tools (www.expasy.ch).

Molecular Dynamics simulation for model refinement

The MD simulations were performed using AMBER03 force field as described previously (33, 43). The simulation cell was filled with water, pH was fixed to 7.4 and the electrostatic potentials were evaluated for water molecules in the simulation cell and adjusted by addition of sodium and chloride ions. The final MD simulations were then run with AMBER03 force field at 298K, 0.9% NaCl and pH 7.4 for 1000 ps to refine the models. Best models were selected for analysis and evaluation of the effect of mutations on monomer and tetramer structures.

Predicting the effect of mutants on protein stability using site directed mutator (SDM)

The SDM tool (44) (45) was used for predicting the effect of mutants on ASL protein stability. SDM software uses environment-specific substitution frequencies within homologous protein families to calculate a stability score. The mutant structures used for analysis were generated using the program ANDANTE (46). SDM provides a pseudo delta G score for prediction of protein stability.

RNA structure and stability prediction

RNA structure and stability prediction was performed using the program RNAsnp (47). A cutoff p value of 0.2 was used for predicting the effect on RNA stability. Both the global as well as local effects were evaluated for predicting the changes in the RNA structure upon mutations. The minimum free energy structures of the WT and mutant RNA were used to display the secondary structures in the graphic format.

Statistics

Statistical analyses were done using student one-tailed T-test using the program GraphPad Prism 4 (GraphPad Software) to describe the differences of K_m and V_{50} values in kinetic and thermal stability assays, respectively, between ASL WT and mutants with significant residual activities. Differences were considered as significant if the *p* value was <0.05.

Results

Expression of recombinant ASL WT and mutants in 293T cells

In order to investigate the molecular characteristics of all known naturally occurring ASL missense mutations associated with a variant clinical course in ASA patients (17), we first constructed the recombinant ASL WT and mutant plasmids followed by introducing them into 293T cells, respectively. To check whether the recombinant diverse ASL mutants can be expressed at the protein level, Western blot analysis was performed. ASL expression could be detected as monomer in cells expressing all recombinant ASL mutant proteins (Figure 2A). Moreover, a similar level of ASL expression as in WT was observed in all ASL mutants except for p.Arg95Cys, p.Arg193Trp and p.Arg445Pro with lower protein yields (37%, 37% and 40% of WT after normalisation with loading control GAPDH by densitometry) indicating that these mutants are less stable at either protein or RNA level. We performed RNA secondary structure prediction to check whether substantial variations from the WT RNA were the cause of lower expression levels. Our analysis showed significant differences for the p.Arg193Trp (p-0.157) and p.Arg445Pro (p-0.118) variants (Figure 3). Thus, combination of RNA and protein stability effects may be responsible for lower expression of some mutant proteins.

Residual ASL enzymatic activities in transfected 293T cell extracts

To determine whether the expressed ASL mutants have any residual enzyme activity, we performed ASL enzyme activity assays with the cell extracts used for Western blot analysis (summary of data in Table 1 and Figure 2B). The residual enzymatic activities were normalized according to the expressed ASL protein levels by densitometry using GAPDH as control. There was no relevant endogenous ASL activity in cells transfected with EV. No significant residual activity (≤ 2% of ASL WT)

was observed in cells respectively transfected with two severe mutants p.Gln286Arg and p.Arg385Leu as well as with two variant mutants p.Asp31Asn and p.Arg385Cys, whereas cells expressing ASL WT yielded high enzymatic activity (Figure 2B). Cells expressing other nine variant mutants (p.Arg12Gln, p.Arg95Cys, p.Ile100Thr, p.Val178Met, p.Glu189Gly, p.Arg193Trp, p.Val335Leu, p.Arg379Cys and p.Arg445Pro) showed a residual activity >3% of ASL WT. Surprisingly, six of them (p.Arg95Cys, p.Ile100Thr, p.Val178Met, p.Glu189Gly, p.Val335Leu, and p.Arg379Cys) displayed a high level of ASL residual activity ≥18% of ASL WT (Table 1 and Figure 2B).

Kinetic study of variant mutants with high residual ASL activities

Next, we wanted to study the molecular pathology in ASA patients identified with variant mutants (p.Arg95Cys, p.Ile100Thr, p.Val178Met, p.Glu189Gly, p.Val335Leu, and p.Arg379Cys) harbouring residual activities ≥18% of ASL WT. Therefore, we analyzed whether the kinetic parameters were impaired in these mutants using different concentrations of the substrate argininosuccinate (summary of data in Table 1 and Figure 2C). The normalized maximal reaction velocity (V_{max}) value in cells expressing recombinant mutant protein p.Arg95Cys showed about 13% of that in cells expressing ASL WT, whereas other five mutants (p.Ile100Thr, p.Val178Met, p.Glu189Glp, Val335Leu, and p.Arg379Cys) exhibited ≥58% of Vmax of ASL WT. Moreover if compared with WT, the Vmax values of mutants were consistent with their residual activities and were all significantly lower (p<0.05). Interestingly, K_m values were not significantly changed in mutants p.Ile100Thr (0.46 mM), p.Val178Met (0.44 mM), p.Glu189Gly (0.49 mM), and p.Val335Leu (0.53 mM). In contrast, K_m values were even slightly decreased in mutants p.Arg95Cys (0.18 mM) and p.Arg379Cys (0.25 mM) compared with that of ASL WT (0.44 mM) indicating an increased substrate affinity in these two mutants. Furthermore, the ratios of V_{max}/K_m in four mutants (p.Arg95Cys, p.Ile100Thr, p.Glu189Gly and p.Val335Leu) were decreased (32%, 61%, 78%, and 48% of ASL WT, respectively), while two mutants p.Val178Met and p.Arg379Cys showed similar V_{max}/K_m ratios (93% and 112%, respectively) compared to that of WT indicating an unchanged catalytic efficiency in these mutants.

Thermal stability analysis of variant mutants with high residual ASL activities

In order to further investigate the molecular basis in variant ASL mutants with significant residual activity, we measured the thermal stability of mutant proteins by incubating the protein at different temperatures prior to activity determination (summary of data in Table 1 and Figure 2D). The V_{50} values, indicating the temperatures at which 50% of ASL activity is lost, were dropped to 46.5, 48.4, 49.9, 48.2, 42.4, and 48.0^{o}C for mutants p.Arg95Cys, p.Ile100Thr, p.Val178Met, p.Glu189Gly, p.Val335Leu and p.Arg379Cys, respectively, compared with ASL WT (52.7^{o}C). All V_{50} values of mutants were significantly decreased (p<0.05) suggesting thermal instability of these ASL variants.

Structural model of ASL tetramer

We analyzed the mutated residues in human ASL by making a structural model using known x-ray crystal structures of ASL protein as template. The structural model of ASL tetramer was generated using the known x-ray crystal structures of ASL available in the PDB database (PDB # 1K62, 1AOS) (25, 48) as templates with YASARA (33) and WHATIF (34). We used in-silico mutagenesis to replace amino acids as utilized previously for other proteins to preserve the core-structure (49). The amino acids identified from structural studies were checked by comparing the positions of these amino acids in different ASL sequences available in the NCBI protein database. We compared human, horse, cow, cat, pig, chimpanzee, dog and rat ASL protein sequences, and amino acids near the substrate binding site and interaction points of the tetrameric protein complex were checked for conservation (Figure 4). Amino acids involved in substrate access and catalysis were conserved across species and no structurally significant substitutions were observed in any of the sequences analyzed (Figure 4). A high resolution x-ray crystal structure of ASL that describes the conformations and topologies of ASL monomers has been described by Sampaleanu et al (25) which formed the basis of our structural analysis. The enzymatically active form of ASL is a homotetramer which is formed by four identical 100A monomer units which have three distinct helix rich subdomains (Figure 5) (25). Domains 1 and 3 of ASL monomeric structure have similar structure and topology with two helix-turn-helix motifs in perpendicular arrangement, while domain 2 has nine helices and five of them form the central five helix bundles with up-down-up-down-up topology (Figure 5) (25).

Three of these five central helices interact with another subunit of ASL to form the dimeric structures. In the catalytically active complex each monomeric chain contributes one central helix that becomes part of the four helix central cores. Three distinct and highly conserved regions (C1, C2 and C3, shown in grey in Supplemental Figure 1) on the ASL monomers contribute towards the formation of active sites in the functional tetramer. In the monomeric structure these conserved regions are located on different domains of the protein but in the tetramer these regions connect together and form an active site of multiple subunits where each region (C1, C2 or C3) is contributed by a different monomeric subunit. The histidine 160 residue located in the conserved region C2 is proposed as the catalytic centre. A comparison with similar structures suggests that histidine 160 in ASL may be involved in binding and neutralizing the carboxylate group of ASA (40). The glutamine 286 residue is located on the highly conserved and flexible loop C3 comprising of residues 270-290 (called 280`s loop) that has been proposed to be involved in entry of the substrate and exit of the product at the catalytic centre (25). The lysine 287 and 288 located on 280`s loop are highly conserved and may be involved in neutralizing negative charges of the reaction intermediate carbanion dicarboxylate or fumarate which is the final product of the reaction.

Structural properties of the ASL mutants

The location of ASL mutants studied in this report on one subunit was depicted in Figure 5. We investigated the structural properties of these mutants to better understand their diseasecausing nature. We created structural models of 13 ASL mutants (Figures 6-8). Amino acids were mutated in-silico and side-chains of mutated residues were optimized by MD simulations. The MD simulations were performed with YASARA using the AMBER03 (43) force field as described previously (33). Refined structures were evaluated with WHAT_CHECK (35), Verify3D (36, 37) and analyzed by programs YASARA (33) and WHATIF (34) for a variety of structural parameters like breaking of salt-bridges and hydrogen bonds, changes in charge, size and volume of the altered amino acid and interaction with neighbouring residues, to evaluate the impact of mutations as described previously for several other proteins and structures (49-51).

Prediction of disorder due to structural changes was done with the site-directed mutator tool based on statistical potential energy calculations (44). In the

SDM analysis a negative score is indicative of a destabilizing effect and a positive score suggests a stabilizing effect. A cut-off of 2 kcal.mol^{-1} was used for predicting a disease causing effect. The p.Ile100Thr, p.Glu189Gly and p.Arg445Pro mutants in ASL were predicted to decrease the structural stability and cause disease (Table 2). Structural stability of the tetramer interface is also crucial for the complex formation which was analyzed in detail by looking at ionic interactions and hydrogen bond network of residues at the interface of central helices in tetrameric structure (Table 3).

Role of arginine 12: The arginine 12 residue is located on the flexible N-terminus loop of the protein (Figure 6A), which does not seem to influence the overall tetramer structure or active site of the enzyme but this loop is very close to the active site and therefore may influence binding/exit of substrate. During MD simulations we found arginine 12 to be located near glutamate 138 and aspartate 145 of another ASL unit and to form ionic contacts. In addition the arginine 12 formed hydrogen bonds with threonine 142, threonine 347 and glycine 348 which were broken in the arg12gln mutant (Table 3). Sampaleanu et al have proposed that due to mutation of arg12 the arg12-asp18 salt bridge is disrupted, allowing alternate confor-mations of the N-terminal loop which come in contact with 280`s loop domain and disturb the conformation of substrate binding site (25). The p.Arg12Gln mutation had been reported to cause a milder form of disease (25).

Role of aspartate 31: The aspartate 31 residue is situated close to the catalytic centre and is part of the substrate access channel formed by three different units of ASL monomers (Figure 6B). A change from aspartate to aspargine seems to result in additional hydrogen bonding with aspartate 87 of the same monomeric unit of ASL. This might cause restrictions in binding of the substrate or exit of the catalytic product.

Role of arginine 95: Arginine 95 forms 4 hydrogen bonds with the glutamate 73 located on a parallel helix within the same monomeric subunit (Figure 6C) which is important for protein stability. The mutation of arginine 95 to cysteine abolished the hydrogen bonds with the glutamate 73, which would impact protein stability. Confirming this hypothesis the p.Arg95Cys variant of ASL showed lower expression

levels and was adversely affected by temperature increases in the protein stability assays. The mutation of arginine 95 to cysteine may have increased the flexibility of the substrate access to the active site and an increase in binding affinity, as implicated from a reduced Km value, was observed.

Role of isoleucine 100: The isoleucine 100 residue is located in the highly conserved C1 region of the protein and is located near the active site but does not have any direct role in substrate binding or catalysis (Figure 6D). The isoleucine 100 residue is participating in multiple interactions with the isoleucine 63, aspargine 62 and 99 leucine. The mutation of isoleucine 100 to threonine did not affect the interactions with neighbouring residues to any significant extent and is predicted not to have any drastic effects on catalytic activity (Figures 2B,C and 6D). The p.Ile100Thr mutation has been reported to cause a mild effect (11) and enzyme kinetic analysis revealed a slight reduction in activity.

Role of valine 178: The valine 178 residue is located in the central core helix bundle that forms the tetramer structure of ASL (Figure 7A) but is not directly involved in stabilizing the central core of the structure. The substitution of valine by methionine group is predicted to have only minor effects on tetramer stability. Moreover, several strong ionic interactions, especially between Arg186, Arg193 and Glu185 and Glu189 on different subunits were not impacted by mutation of valine 178 and the tetrameric structure was not affected. The p.Val178Met mutation had close to WT activity in enzymatic analysis and was comparatively stable in thermal instability assay and has been reported to allow a milder ASLD phenotype in patients carrying this mutant (11, 19, 21).

Roles of glutamate 189 and arginine 193: The ASL tetramer is held together by hydrophobic interactions between the four central helices as well as ionic interactions between arginine and glutamic acid residues on two adjacent dimeric ASL units (Figure 7B). Our structural analysis using in-silico mutagenesis and MD simulations revealed a central role for arginine 193 in the tetramer formation and any changes to arginine 193 residue was predicted to adversely affect the protein stability. We found that charge pair interactions between Arg193 on one subunit with Glu189 and Glu185 of another adjacent subunit are important for the core structure (Figure 7C). The

p.Glu189Gly mutant has been reported to be milder (19) and enzyme assays also showed only a mild effect on activity (23). Analysis of dynamic hydrogen binding patterns and salt bridges in the mutant structure suggested that in addition to glutamate 189, the glutamate 185 also participates in interactions with arginine 193 of the adjacent ASL subunit to stabilize the tetramer. In the p.Glu189Gly variant of ASL tetramer, the arginine 193 of the adjacent ASL monomer formed hydrogen bonds with glutamate 185. This would suggest that the effect of Glu189 mutation is not severe due to compensatory mechanism of alternate interactions in the mutated protein. The partial disruption of salt bridges is reflected in lower thermal stability of the p.Glu189Gly variant.

Role of glutamate 286: The glutamine 286 residue located on the conserved C3 region of the ASL is part of the flexible 280's loop and although it does not seem to participate directly in substrate binding, its mutation affects catalysis and results in severe form of disease (25, 27). It has been suggested that 280`s loop is important for substrate entry and exit (25) and mutation of Gln286 to arginine changes the interactions of this loop by formation of two hydrogen bonds with the glutamine 399, which is part of the active site. This would stabilize the flexible 280's loop and adversely affect substrate binding and exit from the active site (Figure 7D). This is reflected by almost complete loss of activity in the p.Gln286Arg mutant.

Role of valine 335: The valine 335 group is involved in multiple hydrophobic interactions with residues on the same alpha helix as well as another adjacent parallel alpha helix of the same ASL unit (Figure 8A). The mutation of valine 335 to leucine does not seem to impact the structure adversely. An additional hydrophobic interaction with arginine 302 of the same ASL unit was observed upon mutation of valine 335 to leucine. The mutation did not have severe impact on ASL activity but its thermal stability was remarkably lower than the WT protein.

Roles of arginines 379 and 385: The arginine 379 residue has only a minor role in protein stability of the ASL monomer (Figure 8B), mainly through hydrogen bonding with histidine 432 on the same ASL unit and through hydrophobic interactions to leucine 209 of adjacent ASL unit. The mutation of arginine to cysteine abolished both of the contacts but several other interactions are probably able to compensate and

any major impact on protein stability was not predicted. The p.Arg379Cys variant has similar to WT catalytic efficiency (V_{max}/K_m) but there was a significant impact on thermal stability (Table 1 and Figure 2D). The arginine 385 residue is located near the active site and interacts with Glu389 by formation of two hydrogen bonds for stabilization of the carboxy terminus helix bundle (Figure 8C). The mutation of Arg385 has given mixed phenotypes with p.Arg385Cys reported as mild (11, 21, 23) while p.Arg385Leu causes severe form of disease and clinical details of p.Arg385His mutation are unknown (17). It is likely that its impact is determined by side chains of the mutated residue that may interfere with residues near the active site. In our analysis the interactions with Glu389 and of the same ASL unit and Gly105 of the adjacent unit were affected by mutation to cysteine or leucine. In the enzymatic analysis both the p.Arg385Cys and p.Arg385Leu resulted in loss of activity and could not explain the differences in disease phenotype.

Role of arginine 445: The arginine 445 residue is involved in stabilizing the carboxy terminus helix of the ASL monomeric structure (Figure 8D) and its mutation to proline was predicted to have drastic consequences. The hydrogen bonds formed between arginine 455 and aspartate 152 and glutamate 435 were disrupted upon mutation to proline (Table 3). The SDM prediction gave a disordered structure upon mutation of arginine 445 to proline. The loss of enzymatic activity seems to support this prediction.

Discussion

The broad clinical and biochemical variability of ASLD has been subject of various investigations over recent years. More specific, the presence of residual enzyme activities was confirmed in different expression systems, both prokaryotic (23-25) and eukaryotic (26-30), and this was considered as a factor contributing to the spectrum of disease. On the other hand, the finding of cognitive impairment despite higher ASL activity (22) and, in other patients, of normal outcome despite undetectable ASL activities (19) led to the assumption of “no correlation between enzyme activity and neuro-clinical outcome” (3). This overall inconsistent situation may in part be explained by the variety of methods employed including different enzymatic measurements, direct (5, 22) as well as indirect (20, 21) assays, and likewise different ways of expression, yielding recombinant purified ASL protein from

prokaryotic overexpression (23) as well as eukaryotic systems using yeast (26) or human embryonic kidney 293T cell lysates (30).

Here, we exploited our recently established eukaryotic expression system that is based on crude cell extracts of transfected 293T cells (30) to study in detail all known variant ASL mutants (17). The term variant ASL mutant refers to non-classical presentations either as late onset or as mild clinical and biochemical phenotypes. We studied in total eleven variant and two severe missense mutations. The eleven variant mutations represent a substantial proportion of the total 92 known ASL missense mutations of which 25 are known to be associated with a severe phenotype (17).

We confirmed high levels of ASL enzyme activity in the recombinant WT, further validating our expression system. In contrast, severe mutants p.Gln286Arg and p.Arg385Leu yielded levels of residual ASL activity < 1.5% if compared with the WT level. Western blotting confirmed sufficient expression of recombinant protein for all transfected constructs (Figure 2A). Interestingly, while most mutants, including the severe changes p.Gln286Arg and p.Arg385Leu, expressed at levels comparable to ASL WT, we found three variant mutants that yielded clearly lower protein expression (p.Arg95Cys, p.Arg193Trp, p.Arg445Pro) indicating their disease causing role and already pointing towards instability of the mutant proteins. The RNA secondary structure may also play a role in lower levels of expression. Therefore, a combination of lower translation as well as protein instability may affect the overall outcome of some ASL variants.

In the eleven variant ASL constructs, we found levels of residual activity ≥18% of WT in p.Arg95Cys, p.Ile100Thr, p.Val178Met, p.Glu189Gly, p.Val335Leu, and p.Arg379Cys while residual activities were much lower in the remaining mutants (Table 1 and Figure 2B). Based on this, we decided to add kinetic as well as thermal stability studies for the above six mutants. Four of the mutant ASL proteins (p.Ile100Thr, p.Val178Met, p.Glu189Gly, and p.Val335Leu) showed no significant changed Km values and two mutants (p.Arg95Cys and p.Arg379Cys) even displayed slightly decreased Km values (Table 1), which would explain their milder phenotype.

The findings of a decreased thermal stability for mutants p.Arg95Cys, p.Ile100Thr, p.Val178Met, p.Glu189Gly, p.Val335Leu, and p.Arg379Cys as well as the low expression level for mutants p.Arg95Cys, p.Arg193Trp, and p.Arg445Pro point towards an instable and/or lower expressed ASL protein in the aforementioned

mutants. This opens the possibility of stabilising these mutants by pharmacological chaperons as a new therapeutic approach in ASLD. Such small molecule treatment has been well established in experimental settings in other diseases (52, 53) but has not been tested yet for ASLD. Since all of the mutants that possibly qualify for chaperone treatment are recurrent and some even belong to the most frequently found mutants in ASLD patients (17), identification of compounds that can be used for this purpose should become a research priority. This is underlined by the fact that about 25% (n=43) of the 160 known different genotypes (17) are affected at least on one allele by any of the mutations described here as possible targets of chaperone treatment.

Our findings are further substantiated by predictions from structure modelling. The variants studied in this report can be divided in two different groups based on their impact on the structure of the ASL protein. Most of the variants affect the atomic interactions within a monomeric ASL unit while variants p.Glu189Gly and p.Arg193Trp were found to impact the tetramer formation. The enzyme kinetic data and thermal stability analysis were in general agreement with the structural analysis. Mutants with complete or near-complete effects on activity were either near the active site (p.Arg12Gln, p.Asp31Asn, p.Gln286Arg, p.Arg385Cys, and p.Arg385Leu) or hampered the structural stability of monomer (p.Arg445Pro) or tetramer (p.Arg193Trp). Two variants near the tetrameric interface, p.Val178Met and p.Glu189Gly did not have severe effects on enzymatic activity. Further computational analysis showed that multiple strong ionic interactions between arginine 193, lysine 192 of one subunit with the glutamate 185 and glutamate 189 of another interacting ASL monomeric unit could compensate for loss of some interactions. The major result of this analysis is the role of arginine 193 in the structural stability of the ASL complex. Involvement of arginine 193 with several adjacent acidic residues meant that any mutation of arginine 193 residue would have a strong negative impact on protein stability and catalytic activity.

In conclusion, we have found significant residual levels of ASL activity in some of the mutants that are associated with a variant clinical and biochemical phenotype of ASLD. Likewise, this study provides evidence for instability of the mutant proteins and adds ASLD to the list of target diseases for novel therapeutic approaches with small molecules allowing scaffolding to improve folding and stability. Based on recent data on the genotypes found in ASLD it is obvious that the search for compounds

that stabilize the ASL protein should be pursued with highest priority to eventually gain benefit for a substantial proportion (~25%) of ASLD patients.

Funding

This work was supported by the Swiss National Science Foundation [grants No. 310030_127184/1 and 310030_153196/1 to JH and 310031_134926 to AVP] and a grant from Schweizerische Mobiliar Genossenschaft Jubilaumsstiftung to AVP.

Acknowledgements

The authors are grateful for the technical assistance provided by the late M. Groux, Bern.

Conflict of interest

The authors of this paper confirm that there is no conflict of interest.

References

1. Brusilow, S. and Horwich, A. (2001) Urea cycle enzymes. In Scriver, C., Beaudet, A., Sly, W. and Valle, D. (eds.), *The metabolic & molecular bases of inherited disease.* 8th ed. McGraw-Hill, New York, pp. 1909-1963.
2. Brusilow, S.W. and Maestri, N.E. (1996) Urea cycle disorders: diagnosis, pathophysiology, and therapy. *Advances in pediatrics,* **43,** 127-70.
3. Erez, A., Nagamani, S.C. and Lee, B. (2011) Argininosuccinate lyase deficiencyargininosuccinic aciduria and beyond. *Am J Med Genet C Semin Med Genet,* **157,** 45-53.
4. Tomlinson, S. and Westall, R.G. (1960) Argininosuccinase activity in brain tissue. *Nature,* **188,** 235-6.
5. Tomlinson, S. and Westall, R.G. (1964) Argininosuccinic Aciduria. Argininosuccinase and Arginase in Human Blood Cells. *Clinical science,* **26,** 261-9.
6. Solitare, G.B., Shih, V.E., Nelligan, D.J. and Dolan, T.F., Jr. (1969) Argininosuccinic aciduria: clinical, biochemical, anatomical and neuropathological observations. *J Ment Defic Res,* **13,** 153-70.

7. Zimmermann, A., Bachmann, C. and Baumgartner, R. (1986) Severe liver fibrosis in argininosuccinic aciduria. *Archives of pathology & laboratory medicine,* **110,** 136-40.
8. Mori, T., Nagai, K., Mori, M., Nagao, M., Imamura, M., Iijima, M. and Kobayashi, K. (2002) Progressive liver fibrosis in late-onset argininosuccinate lyase deficiency. *Pediatr Dev Pathol,* **5,** 597-601.
9. Brunetti-Pierri, N., Erez, A., Shchelochkov, O., Craigen, W. and Lee, B. (2009) Systemic hypertension in two patients with ASL deficiency: a result of nitric oxide deficiency? *Molecular genetics and metabolism,* **98,** 195-7.
10. Erez, A., Nagamani, S.C., Shchelochkov, O.A., Premkumar, M.H., Campeau, P.M., Chen, Y., Garg, H.K., Li, L., Mian, A., Bertin, T.K. *et al.* (2011) Requirement of argininosuccinate lyase for systemic nitric oxide production. *Nat Med,* **17,** 1619-26.
11. Linnebank, M., Tschiedel, E., Häberle, J., Linnebank, A., Willenbring, H., Kleijer, W.J. and Koch, H.G. (2002) Argininosuccinate lyase (ASL) deficiency: mutation analysis in 27 patients and a completed structure of the human ASL gene. *Human genetics,* **111,** 350-9.
12. O'Brien, W.E., McInnes, R., Kalumuck, K. and Adcock, M. (1986) Cloning and sequence analysis of cDNA for human argininosuccinate lyase. *Proceedings of the National Academy of Sciences of the United States of America,* **83,** 7211-5.
13. Todd, S., McGill, J.R., McCombs, J.L., Moore, C.M., Weider, I. and Naylor, S.L. (1989) cDNA sequence, interspecies comparison, and gene mapping analysis of argininosuccinate lyase. *Genomics,* **4,** 53-9.
14. Palekar, A.G. and Mantagos, S. (1981) Human liver arginiosuccinase purification and partial characterization. *The Journal of biological chemistry,* **256,** 9192-4.
15. O'Brien, W.E. and Barr, R.H. (1981) Argininosuccinate lyase: purification and characterization from human liver. *Biochemistry,* **20,** 2056-60.
16. Trevisson, E., Salviati, L., Baldoin, M.C., Toldo, I., Casarin, A., Sacconi, S., Cesaro, L., Basso, G. and Burlina, A.B. (2007) Argininosuccinate lyase deficiency: mutational spectrum in Italian patients and identification of a novel ASL pseudogene. *Human mutation,* **28,** 694-702.

17. Balmer, C., Pandey, A.V., Rüfenacht, V., Nuoffer, J.M., Fang, P., Wong, L.J. and Häberle, J. (2014) Mutations and polymorphisms in the human argininosuccinate lyase (ASL) gene. *Human mutation,* **35,** 27-35.
18. Tanaka, T., Nagao, M., Mori, T. and Tsutsumi, H. (2002) A novel stop codon mutation (X465Y) in the argininosuccinate lyase gene in a patient with argininosuccinic aciduria. *The Tohoku journal of experimental medicine,* **198,** 119-24.
19. Mercimek-Mahmutoglu, S., Moeslinger, D., Häberle, J., Engel, K., Herle, M., Strobl, M.W., Scheibenreiter, S., Muehl, A. and Stockler-Ipsiroglu, S. (2010) Long-term outcome of patients with argininosuccinate lyase deficiency diagnosed by newborn screening in Austria. *Mol Genet Metab,* **100,** 24-8.
20. Jacoby, L.B., Littlefield, J.W., Milunsky, A., Shih, V.E. and Wilroy, R.S., Jr. (1972) A microassay for argininosuccinase in cultured cells. *Am J Hum Genet,* **24,** 321-4.
21. Kleijer, W.J., Garritsen, V.H., Linnebank, M., Mooyer, P., Huijmans, J.G., Mustonen, A., Simola, K.O., Arslan-Kirchner, M., Battini, R., Briones, P. *et al.* (2002) Clinical, enzymatic, and molecular genetic characterization of a biochemical variant type of argininosuccinic aciduria: prenatal and postnatal diagnosis in five unrelated families. *Journal of inherited metabolic disease,* **25,** 399-410.
22. Ficicioglu, C., Mandell, R. and Shih, V.E. (2009) Argininosuccinate lyase deficiency: longterm outcome of 13 patients detected by newborn screening. *Molecular Genetics and Metabolism,* **98,** 273-7.
23. Engel, K., Vuissoz, J.M., Eggimann, S., Groux, M., Berning, C., Hu, L., Klaus, V., Moeslinger, D., Mercimek-Mahmutoglu, S., Stockler, S., Wermuth, B., Häberle, J., Nuoffer, J.M. (2012) Bacterial expression of mutant argininosuccinate lyase reveals imperfect correlation of in-vitro enzyme activity with clinical phenotype in argininosuccinic aciduria. *J Inherit Metab Dis,* **35,** 133-40.
24. Yu, B., Thompson, G.D., Yip, P., Howell, P.L. and Davidson, A.R. (2001) Mechanisms for intragenic complementation at the human argininosuccinate lyase locus. *Biochemistry,* **40,** 15581-90.

25. Sampaleanu, L.M., Vallee, F., Thompson, G.D. and Howell, P.L. (2001) Threedimensional structure of the argininosuccinate lyase frequently complementing allele Q286R. *Biochemistry,* **40,** 15570-80.
26. Trevisson, E., Burlina, A., Doimo, M., Pertegato, V., Casarin, A., Cesaro, L., Navas, P., Basso, G., Sartori, G. and Salviati, L. (2009) Functional complementation in yeast allows molecular characterization of missense argininosuccinate lyase mutations. *The Journal of biological chemistry,* **284,** 28926-34.
27. Barbosa, P., Cialkowski, M. and O'Brien, W.E. (1991) Analysis of naturally occurring and site-directed mutations in the argininosuccinate lyase gene. *The Journal of biological chemistry,* **266,** 5286-90.
28. Walker, D.C., Christodoulou, J., Craig, H.J., Simard, L.R., Ploder, L., Howell, P.L. and McInnes, R.R. (1997) Intragenic complementation at the human argininosuccinate lyase locus. Identification of the major complementing alleles. *The Journal of biological chemistry,* **272,** 6777-83.
29. Walker, D.C., McCloskey, D.A., Simard, L.R. and McInnes, R.R. (1990) Molecular analysis of human argininosuccinate lyase: mutant characterization and alternative splicing of the coding region. *Proc Natl Acad Sci U S A,* **87,** 9625-9.
30. Hu, L., Pandey, A.V., Eggimann, S., Rüfenacht, V., Moslinger, D., Nuoffer, J.M. and Häberle, J. (2013) Understanding the role of argininosuccinate lyase transcript variants in the clinical and biochemical variability of the urea cycle disorder argininosuccinic aciduria. *J Biol Chem,* **288,** 34599-611.
31. Bradford, M.M. (1976) A rapid and sensitive method for the quantitation of microgram quantities of protein utilizing the principle of protein-dye binding. *Analytical biochemistry,* **72,** 248-54.
32. Laemmli, U.K. (1970) Cleavage of structural proteins during the assembly of the head of bacteriophage T4. *Nature,* **227,** 680-5.
33. Krieger, E., Darden, T., Nabuurs, S.B., Finkelstein, A. and Vriend, G. (2004) Making optimal use of empirical energy functions: force-field parameterization in crystal space. *Proteins,* **57,** 678-83.
34. Vriend, G. (1990) WHAT IF: a molecular modeling and drug design program. *J Mol Graph,* **8,** 52-6, 29.

35. Hooft, R.W., Vriend, G., Sander, C. and Abola, E.E. (1996) Errors in protein structures. *Nature,* **381,** 272.
36. Bowie, J.U., Luthy, R. and Eisenberg, D. (1991) A method to identify protein sequences that fold into a known three-dimensional structure. *Science,* **253,** 164-70.
37. Luthy, R., Bowie, J.U. and Eisenberg, D. (1992) Assessment of protein models with three-dimensional profiles. *Nature,* **356,** 83-5.
38. Ramachandran, G.N., Ramakrishnan, C. and Sasisekharan, V. (1963) Stereochemistry of polypeptide chain configurations. *J Mol Biol,* **7,** 95-9.
39. Hooft, R.W., Sander, C. and Vriend, G. (1997) Objectively judging the quality of a protein structure from a Ramachandran plot. *Comput Appl Biosci,* **13,** 425-30.
40. Vallee, F., Turner, M.A., Lindley, P.L. and Howell, P.L. (1999) Crystal structure of an inactive duck delta II crystallin mutant with bound argininosuccinate. *Biochemistry,* **38,** 2425-34.
41. Shulman-Peleg, A., Nussinov, R. and Wolfson, H.J. (2005) SiteEngines: recognition and comparison of binding sites and protein-protein interfaces. *Nucleic Acids Res,* **33,** W337-41.
42. Shulman-Peleg, A., Nussinov, R. and Wolfson, H.J. (2004) Recognition of functional sites in protein structures. *J Mol Biol,* **339,** 607-33.
43. Liu, H., Elstner, M., Kaxiras, E., Frauenheim, T., Hermans, J. and Yang, W. (2001) Quantum mechanics simulation of protein dynamics on long timescale. *Proteins,* **44,** 484-9.
44. Worth, C.L., Bickerton, G.R., Schreyer, A., Forman, J.R., Cheng, T.M., Lee, S., Gong, S., Burke, D.F. and Blundell, T.L. (2007) A structural bioinformatics approach to the analysis of nonsynonymous single nucleotide polymorphisms (nsSNPs) and their relation to disease. *J Bioinform Comput Biol,* **5,** 1297-318.
45. Topham, C.M., Srinivasan, N. and Blundell, T.L. (1997) Prediction of the stability of protein mutants based on structural environment-dependent amino acid substitution and propensity tables. *Protein Eng,* **10,** 7-21.
46. Smith, R.E., Lovell, S.C., Burke, D.F., Montalvao, R.W. and Blundell, T.L. (2007) Andante: reducing side-chain rotamer search space during comparative modeling using environment-specific substitution probabilities. *Bioinformatics,* **23,** 1099-105.

47. Sabarinathan, R., Tafer, H., Seemann, S.E., Hofacker, I.L., Stadler, P.F. and Gorodkin, J. (2013) RNAsnp: efficient detection of local RNA secondary structure changes induced by SNPs. *Human mutation,* **34,** 546-56.
48. Turner, M.A., Simpson, A., McInnes, R.R. and Howell, P.L. (1997) Human argininosuccinate lyase: a structural basis for intragenic complementation. *Proceedings of the National Academy of Sciences of the United States of America,* **94,** 9063-8.
49. Fluck, C.E., Mullis, P.E. and Pandey, A.V. (2009) Modeling of human P450 oxidoreductase structure by in silico mutagenesis and MD simulation. *Mol Cell Endocrinol,* **313,** 17-22.
50. Pandey, A.V., Kempna, P., Hofer, G., Mullis, P.E. and Fluck, C.E. (2007) Modulation of human CYP19A1 activity by mutant NADPH P450 oxidoreductase. *Mol Endocrinol,* **21,** 2579-95.
51. Pandey, A.V. and Mullis, P.E. (2011) Molecular Genetics and Bioinformatics Methods for Diagnosis of Endocrine Disorders. In Ranke, M.B. and Mullis, P.E. (eds.), *Diagnostics of Endocrine Function in Children and Adolescents.* 4 ed. Karger, Basel, pp. 1-21.
52. Muntau, A.C., Roschinger, W., Habich, M., Demmelmair, H., Hoffmann, B., Som- merhoff, C.P. and Roscher, A.A. (2002) Tetrahydrobiopterin as an alternative treatment for mild phenylketonuria. *N Engl J Med,* **347,** 2122-32.
53. Pey, A.L., Ying, M., Cremades, N., Velazquez-Campoy, A., Scherer, T., Thony, B., Sancho, J. and Martinez, A. (2008) Identification of pharmacological chaperones as potential therapeutic agents to treat phenylketonuria. *J Clin Invest,* **118,** 2858-67.
54. Sobolev, V., Wade, R.C., Vriend, G. and Edelman, M. (1996) Molecular docking using surface complementarity. *Proteins,* **25,** 120-9.

Table 1: Details of naturally occurring ASL missense mutations, clinical course and enzymatic characteristics of recombinant mutant proteins

Nucleotide level	Protein level	Clinical course	ASL activity (± S.D.)[a]		V_{max} (± S.D.)[b]	K_m (± S.D.)[b]	V_{max}/K_m ratio[b]	V_{50} (± S.D.)[b]
			(mIU/mg)	(% of WT)	(mIU/mg)	(mM)	(% of WT)	(°C)
WT	WT	-	1077.2 ± 506.1	100 ± 5.4	769.0 ± 14.2	0.44 ± 0.03	100	52.7 ± 0.2
c.35G>A	p.R12Q	variant	33.4 ± 3.9	4.3 ± 0.5	n.d.	n.d.	n.d.	n.d.
c.91G>A	p.D31N	variant	22.8 ± 2.5	2.0 ± 0.7	n.d.	n.d.	n.d.	n.d.
c.283C>T	p.R95C	variant	192.5 ± 86.5	18.0 ± 5.7	99.2[c] ± 2.7	0.18[c] ± 0.02	32	46.5[c] ± 0.1
c.299T>C	p.I100T	variant	969.0 ± 397.2	98.0 ± 18.3	488.0[c] ±15.1	0.46 ± 0.06	61	48.5[c] ± 0.1
c.532G>A	p.V178M	variant	877.1 ± 335.3	92.1 ± 21.8	714.0[c] ± 14.1	0.44 ± 0.04	93	49.9[c] ± 0.2
c.566A>G	p.E189G	variant	1048.8 ± 426.3	90.3 ± 13.7	669.3[c] ± 16.1	0.49 ± 0.05	78	48.1[c] ± 0.1
c.577C>T	p.R193W	variant	51.3 ± 26.9	4.1 ± 1.3	n.d.	n.d.	n.d.	n.d.
c.857A>G	p.Q286R	severe	9.0 ± 5.9	1.2 ± 0.8	n.d.	n.d.	n.d.	n.d.
c.1003G>T	p.V335L	variant	535.1 ± 130.8	45.2 ± 21.5	443.6[c] ± 10.8	0.53 ± 0.05	48	42.39[c] ± 0.5
c.1135C>T	p.R379C	variant	649.6 ± 244.7	68.0 ± 16.9	487.3[c] ± 9.0	0.25[c] ± 0.02	112	47.95[c] ± 0.1
c.1153C>T	p.R385C	variant	11.6 ± 1.8	1.5 ± 0.2	n.d.	n.d.	n.d.	n.d.
c.1154G>T	p.R385L	severe	10.4 ± 3.3	1.3 ± 0.4	n.d.	n.d.	n.d.	n.d.
c.1334G>C	p.R445P	variant	28.8 ± 2.1	3.2 ± 0.2	n.d.	n.d.	n.d.	n.d.

[a]ASL activities were measured under standard conditions using 13.6 mM argininosuccinate and normalized with GAPDH according to the expressed ASL protein levels by densitometry indicating in mIU/mg protein. The residual activities of ASL mutants were determined as percentage of ASL WT in each transfection under same conditions in triple measurements from at least three independent transfection experiments, respectively.

[b]V_{max} and K_m values were determined by Michaelis-Menten analysis and V50 values by Boltzmann sigmoidal analysis using GraphPad Prism 4 for curve fitting in triple measurements from the same experiment. V_{max} values were normalized according to the expressed ASL protein levels using the same samples for kinetics assay by densitometry.

[c]Significant difference compared with ASL WT (p<0.05)

± S.D.: standard deviation; n.d.: not determined

Table 2: Prediction of protein stability using SDM

ASL Mutants	Sec Str WT	Sec Str mut	Pseudo ΔΔ G (kcal.mol^{-1})
R12Q	L	L	-0.38
D31N	H	H	-0.17
R95C	H	H	1.84
I100T	T	T	**-2.02**
V178M	H	H	0.98
E189G	H	H	**-3.18**
R193W	H	H	1.29
Q286R	T	T	-0.29
V335L	H	H	0.20
R379C	L	L	-1.88
R385C	H	H	-0.21
R385L	H	H	-0.08
R445P	H	H	**-2.28**

Prediction of structural changes were done based on statistical potential energy calculation [300]. In the SDM analysis a negative score is indicative of a destabilizing effect and positive score suggests a stabilizing effect. A cut-off of 2 kcal.mol^{-1} was used for predicting a destabilizing effect (in bold). L: loop; H: helix; T: turn.

Table 3: List of important atomic contacts in WT and mutant ASL tetrameric structures

Mutation	Amino Acid	Residue	Dist	Surf	HB	Phob
R12Q	Arg	**142C Thr**	**5.5**	**4.4**	**+**	**-**
	Arg	**347C Thr**	**4.7**	**5.7**	**+**	**-**
	Arg	348C Gly	5.8	1.2	-	-
	Arg	351C Ser	3.5	39.9	+	-
R12Q	Gln	351C Ser	3.7	29.4	+	-
R95C	Arg	**73A Glu**	**2.8**	**37.9**	**+**	**-**
	Arg	80A Lys	6.1	1.6	-	-
R95C	Cys	73A Glu	3.8	15.9	-	-
V178M	Val	451A Gln	5.2	1.8	-	-
E189G	Glu	193D Arg	3.0	43.7	+	-
R193W	Arg	185D Glu	3.8	19.0	+	-
R193W	Trp	185D Glu	2.8	43.3	-	+
Q286R	Gln	399B Glu	4.6	22.0	+	-
R379C	Arg	**432A His**	**5.5**	**8.9**	**+**	**-**
	Arg	209D Leu	5.5	2.0	-	+
R379C	Cys	209D Leu	4.9	10.8	-	-
R385C	Arg	105D Gly	4.8	10.6	+	-
R445P	Arg	**152A Asp**	**3.3**	**31.7**	**+**	**-**
	Arg	**435A Glu**	**5.6**	**3.6**	**+**	**+**
R445P	Pro	152A Asp	5.0	3.4	-	-
	Pro	435A Glu	4.2	17.5	-	+

Dist: distance (A) between the atoms; Surf: contact surface area (A2) between the atoms; HB: hydrogen bond; Phob: hydrophobic-hydrophobic contact. **+/-** indicates presence/absence of a specific contact. Important interactions are shown in bold. For the hydrogen bond formation contact analysis is based upon the approach developed in (54).

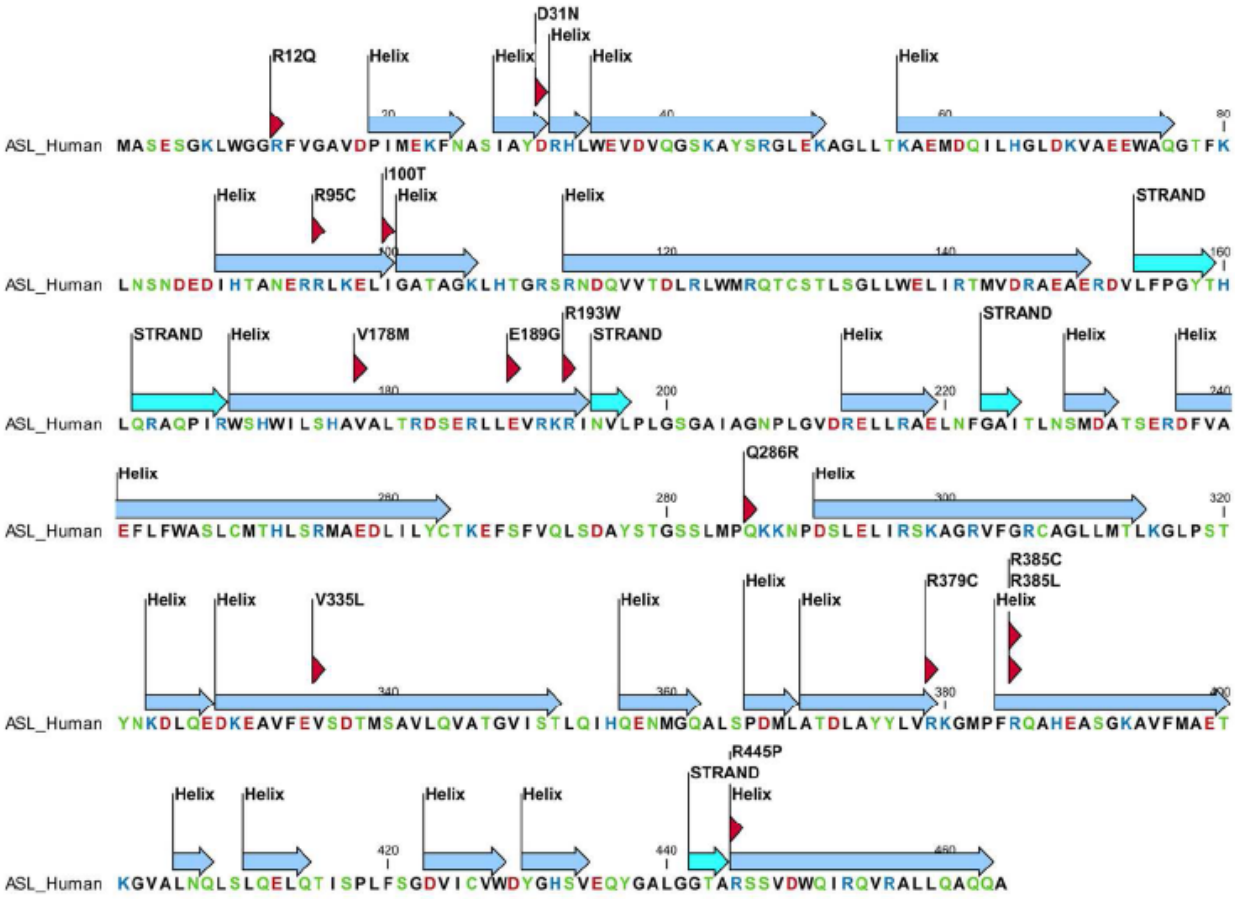

Figure 1: Mutations in the ASL protein mapped onto the secondary structure of the human ASL protein sequence.

Mutations are indicated with red triangles. Helices are shown in light blue and beta strands are shown as cyan arrows. Amino acids are coloured according to chemical properties, with aspartic and glutamic acids are in *red*, arginines and lysines in *blue* and aromatic amino acids are shown in *green*. Secondary structure information was extracted from the known crystal structures of ASL (PDB 1K62) and figure was created with the program CLC Workbench.

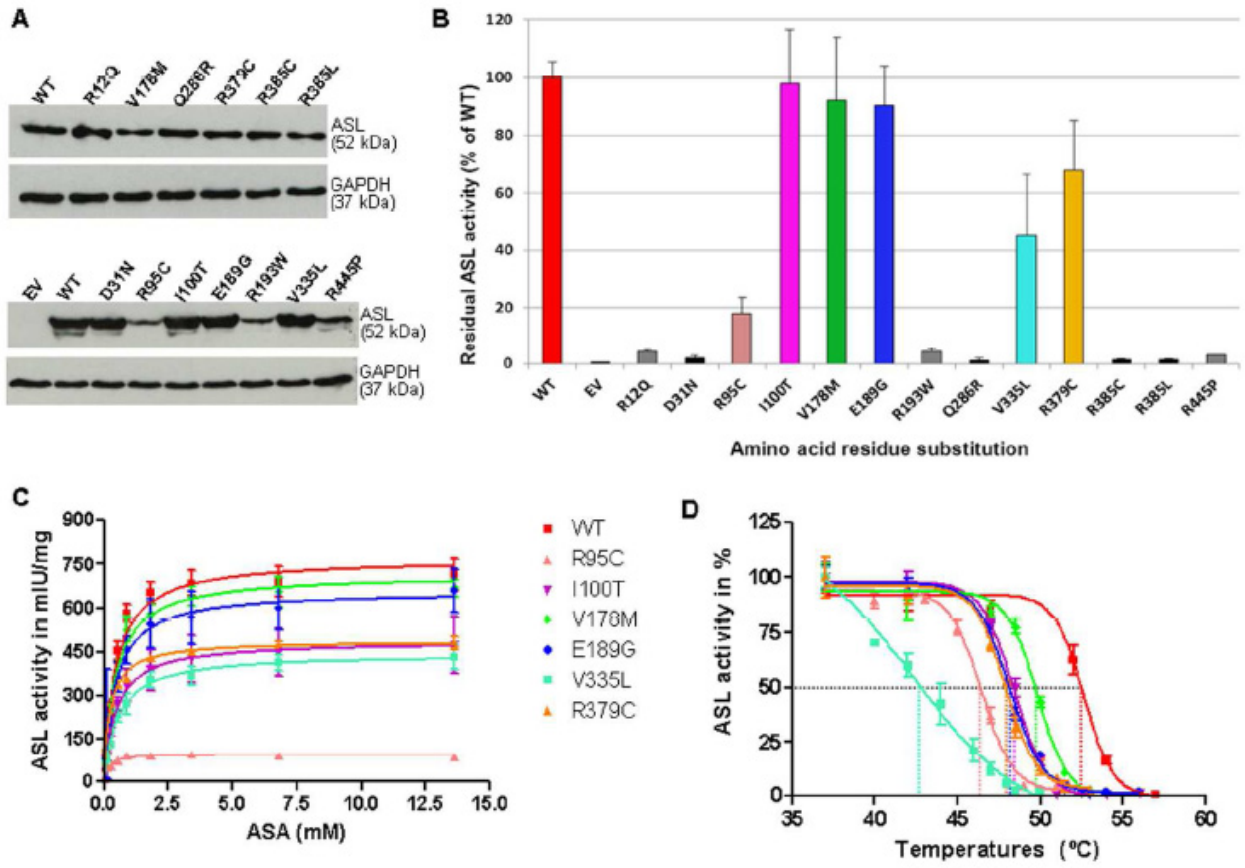

Figure 2: Expression and enzymatic properties of the ASL WT and mutants.

A: Expression of recombinant ASL WT and mutants in 293T cells. 293T cells were transiently transfected with empty vector pcDNA3 (EV), recombinant ASL WT and mutant plasmids, respectively. ASL expression was detected by Western blot analysis using 30 µg of total protein separated by 10% SDS-PAGE. GAPDH (37 kDa) served as loading control. **B: Residual ASL activities of recombinant ASL proteins in 293T cells.** ASL enzymatic activity was measured under standard conditions using 13.6 mM argininosuccinate in cells transiently transfected EV or diverse ASL constructs (6 µg of whole cell extracts), respectively. The residual ASL activities are represented as a percentage of ASL WT activity yielded under same conditions and normalized with GAPDH according to the expressed ASL protein levels by densitometry. ASL severe mutants (Q286R and R385L) and EV served as negative control and were marked in *black*. Nine variant mutants yielded residual activities >3% of ASL WT (in *red*) were marked in different colours: R95C in *salmon*, I100T in *purple*, V178M in *green*, E189G in *blue*, V335L in *cyan*, R379C in *orange*, and R12Q, R193W and R445P in *grey*. Two variant mutants (D31N and R385C) yielded no significant residual activities (≤2% of WT) and were marked also in *black*. All assays were carried out in triplicate measurements of at least three independent

experiments, respectively. **C: Kinetic study of recombinant ASL proteins showing significant residual activities.** Kinetic study was performed for ASL WT and six variant mutants (R95C, I100T, V178M, E189G, V335L, and R379C) (6 µg of whole cell extracts) with ≥18% of WT activity using 10 indicated different argininosuccinate concentrations (ranging from 0.045 to 13.6 mM), respectively. The measured enzymatic activities were normalized according to the expressed ASL protein levels by densitometry using GAPDH as control and represented as mIU/mg of whole cell extract. The kinetic parameters V_{max} in mIU/mg and K_m in mM of argininosuccinate were determined by Michaelis-Menten analysis after curve fitting using GraphPad Prism 4. **D: Thermal stability of recombinant ASL proteins with high residual activities.** A total of 6 µg of protein diluted at 0.15 mg/ml (except for 26 µg of mutant R95C protein, which is expressed less efficient and exhibited only low enzyme activity and was therefore diluted at 0.65 mg/ml) in albumin buffer was heated at the indicated temperatures for 30 min and immediately cooled down on ice prior to ASL activity measurement. ASL activity indicates in percentage of activity of respective protein heated at 37^{o}C. The horizontal dashed line marks 50% of ASL activity, whereas the vertical dashed lines crossing the X-axis indicate the temperatures (V_{50}) at which 50% of each protein is inactivated. The value V_{50} (^{o}C) was determined by Boltzmann sigmoidal analysis after curve fitting using GraphPad Prism 4. All assays were carried out in triplicate. Error bars indicate the standard deviation.

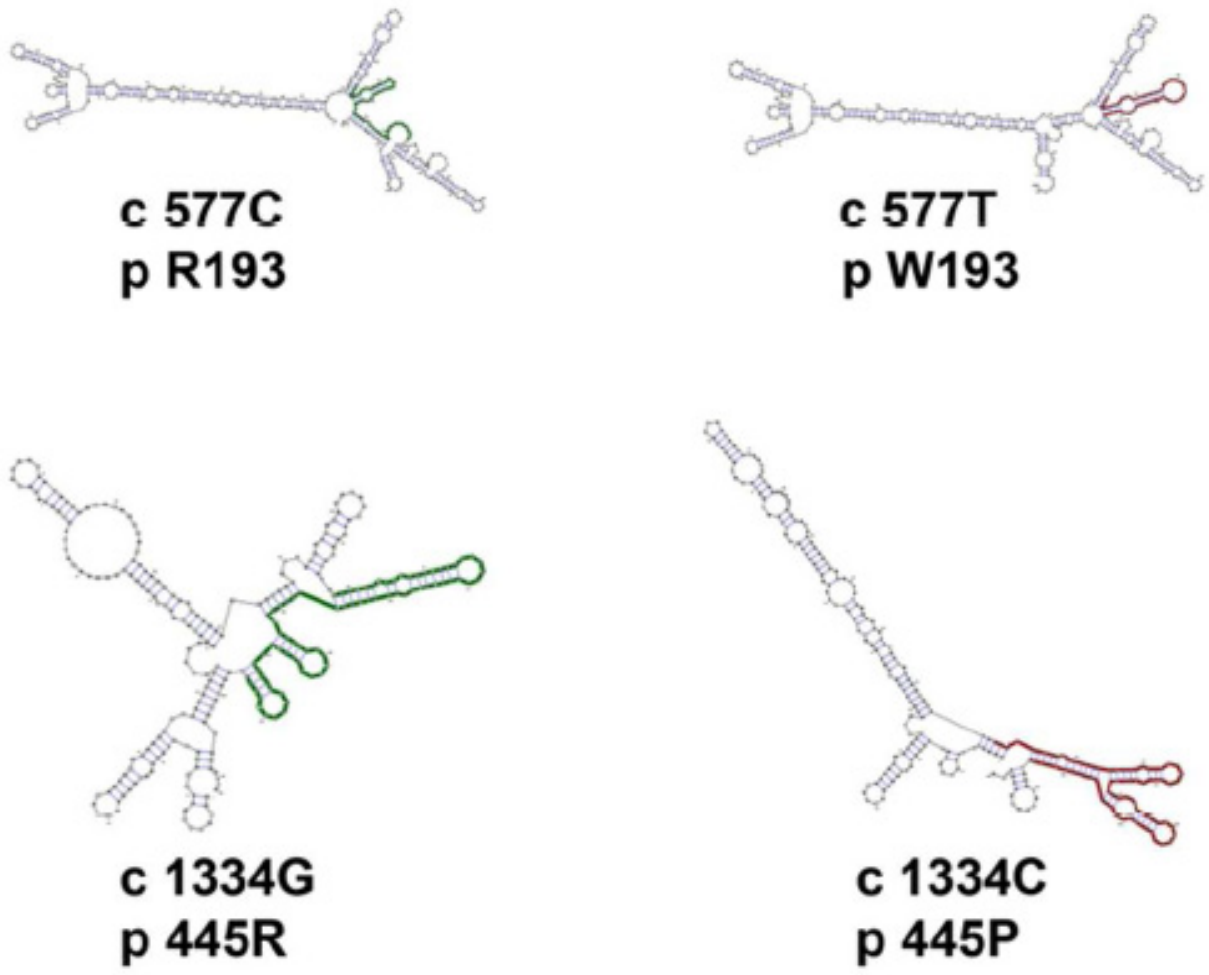

Figure 3: A comparison of the WT and mutant RNA secondary structures of the R193W and R445P variants. The minimum free energy structure of the WT and mutant RNA were used to provide graphical representation of the secondary structures.

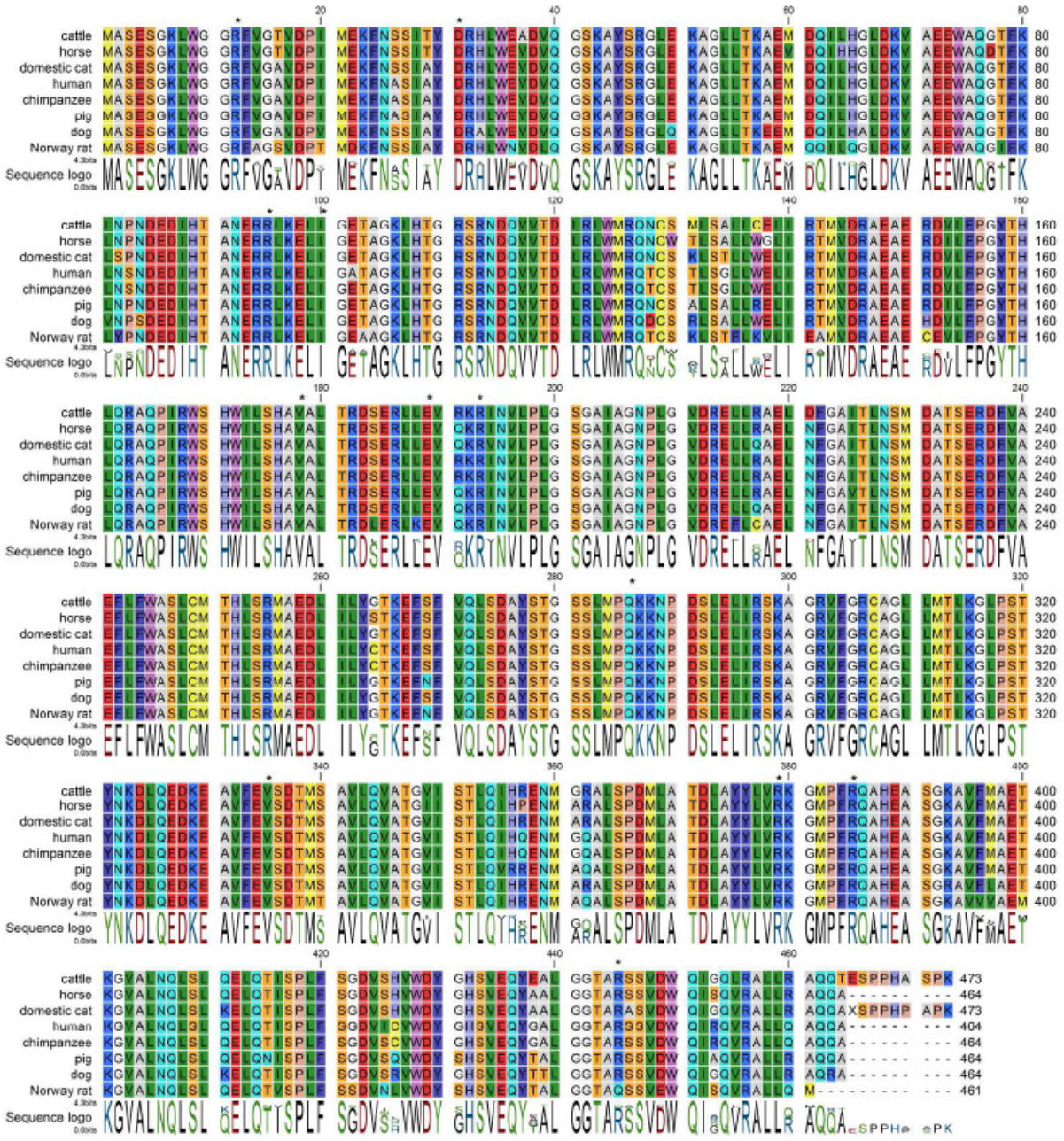

Figure 4: A multiple sequence alignment of ASL protein sequences from human, cow, horse, cat, chimpanzee, pig, dog and rat.

Structurally and catalytically important residues including all residues studied here are conserved across species. As the only exception, in case of rat ASL the arginine 445 residue is replaced by glutamine which may impact the core structure and complex formation of activity. Asterisk indicates mutated residues studied here.

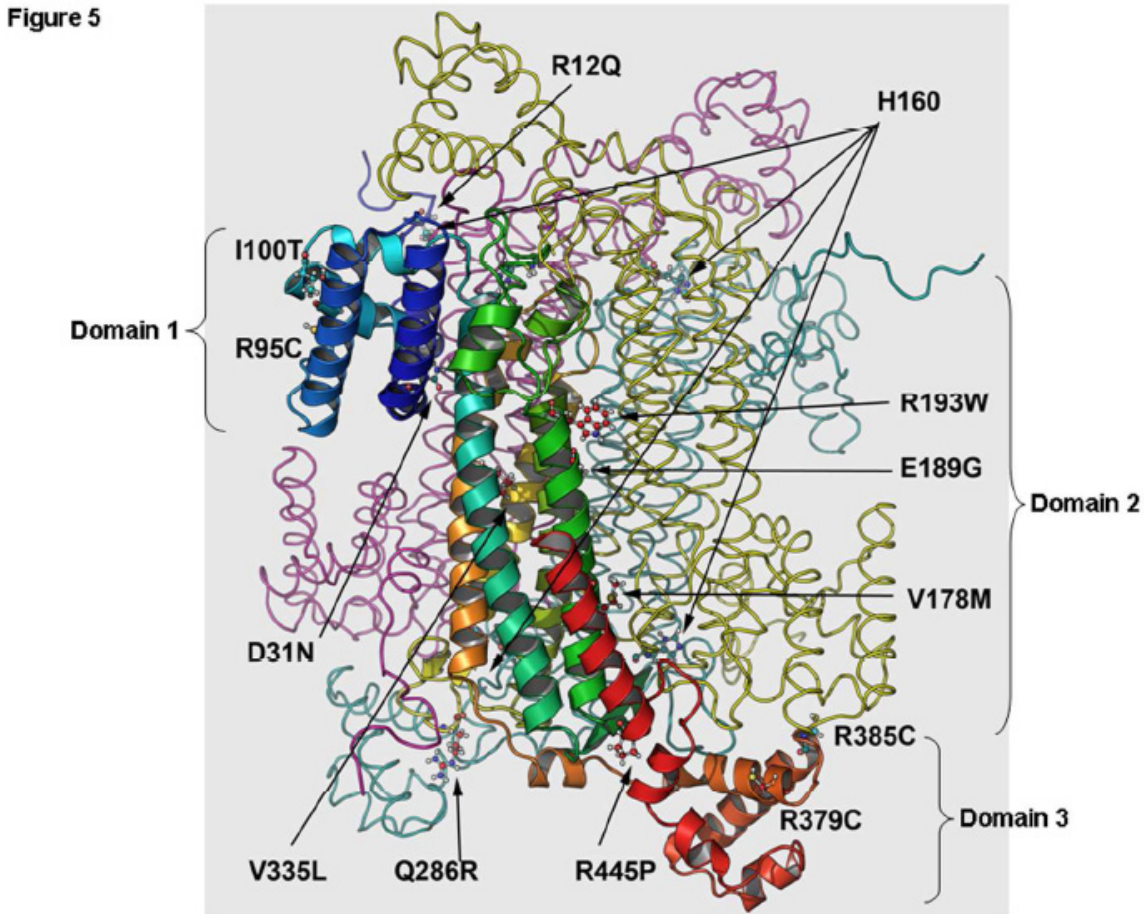

Figure 5: Three dimensional structure of ASL tetramer showing overall structure of ASL tetramer and the location of mutants on one subunit. Monomeric structure of WT ASL has three distinct subdomains. Domains 1 and 3 have similar structure and topology with two helix-turn-helix motifs in perpendicular arrangement. Domain 2 has nine helices and five of them form the central five helix bundle with up-down-up-down-up topology. In the ASL homotetramer, active site residues are contributed by three different subunits. ASL structure is shown as a ribbons model with different subunits coloured in *rainbow*, *cyan*, *magenta* and *yellow*. The green and cyan subunits form a dimer and join with another dimer formed by magenta and yellow subunits to form the tetramer. Active site residues from one of the sites are shown as solid surfaces while catalytic centre (H160) is shown as spheres. For clarity, helices and sheets are only shown for one subunit shown in rainbow colours *violet* at N-terminus and *red* at C-terminus. The mutations studied in this report are shown as ball and stick models. Each active site is formed by residues from three different monomeric subunits, with contributions from three conserved sequences coming from a different subunit. The histidine 160 residues at the catalytic centres are shown for each subunit.

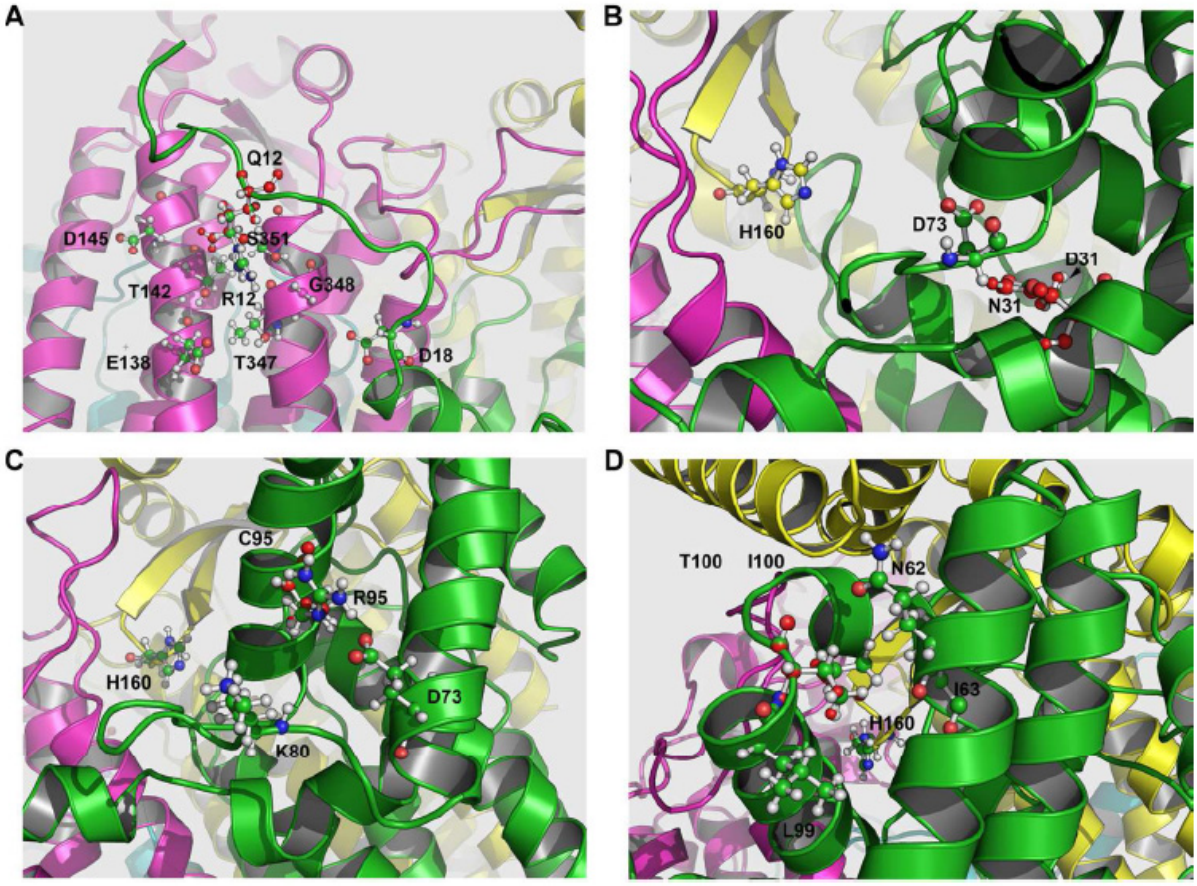

Figure 6: Structural analysis of the ASL mutants R12Q, D31N, R95C and I100T. ASL structure is shown as a ribbons model with different subunits coloured in *green*, *cyan*, *magenta* and *yellow*. Interacting residues are shown as ball and stick models. Mutated residue is shown in *red*. WT and mutant structures were aligned and superimposed to depict the differences between WT and mutated residue. **A: Molecular contacts of arginine 12 and mutagenesis to glutamine.** The arginine 12 residue forms ionic contacts with glutamate 138 and aspartate 145 of the adjacent ASL unit (shown in *magenta*) forms hydrogen bonds with threonine 142, threonine 347 and glycine 348 which were found to be broken in the arg12gln mutant shown in *red*. **B: Molecular contacts of asparate 31 and mutagenesis to asparagine.** The aspartate 31 residue is located close to histidine 160 at catalytic centre and is part of the substrate access channel formed by three different units of ASL monomers, shown in *green*, *magenta* and *yellow*. A change from aspartic acid to aspargine seems to result in hydrogen bond formation with aspartate 87 of the same ASL monomer. This will introduce structural rigidity and may affect the substrate binding and catalysis. **C: Interactions of arginine 95.** The arginine 95 residue is also located near the active site and forms hydrogen bonds with the glutamate 73 on the same ASL monomeric unit (shown in *green*). The arginine 95-glutamate 73 interaction is stabilizing the ASL

monomeric structure and the mutation of arginine 95 to cysteine disrupts the hydrogen bonds with the glutamate 73 which would impact protein stability. **D: Interactions of isoleucine 100.** The isoleucine 100 residue is located near the active site but does not have any direct role in substrate binding or catalysis. The isoleucine 100 residue is participating in multiple interactions with the isoleucine 63, aspargine 62 and 99 leucine but mutation to threonine 100 does not seem to affect the interactions with neighbouring residues.

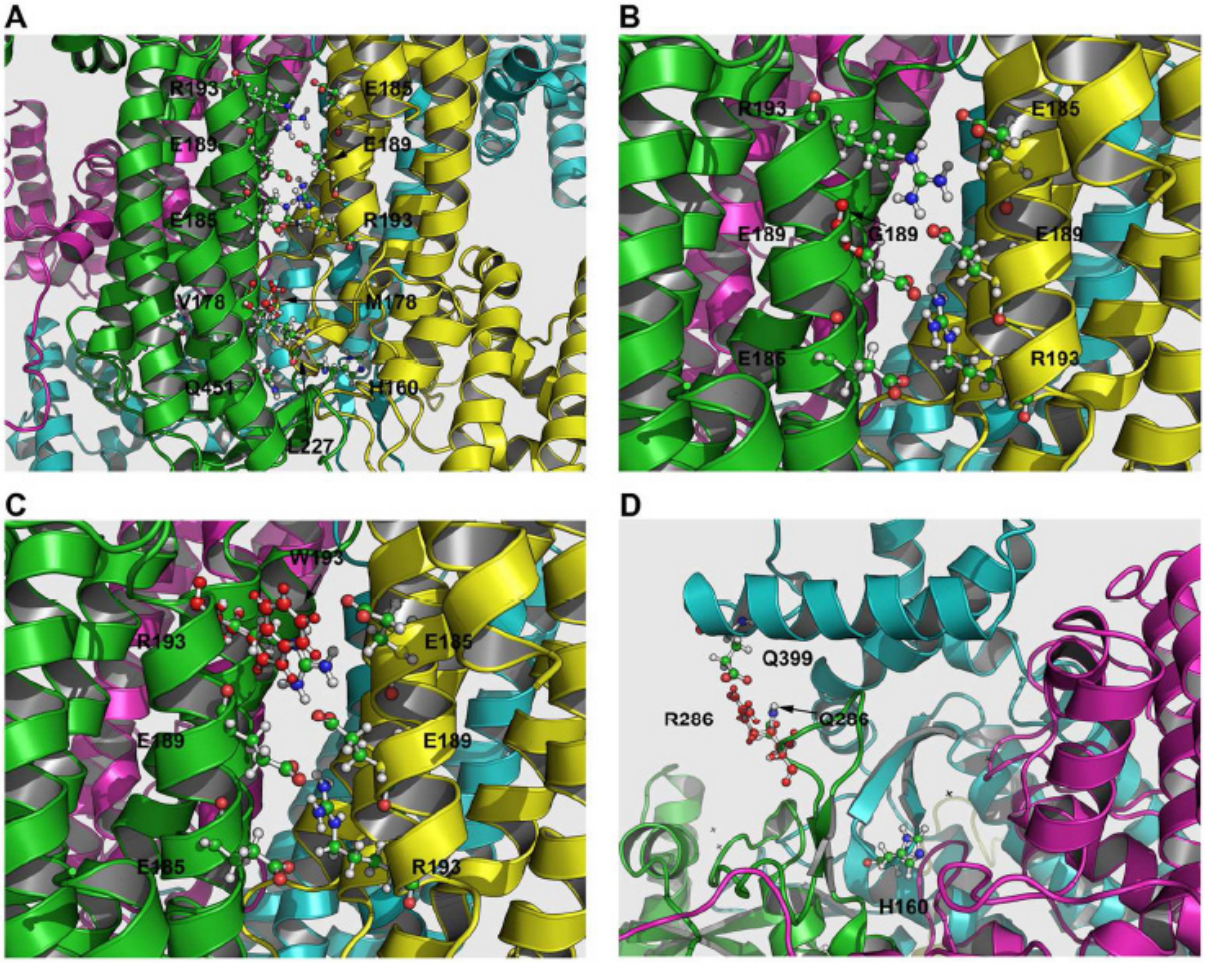

Figure 7: Structural analysis of the ASL mutants V178M, E189G, R193W and Q286R.

ASL structure is shown as a ribbons model with different subunits coloured in *green*, *cyan*, *magenta* and *yellow*. Interacting residues are shown as ball and stick models. Mutated residue is shown in *red*. **A: Interactions of valine 178.** The valine 178 residue is located at the end of the central core helix bundle that forms the ASL tetramer but does not have a major role in formation of the central core of the

structure. The minor effects caused by mutation of valine 178 to methionine are predicted to be stabilized by ionic interactions between arginine 193 and glutamate 185 and glutamate 189 on different subunits (shown in *green* and *yellow*). **B: Interactions of glutamate 189.** The ASL tetramer is formed by ionic interactions between arginine and glutamic acid residues on two adjacent dimeric ASL units (*green-cyan*, *magentayellow*). Ionic interactions between arginine 193 on one subunit with glutamate 189 and glutamate 185 of the adjacent subunit are crucial for the central core helix structure. Upon Glu189Gly mutation, the arginine 193 of the adjacent ASL monomer still forms hydrogen bonds with the glutamate 185 so the structure will still be stable but the overall stability is predicted to be lower than in the WT enzyme. **C: Interactions of arginine 193.** The arginine 193 residue is crucial for complex formation and its mutation to tryptophan destroys ionic interactions with the glutamate 185 and glutamate 189 residues on the opposite subunit (shown in *yellow*) and results in an unstable structure. **D: Interactions of glutamate 286.** The glutamine 286 residue is part of the flexible 280`s loop which is important for substrate entry and exit and mutation of gln286 to arginine results in hydrogen bond formations with the glutamine 399 from another ASL unit (shown in *cyan*). The structural rigidity imposed on the flexible 280’s loop would impact substrate binding and catalysis.

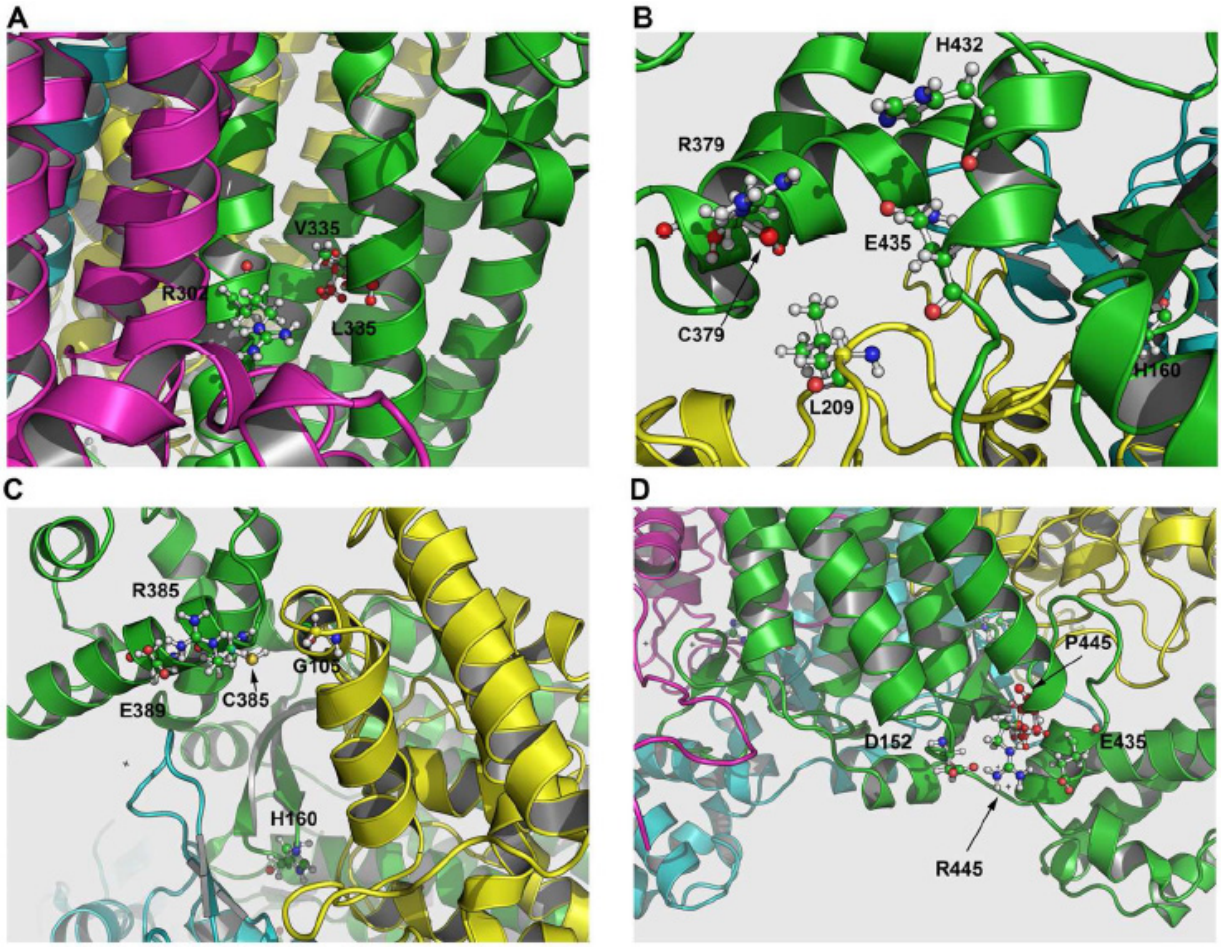

Figure 8: Structural analysis of the ASL mutants V335L, R379C, R385C and R445P.

ASL structure is shown as a ribbons model with different subunits coloured in *green*, *cyan*, *magenta* and *yellow*. Interacting residues are shown as ball and stick models. Mutated residue is shown in *red*. **A: Interactions of valine 335.** The valine 335 group interacts with residues on same alpha helix as well as another adjacent parallel alpha helix of the same ASL unit (shown in *green*). The valine 335 to leucine mutation does not have major impact on the structure. An extra hydrophobic interaction with arginine 302 of the same ASL unit occurs after the mutation of valine 335 to leucine. **B: Interactions of arginine 379.** The arginine 379 forms hydrogen bonds with histidine 432 located on same ASL unit and has hydrophobic interactions with leucine 209 of the adjacent ASL unit. Any major impact on protein structure and function was not predicted. **C: Interactions of arginine 385.** The arginine 385 residue is located near the active site histidine 160 and forms hydrogen bonds with glutamic acid 389 to stabilize the C-terminus helix bundle of ASL monomer. Interactions with glutamic acid 389 of the same ASL unit (*green*) and glycine 105 of the adjacent unit (*yellow*) were affected by mutation to cysteine. **D: Interactions of**

arginine 445. The arginine 445 residue is involved in stabilizing the C-terminus helix of the ASL monomeric structure (*green*) by formation of hydrogen bonds with aspartate 152 and glutamate 435 which are disrupted after mutation to proline (shown in *red*).

Supplemental Table 1: Oligonucleotide primers used for mutagenesis reactions

Mutation		Primer sequence (5'-3')*	Annealing T (°C)
c.35G>A	p.Arg12Gln	forward: TGGGGTGGCC**A**GTTTGTGGGTGCA reverse: AAGCTTCCCACTCTCCGAGGCCAT	81.2 74.4
c.91G>A	p.Asp31Asn	forward: TCCATTGCCTAC**A**ACCGGCACCTT reverse: CGCGTTGAACTTCTCCATGATGGG	74.6 74.2
c.283C>T	p.Arg95Cys	forward: CAATGAGCGC**T**GCCTGAAGGAGCT reverse: GCTGTGTGGATGTCCTCATCATTG	75.2 70
c.299T>C	p.Ile100Thr	forward: AGGGAAGCTGCACACGGGACGGAG reverse: GCCGTTGCACCA**G**TGAGCTCCTTC	78.5 75.7
c.532G>A	p.Val178Met	forward: TGAGCCACGCC**A**TGGCACTGACCC reverse: GAATCCAGTGGCTCCAGCGGATGG	77 81.3
c.566A>G	p.Glu189Gly	forward: CGGATCAATGTCCTGCCCCTGGGG reverse: CTTCCGCACC**C**CCAGCAGCCGCTC	79.8 83.2
c.577 C>T	p.Arg193Trp	forward: GAGGTGCGGAAG**T**GGATCAATGTC reverse: CAGCAGCCGCTCAGAGTCTCGGGT	71.5 77.4
c.857A>G	p.Gln286Arg	forward: CCTGATGCCCCC**G**GAAGAAAAACCC reverse: CTGCTTCCCGTGCTGTAGGCATCT	73.2 75.9
c.1003 G>T	p.Val335Leu	forward: GCTGTGTTTGAA**T**TGTCAGACACT reverse: TTCCTTGTCCTCCTGTAAGTCTTTG	64.6 65.7
c.1135C>T	p.Arg379Cys	forward: ATTACCTGGTC**T**GCAAAGGGATGC reverse: AGGCAAGGTCAGTGGCCAGCATGT	70 75.6
c.1153C>T	p.Arg385Cys	forward: GATGCCATTC**T**GCCAGGCCCACGA reverse: CCTTTGCGGACCAGGTAATAGGCA	79.9 72.3
c.1154G>T	p.Arg385Leu	forward: GATGCCATTCC**T**CCAGGCCCACGA reverse: CCTTTGCGGACCAGGTAATAGGCA	79 72.3
c.1334 G>C	p.Arg445Pro	forward: GGCACTGCGC**C**CTCCAGCGTCGAC reverse: GCCCAGGGCACCATACTGCTCCAC	83.2 76.9

* Primers were purified with high performance liquid chromatography (HPLC) and phosphorylated at the 5'-end. Bold and underlined letters indicate the position of the point mutation.

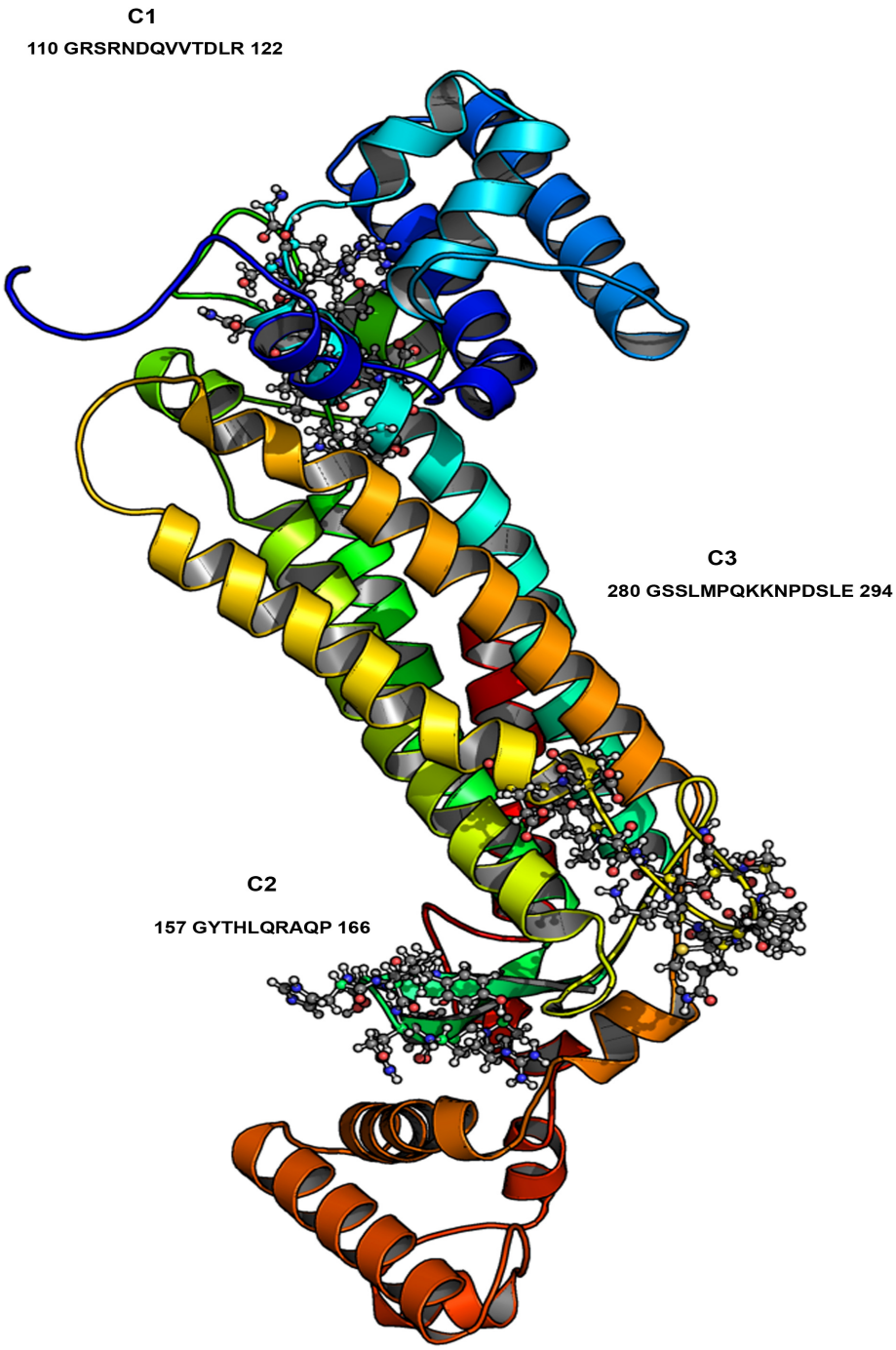

Supplemental Figure 1: Structure of human ASL monomer shown as a ribbon model.

The protein is shown in rainbow colours with *violet* at N-terminus and *red* at C-terminus. The three distinct helix bundles forming distinct domains of the ASL monomer are visible. The highly conserved residues are shown as ball and stick models in *grey*. The three conserved regions are labelled as C1, C2 (contains active site His160) and C3 (contains 280's loop with Gln286).

3.3 Chapter 3

Molecular Characterization of the Only Frequently Recurrent Mutation in Carbamoyl Phosphate Synthetase 1 Deficiency

Liyan Hu[1,2], Carmen Diez-Fernandez[3], Véronique Rüfenacht[1,2], Erdogan Soyucen, Mahmut Çoker, Bilge Tanyeri, Jordi Pérez Tur[3], Vicente Rubio[3,4], Johannes Häberle[1,2]

[1]*Division of Metabolism, University Children's Hospital, 8032 Zurich, Switzerland*
[2]*Children's Research Center, 8032 Zurich, Switzerland*
[3]*Instituto de Biomedicina de Valencia (IBV-CSIC), Valencia, Spain*
[4]*Group 739, Centro de Investigación Biomédica en Red para Enfermedades Raras (CIBERER-ISCIII), Valencia, Spain*

(Manuscript in preparation)

Keywords
Urea cycle, carbamoyl phosphate synthetase 1 (CPS1) deficiency, recurrent mutation, recombinant protein, baculovirus/insect cell expression system, enzyme activity, thermostability

Abbreviations
hCPS1, human carbamoyl phosphate synthetase 1; CPS1D, carbamoyl phosphate synthetase 1 deficiency; DSF, differential scanning fluorimetry; V1013del, CPS1-valine 1013 deletion; CP, carbamoyl phosphate; NAG, N-acetyl-L-glutamate

Abstract

Carbamoyl phosphate synthetase 1 deficiency (CPS1D), due to *CPS1* mutations, is a rare autosomal-recessive urea cycle disorder causing hyperammonemia that can lead to death or severe neurological impairment. CPS1 catalyzes carbamoyl phosphate formation from ammonia, bicarbonate and two ATPs, and requires the essential allosteric activator N-acetyl-L-glutamate. Clinical mutations were found spreading over the entire *CPS1* coding region, occurring mainly in single families, with little recurrence. We characterize here the only known frequently recurrent *CPS1* mutation, p.Val1013del, found in nine unrelated patients of Turkish descent using recombinant His-tagged wild type (WT) or mutant CPS1 expressed in baculovirus/insect cells. The global CPS1 reaction and the ATPase and ATP synthesis partial reactions that reflect, respectively, the bicarbonate and the carbamate phosphorylation steps, were assayed. Structural modelling was performed to rationalize the p.Val1013del effects. We found that CPS1 WT and V1013del mutant were expressed at comparable level and were purified to homogeneity but the mutant CPS1 exhibited no significant residual activities in the assays for the global or partial reactions. In the CPS1 structural model, V1013 belongs to a highly hydrophobic β-strand at the middle of the central β-sheet of the A subdomain of the carbamate phosphorylation domain (an ATP-grasp domain). It is close to the predicted carbamate tunnel that links both phosphorylation sites, being just five residues away from E1018, which is predicted to belong to the tunnel wall. The mutation p.V1013del inactivates the enzyme but does not render the enzyme grossly unstable or insoluble. The deletion, by shortening the β-strand, could pull E1018 away from the carbamate tunnel, distorting this tunnel and possibly hampering the connection between both phosphorylation steps.

Introduction

Carbamoyl phosphate synthetase 1 deficiency (CPS1D; OMIM #237300) caused by mutations in the human *Carbamoyl phosphate synthetase 1* (*CPS1*, MIM #608307) gene is a rare autosomal-recessive urea cycle disorder (UCD) with an estimated incidence of 1:50,000-1:100,000 based on the reports of the Japanese and American cohorts [1]. Like in other urea cycle disorders, CPS1D patients present hyperammonemia leading to death or to severe neurological impairments. CPS1D is biochemically in plasma characterized by high ammonia and glutamine and low

citrulline levels with no increase in urine orotic acid (which is the marker for another mitochondrial UCD, ornithine transcarbamylase (OTC) deficiency). CPS1D can be identified as lethal neonatal onset within the first days of life but also less severe late onset is described in children or adults [2-3]. The severity of the clinical presentation varies depending on the time of onset and the level of residual enzyme activity.

Human *CPS1* is located on chromosome 2q34-35 [4] and is comprised of 38 exons with 4500 nucleotides coding sequence [5-7]. To date, more than 220 mutations have been detected over the entire *hCPS1* coding region [1-3, 8-13]. Different types of mutations were described, including single-nucleotide substitutions (~77%) with preference of missense changes (~61%), deletions (~14%), small insertions or duplications (~7%), indels (~2%), and nonsense mutations (~7%) [1]. A certain number of missense mutations are non-recurrent [1, 5-6, 8, 10, 12-14]. Only very few of the missense mutations (<10%) recur in different families [1].

CPS1 (EC 6.3.4.16) is the first rate-limiting urea cycle enzyme which catalyzes the synthesis of carbamoyl phosphate (CP) from ammonia, bicarbonate and two molecules of ATP [1, 7, 15-22]. The complex reaction requires the cofactor N-acetyl-L-glutamate [23] and takes place in three sequential steps, namely, bicarbonate phosphorylation, carbamate formation from carboxyphosphate and ammonia, and carbamate phosphorylation [24-25]. The bicarbonate-dependent ATPase partial reaction and the partial reaction of ATP synthesis from ADP and carbamoyl phosphate reflects the steps of bicarbonate phosphorylation, respectively [18, 24-26]. CPS1 is highly expressed in liver [27] and can also be detected in small intestine [28] as well as in pancreas [27].

Expression systems for investigations of the functional relevance of missense mutations associated with CPS1D were developed using bacteria [26] or insect cells [29-30], or, in the case of a common single nucleotide polymorphism (p.Thr1406Asn), yeast (*Schizosaccharomyces pombe*) [31]. Hereby, the role of specific residues and amino acid changes and their functional consequences for CPS1 function were defined. Importantly, at least the recombinant human CPS1 expressed in the baculovirus/insect system showed essentially the same kinetic and molecular properties as the natural human enzyme allowing reliable characterization of disease-causing mutations [30].

In this study, we expressed the recombinant human CPS1 in insect Sf9 cells to characterize the molecular basis of the only recurrent mutation, the deletion of a

valine 1013 residue (p.Val1013del) in the carbamate phosphorylation domain of the *CPS1* gene, which was found in nine Turkish CPS1D patients from apparently unrelated families. We found that CPS1 WT and p.Val1013 deleted mutant (CPS1-V1013del) were expressed at comparable level and both purified to >97% purity as judged by SDS-PAGE. However, the CPS1-V1013del mutant yielded no significant residual activity in the global as well as the partial reactions and exhibited thermal instability.

Materials and Methods

Patients' information

The mutation p.Val1013del was found in a homozygous state in nine CPS1D patients of Turkish origin with neonatal onset of disease when mutation analysis using cDNA derived from cultured fibroblasts or stimulated lymphocytes were used as described [8, 32]. Although some of the families originated from Eastern regions in Turkey, there was no apparent relationship between the families. All parents of whom DNA was available (which was the case in five of the nine families) were carriers of the respective mutation confirming segregation on each one parental allele. Clinical information was available for 5/9 patients confirming the severity of CPS1D in all cases. Detailed are listed in Table 1.

Table 1: Details to patients and their families described in this study

Patient	Consanguinity (of parents)	Onset	Max. ammonia (µmol/L)	Extracorporeal detoxification	outcome
1	n.a.	n.a.	n.a.	n.a.	n.a.
2	2nd degree cousins	day 3	2400	PD	died month 4
3	n.a.	n.a.	n.a.	n.a.	n.a.
4	"related"	day 2	1700	CAVHDF	died day 6
5	n.a.	n.a.	n.a.	n.a.	n.a.
6	"related"	day 3	2400	HDF	died week 3
7	"related"	day 3	2500	n.a.	died week 1
8	1st degree cousins	day 1	1980	PD	died day 5
9	n.a.	n.a.	n.a.	n.a.	n.a.

CAVHDF: continuous arterio-venous hemodiafiltration; HDF: hemodiafiltration; n.a.: no information available; PD: peritoneal dialysis

Generation of wild type and mutant CPS1 constructs

The recombinant mature human CPS1 WT construct carrying a His6-tag at the N-terminal position hereby replacing the mitochondrial targeting sequence (pFastBac-CPS1-WT) was generated as described previously [30]. Based on the pFastBac-CPS1-WT, site-directed mutagenesis was performed by the overlapping extension method (Quickchange kit from Stratagene) using the forward V1013delF' (5'GACGGTGGTGAATTGCAATCCTGAGAC3') and reverse V1013delR' (5'GTCTCAGGATTGCAATTCACCACCGTC3') primers yielding the mutant pFastBac-CPS1-V1013del. The established CPS1 constructs were verified by sequencing using the BigDye Terminator cycle sequencing kit version 1.1 (ABI sequence, Applied Biosystems).

Recombinant human CPS1 protein expression, purification and Western blot analysis

The CPS1 constructs were expressed by using the Bac-to-Bac® Baculovirus Expression System (Invitrogen) as described before [30]. In brief, the plasmids pFastBac-CPS1-WT and pFastBac-CPS1-V1013del were transformed into *E. coli* DH10Bac competent cells by heat shock. The individual bacmids containing the recombinant CPS1 constructs were extracted using the blue white screen and further verified by PCR screening. The Sf9 insect cells were grown in a shaker flask with serum-free SF 900 II SFM cell culture medium (Invitrogen) containing 0.1% Pluronic F-68 (Invitrogen) and 0.5% penicillin/streptomycin solution (Sigma) and incubated at 27^{o}C with orbital shaking at 125 rpm in a humidified atmosphere. Cells were transfected with bacmids carrying CPS1 WT or mutant (CPS1 c.3037-3039del) cDNA using Cellfectin II Reagent/Grace medium in a 6-well plate for 5 hours according to the manufacturer's instructions (Invitrogen) followed by 3-day culture in growth medium without shaking. The produced baculovirus was enriched for 2 days prior to infecting the Sf9 cells for CPS1 expression. The infected cells were harvested after 3 days by centrifugation at 300g for 10 min.

The cell pellets containing recombinant His-tagged human CPS1 WT or mutant proteins were lysed followed by purification using a HisTrap HP 1-ml column fitted in an AKTA FPLC system (GE Healthcare). The CPS1-containing fractions monitored by SDS-PAGE (8% polyacrylamide gel) with Coomassie staining were pooled, concentrated to >1 mg protein/ml using centrifugal ultrafiltration (100-kDa

cutoff membrane, Amicon Ultra, Millipore), enriched with extra 10% glycerol and 1mM dithiothreitol (DTT), and snap frozen at –80°C. The concentrations of purified CPS1 proteins were determined by the method of Bradford [33] using bovine serum albumin as a standard.

Western blotting was performed as described by Laemmli [34]. Cell extracts (~ 20 µg of with baculovirus infected CPS1 protein) were separated by 8% denaturing SDS-PAGE, and subsequently transferred to nitrocellulose transfer membranes (Whatman GmbH, Dassel, Germany). The primary monoclonal antibody anti-6xHis (Clontech, CA) was used at a dilution of 1:7500, and the horseradish peroxidase-conjugated secondary antibody anti-mouse (Santa Cruz Biotechnology) was used at a dilution of 1:5000. Antibody against β-actin (Santa Cruz Biotechnology) served as loading controls. Protein detection was done using ECL reagents (GE Healthcare) for chemiluminescent labelling and the densitometry of detected bands was analysed by Carestream Molecular Imaging software (Carestream Health) to judge the purity of produced proteins.

Enzyme activity assays

The CPS1 enzyme overall and partial activities were determined colorimetrically as described before [26, 30, 35-36]. The overall CPS1 activity was measured as the citrulline production converted from CP by coupling with ornithine and ornithine transcarbamylase (OTC) [37-38]. Briefly, the purified CPS1 proteins were diluted at 1 mg/ml in a solution (50mM glycyl-glycine pH 7.4, 0.5 M NaCl, 10% Glycerol and 2 mM DTT) and incubated at 37^{o}C for 10 min following another incubation for 10 min in a standard assay mixture (50mM glycyl-glycine pH 7.4, 70 mM KCl, 1 mM DTT, 20 mM $MgSO_4$, 5 mM ATP, 35 mM NH_4Cl, 50 mM $KHCO_3$, 10 mM NAG, 5 mM L-ornithine, and 4 U/ml OTC (Sigma)). The reaction was stopped by adding 800 µl of a stop solution containing 0.04 M antipyrine, 0.01 M ammonium iron (III) sulphate, 50% sulfuric acid, 50% orto-phosphoric acid, 7.5% NaCl and 0.4% 2,3-butanedione and followed by incubation in a boiling water bath for 16 min prior to photometrically measurement at 464 nm. The partial ATPase reaction was measured in pyruvate kinase/lactate dehydrogenase coupled assay by monitoring continuously ADP production as NADH oxidation at 340 nm [30, 39] with the following modifications: 50 mM $KHCO_3$ and 10 mM NAG were sequentially added to the assay mixture after respective measurement for 10 min at 37^{o}C. The partial reaction of ATP synthesis

was measured by monitoring continuously ATP production with the increase in the absorbance at 340 nm [26, 30] with the following modifications: 50 mM, 6 µg/ml and 20 µg/ml replaced 15 mM $MgSO_4$, 0.1 mg/ml hexokinase and 25 µg/ml glucose-6-phosphate dehydrogenase, respectively; 5 mM CP and 10 mM NAG were sequentially added to the assay mixture after respective measurement for 10 min at 37^{o}C. The measured extinctions were corrected with the extinctions of a blank containing protein and all reagents except for NAG. One CPS1 unit produces per minute 1 µmol citrulline or 2 µmol ADP. All assays were carried out in duplicate for at least three independent measurements.

Differential scanning fluorimetry

To monitor thermal unfolding of proteins in the presence of a fluorescent dye, differential scanning fluorimetry (DSF) was performed and analyzed as described previously [40-41] with following modifications: purified CPS1 proteins were diluted to 0.1 mg/ml in buffer (50mM glycyl-glycine pH 7.4) with Sypro Orange (Roche) at final concentration of 2-folds and run in duplicate. Briefly, the proteins were heated from 20 to 95^{o}C with a ramp rate of 0.57^{o}C/sec in a LightCycler 480 (Roche, Switzerland). The obtained fluorescence was normalized as relative fluorescence so that minimum fluorescence was set to 0 and maximum fluorescence set to 1. The value V_{50} (^{o}C) indicating the temperature at which 50% of protein is melted (T_m), was determined by Boltzmann sigmoidal analysis after curve fitting using GraphPad Prism 4 (GraphPad Software, San Diego, CA, USA).

Structural modelling

The computational structural modelling was performed using previously reported atomic structure model of CPS1 based on the experimental crystal structure of *E. coli* CPS [42] to rationalize the mutation effect. Pymol (DeLano Scientific; http://www.pymol.org) was used for visual analysis, for structural superimposition and for depicting protein structures.

Statistics

All statistics were analysed by one-tailed and two-tailed Student's T-tests using the program GraphPad Prism 4 (GraphPad Software). Differences were considered as significant if the *p* value was <0.05.

Results

Recombinant CPS1-V1013del mutant yields highly purified protein production

In order to characterize the molecular basis of the only known frequently recurrent *CPS1* mutation p.Val1013del, we first introduced recombinant His-tagged CPS1 constructs carrying WT or mutant V1013del cDNA into insect Sf9 cells to express CPS1 proteins using the previously reported baculovirus/insect cell system. At the protein level, expression of mature CPS1 WT or V1013del was detected in the infected Sf9 cells at comparable level by Western blot analysis (Fig. 1A) indicating the recombinant mutant V1013del was as stable expressed as WT. A multiplicity of bands of lower molecular weight could be observed in both CPS1 forms indicating the occurrence of CPS1 degradation. Next, we purified the two CPS1 proteins using Ni-affinity chromatography and yielded >97% purity for both as judged by Coomassie-stained SDS-PAGE (Fig. 1B). Taken together, these findings suggest that the deletion of valine 1013 in the CPS1 protein does not lead to misfolding or lower expression levels of mutated CPS1.

Figure 1: Expression and purification of CPS1 WT and V1013del

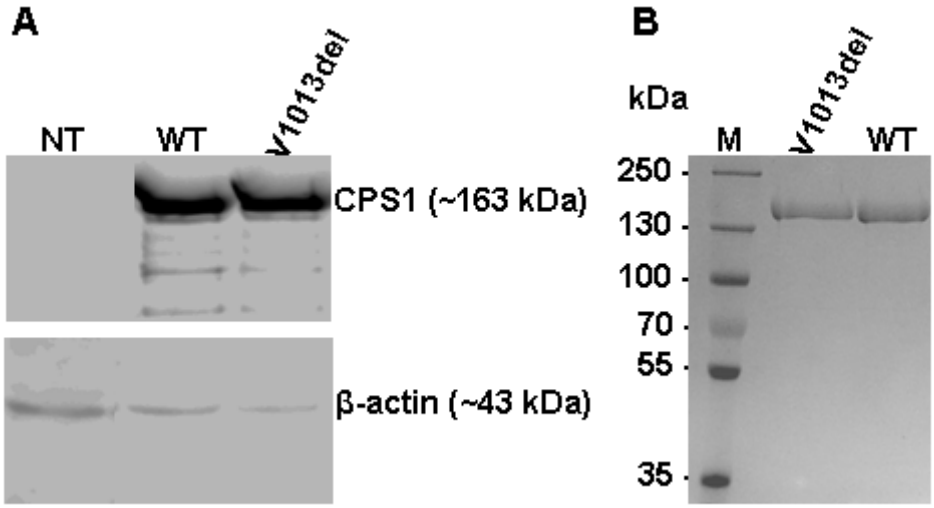

Fig. 1: A: Western blot analysis of CPS1 expression (~163 kDa) of WT and V1013del in baculovirus-infected Sf9 cell extracts (~20 µg of total protein) by 8% SDS-PAGE. NT: non-transfected Sf9 cells. β-actin (~ 43 kDa) served as loading control. **B:** Coomassie-stained SDS-PAGE (8%) analysis showing the purity of purified CPS1 WT and V1013del proteins. M: protein ladder.

CPS1-V1013del yields no significant CPS1 activity

To determine whether the stably expressed CPS1-V1013del mutant harbours residual CPS1 activity compared to WT, we measured the CPS1 global activity as well as the partial reactions of ATPase and ATP synthesis by monitoring continuously ADP or ATP production, respectively (Table 2, Fig. 2). The mutant V1013del yielded no significant residual activities in the enzyme activity assays for the CP synthesis reaction or for the ATPase and ATP synthesis (Fig. 2) partial reactions compared to those of WT, suggesting that the deletion strongly impaired global CPS1 activity as well as both ATPase and ATP synthesis partial CPS1 activities reflecting the bicarbonate and the carbamate phosphorylation reactions, respectively. Our findings indicate that the deletion of V1013 residue hampers both bicarbonate and carbamate phosphorylation steps.

Table 2: Enzymatic properties of CPS1 WT and mutant V1013del

Enyzme	**Global reaction** (µmol CP/min*mg)	**Partial reactions** (µmol ADP/min*mg)		**Thermostability**
	CP synthesis	**ATPase**	**ATP synthesis**	**T_m=V_{50} (^oC)**
WT (± S.D)	0.8184 ± 0.1441	0.0561 ± 0.0046	0.0233 ± 0.0136	58.99 ± 0.49
V1013del (± S.D)	0.0056 ± 0.0023	0.0010 ± 0.0017	0.0004 ± 0.0002	57.51 ± 0.66[#]

Assays were carried out at 37^{o}C. S.D.: standard deviation.

[#] indicates a V_{50} value significantly lower than WT ($p<0.0001$).

Figure 2: Relative CPS1 enzyme global activity and partial activities

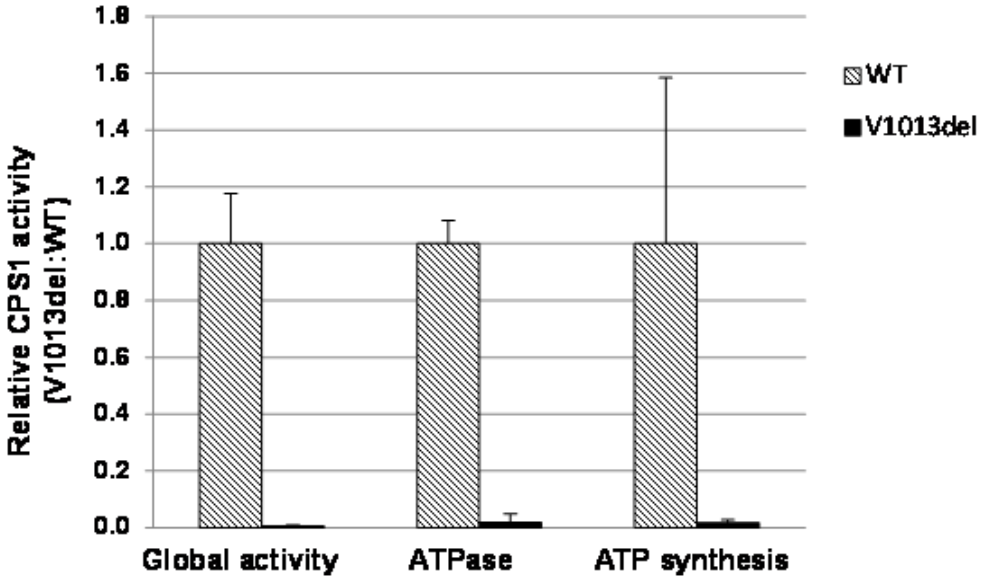

Fig. 2: Relative CPS1 enzyme global activity and partial activities of ATPase and ATP synthesis (standard assay conditions) of the purified V1013del to WT CPS1 protein. CPS1 global activity in µmol CP/min*mg protein, partial ATPase and ATP synthesis activity in µmol ADP/min*mg protein. Error bars indicate standard deviations.

CPS1-V1013del is less stable than wild type

In order to further investigate whether the mutation p.Val1013del causes protein instability, we performed the thermostability assay by DSF. The melting point of the protein (T_m) is determined by using heat-caused denaturated protein which is bound to a sensitive dye (such as Sypro orange) with high fluorescence [43-44]. We found that the mutant V1013del showed a lower melting temperature (57.51 ± 0.66^{o}C) than that of WT (58.99 ± 0.49^{o}C) (Table 2 and Fig. 3), and this difference was significant ($p<0.0001$) indicating that the mutant V1013del is less stable than WT CPS1.

Figure 3: Thermostability assay of CPS1 WT and V1013del

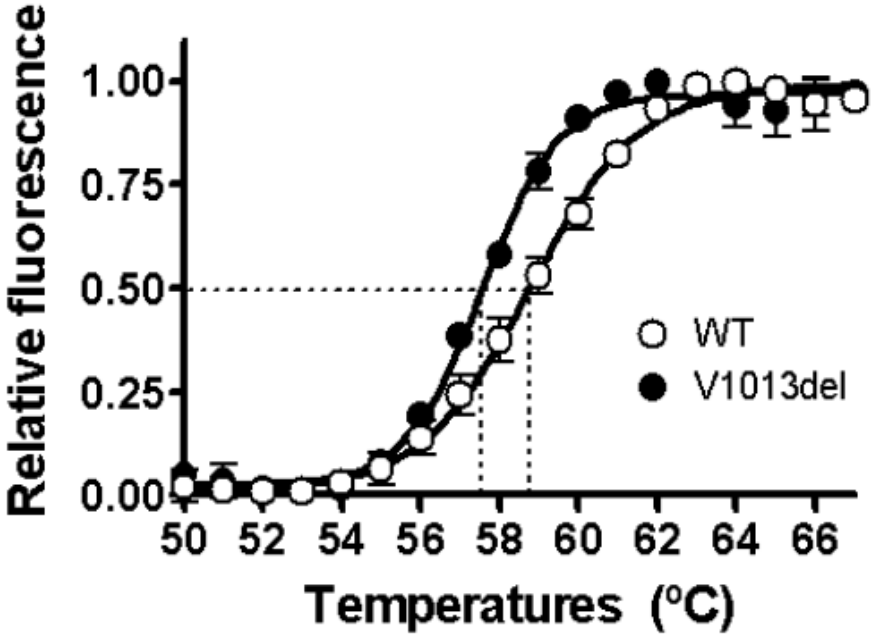

Fig. 3: Protein stability was determined by DSF. The horizontal dashed line marks 50% of fluorescence, whereas the vertical dashed lines crossing the X-axis indicate the melting temperatures (T_m) at which 50% of each protein is melted. The value V_{50} (^oC) was determined as T_m by Boltzmann sigmoidal analysis after curve fitting using GraphPad Prism 4. All assays were carried out in duplicate at least from three experiments. Error bars indicate the standard deviation.

Role of V1013 residue in the CPS1 protein structure

To rationalize the mutation effect, the computational structural modelling was performed based on the experimental crystal structure of *E. coli* CPS [42]. In the CPS1 structural model, valine 1013 belongs to a highly hydrophobic β-strand at the middle of the central β-sheet of the A subdomain of the carbamate phosphorylation domain (the second ATP-grasp domain) (Fig. 4). It is close to the predicted carbamate tunnel that links both phosphorylation sites, being just 5 residues away from E1018, which is predicted to belong to the tunnel wall and located near the carboxy phosphate binding site [26, 45-46]. Additionally, V1013 residue also belongs to a hydrophobic core consisting of 3 consecutive valines, which is conserved in all CPS1 and CPSIII. Moreover, V1013 residue is in the vicinity of a D1025-K450 interaction. The residue K450, located at bicarbonate phosphorylation domain, was shown to be important since there exists a mutation affecting this residue,

p.Lys450Glu [1]. Taken together, the deletion of V1013, by shortening the β-strand, could pull E1018 away from the carbamate tunnel, distorting this tunnel and possibly hampering the connection between both phosphorylation steps abolishing CP production. Moreover, the deletion could abolish the D1025-K450 interaction by shifting the peptides in the vicinity of V1013del, leading to interference of the allosteric signal transmitted between ATP-grasps. Although the mutation inactivates the CPS1 enzyme activity (Table 2, Fig. 2), it does not render the enzyme grossly unstable or insoluble (Fig. 1).

Figure 4: CPS1 computational structural modelling based on the crystal structure of *E. coli* CPS

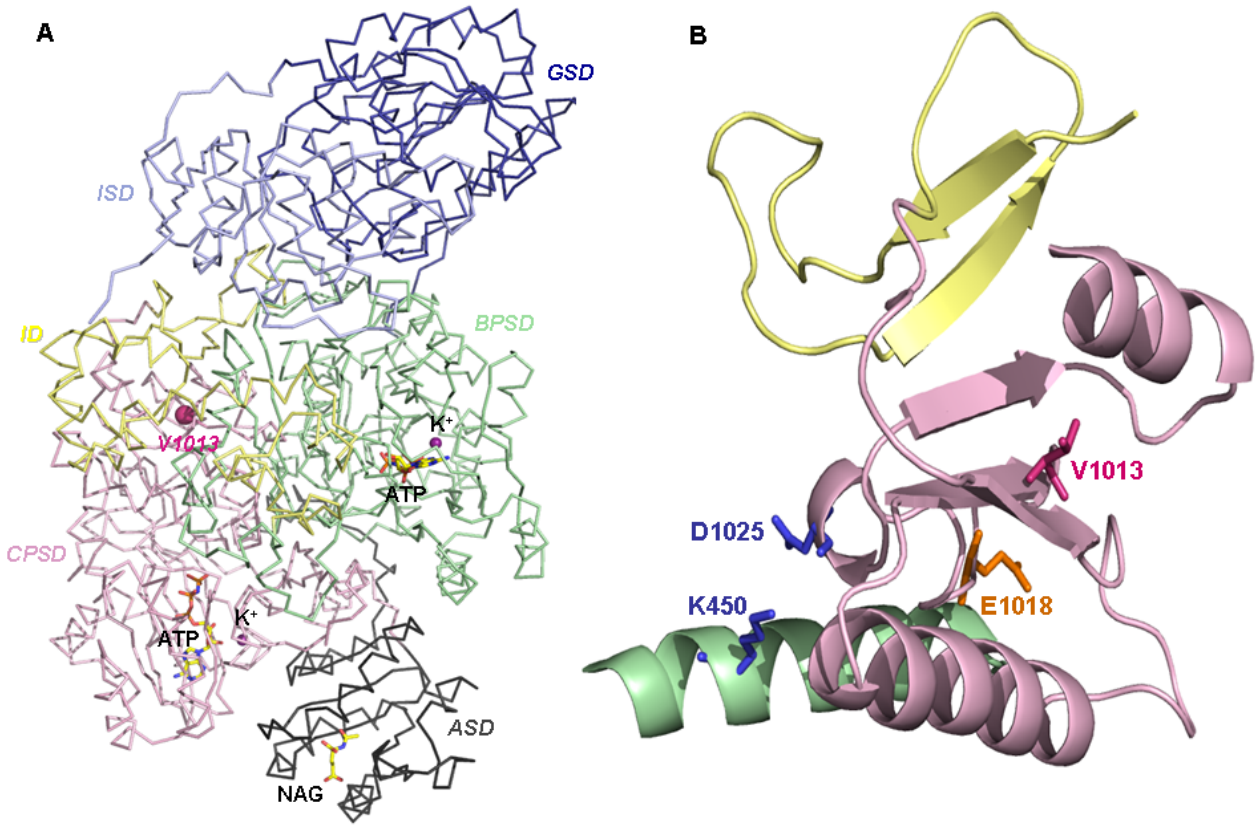

Fig. 4: A: Location of V1013 residual (big atomic structure in *pink*) in structural model of CPS1 consisting of small subunit of N-terminal domain (intersubunit interaction domain (ISD, in *light blue*) and glutaminase domain (GSD, in *blue*)), bicarbonate phosphorylation domain (BPSD, in *light green*), integrating domain (ID, in *yellow*), carbamate phosphorylation domain (CPSB, in *ligh pink*) and allosteric NAG binding domain (in *black*). Other atomic structures indicate the locations of ligands. **B:** Close-up of V1013 residue and its relevant surrounding residues E1018 (in *orange*), D1025 and K450 (both in *blue*).

Discussion

Most mutations known so far in the *CPS1* gene are “private” to the individual families [1]. In this study, we characterized the only frequently recurrent *CPS1* mutation p.V1013del using the recombinant hCPS1 protein expressed in baculovirus/insect cells which allowed production of sufficient amounts of pure CPS1. Importantly, this expression system was shown to reliably predict the disease-causing nature of CPS1 mutations as demonstrated in 35 mutations studied so far [29-30, 47]

The naturally occurring recurrent deletion located at the carbamate phosphorylation domain was found in CPS1D patients with neonatal onset of disease. Since all patients, of whom data were available (5/9), presented shortly after birth on day 1 to 3 and furthermore all died during the neonatal period or in early infancy, a severe impact of p.Val1013del on CPS1 function could be expected. In fact, we show here that the mutant p.V1013del, despite high protein expression levels and purity (>97%) (Fig. 1) did not exhibit any significant residual activities in the global reaction of CP production or in both ATPase and ATP synthesis partial reactions (Fig. 2). The low yields of most mutants studied so far were considered to be due to poor CPS1 polypeptide production and to gross misfolding resulting in less solubility of pure CPS1 protein and this was identified as a key element in determining the disease-causing role in missense mutations [47]. Our results indicate that the deletion of valine1013 residue does not hamper global CPS1 folding and architecture, as suggested by the unaffected production of soluble CPS1 protein.

The CPS1 activity assays for the overall and partial reactions allow a detailed investigation of the single CPS1 reactions and, in addition, to reveal the specific role of individual residues [26]. In general, the CPS1 mutations located within the bicarbonate domain interfere with the enzyme’s ability to phosphorylate bicarbonate, whereas mutations in the carbamate domain specifically perturbe carbamate phosphorylation, which is reflected in the ATPase and ATP synthesis partial reactions, respectively [26, 46, 48]. As expected, the mutant p.V1013del yielded no significant residual activity in the overall rate of CP synthesis nor in ATP synthesis partial reaction compared with CPS1 WT protein (Fig. 2A,C). The perturbation of the rate of the partial ATP synthesis reaction indicates that the catalytic machinery at the carbamate phosphorylation domain is seriously affected. Furthermore, the mutant also completely impaired the ATPase partial reaction, even though the site of

mutation is distant from the catalytic site of bicarbonate phosphorylation domain (Fig. 2B).

Since the human CPS1 crystal structure is not yet elucidated, structural predictions rely on the *E. coli* CPS structural modelling. According to this, the deletion of V1013 residue is expected to deform the carbamate tunnel, since it is located close to Glu1018, which is part of the carbamate tunnel, and corresponds to Glu604 in *E. coli* CPS [42, 46, 49]. Additionally, deletion of V1013 residue probably causes the abolishment of an interaction K450-D1025, which bridges the two ATP grasps, leading to the blockage of allosteric signal transmission between ATP-grasps. Moreover, deletion of V1013 residue perturbs the conserved hydrophobic core which might result in instability in the enzyme. Indeed, the thermostability analysis using DSF showed that the mutant is less stable (Fig. 3). Thus, the diminished rate of CP production can be rationalized by a deformed carbamate tunnel resulting in disconnection between both phosphorylation sites and by the perturbation of an interaction between both ATP-grasps. Taken together, these findings suggest the pathogenic role of this recurrent deletion found in CPS1D patients.

Acknowledgements

We thank Dr. D.S. Froese and P. Forny (Zurich, Switzerland) for the technical assistance and helpful suggestions by DSF experiments. This work was supported by Swiss National Science Foundation (grant 310030_127184 to J.H.).

References

1. Häberle, J., et al., *Molecular defects in human carbamoyl phosphate synthetase I: mutational spectrum, diagnostic and protein structure considerations.* Hum Mutat, 2011. **32**(6): p. 579-89.
2. Ono, H., et al., *A case of carbamoyl phosphate synthetase 1 deficiency presenting symptoms at one month of age.* Brain Dev, 2009. **31**(10): p. 779-81.
3. Klaus, V., et al., *Highly variable clinical phenotype of carbamylphosphate synthetase 1 deficiency in one family: an effect of allelic variation in gene expression?* Clin Genet, 2009. **76**(3): p. 263-9.

4. Summar, M.L., et al., *Physical and linkage mapping of human carbamyl phosphate synthetase I (CPS1) and reassignment from 2p to 2q35.* Cytogenet Cell Genet, 1995. **71**(3): p. 266-7.
5. Häberle, J., et al., *Gene structure of human carbamylphosphate synthetase 1 and novel mutations in patients with neonatal onset.* Hum Mutat, 2003. **21**(4): p. 444.
6. Funghini, S., et al., *Structural organization of the human carbamyl phosphate synthetase I gene (CPS1) and identification of two novel genetic lesions.* Hum Mutat, 2003. **22**(4): p. 340-1.
7. Summar, M.L., et al., *Characterization of genomic structure and polymorphisms in the human carbamyl phosphate synthetase I gene.* Gene, 2003. **311**: p. 51-7.
8. Rapp, B., et al., *Genetic analysis of carbamoylphosphate synthetase I and ornithine transcarbamylase deficiency using fibroblasts.* Eur J Pediatr, 2001. **160**(5): p. 283-7.
9. Funghini, S., et al., *Carbamoyl phosphate synthetase 1 deficiency in Italy: clinical and genetic findings in a heterogeneous cohort.* Gene, 2012. **493**(2): p. 228-34.
10. Summar, M.L., *Molecular genetic research into carbamoyl-phosphate synthase I: molecular defects and linkage markers.* J Inherit Metab Dis, 1998. **21 Suppl 1**: p. 30-9.
11. Wang, J., et al., *Molecular characterization of CPS1 deletions by array CGH.* Mol Genet Metab, 2011. **102**(1): p. 103-6.
12. Aoshima, T., et al., *Novel mutations (H337R and 238-362del) in the CPS1 gene cause carbamoyl phosphate synthetase I deficiency.* Hum Hered, 2001. **52**(2): p. 99-101.
13. Aoshima, T., et al., *Carbamoyl phosphate synthetase I deficiency: molecular genetic findings and prenatal diagnosis.* Prenat Diagn, 2001. **21**(8): p. 634-7.
14. Finckh, U., et al., *Prenatal diagnosis of carbamoyl phosphate synthetase I deficiency by identification of a missense mutation in CPS1.* Hum Mutat, 1998. **12**(3): p. 206-11.
15. Nyunoya, H., et al., *Characterization and derivation of the gene coding for mitochondrial carbamyl phosphate synthetase I of rat.* J Biol Chem, 1985. **260**(16): p. 9346-56.

16. Oyanagi, K., et al., *A study of urea-synthesizing enzymes in prenatal and postnatal human liver.* Pediatr Res, 1980. **14**(3): p. 236-41.
17. Rubio, V. and S. Grisolia, *Human carbamoylphosphate synthetase I.* Enzyme, 1981. **26**(5): p. 233-9.
18. Rubio, V., G. Ramponi, and S. Grisolia, *Carbamoyl phosphate synthetase I of human liver. Purification, some properties and immunological cross-reactivity with the rat liver enzyme.* Biochim Biophys Acta, 1981. **659**(1): p. 150-60.
19. Rubio, V., *Structure-function studies in carbamoyl phosphate synthetases.* Biochem Soc Trans, 1993. **21**(1): p. 198-202.
20. Rubio, V. and J. Cervera, *The carbamoyl-phosphate synthase family and carbamate kinase: structure-function studies.* Biochem Soc Trans, 1995. **23**(4): p. 879-83.
21. Ryall, J., et al., *Expression of nuclear genes encoding the urea cycle enzymes, carbamoyl-phosphate synthetase I and ornithine carbamoyl transferase, in rat liver and intestinal mucosa.* Eur J Biochem, 1985. **152**(2): p. 287-92.
22. Schofield, J.P., *Molecular studies on an ancient gene encoding for carbamoyl-phosphate synthetase.* Clin Sci (Lond), 1993. **84**(2): p. 119-28.
23. Grisolia, S. and P.P. Cohen, *Catalytic role of of glutamate derivatives in citrulline biosynthesis.* J Biol Chem, 1953. **204**(2): p. 753-7.
24. Lusty, C.J., *The molecular structure and function of carbamyl phosphate synthetase I.* Trans N Y Acad Sci, 1983. **41**: p. 103-15.
25. Metzenberg, R.L., M. Marshall, and P.P. Cohen, *Carbamyl phosphate synthetase: studies on the mechanism of action.* J Biol Chem, 1958. **233**(6): p. 1560-4.
26. Yefimenko, I., et al., *Understanding carbamoyl phosphate synthetase deficiency: impact of clinical mutations on enzyme functionality.* J Mol Biol, 2005. **349**(1): p. 127-41.
27. Neill, M.A., et al., *Quantitative RT-PCR comparison of the urea and nitric oxide cycle gene transcripts in adult human tissues.* Mol Genet Metab, 2009. **97**(2): p. 121-7.
28. Windmueller, H.G. and A.E. Spaeth, *Source and fate of circulating citrulline.* Am J Physiol, 1981. **241**(6): p. E473-80.

29. Pekkala, S., et al., *Understanding carbamoyl-phosphate synthetase I (CPS1) deficiency by using expression studies and structure-based analysis.* Hum Mutat, 2010. **31**(7): p. 801-8.
30. Diez-Fernandez, C., et al., *Molecular characterization of carbamoyl-phosphate synthetase (CPS1) deficiency using human recombinant CPS1 as a key tool.* Hum Mutat, 2013. **34**(8): p. 1149-59.
31. Ahuja, V. and S.G. Powers-Lee, *Human carbamoyl-phosphate synthetase: insight into N-acetylglutamate interaction and the functional effects of a common single nucleotide polymorphism.* J Inherit Metab Dis, 2008. **31**(4): p. 481-91.
32. Kretz, R., et al., *Phytohemagglutinin stimulation of lymphocytes improves mutation analysis of carbamoylphosphate synthetase 1.* Mol Genet Metab, 2012. **106**(3): p. 375-8.
33. Bradford, M.M., *A rapid and sensitive method for the quantitation of microgram quantities of protein utilizing the principle of protein-dye binding.* Anal Biochem, 1976. **72**: p. 248-54.
34. Laemmli, U.K., *Cleavage of structural proteins during the assembly of the head of bacteriophage T4.* Nature, 1970. **227**(5259): p. 680-5.
35. Pekkala, S., et al., *Structural insight on the control of urea synthesis: identification of the binding site for N-acetyl-L-glutamate, the essential allosteric activator of mitochondrial carbamoyl phosphate synthetase.* Biochem J, 2009. **424**(2): p. 211-20.
36. Britton, H.G., et al., *A structure-reactivity study of the binding of acetylglutamate to carbamoyl phosphate synthetase I.* Eur J Biochem, 1990. **188**(1): p. 47-53.
37. Uriarte, M., et al., *The carbamoyl-phosphate synthetase of Pyrococcus furiosus is enzymologically and structurally a carbamate kinase.* J Biol Chem, 1999. **274**(23): p. 16295-303.
38. Nuzum, C., and Snodgrass, PJ., *in The Urea Cycle* (Grisolía, S., Báguena, R., and Mayor, F., eds), 1975: p. 325-349, John Wiley & Sons, Inc., New York.
39. Guthohrlein, G. and J. Knappe, *Structure and function of carbamoylphosphate synthase. I. Transitions between two catalytically inactive forms and the active form.* Eur J Biochem, 1968. **7**(1): p. 119-27.

40. Niesen, F.H., H. Berglund, and M. Vedadi, *The use of differential scanning fluorimetry to detect ligand interactions that promote protein stability.* Nat Protoc, 2007. **2**(9): p. 2212-21.
41. Froese, D.S., et al., *Thermolability of mutant MMACHC protein in the vitamin B12-responsive cblC disorder.* Mol Genet Metab, 2010. **100**(1): p. 29-36.
42. Martinez, A.I., et al., *Genetic, structural and biochemical basis of carbamoyl phosphate synthetase 1 deficiency.* Mol Genet Metab, 2010. **101**(4): p. 311-23.
43. Lo, M.C., et al., *Evaluation of fluorescence-based thermal shift assays for hit identification in drug discovery.* Anal Biochem, 2004. **332**(1): p. 153-9.
44. Hopper, E.D., et al., *In vivo and in vitro examination of stability of primary hyperoxaluria-associated human alanine:glyoxylate aminotransferase.* J Biol Chem, 2008. **283**(45): p. 30493-502.
45. Kim, J., et al., *Structural defects within the carbamate tunnel of carbamoyl phosphate synthetase.* Biochemistry, 2002. **41**(42): p. 12575-81.
46. Kim, J. and F.M. Raushel, *Access to the carbamate tunnel of carbamoyl phosphate synthetase.* Arch Biochem Biophys, 2004. **425**(1): p. 33-41.
47. Diez-Fernandez, C., et al., *Understanding carbamoyl phosphate synthetase (CPS1) deficiency by using the recombinantly purified human enzyme: effects of clincial CPS1 mutations that concentrate in a central domain of unkown function.* Molecular Genetics and Metabolism (Currently minor revisions), 2014.
48. Javid-Majd, F., et al., *Comparison of the functional differences for the homologous residues within the carboxy phosphate and carbamate domains of carbamoyl phosphate synthetase.* Biochemistry, 1996. **35**(45): p. 14362-9.
49. Thoden, J.B., et al., *Carbamoyl phosphate synthetase: closure of the B-domain as a result of nucleotide binding.* Biochemistry, 1999. **38**(8): p. 2347-57.

4 Concluding remarks and future prospects

In the present work, the established eukaryotic expression systems in mammalian HEK 293T cells and in insect Sf9 cells allow us to study the molecular basis of phenotypic variability and pathology in UCDs referring to ASA and CPS1D, respectively. For instance, we were able to reveal the role of the naturally occurring ASL transcript variants in the phenotypic variability in ASA by co-expression with ASL WT or mutants in 293T cells [159]. This provides a new explanation for the molecular basis in an inherited disease and adds to our understanding of the clinical variability in ASA patients. Further, the established expression system was validated as a reliable system to confirm that relevant residual enzyme activities contribute to the clinical and biochemical variability of ASA.

In addition, we were able to characterize the molecular basis of the only known frequently recurrent *CPS1* mutation (p.Val1013del) using human recombinant CPS1 in a baculovirus/insect cell expression system. This mutation, affecting Val1013 residue, is predicted to be involved in the structural elements of the carbamate tunnel and hereby explains the pathological effect of the mutation. This underlines the value of this model by elucidating the effect of a mutation based on structural and biochemical properties.

With the development of the technology in next generation sequencing and NBS, an increasing number of disease-causing genetic alterations will be identified. However, it remains challenging to determine the relevance of clinical mutations. Generally, genotype-phenotype correlations are still poor in all UCDs. The expression systems we have established can serve as a tool with the intention to facilitate genotype-phenotype studies, in particularly those involving late-onset missense mutations with partial residual enzyme activities. By expression of all known variant ASL mutants associated with late-onset and/or mild clinical and biochemical courses of ASA in 293T cells, this expression system provides higher sensitivity for enzymatic activities and better correlations between the enzyme activity and phenotype compared to those in other reported systems so far [141, 279].

While establishment of *in vitro-in vivo* correlation is feasibly in severe neonatal mutations which cause complete absence of enzyme activity, it is rather difficult in variant mutants with partial residual catalytic activity. In addition, environmental, genetic and biochemical factors need to be considered. First, the *in vivo* enzyme

activity might be sufficient or insufficient to detoxify the nitrogen load depending on the external conditions (e.g. increased protein intake, stress, and medication), intrinsic factors (e.g. age, pregnancy, and health state) or other regulatory factors (e.g. hormones such as glucocorticosteroids and insulin). Second, mechanisms of intragenic complementation within the *ASL* gene [182-185] and of allelic imbalance affecting the *CPS1* gene [261] may also contribute to the difficulty in predicting outcome in these UCDs. Additionally, the co-occurrence of a missense mutation and a splicing variant can contribute to the clinical and biochemical variability [159]. Moreover, the urea cycle enzymes such as ASS and ASL, and intermediate metabolites such as citrulline and arginine are involved in further pathways such as the citrulline-NO cycle. Besides for ureagenesis, arginine is substrate for synthesis of NO, creatine, and polyamines. The involvement of urea cycle metabolites in other pathways adds further to the complexity of disease(s). Ultimately, the different sensitivity of *in-vitro* enzymatic measurements can also be a factor. Thus, additional research is required to further establish more reliable genotype-phenotype correlations.

Better understanding of the disease-causing mechanisms of clinical mutations in UCDs can provide more clues for development of novel therapeutic strategies. Interestingly, in addition to generating a tool for the study of genotype-phenotype correlations, our results also elucidated that some ASL mutants, despite displaying high residual activity, probably affect protein folding caused by thermal instability. This indicates potential novel therapeutic approaches with small molecules as pharmachaperone treatment in order to stabilize those mutants in ASLD, as well as in other UCDs.

Recently, structurally intact ASL was described as a requirement for NO production [124]. Frequent occurrence of alternative splicing is a common phenomenon in *ASL* gene. We identified a predominant presence of one of the most common transcript variants, ex7del ASL, in two ASA patients [159]. In view of these findings, it will be interesting to investigate whether the ASL transcript variants as well as those instable mutants will affect the formation of the NOS complex ultimately leading to NO deficiency. Additionally, it was suggested that NO supplementation should be considered to treat or prevent long-term complications in ASA [237]. However, more clinical trials are necessary to evaluate the effect of NO donor

therapy. Further, a better understanding of the genotype-phenotype correlations will be useful to select certain ASA patients who will benefit from NO therapy.

Currently, the mortality of UCDs is still high and the outcome of severely affected patients is generally poor. Novel therapeutic strategies are required. An optimized reliable animal model for individual UCDs will be helpful to explore potential novel treatment modalities including liver and hepatic cells transplantation, pharmachaperons as well as gene therapy.

In the past few years, there has been a dramatic increase in studying UCDs. Since UCDs are rare inherited disease, a large network including UCD patients and families, clinicians, researchers, and pharmaceutical companies around the world will facilitate joint projects, as already shown by recently established “The Urea Cycle Disorders Consortium (UCDC)” in the USA and “European Initiative for Intoxication Type Metabolic Disorders (E-IMD)” in Europe. This will contribute to create a global knowledge about the prevalence of individual UCDs, clinical and biochemical phenotypes, diagnosis, prognosis, care and treatment, from which the prevention of the disease and the development of novel therapeutic strategies will eventually result.

In summary, the studies on ASLD and CPS1D can serve as examples for understanding the molecular basis and pathology of phenotypic variability in UCDs. Accordingly, the strategies and models used in this work provide a general applicability which can be further adapted to study other UCDs or to be extended to other IEMs.

5 References

1. Wilkinson, D.J., N.J. Smeeton, and P.W. Watt, *Ammonia metabolism, the brain and fatigue; revisiting the link.* Prog Neurobiol, 2010. **91**(3): p. 200-19.
2. Haussinger, D., *Hepatocyte heterogeneity in glutamine and ammonia metabolism and the role of an intercellular glutamine cycle during ureogenesis in perfused rat liver.* Eur J Biochem, 1983. **133**(2): p. 269-75.
3. Haussinger, D., W.H. Lamers, and A.F. Moorman, *Hepatocyte heterogeneity in the metabolism of amino acids and ammonia.* Enzyme, 1992. **46**(1-3): p. 72-93.
4. Olde Damink, S.W., R. Jalan, and C.H. Dejong, *Interorgan ammonia trafficking in liver disease.* Metab Brain Dis, 2009. **24**(1): p. 169-81.
5. Haussinger, D., *Regulation of hepatic ammonia metabolism: the intercellular glutamine cycle.* Adv Enzyme Regul, 1986. **25**: p. 159-80.
6. Subcommittee on Ammonia, N.R.C., *Ammonia.* 1979: p. 1-303.
7. Nelson, D., and Cox MM., *Lehninger Principles of Biochemistry.* W.H. Freemann and Company, New York, 2005. **4th edition**(Part II): p. 481-917.
8. Cooper, A.J., *Ammonia metabolism in normal and portacaval-shunted rats.* Adv Exp Med Biol, 1990. **272**: p. 23-46.
9. Meijer, A.J., W.H. Lamers, and R.A. Chamuleau, *Nitrogen metabolism and ornithine cycle function.* Physiol Rev, 1990. **70**(3): p. 701-48.
10. Rolfes, S.R., K. Pinna, and E. Whitney, *Understanding Normal and Clinical Nutrition.* Wadsworth, Cengage Learning, Chapter 6, 2009: p. 173-204.
11. Millward, D.J., *The physiological regulation of proteolysis in muscle.* Biochem Soc Trans, 1985. **13**(6): p. 1023-6.
12. Mortimore, G.E. and A.R. Poso, *Intracellular protein catabolism and its control during nutrient deprivation and supply.* Annu Rev Nutr, 1987. **7**: p. 539-64.
13. Berg JM, Tymoczko JL, and Stryer L, *Biochemistry.* New York: W H Freeman, 2002. **5th edition**(Section 23).
14. Erecinska, M. and I.A. Silver, *Metabolism and role of glutamate in mammalian brain.* Prog Neurobiol, 1990. **35**(4): p. 245-96.
15. Benjamin, A.M. and J.H. Quastel, *Fate of L-glutamate in the brain.* J Neurochem, 1974. **23**(3): p. 457-64.
16. Cooper, A.J., *Role of glutamine in cerebral nitrogen metabolism and ammonia neurotoxicity.* Ment Retard Dev Disabil Res Rev, 2001. **7**(4): p. 280-6.
17. Haussinger, D., W. Gerok, and H. Sies, *Regulation of flux through glutaminase and glutamine synthetase in isolated perfused rat liver.* Biochim Biophys Acta, 1983. **755**(2): p. 272-8.
18. Haussinger, D. and H. Sies, *Hepatic glutamine metabolism under the influence of the portal ammonia concentration in the perfused rat liver.* Eur J Biochem, 1979. **101**(1): p. 179-84.
19. Häberle, J., *Clinical practice: the management of hyperammonemia.* Eur J Pediatr, 2010. **170**(1): p. 21-34.
20. Auron, A. and P.D. Brophy, *Hyperammonemia in review: pathophysiology, diagnosis, and treatment.* Pediatric nephrology, 2012. **27**(2): p. 207-22.
21. Braissant, O., V.A. McLin, and C. Cudalbu, *Ammonia toxicity to the brain.* Journal of inherited metabolic disease, 2013. **36**(4): p. 595-612.
22. Gropman, A.L., M. Summar, and J.V. Leonard, *Neurological implications of urea cycle disorders.* Journal of inherited metabolic disease, 2007. **30**(6): p. 865-79.

23. Braissant, O., *Current concepts in the pathogenesis of urea cycle disorders.* Molecular genetics and metabolism, 2010. **100 Suppl 1**: p. S3-S12.
24. Rose, C., *Effect of ammonia on astrocytic glutamate uptake/release mechanisms.* Journal of neurochemistry, 2006. **97 Suppl 1**: p. 11-5.
25. Ratnakumari, L., I.A. Qureshi, and R.F. Butterworth, *Evidence for cholinergic neuronal loss in brain in congenital ornithine transcarbamylase deficiency.* Neuroscience letters, 1994. **178**(1): p. 63-5.
26. Robinson, M.B., et al., *Brain serotonin2 and serotonin1A receptors are altered in the congenitally hyperammonemic sparse fur mouse.* Journal of neurochemistry, 1992. **58**(3): p. 1016-22.
27. Bachmann, C. and J.P. Colombo, *Increase of tryptophan and 5-hydroxyindole acetic acid in the brain of ornithine carbamoyltransferase deficient sparse-fur mice.* Pediatric research, 1984. **18**(4): p. 372-5.
28. Hyman, S.L., et al., *Anorexia and altered serotonin metabolism in a patient with argininosuccinic aciduria.* The Journal of pediatrics, 1986. **108**(5 Pt 1): p. 705-9.
29. Rao, K.V., Y.R. Mawal, and I.A. Qureshi, *Progressive decrease of cerebral cytochrome C oxidase activity in sparse-fur mice: role of acetyl-L-carnitine in restoring the ammonia-induced cerebral energy depletion.* Neuroscience letters, 1997. **224**(2): p. 83-6.
30. Zanelli, S.A., et al., *Mechanisms of ischemic neuroprotection by acetyl-L-carnitine.* Annals of the New York Academy of Sciences, 2005. **1053**: p. 153-61.
31. Braissant, O., et al., *Ammonium alters creatine transport and synthesis in a 3D culture of developing brain cells, resulting in secondary cerebral creatine deficiency.* The European journal of neuroscience, 2008. **27**(7): p. 1673-85.
32. Lichter-Konecki, U., et al., *Gene expression profiling of astrocytes from hyperammonemic mice reveals altered pathways for water and potassium homeostasis in vivo.* Glia, 2008. **56**(4): p. 365-77.
33. Bosoi, C.R. and C.F. Rose, *Identifying the direct effects of ammonia on the brain.* Metabolic brain disease, 2009. **24**(1): p. 95-102.
34. Krebs, H.A., and Henseleit, K., *Untersuchungen über die Harnstoffbildung in Tierkröper.* Hoppe-Seyler's Z. Physiol. Chem, 1932. **210**: p. 33-66.
35. Häberle, J., et al., *Suggested guidelines for the diagnosis and management of urea cycle disorders.* Orphanet J Rare Dis, 2012. **7**: p. 32.
36. Rubio, V. and S. Grisolia, *Human carbamoylphosphate synthetase I.* Enzyme, 1981. **26**(5): p. 233-9.
37. Rubio, V., G. Ramponi, and S. Grisolia, *Carbamoyl phosphate synthetase I of human liver. Purification, some properties and immunological cross-reactivity with the rat liver enzyme.* Biochim Biophys Acta, 1981. **659**(1): p. 150-60.
38. Rubio, V., *Structure-function studies in carbamoyl phosphate synthetases.* Biochem Soc Trans, 1993. **21**(1): p. 198-202.
39. Rubio, V. and J. Cervera, *The carbamoyl-phosphate synthase family and carbamate kinase: structure-function studies.* Biochem Soc Trans, 1995. **23**(4): p. 879-83.
40. Nyunoya, H., et al., *Characterization and derivation of the gene coding for mitochondrial carbamyl phosphate synthetase I of rat.* J Biol Chem, 1985. **260**(16): p. 9346-56.
41. Oyanagi, K., et al., *A study of urea-synthesizing enzymes in prenatal and postnatal human liver.* Pediatr Res, 1980. **14**(3): p. 236-41.

42. Ryall, J., et al., *Expression of nuclear genes encoding the urea cycle enzymes, carbamoyl-phosphate synthetase I and ornithine carbamoyl transferase, in rat liver and intestinal mucosa.* Eur J Biochem, 1985. **152**(2): p. 287-92.
43. Schofield, J.P., *Molecular studies on an ancient gene encoding for carbamoyl-phosphate synthetase.* Clin Sci (Lond), 1993. **84**(2): p. 119-28.
44. Summar, M.L., et al., *Characterization of genomic structure and polymorphisms in the human carbamyl phosphate synthetase I gene.* Gene, 2003. **311**: p. 51-7.
45. Fresquet, V., et al., *Site-directed mutagenesis of the regulatory domain of Escherichia coli carbamoyl phosphate synthetase identifies crucial residues for allosteric regulation and for transduction of the regulatory signals.* J Mol Biol, 2000. **299**(4): p. 979-91.
46. Javid-Majd, F., et al., *Comparison of the functional differences for the homologous residues within the carboxy phosphate and carbamate domains of carbamoyl phosphate synthetase.* Biochemistry, 1996. **35**(45): p. 14362-9.
47. Stapleton, M.A., et al., *Role of conserved residues within the carboxy phosphate domain of carbamoyl phosphate synthetase.* Biochemistry, 1996. **35**(45): p. 14352-61.
48. Pierrat, O.A. and F.M. Raushel, *A functional analysis of the allosteric nucleotide monophosphate binding site of carbamoyl phosphate synthetase.* Arch Biochem Biophys, 2002. **400**(1): p. 34-42.
49. Hart, E.J. and S.G. Powers-Lee, *Role of Cys-1327 and Cys-1337 in redox sensitivity and allosteric monitoring in human carbamoyl phosphate synthetase.* J Biol Chem, 2009. **284**(9): p. 5977-85.
50. Häberle, J., et al., *Molecular defects in human carbamoy phosphate synthetase I: mutational spectrum, diagnostic and protein structure considerations.* Hum Mutat, 2011. **32**(6): p. 579-89.
51. Pierson, D.L. and J.M. Brien, *Human carbamylphosphate synthetase I. Stabilization, purification, and partial characterization of the enzyme from human liver.* J Biol Chem, 1980. **255**(16): p. 7891-5.
52. Pekkala, S., et al., *Structural insight on the control of urea synthesis: identification of the binding site for N-acetyl-L-glutamate, the essential allosteric activator of mitochondrial carbamoyl phosphate synthetase.* Biochem J, 2009. **424**(2): p. 211-20.
53. Meijer, A.J., et al., *Control of ureogenesis.* European journal of biochemistry / FEBS, 1985. **148**(1): p. 189-96.
54. Caldovic, L., et al., *Cloning and expression of the human N-acetylglutamate synthase gene.* Biochemical and biophysical research communications, 2002. **299**(4): p. 581-6.
55. Morizono, H., et al., *Mammalian N-acetylglutamate synthase.* Molecular Genetics and Metabolism, 2004. **81 Suppl 1**: p. S4-11.
56. Neupert, W., *Protein import into mitochondria.* Annual review of biochemistry, 1997. **66**: p. 863-917.
57. Sonoda, T. and M. Tatibana, *Purification of N-acetyl-L-glutamate synthetase from rat liver mitochondria and substrate and activator specificity of the enzyme.* J Biol Chem, 1983. **258**(16): p. 9839-44.
58. Shambaugh, G.E., 3rd, *Urea biosynthesis I. The urea cycle and relationships to the citric acid cycle.* Am J Clin Nutr, 1977. **30**(12): p. 2083-7.

59. Rubio, V. and S. Grisolia, *Mechanism of mitochondrial carbamoyl-phosphate synthetase: synthesis and properties of active CO2, precursor of carbamoyl phosphate.* Biochemistry, 1977. **16**(2): p. 321-9.
60. Britton, H.G., V. Rubio, and S. Grisolia, *Mechanism of carbamoyl-phosphate synthetase. Properties of the two binding sites for ATP.* European journal of biochemistry / FEBS, 1979. **102**(2): p. 521-30.
61. Rubio, V., H.G. Britton, and S. Grisolia, *Mechanism of carbamoyl-phosphate synthetase. Binding of ATP by the rat-liver mitochondrial enzyme.* European journal of biochemistry / FEBS, 1979. **93**(2): p. 245-56.
62. Rubio, V., et al., *Mechanism of activation of bicarbonate ion by mitochondrial carbamoyl-phosphate synthetase: formation of enzyme-bound adenosine diphosphate from the adenosine triphosphate that yields inorganic phosphate.* Biochemistry, 1981. **20**(7): p. 1969-74.
63. Martinez, A.I., et al., *Genetic, structural and biochemical basis of carbamoyl phosphate synthetase 1 deficiency.* Mol Genet Metab, 2010. **101**(4): p. 311-23.
64. Foley, R., J. Poon, and P.M. Anderson, *Characterization of the reactive sulfhydryl groups in carbamyl phosphate synthetase of Escherichia coli.* Biochemistry, 1971. **10**(24): p. 4562-9.
65. Miles, B.W. and F.M. Raushel, *Synchronization of the three reaction centers within carbamoyl phosphate synthetase.* Biochemistry, 2000. **39**(17): p. 5051-6.
66. Thoden, J.B., et al., *Carbamoyl phosphate synthetase: closure of the B-domain as a result of nucleotide binding.* Biochemistry, 1999. **38**(8): p. 2347-57.
67. Johnson, J.L., et al., *Resolving the fluorescence response of Escherichia coli carbamoyl phosphate synthetase: mapping intra- and intersubunit conformational changes.* Biochemistry, 2007. **46**(2): p. 387-97.
68. Rubio, V., H.G. Britton, and S. Grisolia, *Mitochondrial carbamoyl phosphate synthetase activity in the absence of N-acetyl-L-glutamate. Mechanism of activation by this cofactor.* European journal of biochemistry / FEBS, 1983. **134**(2): p. 337-43.
69. Braxton, B.L., et al., *Quantifying the allosteric properties of Escherichia coli carbamyl phosphate synthetase: determination of thermodynamic linked-function parameters in an ordered kinetic mechanism.* Biochemistry, 1992. **31**(8): p. 2309-16.
70. Raijman, L. and M.E. Jones, *Purification, composition, and some properties of rat liver carbamyl phosphate synthetase (ammonia).* Arch Biochem Biophys, 1976. **175**(1): p. 270-8.
71. Elliott, K.R. and K.F. Tipton, *Purification and characterisation of carbamoyl phosphate synthetase from beef liver.* FEBS letters, 1973. **37**(1): p. 79-81.
72. Mori, M., et al., *Cell-free translation of carbamyl phosphate synthetase I and ornithine transcarbamylase messenger RNAs of rat liver. Effect of dietary protein and fasting on translatable mRNA levels.* J Biol Chem, 1981. **256**(8): p. 4127-32.
73. Mori, M., et al., *Synthesis, intracellular transport, and processing of the precursors for mitochondrial ornithine transcarbamylase and carbamoyl-phosphate synthetase I in isolated hepatocytes.* Proceedings of the National Academy of Sciences of the United States of America, 1981. **78**(10): p. 6056-60.

74. Haraguchi, Y., et al., *Cloning and sequence of a cDNA encoding human carbamyl phosphate synthetase I: molecular analysis of hyperammonemia.* Gene, 1991. **107**(2): p. 335-40.
75. Meister, A., *Mechanism and regulation of the glutamine-dependent carbamyl phosphate synthetase of Escherichia coli.* Advances in enzymology and related areas of molecular biology, 1989. **62**: p. 315-74.
76. Ahuja, V. and S.G. Powers-Lee, *Human carbamoyl-phosphate synthetase: insight into N-acetylglutamate interaction and the functional effects of a common single nucleotide polymorphism.* J Inherit Metab Dis, 2008. **31**(4): p. 481-91.
77. Marshall, M. and L.A. Fahien, *Proteolysis as a probe of ligand-associated conformational changes in rat carbamyl phosphate synthetase I.* Arch Biochem Biophys, 1988. **262**(2): p. 455-70.
78. Powers-Lee, S.G. and K. Corina, *Domain structure of rat liver carbamoyl phosphate synthetase I.* J Biol Chem, 1986. **261**(33): p. 15349-52.
79. Nyunoya, H., K.E. Broglie, and C.J. Lusty, *The gene coding for carbamoyl-phosphate synthetase I was formed by fusion of an ancestral glutaminase gene and a synthetase gene.* Proceedings of the National Academy of Sciences of the United States of America, 1985. **82**(8): p. 2244-6.
80. Alonso, E., et al., *Oxidative inactivation of carbamoyl phosphate synthetase (ammonia). Mechanism and sites of oxidation, degradation of the oxidized enzyme, and inactivation by glycerol, EDTA, and thiol protecting agents.* J Biol Chem, 1992. **267**(7): p. 4524-32.
81. Alonso, E. and V. Rubio, *Affinity cleavage of carbamoyl-phosphate synthetase I localizes regions of the enzyme interacting with the molecule of ATP that phosphorylates carbamate.* Eur J Biochem, 1995. **229**(2): p. 377-84.
82. Rodriguez-Aparicio, L.B., A.M. Guadalajara, and V. Rubio, *Physical location of the site for N-acetyl-L-glutamate, the allosteric activator of carbamoyl phosphate synthetase, in the 20-kilodalton COOH-terminal domain.* Biochemistry, 1989. **28**(7): p. 3070-4.
83. Diez-Fernandez, C., et al., *Understanding carbamoyl phosphate synthetase (CPS1) deficiency by using the recombinantly purified human enzyme: effects of clincial CPS1 mutations that concentrate in a central domain of unkown function.* Molecular Genetics and Metabolism (Currently minor revisions), 2014.
84. Thoden, J.B., et al., *Structure of carbamoyl phosphate synthetase: a journey of 96 A from substrate to product.* Biochemistry, 1997. **36**(21): p. 6305-16.
85. Thoden, J.B., et al., *The binding of inosine monophosphate to Escherichia coli carbamoyl phosphate synthetase.* J Biol Chem, 1999. **274**(32): p. 22502-7.
86. Liu, X., H.I. Guy, and D.R. Evans, *Identification of the regulatory domain of the mammalian multifunctional protein CAD by the construction of an Escherichia coli hamster hybrid carbamyl-phosphate synthetase.* J Biol Chem, 1994. **269**(44): p. 27747-55.
87. Cervera, J., et al., *The influence of effectors and subunit interactions on Escherichia coli carbamoyl-phosphate synthetase studied by differential scanning calorimetry.* J Biol Chem, 1993. **268**(17): p. 12504-11.
88. Carrey, E.A., D.G. Campbell, and D.G. Hardie, *Phosphorylation and activation of hamster carbamyl phosphate synthetase II by cAMP-dependent protein kinase. A novel mechanism for regulation of pyrimidine nucleotide biosynthesis.* The EMBO journal, 1985. **4**(13B): p. 3735-42.

89. Holden, H.M., J.B. Thoden, and F.M. Raushel, *Carbamoyl phosphate synthetase: an amazing biochemical odyssey from substrate to product.* Cellular and molecular life sciences : CMLS, 1999. **56**(5-6): p. 507-22.
90. Piette, J., et al., *DNA sequence of the carA gene and the control region of carAB: tandem promoters, respectively controlled by arginine and the pyrimidines, regulate the synthesis of carbamoyl-phosphate synthetase in Escherichia coli K-12.* Proceedings of the National Academy of Sciences of the United States of America, 1984. **81**(13): p. 4134-8.
91. Nyunoya, H. and C.J. Lusty, *The carB gene of Escherichia coli: a duplicated gene coding for the large subunit of carbamoyl-phosphate synthetase.* Proceedings of the National Academy of Sciences of the United States of America, 1983. **80**(15): p. 4629-33.
92. Thoden, J.B., et al., *The structure of carbamoyl phosphate synthetase determined to 2.1 A resolution.* Acta Crystallogr D Biol Crystallogr, 1999. **55**(Pt 1): p. 8-24.
93. Hoshide, R., et al., *Assignment of the human carbamyl phosphate synthetase I gene (CPS1) to 2q35 by fluorescence in situ hybridization.* Genomics, 1995. **28**(1): p. 124-5.
94. Summar, M.L., et al., *Physical and linkage mapping of human carbamyl phosphate synthetase I (CPS1) and reassignment from 2p to 2q35.* Cytogenet Cell Genet, 1995. **71**(3): p. 266-7.
95. Häberle, J., et al., *Gene structure of human carbamylphosphate synthetase 1 and novel mutations in patients with neonatal onset.* Hum Mutat, 2003. **21**(4): p. 444.
96. Funghini, S., et al., *Structural organization of the human carbamyl phosphate synthetase I gene (CPS1) and identification of two novel genetic lesions.* Hum Mutat, 2003. **22**(4): p. 340-1.
97. Saeed-Kothe, A. and S.G. Powers-Lee, *Gain of glutaminase function in mutants of the ammonia-specific frog carbamoyl phosphate synthetase.* J Biol Chem, 2003. **278**(29): p. 26722-6.
98. Windmueller, H.G. and A.E. Spaeth, *Source and fate of circulating citrulline.* Am J Physiol, 1981. **241**(6): p. E473-80.
99. Neill, M.A., et al., *Quantitative RT-PCR comparison of the urea and nitric oxide cycle gene transcripts in adult human tissues.* Mol Genet Metab, 2009. **97**(2): p. 121-7.
100. Rapp, B., et al., *Genetic analysis of carbamoylphosphate synthetase I and ornithine transcarbamylase deficiency using fibroblasts.* Eur J Pediatr, 2001. **160**(5): p. 283-7.
101. Pekkala, S., et al., *Understanding carbamoyl-phosphate synthetase I (CPS1) deficiency by using expression studies and structure-based analysis.* Hum Mutat, 2010. **31**(7): p. 801-8.
102. Yefimenko, I., et al., *Understanding carbamoyl phosphate synthetase deficiency: impact of clinical mutations on enzyme functionality.* J Mol Biol, 2005. **349**(1): p. 127-41.
103. Diez-Fernandez, C., et al., *Molecular characterization of carbamoyl-phosphate synthetase (CPS1) deficiency using human recombinant CPS1 as a key tool.* Hum Mutat, 2013. **34**(8): p. 1149-59.
104. Marshall, M. and P.P. Cohen, *Ornithine transcarbamylase from Streptococcus faecalis and bovine liver. I. Isolation and subunit structure.* J Biol Chem, 1972. **247**(6): p. 1641-53.

105. Marshall, M. and P.P. Cohen, *Ornithine transcarbamylase from Streptococcus faecalis and bovine liver. II. Multiple binding sites for carbamyl-P and L-norvaline, correlation with steady state kinetics.* J Biol Chem, 1972. **247**(6): p. 1654-68.
106. Marshall, M. and P.P. Cohen, *Ornithine transcarbamylase from Streptococcus faecalis and bovine liver. 3. Effects of chemical modifications of specific residues on ligand binding and enzymatic activity.* J Biol Chem, 1972. **247**(6): p. 1669-82.
107. Pierson, D.L., S.L. Cox, and B.E. Gilbert, *Human ornithine transcarbamylase. Purification and characterization of the enzyme from normal liver and the liver of a Reye's syndrome patient.* J Biol Chem, 1977. **252**(18): p. 6464-9.
108. Kalousek, F., B. Francois, and L.E. Rosenberg, *Isolation and characterization of ornithine transcarbamylase from normal human liver.* J Biol Chem, 1978. **253**(11): p. 3939-44.
109. Clarke, S., *The polypeptides of rat liver mitochondria: identification of a 36,000 dalton polypeptide as the subunit of ornithine transcarbamylase.* Biochemical and biophysical research communications, 1976. **71**(4): p. 1118-24.
110. Lindgren, V., et al., *Human ornithine transcarbamylase locus mapped to band Xp21.1 near the Duchenne muscular dystrophy locus.* Science, 1984. **226**(4675): p. 698-700.
111. Horwich, A.L., et al., *Structure and expression of a complementary DNA for the nuclear coded precursor of human mitochondrial ornithine transcarbamylase.* Science, 1984. **224**(4653): p. 1068-74.
112. Hata, A., et al., *Structure of the human ornithine transcarbamylase gene.* Journal of biochemistry, 1988. **103**(2): p. 302-8.
113. Tuchman, M., et al., *Mutations and polymorphisms in the human ornithine transcarbamylase gene.* Human mutation, 2002. **19**(2): p. 93-107.
114. Kolansky, D.M., et al., *Energy-dependent translocation of the precursor of ornithine transcarbamylase by isolated rat liver mitochondria.* J Biol Chem, 1982. **257**(14): p. 8467-71.
115. Mori, M., et al., *Uptake and processing of the precursor for rat liver ornithine transcarbamylase by isolated mitochondria. Inhibition by uncouplers.* J Biol Chem, 1981. **256**(16): p. 8263-6.
116. Sztul, E.S., et al., *Import of rat ornithine transcarbamylase precursor into mitochondria: two-step processing of the leader peptide.* The Journal of cell biology, 1987. **105**(6 Pt 1): p. 2631-9.
117. Shi, D., et al., *1.85-A resolution crystal structure of human ornithine transcarbamoylase complexed with N-phosphonacetyl-L-ornithine. Catalytic mechanism and correlation with inherited deficiency.* J Biol Chem, 1998. **273**(51): p. 34247-54.
118. Shi, D., et al., *Human ornithine transcarbamylase: crystallographic insights into substrate recognition and conformational changes.* The Biochemical journal, 2001. **354**(Pt 3): p. 501-9.
119. Diaz-Munoz, M. and R. Hernandez-Munoz, *Molecular and biochemical features of the mitochondrial enzyme ornithine transcarbamylase: a possible new role as a signaling factor.* Current medicinal chemistry, 2010. **17**(21): p. 2253-60.
120. Engel, K., W. Hohne, and J. Häberle, *Mutations and polymorphisms in the human argininosuccinate synthetase (ASS1) gene.* Human mutation, 2009. **30**(3): p. 300-7.

121. Beaudet, A.L., et al., *The human argininosuccinate synthetase locus and citrullinemia.* Advances in human genetics, 1986. **15**: p. 161-96, 291-2.
122. Kobayashi, K., et al., *Heterogeneity of mutations in argininosuccinate synthetase causing human citrullinemia.* J Biol Chem, 1990. **265**(19): p. 11361-7.
123. Husson, A., et al., *Argininosuccinate synthetase from the urea cycle to the citrulline-NO cycle.* European journal of biochemistry / FEBS, 2003. **270**(9): p. 1887-99.
124. Erez, A., et al., *Requirement of argininosuccinate lyase for systemic nitric oxide production.* Nat Med, 2011. **17**(12): p. 1619-26.
125. Su, T.S., et al., *Human chromosomal assignments for 14 argininosuccinate synthetase pseudogenes: cloned DNAs as reagents for cytogenetic analysis.* American journal of human genetics, 1984. **36**(5): p. 954-64.
126. Freytag, S.O., et al., *Molecular structures of human argininosuccinate synthetase pseudogenes. Evolutionary and mechanistic implications.* J Biol Chem, 1984. **259**(5): p. 3160-6.
127. Su, T.S., et al., *Molecular analysis of argininosuccinate synthetase deficiency in human fibroblasts.* The Journal of clinical investigation, 1982. **70**(6): p. 1334-9.
128. Su, T.S., A.L. Beaudet, and W.E. O'Brien, *Abnormal mRNA for argininosuccinate synthetase in citrullinaemia.* Nature, 1983. **301**(5900): p. 533-4.
129. Bock, H.G., et al., *Sequence for human argininosuccinate synthetase cDNA.* Nucleic acids research, 1983. **11**(18): p. 6505-12.
130. Ratner, S., *Argininosuccinate synthetase of bovine liver: chemical and physical properties.* Proceedings of the National Academy of Sciences of the United States of America, 1982. **79**(17): p. 5197-9.
131. Brusilow, S.W. and A.L. Horwich, *Urea cycle enzymes.* In: Scriver CR, Valle D, Beaudet AL, et al, eds. The Metabolic and Molecular Basis of Inherited Disease. 7th ed. New York: McGraw Hill, 1995: p. 1187-1232.
132. Freytag, S.O., et al., *Molecular structure of the human argininosuccinate synthetase gene: occurrence of alternative mRNA splicing.* Molecular and cellular biology, 1984. **4**(10): p. 1978-84.
133. Ratner, S., *Enzymes of arginine and urea synthesis.* Advances in enzymology and related areas of molecular biology, 1973. **39**: p. 1-90.
134. Tsuda, M., Y. Shikata, and T. Katsunuma, *Effect of dietary proteins on the turnover of rat liver argininosuccinate synthetase.* Journal of biochemistry, 1979. **85**(3): p. 699-704.
135. Morris, S.M., Jr., et al., *Regulation of mRNA levels for five urea cycle enzymes in rat liver by diet, cyclic AMP, and glucocorticoids.* Arch Biochem Biophys, 1987. **256**(1): p. 343-53.
136. Quillard, M., A. Husson, and A. Lavoinne, *Glutamine increases argininosuccinate synthetase mRNA levels in rat hepatocytes. The involvement of cell swelling.* European journal of biochemistry / FEBS, 1996. **236**(1): p. 56-9.
137. Irr, J.D. and L.B. Jacoby, *Control of argininosuccinate synthetase by arginine in human lymphoblasts.* Somatic cell genetics, 1978. **4**(1): p. 111-24.
138. Schimke, R.T., *Enzymes of Arginine Metabolism in Mammalian Cell Culture. I. Repression of Argininosuccinate Synthetase and Argininosuccinase.* J Biol Chem, 1964. **239**: p. 136-45.

139. Su, T.S., A.L. Beaudet, and W.E. O'Brien, *Increased translatable messenger ribonucleic acid for argininosuccinate synthetase in canavanine-resistant human cells.* Biochemistry, 1981. **20**(10): p. 2956-60.
140. Karlberg, T., et al., *Structure of human argininosuccinate synthetase.* Acta crystallographica. Section D, Biological crystallography, 2008. **64**(Pt 3): p. 279-86.
141. Trevisson, E., et al., *Functional complementation in yeast allows molecular characterization of missense argininosuccinate lyase mutations.* J Biol Chem, 2009. **284**(42): p. 28926-34.
142. Woods, S.A., et al., *Structural and functional relationships between fumarase and aspartase. Nucleotide sequences of the fumarase (fumC) and aspartase (aspA) genes of Escherichia coli K12.* The Biochemical journal, 1986. **237**(2): p. 547-57.
143. Stone, R.L., H. Zalkin, and J.E. Dixon, *Expression, purification, and kinetic characterization of recombinant human adenylosuccinate lyase.* J Biol Chem, 1993. **268**(26): p. 19710-6.
144. Woods, S.A., S.D. Schwartzbach, and J.R. Guest, *Two biochemically distinct classes of fumarase in Escherichia coli.* Biochimica et biophysica acta, 1988. **954**(1): p. 14-26.
145. Williams, S.E., et al., *3-Carboxy-cis,cis-muconate lactonizing enzyme from Pseudomonas putida is homologous to the class II fumarase family: a new reaction in the evolution of a mechanistic motif.* Biochemistry, 1992. **31**(40): p. 9768-76.
146. Erez, A., S.C. Nagamani, and B. Lee, *Argininosuccinate lyase deficiency-argininosuccinic aciduria and beyond.* Am J Med Genet C Semin Med Genet, 2011. **157**(1): p. 45-53.
147. O'Brien, W.E., et al., *Cloning and sequence analysis of cDNA for human argininosuccinate lyase.* Proceedings of the National Academy of Sciences of the United States of America, 1986. **83**(19): p. 7211-5.
148. Tomlinson, S. and R.G. Westall, *Argininosuccinic Aciduria. Argininosuccinase and Arginase in Human Blood Cells.* Clin Sci, 1964. **26**: p. 261-9.
149. O'Brien, W.E. and R.H. Barr, *Argininosuccinate lyase: purification and characterization from human liver.* Biochemistry, 1981. **20**(7): p. 2056-60.
150. Ratner, S. and B. Petrack, *The mechanism of arginine synthesis from citrulline in kidney.* J Biol Chem, 1953. **200**(1): p. 175-85.
151. Wu, G., D.A. Knabe, and N.E. Flynn, *Synthesis of citrulline from glutamine in pig enterocytes.* The Biochemical journal, 1994. **299 (Pt 1)**: p. 115-21.
152. Ratner, S., H. Morell, and E. Carvalho, *Enzymes of arginine metabolism in brain.* Arch Biochem Biophys, 1960. **91**: p. 280-9.
153. Bizzoco, E., M.S. Faussone-Pellegrini, and M.G. Vannucchi, *Activated microglia cells express argininosuccinate synthetase and argininosuccinate lyase in the rat brain after transient ischemia.* Experimental neurology, 2007. **208**(1): p. 100-9.
154. Yu, B. and P.L. Howell, *Intragenic complementation and the structure and function of argininosuccinate lyase.* Cellular and molecular life sciences : CMLS, 2000. **57**(11): p. 1637-51.
155. Todd, S., et al., *cDNA sequence, interspecies comparison, and gene mapping analysis of argininosuccinate lyase.* Genomics, 1989. **4**(1): p. 53-9.
156. Naylor, S.L., R.J. Klebe, and T.B. Shows, *Argininosuccinic aciduria: assignment of the argininosuccinate lyase gene to the pter to q22 region of*

human chromosome 7 by bioautography. Proc Natl Acad Sci U S A, 1978. **75**(12): p. 6159-62.
157. Linnebank, M., et al., *Argininosuccinate lyase (ASL) deficiency: mutation analysis in 27 patients and a completed structure of the human ASL gene.* Human genetics, 2002. **111**(4-5): p. 350-9.
158. Trevisson, E., et al., *Argininosuccinate lyase deficiency: mutational spectrum in Italian patients and identification of a novel ASL pseudogene.* Human mutation, 2007. **28**(7): p. 694-702.
159. Hu, L., et al., *Understanding the role of argininosuccinate lyase transcript variants in the clinical and biochemical variability of the urea cycle disorder argininosuccinic aciduria.* J Biol Chem, 2013. **288**(48): p. 34599-611.
160. Piatigorsky, J., *Lens crystallins and their gene families.* Cell, 1984. **38**(3): p. 620-1.
161. Wistow, G.J. and J. Piatigorsky, *Lens crystallins: the evolution and expression of proteins for a highly specialized tissue.* Annual review of biochemistry, 1988. **57**: p. 479-504.
162. Bloemendal, H. and W.W. de Jong, *Lens proteins and their genes.* Progress in nucleic acid research and molecular biology, 1991. **41**: p. 259-81.
163. Piatigorsky, J. and G.J. Wistow, *Enzyme/crystallins: gene sharing as an evolutionary strategy.* Cell, 1989. **57**(2): p. 197-9.
164. Chen, Y.H., et al., *Distinct interactions of alphaA-crystallin with homologous substrate proteins, delta-crystallin and argininosuccinate lyase, under thermal stress.* Biochimie, 2011. **93**(2): p. 314-20.
165. Bloemendal, H., et al., *Ageing and vision: structure, stability and function of lens crystallins.* Progress in biophysics and molecular biology, 2004. **86**(3): p. 407-85.
166. Horwitz, J., *Alpha-crystallin.* Experimental eye research, 2003. **76**(2): p. 145-53.
167. Horwitz, J., *Alpha-crystallin can function as a molecular chaperone.* Proceedings of the National Academy of Sciences of the United States of America, 1992. **89**(21): p. 10449-53.
168. de Jong, W.W., E.C. Terwindt, and H. Bloemendal, *The amino acid sequence of the A chain of human alpha-crystallin.* FEBS letters, 1975. **58**(1): p. 310-3.
169. Iwaki, T., A. Kume-Iwaki, and J.E. Goldman, *Cellular distribution of alpha B-crystallin in non-lenticular tissues.* The journal of histochemistry and cytochemistry : official journal of the Histochemistry Society, 1990. **38**(1): p. 31-9.
170. Wei, Y.Y., et al., *alpha-Crystallin protects human arginosuccinate lyase activity under freeze-thaw conditions.* Biochimie, 2012. **94**(2): p. 566-73.
171. Piatigorsky, J., et al., *Gene sharing by delta-crystallin and argininosuccinate lyase.* Proc Natl Acad Sci U S A, 1988. **85**(10): p. 3479-83.
172. Li, X., G.J. Wistow, and J. Piatigorsky, *Linkage and expression of the argininosuccinate lyase/delta-crystallin genes of the duck: insertion of a CR1 element in the intergenic spacer.* Biochimica et biophysica acta, 1995. **1261**(1): p. 25-34.
173. Parker, D.S., E.F. Wawrousek, and J. Piatigorsky, *Expression of the delta-crystallin genes in the embryonic chicken lens.* Developmental biology, 1988. **126**(2): p. 375-81.
174. Li, X., P.S. Zelenka, and J. Piatigorsky, *Differential expression of the two delta-crystallin genes in lens and non-lens tissues: shift favoring delta 2 expression from embryonic to adult chickens.* Developmental dynamics : an

official publication of the American Association of Anatomists, 1993. **196**(2): p. 114-23.
175. Kondoh, H., et al., *Expression of the chicken 'delta 2-crystallin' gene in mouse cells: evidence for encoding of argininosuccinate lyase.* Gene, 1991. **99**(2): p. 267-71.
176. Barbosa, P., et al., *Expression of duck lens delta-crystallin cDNAs in yeast and bacterial hosts. Delta 2-crystallin is an active argininosuccinate lyase.* J Biol Chem, 1991. **266**(33): p. 22319-22.
177. Piatigorsky, J. and J. Horwitz, *Characterization and enzyme activity of argininosuccinate lyase/delta-crystallin of the embryonic duck lens.* Biochimica et biophysica acta, 1996. **1295**(2): p. 158-64.
178. Chiou, S.H., C.C. Hung, and C.W. Lin, *Biochemical characterization of crystallins from pigeon lenses: structural and sequence analysis of pigeon delta-crystallin.* Biochimica et biophysica acta, 1992. **1160**(3): p. 317-24.
179. Lee, H.J., S.H. Chiou, and G.G. Chang, *Biochemical characterization and kinetic analysis of duck delta-crystallin with endogenous argininosuccinate lyase activity.* The Biochemical journal, 1992. **283 (Pt 2)**: p. 597-603.
180. Chiou, S.H., et al., *Ostrich crystallins. Structural characterization of delta-crystallin with enzymic activity.* The Biochemical journal, 1991. **273(Pt 2)**: p. 295-300.
181. Yu, C.W. and S.H. Chiou, *Facile cloning and sequence analysis of goose delta-crystallin gene based on polymerase chain reaction.* Biochemical and biophysical research communications, 1993. **192**(2): p. 948-53.
182. Walker, D.C., et al., *Intragenic complementation at the human argininosuccinate lyase locus. Identification of the major complementing alleles.* J Biol Chem, 1997. **272**(10): p. 6777-83.
183. McInnes, R.R., V. Shih, and S. Chilton, *Interallelic complementation in an inborn error of metabolism: genetic heterogeneity in argininosuccinate lyase deficiency.* Proc Natl Acad Sci U S A, 1984. **81**(14): p. 4480-4.
184. Howell, P.L., et al., *Intragenic complementation at the argininosuccinate lyase locus: reconstruction of the active site.* J Inherit Metab Dis, 1998. **21 Suppl 1**: p. 72-85.
185. Turner, M.A., et al., *Human argininosuccinate lyase: a structural basis for intragenic complementation.* Proc Natl Acad Sci U S A, 1997. **94**(17): p. 9063-8.
186. Abu-Abed, M., et al., *Structural comparison of the enzymatically active and inactive forms of delta crystallin and the role of histidine 91.* Biochemistry, 1997. **36**(46): p. 14012-22.
187. Jenkinson, C.P., W.W. Grody, and S.D. Cederbaum, *Comparative properties of arginases.* Comparative biochemistry and physiology. Part B, Biochemistry & molecular biology, 1996. **114**(1): p. 107-32.
188. Sparkes, R.S., et al., *The gene for human liver arginase (ARG1) is assigned to chromosome band 6q23.* American journal of human genetics, 1986. **39**(2): p. 186-93.
189. Morris, S.M., Jr., *Regulation of enzymes of the urea cycle and arginine metabolism.* Annual review of nutrition, 2002. **22**: p. 87-105.
190. Kanyo, Z.F., et al., *Structure of a unique binuclear manganese cluster in arginase.* Nature, 1996. **383**(6600): p. 554-7.
191. Mori, M. and T. Gotoh, *Arginine metabolic enzymes, nitric oxide and infection.* J Nutr, 2004. **134**(10 Suppl): p. 2820S-2825S; discussion 2853S.

192. Christowitz, D., F.J. Mattheyse, and J.B. Balinsky, *Dietary and hormonal regulation of urea cycle enzymes in rat liver.* Enzyme, 1981. **26**(3): p. 113-21.
193. Ulbright, C. and P.J. Snodgrass, *Coordinate induction of the urea cycle enzymes by glucagon and dexamethasone is accomplished by three different mechanisms.* Arch Biochem Biophys, 1993. **301**(2): p. 237-43.
194. Stewart, P.M. and M. Walser, *Short term regulation of ureagenesis.* J Biol Chem, 1980. **255**(11): p. 5270-80.
195. Takiguchi, M. and M. Mori, *Transcriptional regulation of genes for ornithine cycle enzymes.* The Biochemical journal, 1995. **312 (Pt 3)**: p. 649-59.
196. van den Hoff, M.J., et al., *Isolation and characterization of the rat gene for carbamoylphosphate synthetase I.* European journal of biochemistry / FEBS, 1995. **228**(2): p. 351-61.
197. Christoffels, V.M., et al., *The upstream regulatory region of the carbamoyl-phosphate synthetase I gene controls its tissue-specific, developmental, and hormonal regulation in vivo.* J Biol Chem, 1996. **271**(49): p. 31243-50.
198. Christoffels, V.M., et al., *A single regulatory module of the carbamoylphosphate synthetase I gene executes its hepatic program of expression.* J Biol Chem, 2000. **275**(51): p. 40020-7.
199. Summar, M.L., et al., *The incidence of urea cycle disorders.* Mol Genet Metab, 2013. **110**(1-2): p. 179-80.
200. Seminara, J., et al., *Establishing a consortium for the study of rare diseases: The Urea Cycle Disorders Consortium.* Mol Genet Metab, 2010. **100 Suppl 1**: p. S97-105.
201. Batshaw, M.L., *Hyperammonemia.* Curr Probl Pediatr, 1984. **14**(11): p. 1-69.
202. Summar, M., *Current strategies for the management of neonatal urea cycle disorders.* J Pediatr, 2001. **138**(1 Suppl): p. S30-9.
203. Brusilow, S.W., *Inborn errors of urea synthesis.* In: Genetic and Metabolic Disease in Pediatrics, edited by J.K. Lloyd and C.R. Scriver. London: Butterworths, 1985: p. 140-165.
204. Summar, M.L., et al., *Diagnosis, symptoms, frequency and mortality of 260 patients with urea cycle disorders from a 21-year, multicentre study of acute hyperammonaemic episodes.* Acta paediatrica, 2008. **97**(10): p. 1420-5.
205. Teufel, U., et al., *High urgency liver transplantation in ornithine transcarbamylase deficiency presenting with acute liver failure.* Pediatric transplantation, 2011. **15**(6): p. E110-5.
206. Nassogne, M.C., et al., *Urea cycle defects: management and outcome.* Journal of inherited metabolic disease, 2005. **28**(3): p. 407-14.
207. Iorio, R., et al., *Hypertransaminasemia in childhood as a marker of genetic liver disorders.* Journal of gastroenterology, 2005. **40**(8): p. 820-6.
208. Miles, L., J.E. Heubi, and K.E. Bove, *Hepatocyte glycogen accumulation in patients undergoing dietary management of urea cycle defects mimics storage disease.* Journal of pediatric gastroenterology and nutrition, 2005. **40**(4): p. 471-6.
209. Yamaguchi, S., et al., *Mutations and polymorphisms in the human ornithine transcarbamylase (OTC) gene.* Human mutation, 2006. **27**(7): p. 626-32.
210. Landsverk, M.L., et al., *Utilization of targeted array comparative genomic hybridization, MitoMet, in prenatal diagnosis of metabolic disorders.* Molecular Genetics and Metabolism, 2011. **103**(2): p. 148-52.
211. Kretz, R., et al., *Phytohemagglutinin stimulation of lymphocytes improves mutation analysis of carbamoylphosphate synthetase 1.* Mol Genet Metab, 2012. **106**(3): p. 375-8.

212. Bamshad, M.J., et al., *Exome sequencing as a tool for Mendelian disease gene discovery.* Nature reviews. Genetics, 2011. **12**(11): p. 745-55.
213. Mandell, R., et al., *Use of amniotic fluid amino acids in prenatal testing for argininosuccinic aciduria and citrullinaemia.* Prenatal diagnosis, 1996. **16**(5): p. 419-24.
214. Häberle, J., *Diagnosis and treatment of urea cycle disorders.* Journal of Pediatric Science, 2010: p. 2-11.
215. Cavicchi, C., et al., *Hypocitrullinemia in expanded newborn screening by LC-MS/MS is not a reliable marker for ornithine transcarbamylase deficiency.* Journal of pharmaceutical and biomedical analysis, 2009. **49**(5): p. 1292-5.
216. Mercimek-Mahmutoglu, S., et al., *Long-term outcome of patients with argininosuccinate lyase deficiency diagnosed by newborn screening in Austria.* Mol Genet Metab, 2010. **100**(1): p. 24-8.
217. Bachmann, C., *Long-term outcome of patients with urea cycle disorders and the question of neonatal screening.* Eur J Pediatr, 2003. **162 Suppl 1**: p. S29-33.
218. Feillet, F. and J.V. Leonard, *Alternative pathway therapy for urea cycle disorders.* Journal of inherited metabolic disease, 1998. **21 Suppl 1**: p. 101-11.
219. Endo, F., et al., *Clinical manifestations of inborn errors of the urea cycle and related metabolic disorders during childhood.* The Journal of nutrition, 2004. **134**(6 Suppl): p. 1605S-1609S; discussion 1630S-1632S, 1667S-1672S.
220. Berry, G.T. and R.D. Steiner, *Long-term management of patients with urea cycle disorders.* The Journal of pediatrics, 2001. **138**(1 Suppl): p. S56-60; discussion S60-1.
221. Morioka, D., et al., *Current role of liver transplantation for the treatment of urea cycle disorders: a review of the worldwide English literature and 13 cases at Kyoto University.* Liver transplantation : official publication of the American Association for the Study of Liver Diseases and the International Liver Transplantation Society, 2005. **11**(11): p. 1332-42.
222. Whitington, P.F., et al., *Liver transplantation for the treatment of urea cycle disorders.* Journal of inherited metabolic disease, 1998. **21 Suppl 1**: p. 112-8.
223. Meyburg, J., et al., *One liver for four children: first clinical series of liver cell transplantation for severe neonatal urea cycle defects.* Transplantation, 2009. **87**(5): p. 636-41.
224. Meyburg, J. and G.F. Hoffmann, *Liver, liver cell and stem cell transplantation for the treatment of urea cycle defects.* Molecular Genetics and Metabolism, 2010. **100 Suppl 1**: p. S77-83.
225. Jorns, C., et al., *Hepatocyte transplantation for inherited metabolic diseases of the liver.* Journal of internal medicine, 2012. **272**(3): p. 201-23.
226. Wirth, T., *A short perspective on gene therapy: Clinical experience on gene therapy of gliomablastoma multiforme.* World journal of experimental medicine, 2011. **1**(1): p. 10-16.
227. Ye, X., et al., *Prolonged metabolic correction in adult ornithine transcarbamylase-deficient mice with adenoviral vectors.* J Biol Chem, 1996. **271**(7): p. 3639-46.
228. Mian, A., et al., *Long-term correction of ornithine transcarbamylase deficiency by WPRE-mediated overexpression using a helper-dependent adenovirus.* Molecular therapy : the journal of the American Society of Gene Therapy, 2004. **10**(3): p. 492-9.

229. Brunetti-Pierri, N., et al., *Phenotypic correction of ornithine transcarbamylase deficiency using low dose helper-dependent adenoviral vectors.* The journal of gene medicine, 2008. **10**(8): p. 890-6.
230. Moscioni, D., et al., *Long-term correction of ammonia metabolism and prolonged survival in ornithine transcarbamylase-deficient mice following liver-directed treatment with adeno-associated viral vectors.* Molecular therapy : the journal of the American Society of Gene Therapy, 2006. **14**(1): p. 25-33.
231. Kiwaki, K., et al., *Correction of ornithine transcarbamylase deficiency in adult spf(ash) mice and in OTC-deficient human hepatocytes with recombinant adenoviruses bearing the CAG promoter.* Human gene therapy, 1996. **7**(7): p. 821-30.
232. Cunningham, S.C., et al., *AAV2/8-mediated correction of OTC deficiency is robust in adult but not neonatal Spf(ash) mice.* Molecular therapy : the journal of the American Society of Gene Therapy, 2009. **17**(8): p. 1340-6.
233. Cunningham, S.C., et al., *Induction and prevention of severe hyperammonemia in the spfash mouse model of ornithine transcarbamylase deficiency using shRNA and rAAV-mediated gene delivery.* Molecular therapy : the journal of the American Society of Gene Therapy, 2011. **19**(5): p. 854-9.
234. Lee, B., et al., *Hepatocyte gene therapy in a large animal: a neonatal bovine model of citrullinemia.* Proceedings of the National Academy of Sciences of the United States of America, 1999. **96**(7): p. 3981-6.
235. Ye, X., et al., *Correction of argininosuccinate synthetase (AS) deficiency in a murine model of citrullinemia with recombinant adenovirus carrying human AS cDNA.* Gene therapy, 2000. **7**(20): p. 1777-82.
236. Yang, Y., et al., *Cellular immunity to viral antigens limits E1-deleted adenoviruses for gene therapy.* Proceedings of the National Academy of Sciences of the United States of America, 1994. **91**(10): p. 4407-11.
237. Nagamani, S.C., et al., *Nitric-oxide supplementation for treatment of long-term complications in argininosuccinic aciduria.* American journal of human genetics, 2012. **90**(5): p. 836-46.
238. Gau, C.L., et al., *Short-term correction of arginase deficiency in a neonatal murine model with a helper-dependent adenoviral vector.* Molecular therapy : the journal of the American Society of Gene Therapy, 2009. **17**(7): p. 1155-63.
239. Raper, S.E., et al., *Fatal systemic inflammatory response syndrome in a ornithine transcarbamylase deficient patient following adenoviral gene transfer.* Molecular Genetics and Metabolism, 2003. **80**(1-2): p. 148-58.
240. Mueller, C. and T.R. Flotte, *Clinical gene therapy using recombinant adeno-associated virus vectors.* Gene therapy, 2008. **15**(11): p. 858-63.
241. Nathwani, A.C., et al., *Adenovirus-associated virus vector-mediated gene transfer in hemophilia B.* The New England journal of medicine, 2011. **365**(25): p. 2357-65.
242. Wang, L., et al., *Preclinical evaluation of a clinical candidate AAV8 vector for ornithine transcarbamylase (OTC) deficiency reveals functional enzyme from each persisting vector genome.* Molecular Genetics and Metabolism, 2012. **105**(2): p. 203-11.
243. Wang, L., et al., *Sustained correction of OTC deficiency in spf(ash) mice using optimized self-complementary AAV2/8 vectors.* Gene therapy, 2012. **19**(4): p. 404-10.
244. Lee, E.K., et al., *Long-term survival of the juvenile lethal arginase-deficient mouse with AAV gene therapy.* Molecular therapy : the journal of the American Society of Gene Therapy, 2012. **20**(10): p. 1844-51.

245. Lee, E.K., et al., *AAV-based gene therapy prevents neuropathology and results in normal cognitive development in the hyperargininemic mouse.* Gene therapy, 2013. **20**(8): p. 785-96.
246. Deignan, J.L., S.D. Cederbaum, and W.W. Grody, *Contrasting features of urea cycle disorders in human patients and knockout mouse models.* Molecular Genetics and Metabolism, 2008. **93**(1): p. 7-14.
247. Senkevitch, E., et al., *A novel biochemically salvageable animal model of hyperammonemia devoid of N-acetylglutamate synthase.* Molecular Genetics and Metabolism, 2012. **106**(2): p. 160-8.
248. Schofield, J.P., et al., *Mice deficient in the urea-cycle enzyme, carbamoyl phosphate synthetase I, die during the early neonatal period from hyperammonemia.* Hepatology, 1999. **29**(1): p. 181-5.
249. DeMars, R., et al., *Abnormal ornithine carbamoyltransferase in mice having the sparse-fur mutation.* Proceedings of the National Academy of Sciences of the United States of America, 1976. **73**(5): p. 1693-7.
250. Doolittle, D.P., L.L. Hulbert, and C. Cordy, *A new allele of the sparse fur gene in the mouse.* The Journal of heredity, 1974. **65**(3): p. 194-5.
251. Dennis, J.A., et al., *Molecular definition of bovine argininosuccinate synthetase deficiency.* Proceedings of the National Academy of Sciences of the United States of America, 1989. **86**(20): p. 7947-51.
252. Patejunas, G., et al., *Generation of a mouse model for citrullinemia by targeted disruption of the argininosuccinate synthetase gene.* Somatic cell and molecular genetics, 1994. **20**(1): p. 55-60.
253. Perez, C.J., et al., *Two hypomorphic alleles of mouse Ass1 as a new animal model of citrullinemia type I and other hyperammonemic syndromes.* The American journal of pathology, 2010. **177**(4): p. 1958-68.
254. Reid Sutton, V., et al., *A mouse model of argininosuccinic aciduria: biochemical characterization.* Molecular Genetics and Metabolism, 2003. **78**(1): p. 11-6.
255. Iyer, R.K., et al., *Mouse model for human arginase deficiency.* Molecular and cellular biology, 2002. **22**(13): p. 4491-8.
256. Caldovic, L., et al., *N-acetylglutamate synthase: structure, function and defects.* Molecular Genetics and Metabolism, 2010. **100 Suppl 1**: p. S13-9.
257. Bachmann, C., J.P. Colombo, and K. Jaggi, *N-acetylglutamate synthetase (NAGS) deficiency: diagnosis, clinical observations and treatment.* Advances in experimental medicine and biology, 1982. **153**: p. 39-45.
258. Häberle, J., et al., *Mutation analysis in patients with N-acetylglutamate synthase deficiency.* Human mutation, 2003. **21**(6): p. 593-7.
259. Caldovic, L., H. Morizono, and M. Tuchman, *Mutations and polymorphisms in the human N-acetylglutamate synthase (NAGS) gene.* Human mutation, 2007. **28**(8): p. 754-9.
260. Grisolia, S. and P.P. Cohen, *The catalytic role of carbamyl glutamate in citrulline biosynthesis.* J Biol Chem, 1952. **198**(2): p. 561-71.
261. Klaus, V., et al., *Highly variable clinical phenotype of carbamylphosphate synthetase 1 deficiency in one family: an effect of allelic variation in gene expression?* Clin Genet, 2009. **76**(3): p. 263-9.
262. Eeds, A.M., et al., *Assessing the functional characteristics of synonymous and nonsynonymous mutation candidates by use of large DNA constructs.* Am J Hum Genet, 2007. **80**(4): p. 740-50.
263. Brusilow, S.W. and N.E. Maestri, *Urea cycle disorders: diagnosis, pathophysiology, and therapy.* Adv Pediatr, 1996. **43**: p. 127-70.

264. Matsuda, I., et al., *Phenotypic variability in male patients carrying the mutant ornithine transcarbamylase (OTC) allele, Arg40His, ranging from a child with an unfavourable prognosis to an asymptomatic older adult.* J Med Genet, 1996. **33**(8): p. 645-8.
265. Maestri, N.E., et al., *The phenotype of ostensibly healthy women who are carriers for ornithine transcarbamylase deficiency.* Medicine (Baltimore), 1998. **77**(6): p. 389-97.
266. McCullough, B.A., et al., *Genotype spectrum of ornithine transcarbamylase deficiency: correlation with the clinical and biochemical phenotype.* Am J Med Genet, 2000. **93**(4): p. 313-9.
267. Ricciuti, F.C., T.D. Gelehrter, and L.E. Rosenberg, *X-chromosome inactivation in human liver: confirmation of X-linkage of ornithine transcarbamylase.* Am J Hum Genet, 1976. **28**(4): p. 332-8.
268. Leonard, J.V. and A.A. Morris, *Urea cycle disorders.* Seminars in neonatology : SN, 2002. **7**(1): p. 27-35.
269. Woo, H.I., H.D. Park, and Y.W. Lee, *Molecular genetics of citrullinemia types I and II.* Clinica chimica acta; international journal of clinical chemistry, 2014. **431C**: p. 1-8.
270. Gao, H.Z., et al., *Identification of 16 novel mutations in the argininosuccinate synthetase gene and genotype-phenotype correlation in 38 classical citrullinemia patients.* Human mutation, 2003. **22**(1): p. 24-34.
271. Lee, B.H., et al., *High prevalence of neonatal presentation in Korean patients with citrullinemia type 1, and their shared mutations.* Molecular Genetics and Metabolism, 2013. **108**(1): p. 18-24.
272. Allan, J.D., et al., *A disease, probably hereditary characterised by severe mental deficiency and a constant gross abnormality of aminoacid metabolism.* Lancet, 1958. **1**(7013): p. 182-7.
273. Nagamani, S.C., B. Lee, and A. Erez, *Optimizing therapy for argininosuccinic aciduria.* Molecular Genetics and Metabolism, 2012. **107**(1-2): p. 10-4.
274. Nagamani, S.C., A. Erez, and B. Lee, *Argininosuccinate lyase deficiency.* Genetics in medicine : official journal of the American College of Medical Genetics, 2012. **14**(5): p. 501-7.
275. Ficicioglu, C., R. Mandell, and V.E. Shih, *Argininosuccinate lyase deficiency: longterm outcome of 13 patients detected by newborn screening.* Molecular Genetics and Metabolism, 2009. **98**(3): p. 273-7.
276. Glick, N.R., P.J. Snodgrass, and I.A. Schafer, *Neonatal argininosuccinic aciduria with normal brain and kidney but absent liver argininosuccinate lyase activity.* Am J Hum Genet, 1976. **28**(1): p. 22-30.
277. Perry, T.L., et al., *Amino acid and enzyme studies of brain and other tissues in an infant with argininosuccinic aciduria.* Clin Chim Acta, 1980. **105**(2): p. 257-67.
278. Barbosa, P., M. Cialkowski, and W.E. O'Brien, *Analysis of naturally occurring and site-directed mutations in the argininosuccinate lyase gene.* J Biol Chem, 1991. **266**(8): p. 5286-90.
279. Engel, K., et al., *Bacterial expression of mutant argininosuccinate lyase reveals imperfect correlation of in-vitro enzyme activity with clinical phenotype in argininosuccinic aciduria.* J Inherit Metab Dis, 2012. **35**(1): p. 133-40.
280. Renouf, S., A. Fairand, and A. Husson, *Developmental control of argininosuccinate lyase gene by methylation.* Biol Neonate, 1998. **73**(3): p. 190-7.

281. Abramson, R.D., et al., *Characterization of the human argininosuccinate lyase gene and analysis of exon skipping.* Genomics, 1991. **10**(1): p. 126-32.
282. Linnebank, M., et al., *Two novel mutations (E86A, R113W) in argininosuccinate lyase deficiency and evidence for highly variable splicing of the human argininosuccinate lyase gene.* J Inherit Metab Dis, 2000. **23**(4): p. 308-12.
283. Walker, D.C., et al., *Molecular analysis of human argininosuccinate lyase: mutant characterization and alternative splicing of the coding region.* Proc Natl Acad Sci U S A, 1990. **87**(24): p. 9625-9.
284. Stuehr, D., S. Pou, and G.M. Rosen, *Oxygen reduction by nitric-oxide synthases.* J Biol Chem, 2001. **276**(18): p. 14533-6.
285. Lin, M.I., et al., *Phosphorylation of threonine 497 in endothelial nitric-oxide synthase coordinates the coupling of L-arginine metabolism to efficient nitric oxide production.* J Biol Chem, 2003. **278**(45): p. 44719-26.
286. Pignitter, M., et al., *Inefficient spin trapping of superoxide in the presence of nitric-oxide: implications for studies on nitric-oxide synthase uncoupling.* Free radical biology & medicine, 2006. **41**(3): p. 455-63.
287. D'Hooge, R., et al., *Convulsive action and toxicity of uremic guanidino compounds: behavioral assessment and relation to brain concentration in adult mice.* Journal of the neurological sciences, 1992. **112**(1-2): p. 96-105.
288. Aoyagi, K., et al., *Role of nitric oxide in the synthesis of guanidinosuccinic acid, an activator of the N-methyl-D-aspartate receptor.* Kidney international. Supplement, 2001. **78**: p. S93-6.
289. Aoyagi, K., *Inhibition of arginine synthesis by urea: a mechanism for arginine deficiency in renal failure which leads to increased hydroxyl radical generation.* Molecular and cellular biochemistry, 2003. **244**(1-2): p. 11-5.
290. Balmer, C., et al., *Mutations and polymorphisms in the human argininosuccinate lyase (ASL) gene.* Human mutation, 2014. **35**(1): p. 27-35.
291. Kleijer, W.J., et al., *Clinical, enzymatic, and molecular genetic characterization of a biochemical variant type of argininosuccinic aciduria: prenatal and postnatal diagnosis in five unrelated families.* J Inherit Metab Dis, 2002. **25**(5): p. 399-410.
292. Nagamani, S.C., et al., *A randomized controlled trial to evaluate the effects of high-dose versus low-dose of arginine therapy on hepatic function tests in argininosuccinic aciduria.* Molecular Genetics and Metabolism, 2012. **107**(3): p. 315-21.
293. Yu, B., et al., *Mechanisms for intragenic complementation at the human argininosuccinate lyase locus.* Biochemistry, 2001. **40**(51): p. 15581-90.
294. Sampaleanu, L.M., et al., *Three-dimensional structure of the argininosuccinate lyase frequently complementing allele Q286R.* Biochemistry, 2001. **40**(51): p. 15570-80.
295. Ash, D.E., et al., *Molecular basis of hyperargininemia: structure-function consequences of mutations in human liver arginase.* Molecular Genetics and Metabolism, 1998. **64**(4): p. 243-9.
296. Vockley, J.G., et al., *Loss of function mutations in conserved regions of the human arginase I gene.* Biochemical and molecular medicine, 1996. **59**(1): p. 44-51.
297. Cederbaum, S.D., et al., *Hyperargininemia with arginase deficiency.* Pediatric research, 1979. **13**(7): p. 827-33.
298. Iyer, R., et al., *The human arginases and arginase deficiency.* Journal of inherited metabolic disease, 1998. **21 Suppl 1**: p. 86-100.

299. Uchino, T., et al., *Molecular basis of phenotypic variation in patients with argininemia.* Human genetics, 1995. **96**(3): p. 255-60.
300. Worth, C.L., et al., *A structural bioinformatics approach to the analysis of nonsynonymous single nucleotide polymorphisms (nsSNPs) and their relation to disease.* J Bioinform Comput Biol, 2007. **5**(6): p. 1297-318.

6 Acknowledgments

A major research project like this thesis is never the effort of a single person. Different contributions from different people, in their own differing styles, have made this thesis possible. I would like to express my appreciation particularly to the following persons.

First and foremost, I am extremely grateful to Prof. Dr. med. Johannes Häberle for offering me the great opportunity to complete my doctoral thesis in his laboratory as well as for the correction and critical reading of this thesis. His valuable guidance, sincere, patience, encouragement as well as personal care accompanied me through the entire period, which helped me grow not only in doing the research tasks, but also in my personal development.

I wish to express my sincere thanks to my thesis committee chair Prof. Dr. Beat Schäfer and the other committee members Prof. Dr. Thierry Hennet and PD. Dr. med. Jean-Marc Nuoffer for supervising me through the PhD with their insightful comments and suggestions, encouragement as well as critical feedback and questions.

Many thanks must go to PD. Dr. Amit Pandey (Bern), PD. Jean-Marc Nuoffer (Bern) and Prof. Dr. Vicente Rubio (Valencia) for their excellent collaboration. Also I like to thank all the people directly or indirectly involved in my research project, especially for the excellent technical assistance provided by Dana Leiteritz, Véronique Rüfenacht, Sandra Eggimann, and the late Murielle Groux. Special thanks go to Carmen Diez for helping me with the establishment of the baculovirus/insect expression system as well as for her generous support.

I would like to thank the director of Division of Metabolism at Kispi Zurich, Prof. Dr. med. Matthias Baumgartner, for providing me all the necessary facilities and nice work place. Thanks also go to people from the Divisions of Clinical Chemistry, Hematology, and Immunology at Kispi for allowing me to use their facilities.

The fruitful discussions and suggestions during our seminars provided by members of Kispi's StoMol team including Matthias, Beat, David, Cecilia, Terttu, Patricie, Uschi, Sean, Patrick, Hiu Man, Marianne, and people from Divisions of Clinical Chemistry were valuable and inspirational. Taking this opportunity, I would like to thank all the other former and current members of StoMol team, such as Angelika, Seraine, Céline, Trinh, Micha, Merima, Corinne, Dorothea, Michele, Martin

etc. for their help, suggestions, encouragement as well as personal care. Many thanks also go to the people in Jean-Marc Nuoffer's lab who made me feel like being part of their lab at the Inselspital Bern.

Special gratitude should go to my friends for their continuous motivation and support, especially Dan, Furong, Paulette and Maite.

Finally, I would like to thank my family: my parents, brother, sister and aunt for their unlimited love and unconditional support, both financially and spiritually, not least the love of my father, who passed away, that encouraged me to overcome any difficult situations. Also, great support came from my Dutch family in Terneuzen.

Finally to my husband Ad, who always inspires me to engage into the competing demands of work, study and personal development, thanks for always being there for me, for his belief in my abilities and for his constant support and love.

7 Curriculum vitae

Personal Information:

Family name:	HU
Given name:	Liyan
Gender:	Female
Date of Birth:	29th. Sep. 1976
Family status:	Married
Nationality:	China
Address:	Hinterbrunnenstrasse 10 8312 Winterberg ZH, Switzerland
Telefon:	+41 52 347 1570
Mobile:	+41 79 299 2983
E-Mail:	Liyan@gmx.ch

Educational Background:

Oct. 2010- Mar. 2014 **Doctoral thesis** in Division of Metabolism at University of Children's Hospital Zurich, PhD program of Neuroscience, Faculty of Science, University of Zurich, Switzerland
Apr. 2003- Mar. 2010 **Master** major in Biology, Free University of Berlin, Germany
Jun. 2002- Mar. 2003 **German course** at Goethe-Institute Göttingen, Germany
Sep.1998- Jul. 2001 **Undergraduate** major in Clinical Medicine, University of Zhejiang, Hangzhou, China
Sep.1994- Jul.1997 Three-year **College** major in Osteology, Zhejiang College of Traditional Chinese Medicine, Hangzhou, China
Sep.1983- Jul.1994 Primary and secondary education in Taizhou, Zhejiang, China

Research/Work Experience:

Oct. 2010 – Mar. 2014

Doctoral thesis in the group of Prof. Dr. med. Johannes Häberle in the metabolic laboratory at the Division of Metabolism, University Children's Hospital Zurich with the following title:
The Molecular Basis and Pathology of Phenotypic Variability in Urea Cycle Disorders

Jun. 2009 – Mar. 2010

Diploma thesis in the group of Prof. Dr. Josef Jiricny at the Institute of Molecular Cancer Research of the University of Zurich with the following title:
Doxycycline-inducible Gene Replacement of DNA Polymerase-δ and Downregulation of Human Exonuclease1 (EXO1): A Model System for Studying EXO1-independent Mismatch Repair in Human Cell Lines

Apr. 2007 – Dec. 2008

Student Research Associate in the Research Group of Dr. Elena Elstner in the Division of Hematology/Oncology, University Medicine Berlin, Charite with Research Interests:
The nuclear hormone receptors (NHRs) as molecular targets for breast cancer therapy

Jul. 1996 – Jul. 1997

Practical year as resident doctor in Hangzhou Hospital of Traditional Chinese Medicine, Hangzhou, China

Language Skills:

Chinese (mother tongue), German and English (spoken and written good)

Personal interests:

Sports (volleyball, cycling, hiking); general interest in culture, history, economy and travel

Abstracts (with posters)

Hu L, Diez-Fernandez C, Rüfenacht V, Rubio V, Häberle J (2014) Molecular characterization of the only frequently recurrent mutation in carbamoyl phosphate synthetase 1 (CPS1) deficiency. *Mol Syndromol* 5 (2): 95 (poster at the 2nd Re(ACT) congress, 5th-8th Mar 2014, Basel)

Hu L, Rüfenacht V, Pandey A, Nuoffer JM, Möslinger D, Häberle J (2013) Predominant expression of exon 7-deleted argininosuccinate lyase in a patien with argininosuccinic aciduria. *J Inher Metab Dis* 36: S142 (poster at the ICIEM congress, 3th-6th Sep 2013, Barcelona)

Hu L, Eggimann S, Pandey A, Nuoffer JM, Häberle J (2012) Variability of argininosuccinate lyase deficiency can be caused by splice variants resulting in heterotetramer formation *J Inher Metab Dis* 35: S48 (poster at the SSIEM congress, 4th-7th Sep 2012, Birmingham)

Balmer C, **Hu L**, Eggimann S, Pandey A, Wettstein V, Nuoffer JM, Häberle J (2012) Expression of naturally occurring argininosuccinate lyase mutants in 293T cells improves the correlation of residual enzyme activity with the clinical phenotype. *J Inher Metab Dis* 35: S48 (poster at the SSIEM congress, 4th-7th Sep 2012, Birmingham)

Hu L, Frapolli M, Stucki M, Ben-Omran T, Häberle J (2011) Lessons from an ultra-rare disorder: a new insight into glutamine synthetase deficiency. *Mol Syndromol* 2: 276 (poster at the 1st Re(ACT) congress, 29th Feb-2nd Mar 2012, Basel)

Hu L, Vuissoz JM, Eggimann S, Nuoffer JM, Häberle J (2011) The role of transcript variants of argininosuccinate lyase for clinical variability. *J Inher Metab Dis* 34: S92 (poster at the SSIEM congress, 30th Aug.-2nd Sep 2011, Geneva)

Oral presentations

"The role of transcript variants of argininosuccinate lyase for clinical variability" at the ZNZ PhD retreat 11, 12th-14th May.2011, Valens

"Dominant negative effect of a naturally occurring splice variant on argininosuccinate lyase activity" at the FZK retreat, 25th Oct 2012, Zurich

Poster presentations

"Understanding the role of a predominantly expressed exon 7-deleted argininosuccinate lyase transcript in 2 patients" at the FZK retreat, 31st Oct 2013, Zurich

"The molecular mechanism and pathology of clinical variability in one of urea cycle disorders (argininosuccinic aciduria)" at ZNZ symposium, 13th Sep 2013, Zurich

"Surprisingly high recombinant mutant activity levels may partly explain the wide clinical spectrum of argininosuccinic aciduria" at the 4th international symposium on UCD, 1st-2nd Sep. 2013, Barcelona

"Dominant negative effect of a naturally occurring splice variant on argininosuccinate lyase activity" and "Surprisingly high mutant activity levels might partly explain the wide clinical spectrum of argininosuccinic aciduria" at 12th Day of Clinical Research, 4th Apr 2013, Zurich
"Surprisingly high mutant activity levels might partly explain the wide clinical spectrum of argininosuccinic aciduria" at the FZK retreat, 25th Oct 2012, Zurich

"The role of transcript variants of argininosuccinate lyase for clinical variability" at the FZK retreat, 7th Oct 2011, Zurich

Prior to PhD:

Ghodgaonkar M, Kehl P, Ventura I, **Hu L**, Bignami M, and Jiricny J (2014) *An inducible protein replacement system for the study of genotypephenotype correlations: polymerase-δ mutations in hereditary colon cancer*. Manuscript (from master thesis) submitted to *Nature Genetics*